70th Conference on Glass Problems

Ceramic Engineering and Science Proceedings

Volume 31, Issue 1, 2010

Charles H. Drummond, III
Editor

WILEY

The American Ceramic Society

70th Conference on Glass Problems

A Collection of Papers Presented at the 70th Conference on Glass Problems The Ohio State University, Columbus, Ohio October 11–12, 2009

Edited by
Charles H. Drummond, III

WILEY

A John Wiley & Sons, Inc., Publication

This Page Intentionally Left Blank

70th Conference on Glass Problems

This Page Intentionally Left Blank

70th Conference on Glass Problems

A Collection of Papers Presented at the 70th Conference on Glass Problems The Ohio State University, Columbus, Ohio October 11–12, 2009

Edited by
Charles H. Drummond, III

WILEY

A John Wiley & Sons, Inc., Publication

Published by John Wiley & Sons, Inc., Hoboken, New Jersey.
Published simultaneously in Canada.

Library of Congress Cataloging-in-Publication Data is available.

ISBN 978-0-470-59466-7
ISBN 978-0-470-64415-7 (special edition)

Printed in the United States of America.

10 9 8 7 6 5 4 3 2 1

Contents

This Page Intentionally Left Blank

Foreword

The conference was sponsored by the Department of Materials Science and Engineering at The Ohio State University.

The director of the conference was Charles H. Drummond, III, Associate Professor, Department of Materials Science and Engineering, The Ohio State University.

Randy Moses, Interim Associate Dean, College of Engineering, The Ohio State University, gave the welcoming address. Rudolph Buchheit, Chair, Department of Materials Science and Engineering, The Ohio State University, gave the Departmental welcome.

The themes and chairs of the five half-day sessions were as follows:

Glass Melting
Ruud Beerkens, TNO Glass Technology - Glass Group, Eindhoven, The Netherlands, Tom Dankert, O-I, Toledo OH and Larry McCloskey, Toledo Engineering, Toledo OH

The Future of the Glass Industry and Environment Regulations
Dick Bennett, Johns Manville, Littleton CO, Terry Berg, CertainTeed, Athens GA and Phil Ross, Glass Industry Consulting, Laguna Niguel CA

Energy
Martin H. Goller, Corning, Corning NY, Elmer Sperry, Libbey Glass, Toledo OH and Carsten Weinhold, Schott, Dyrea PA

Refractories
Warren F. Curtis, PPG Industries, Pittsburgh PA, Dan Wishnick, Siemens, Spring House PA and John Tracey, North American Refractories, Cincinnati OH

This Page Intentionally Left Blank

Preface

In the tradition of previous conferences, started in 1934 at the University of Illinois, the papers presented at the 70th Annual Conference on Glass Problems have been collected and published as the 2009 edition of The Collected Papers.

The manuscripts are reproduced as furnished by the authors, but were reviewed prior to presentation by the respective session chairs. Their assistance is greatly appreciated. C. H. Drummond did minor editing with further editing by the American Ceramic Society. The Ohio State University is not responsible for the statements and opinions expressed in this publication.

The following presentations were made at the conference but the manuscripts were not received in time for publication in this proceedings: Heat Recovery on a 500MT/D Float Furnace by Niels A. Rozendaal, OPTIMUM Environmental & Energy Technologies, Arnhem, The Netherlands and Gob Assist, an Indispensable Tool for the Glass Industry by Joop Dalstra, XPAR Vision, Groningen, The Netherlands

CHARLES H. DRUMMOND, III
Columbus, OH
December 2009

This Page Intentionally Left Blank

Acknowledgments

It is a pleasure to acknowledge the assistance and advice provided by the members of Program Advisory Committee in reviewing the presentations and the planning of the program:

Ruud G. C. Beerkens—TNO

Dick Bennett—Johns Manville

Terry Berg—CertainTeed

Warren Curtis—PPG Industries

Tom Dankert—O-I

Martin H. Goller—Corning

Larry McCloskey—Toledo Engineering

C. Philip Ross—Glass Industry Consulting

Elmer Sperry—Libbey Glass

John Tracey—North American Refractories

Carsten Weinhold—Schott

Dan Wishnick—Siemens

This Page Intentionally Left Blank

Glass Melting

This Page Intentionally Left Blank

RAPID REFINING OF SUBMERGED COMBUSTION MELTER PRODUCT GLASS

David Rue, Walter Kunc, and John Wagner
Gas Technology Institute

Bruno Purnode
Owens Corning

Aaron Huber
Johns Manville

Segmented glass melting processes require special attention to glass refining before glass is delivered to the forming process. Refining levels vary based on product requirements, allowing this step to be designed as needed, but most commercial glasses require refining. Submerged combustion melting (SCM) produces a homogeneous molten glass that contains a large number of bubbles ranging all the way up to 2 cm. in diameter. Efforts to rapidly refine SCM glass have led to an understanding of methods that hold promise and those that are ineffective for this glass. A crucial factor involves the number and distribution of bubbles and how they move within the viscous glass. A two-stage refining approach holds promise. This approach enables attainment of glass for fiber quality in the first stage and glass for higher quality applications (container, float, etc.) in a second stage. This paper describes efforts to develop and study batch and continuous refining of SCM product glass. A wide range of refining approaches have been proposed and explored in the past, and the current work is reviewed in the context of this body of earlier work.

CONVENTIONAL MELTING AND SUBMERGED COMBUSTION MELTING

The great majority of glass made industrially is produced in refractory melters. While these furnaces vary significantly in size, temperature, residence time, and refractory composition based on the glass composition and fining quality required, the overall approach of using a single large tank with a long residence time is the same. Glass batch and cullet (if included) is charged at the back of the furnace, and fined glass ready for a final conditioning step, a forehearth, or a forming process is discharged at a controlled rate from a throat on the front wall of the furnace. Usually heat is supplied by air-gas or oxygen-gas burners above the melt surface. In some furnaces electrodes below the melt surface provide a portion or even all of the heat needed for batch heating and glass forming reactions, and to hold temperature for homogenization and glass fining.

Submerged combustion melting provides a different path to a homogeneous molten glass. In SCM[1], batch and cullet (if used) is also charged at the back of the furnace and molten, homogeneous glass is discharged at a controlled rate from a throat or opening on the front wall. The means of heating in SCM is a carefully arranged group of oxygen-gas burners firing directly up into the melt pool. This provides excellent heat transfer and mixing along with a much shorter average residence time of one to four hours. With a residence ti me of 10 to 20 percent of conventional

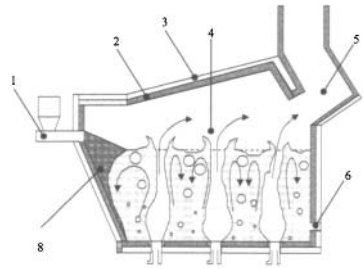

Figure 1. 1 Feeder, 2 Refractory, 3 Cooled walls, 4 Melt, 5 Vent, 6 Tap, 7 Burners, 8 Feed pocket

melters and with the refractory walls replaced with water-cooled panels, an SCM has a much smaller footprint and lower capital cost than a conventional tank.

SCM product glass needs fining, thus the need for a segmented production process. Glass leaving the SCM has been measured to contain up to 35% voids by volume. These voids are predominantly carbon dioxide from the combustion process, with lower levels of oxygen and argon, and trace amounts of CO and NO_x. Combustion is carried out, as in conventional melters, slightly fuel-lean, so the oxygen in the bubbles is unused oxygen. Because of the differences between glass melted in conventional melters and SCM, the approach to refining could be different.

GLASS FINING APPROACHES

One reason for the large size of conventional melters is to allow time for bubbles and seeds to rise to the glass surface. Buoyancy in the viscous melt can be enhanced by one or more methods that take advantage of the relationships described by Stokes Law as modified for viscous liquids[2].

$$V_b = \frac{3}{2}V_r = \frac{g\Delta\rho r^2}{9\eta}$$

Stokes Law states that the bubble velocity (V_b) is proportional to the gravitational constant (g), the difference in density of the gas and liquid ($\Delta\rho$), and the square of the bubble radius (r), and is inversely proportional to the melt viscosity (η). Industrially practiced methods include the use of bubblers and bubble curtains to combine smaller bubbles into faster rising larger bubbles, the use of fining agents (As_2O_5, Sb_2O_5, Na_2SO_4, other sulfates, and sometimes other oxides (such as CeO) to add additional gases to increase bubble size, and the use of refining to allow the tiniest seeds to dissolve fully into the glass.

The physics of bubble buoyancy behavior is the same for SCM. Process dynamics, however, dictate which approaches can be considered for rapid fining of SCM glass. SCM glass is homogeneous with large numbers of bubbles that range from tiny up to 2 cm. in diameter. The large number of inclusions eliminates any possible benefits of bubblers, bubble curtains, and chemical fining agents that are used industrially. Also, SCM fining should be rapid or the benefits of a small, intense melting process are lost. A number of other fining methods have been proposed and sometimes employed over the years[3]. These have been studied and evaluated with reference to SCM glass fining requirements.

The most common of the alternate fining approaches is the use of a thin layer zone or fining shelf. By creating a zone with a shallow depth, bubbles have less distance to travel, and fining time is reduced[4]. This approach is commonly applied with electric melters and specially designed furnaces such as the Sorg LoNOx melter. Thin layer refining can accelerate refining, but the method can require large surface areas for glasses that are slow to refine. A second alternative approach is to extract bubbles under reduced pressure or vacuum. The method was demonstrated at industrial scale by PPG in the P-10 process[5] and has been applied in a different way by Asahi. Reduced pressure can accelerate fining but drawbacks include the mechanical complexity, sealing concerns, and the need for foam control.

A third means to speed refining is to use mechanical methods to either screen out bubbles or to gently stir glass to bring bubbles to the surface more quickly[6]. Care must be taken to devise approaches that do not add new bubbles to the glass. Even when well executed, issues remain regarding mechanical wear of stirrers. Also, stirring alone is likely to help refining but not lead to complete refining. A fourth proposed fining method is the application of heat in precise locations to lower glass viscosity and increase bubble velocity. Microwaves have been proposed as one way to

accomplish this[7] since silicate melts are susceptible to microwave heating. The approach is energy-intensive and the means to carry out this approach industrially are not yet demonstrated.

Two related approaches to fining are the injection of steam[8] and the injection of helium[9] to replace or supplement some or all of the fining agents normally used. Steam, particularly in conjunction with sulfates, can accelerate refining. Helium has the virtue of very low density and is expected to very effectively combine with other gas inclusions and increase bubble buoyancy rates. Steam can be understood as a practical way to reduce sulfate requirements, but high temperature steam must be generated and injected uniformly into the melt. Helium refining is promising, but care must be taken to use only a small amount of helium, to distribute helium uniformly in the glass, and to capture and recycle helium if possible.

Centrifugal refining holds promise as a very fast fining approach[10]. Spinning the molten glass at up to 1500 rpm has been shown in lab testing to reduce fining time to minutes. Complexities in scaling to industrial capacities and concerns over high speed rotational equipment have prevented adoption of this approach. A final proposed fining method, acoustic or ultrasonic refining, relies on bubble exclusion rather than Stokes Law[11]. In this approach bubbles are prevented by the acoustic field from passing out of the melter. This promising approach has not been demonstrated at large scale and the materials required for long service life have not been identified.

SCM RAPID FINING TESTING

The selection of the first rapid refining approach to evaluate with SCM glass was made in the following manner. Helium refining and acoustic refining were considered immature and would require research programs of their own to test. Steam refining and mechanical stirring were considered inapplicable to SCM glass because large numbers of bubbles and high water levels are already present in the glass. Rapid refining by application of precise heating using microwaves or other methods was determined to be too energy intensive and to mot be easily adapted to the SCM process. Reduced pressure refining has been proven at industrial scale, but foam control is challenging. The large number of small to large bubbles in SCM glass may be manageable during vacuum refining, but the development of the process would be complex and likely beyond the available development resources. Centrifugal refining also would appear compatible with SCM glass, but the development of the process equipment would require resources beyond those available. Both vacuum refining and centrifugal refining have not been adopted by the glass industry, despite demonstrated successes, therefore these methods were set aside temporarily but kept in mind as possible matches to the SCM process.

Short residence time refining, or holding SCM glass at constant temperature for precise time periods in a chamber with relatively shallow depth, was deemed promising. Because SCM glass is already homogeneous, no further mixing is required. The large number of bubbles, with many of the bubbles having a large enough size that they should quickly rise to the surface, and the high oxygen and steam content in the SCM glass, were supportive of the potential to refine the glass in a reasonable residence time of no more than several hours.

To quickly assess the potential for refining SCM glass with short residence times, an SCM test was conducted with a commercial non-boron E glass composition. Fully melted glass was collected in mullite crucibles that were placed in an electric oven held at 1250°, 1350°, and 1450°C for 0, 20, 60, and 120 min. The crucibles were then placed in a second electric oven held at 800°C overnight to anneal the glass. Once cooled, the crucibles were cut in half as shown in Figure 2 so the refining potential could be determined. Quantitative void fractions were not measured, but visual observation showed that residence times as short as 20 min. led to significant clarification of the glass at the bottom of the crucible, and residence times of 120 min. produced a much more clarified glass.

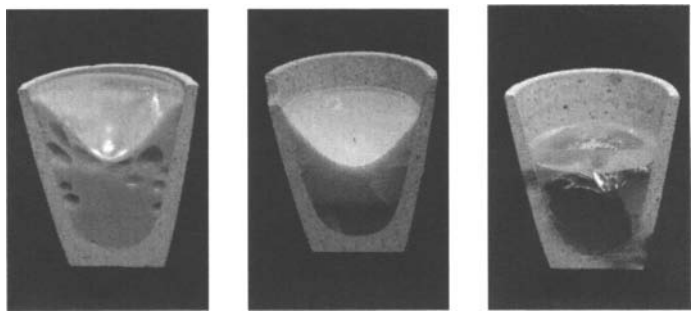

(a) 0 min. (b) 20 min. (c) 120 min.

Figure 2. Static Clarification of SCM E Glass at 1350°C, (a) no refining, (b) clearing at bottom, (c) clearing throughout

Promising results from the static crucible refining tests led to preparation of equipment for continuous SCM-short residence time refining tests. An electrically-heated refractory conditioning channel was designed and built. The channel allows steady flow of glass at constant temperature with no stirring. Glass depth can be varied from 7 to 18 cm, and temperature can be as high as 1450°C. Glass flow rates can be 150 to 750 kg/h, giving residence times up to several hours as desired. The channel was close-couple to the SCM with a heated refractory chute. An oxy-gas torch was placed at the exit from the channel to prevent heat losses and to provide a combustion gas environment over the surface of the glass in the channel that simulates expected industrial conditions.

Two continuous steady-state tests were conducted with SCM glass produced from the same borosilicate E glass batch and then sent into and through the conditioning channel. In Test SCM-R-1 two SCM steady state temperature periods were maintained (1370° and 1425°C). SCM discharge rates were varied over a small range between 400 and 550 kg/h giving a similarly small range, and fairly short, residence time range.

The second combined SCM-refining test was conducted under similar operating conditions but with improved process control and more detailed analyses. After the first test, a slide gate was devised for the discharge end of the SCM tap. This electrically-driven and externally heated ceramic plate allowed control of melt flow in test SCM-R-2 over a much wider range from 175 to 450 kg/h. This allowed the refining residence time to be set and varied by nearly a 3:1 ratio. To collect more detailed data than in the first test, the SCM temperature during constant batch charging and glass discharge was held steady at 1425°C, $\pm$10°C, throughout the second test. The chute connecting the SCM and the conditioning channel was better insulated with improved heating to prevent loss of glass temperature. The conditioning channel was held at 1355°C, as measured by an optical pyrometer at the channel discharge. Limited analyses were conducted with SCM and refined glass from the first test, but care was taken in the second test to collect more samples using a graphite mold, to anneal samples at 800°C, and to conduct more extensive analyses of the collected samples from the melter and the conditioning channel.

RESULTS

Assessment of the short residence time refining of SCM glass has been made with samples collected from similar operating conditions of tests SCM-R-1 and SCM-R-2. The SCM was maintained under continuous steady state operation at 1425°C using the same borosilicate E glass pre-mixed batch. Samples weighing approximately 0.5 kg were collected from the SCM tap and from the conditioning channel discharge in graphite molds. Samples were allowed to cool, with some samples annealed at 800°C. Chemical analyses found the glass samples from the conditioning channel were fully melted and homogeneous, with uniform compositions across both tests. The collected glass samples were split in half, and chemists at GTI and Johns Manville independently measured void fractions of the samples.

Void fraction analyses from test SCM-R-2 tap and refiner samples are presented in Figure 3. Analyses show the void fraction of the tap samples was similar throughout the day of operation. Voids were measured between 25 and 33%. The test was conducted with melt flow rate decreasing (and refiner residence time increasing) as the day continued. Results show that as residence time increases, a large decrease in void fraction is obtained. Average void fraction of samples after the conditioning channel decreased from 16 to as low as 0.3%, equivalent to a decrease in void fraction from 45 to 99% relative to the voids in the SCM product glass. Refining with short residence time was able to convert the foamy SCM glass to a solid glass with remaining bubbles by removing 99% of the gaseous inclusions.

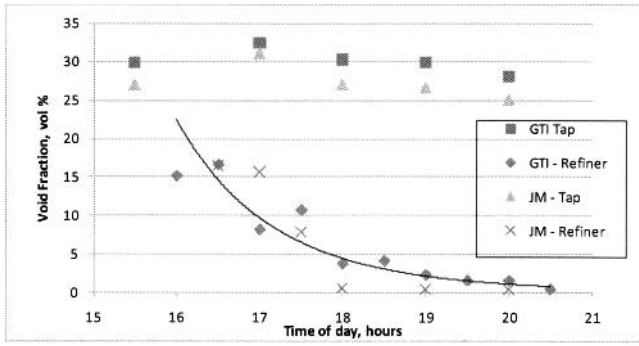

Figure 3. Test SCM-R-2 Tap Glass and Refiner Glass Void Fractions, SCM at 1425°C, Refiner at 1355°C, Pull Rate 175-450 kg/h (Samples Measured Independently by GTI and JM)

The relationship between void fraction in refined glass and residence time in the conditioning channel is shown in Figure 4 for samples collected during both tests. Residence times were shorter in the first test and were longer, covering a wider residence time range, in the second test. All samples were measured for void fraction independently by GTI and Johns Manville chemists. Glass samples from the two tests present the same pattern of reduced void fraction with increased residence time. A short relative residence time period produced a reduction in void fraction to 16%, a removal of inclusions of around 45%. By increasing the residence time, the void fraction decreased. A relative residence time of 3.5 times the initial short residence time produced glass with gaseous inclusions reduced to as low as 0.3%, a removal equivalent to 99% of the SCM glass voids.

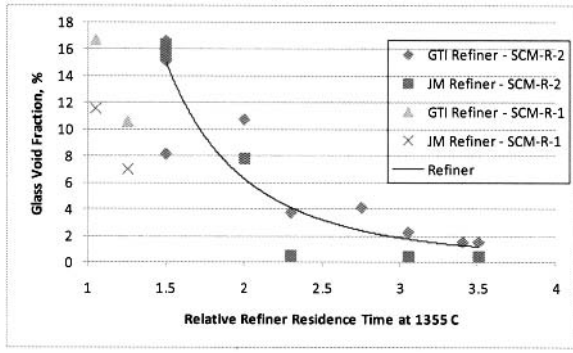

Figure 4. Refiner Glass Void Fractions From Two Tests, Samples With SCM at 1425°C, Refiner at 1355°C, Pull Rate 175-600 kg/h (Samples Measured Independently by GTI and JM)

Inclusions in SCM glass have been found to range from microns to as large as 2 cm. Centimeter sized bubbles are not common, but many bubbles are in the range of 10 mm. to 1 cm. Figure 5(a) provides a close-up view of SCM glass with no refining. The bubbles are uniformly dispersed throughout the glass, and relatively large bubbles can be easily identified.

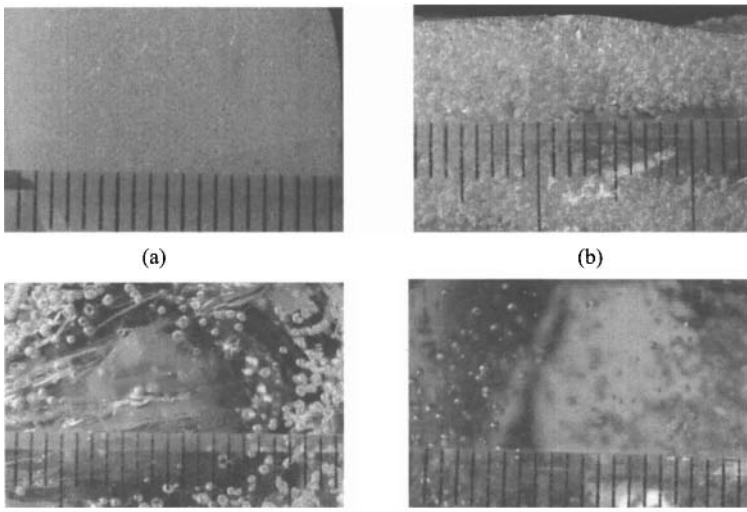

Figure 5. SCM-R-2 Glass (a) SCM Tap (29% voids) and With Relative Refining Residence Times of (b) 1.5 (16% voids), (c) 2 (11% voids), and (d) 3 (<1% voids) – 1 mm Line Spacing

The other photographs in Figure 5 show examples of the level of refining achieved with various refining time periods. With extended refining times the number of inclusions clearly decreased. The longest relative refining time of 3.5 produced isolated bubbles in the glass matrix. Viewing the photographs as a set shows that the average bubble size increases with additional refining time. This is speculated to be the result of bubble coalescence as larger bubbles rise the fastest and merge with smaller bubbles. An advantage of this process is that bubbles will rise more quickly as they merge and become larger, therefore reducing overall refining time.

As higher levels of refining are reached in future tests, different means will be needed to collect samples. Hand sampling with graphite molds will add bubbles to the molten glass. At high refining levels, this will impact the quality of the product glass.

SUMMARY

The short residence time refining step has proven capable of removing 99% of the bubbles in SCM glass. This level of refining may be sufficient for certain market segments such as wool insulation and large diameter continuous fibers. However, most glass applications require much higher quality. Glass ready for forming into fine continuous fibers, containers, tableware, flat glass, and other items requires gaseous inclusion levels from a thousand to a million times better than has been achieved to date. Short residence time refining is anticipated to able to achieve at least a further ten-fold improvement in quality with careful control, but higher quality levels will require a different or supplemental refining approach.

Future work with the SCM technology will focus on more detailed study and testing of short residence time refining. Variables to be explored include melt depth, refiner residence time, temperature, and conditioning channel introduction and removal methods. Other work will consider further refining of SCM glass by new methods. These methods may be on the list of those described above or may be wholly new to the glass industry but well adapted to SCM glass.

REFERENCES

1. Rue, D., Wagner, J., Aronchik, A., "Recent Developments in Submerged Combustion Melting", 67th Glass Problems Conference, Oct. 2006.
2. Shelby J., *Introduction to Glass Science and Technology*, 2nd ed., p. 42, Roy. Scty., of Chem., 2005.
3. Ross, C.P., Tincher, G., Glass Melting Technology: A Technical and Economic Assessment, GMIC, at www.gmic.org, Oct. 2004.
4. Beerkens, R., "Analysis of Elementary Process Steps in Glass Melting Tanks", Ceramics – Silikaty, 52(4), 2008, p. 206-17.
5. Pecoraro, G., Shelestak, L., Cooper, J., "Vacuum Refining of Glassy Materials With Selected Water Content", U.S. Pat. 4,919,700, 1989.
6. Demarest, H., "Method of and Apparatus for Removal of Gas Inclusions From a Molten Glass Pool", U.S. Pat. 4,406,683, 1983.
7. Berson, X., Vivet, A., Bertrand, E., "Microwave Refining and Melting Furnace", U.S. Pat. 5,597,504, 1997.
8. Kobayashi, H., Beerkens, R., "Water Enhanced Fining Process A Method to Reduce Toxic Emissions From Glass Melting Furnaces", U.S. Pat. 5,922,097, 1999.
9. Buehl, W., "Method of Fining Glass", U.S. Pat. 3,622,296, 1971.
10. Richards, R., "Glass Melting Method", U.S. Pat. 5,573,564, 1996.
11. Spinosa, E., Ensminger, D., "Removing Inclusions", U.S. Pat. 4,316,734, 1982.

This Page Intentionally Left Blank

MODELING THE QUALITY OF GLASS MELTING PROCESSES

Adriaan Lankhorst[1], Andries Habraken,
Mathi Rongen, Philip Simons and Ruud Beerkens[2]

TNO Glass Group, Eindhoven, the Netherlands

INTRODUCTION

For a regenerative TV-panel furnace as an example, the effect of changes in combustion firing profile on glass quality has been investigated for two different pull rates and two different cullet fractions. This has been done by simulation of the temperatures, heat transfer, flow patterns and elementary processes in the complete furnace, which includes melting tank, melter combustion space with port necks and burners, doghouse and throat. As the reliability of the predicted glass melt quality indicator values very much depends on the accuracy and the details of the predicted glass melt flows and temperature levels, the glass depth temperature profiles on various locations are validated against actual measured temperature profiles in the existing furnace, at two process settings.

Glass quality parameters have been determined by statistical analysis of simulated trajectories of 50.000 particles that are released in the batch chargers, as well as for bubbles starting from different sources. The rate of growth and shrinkage of bubbles has been determined from relations describing the physical fining process. These derived glass quality parameters from modeling are correlated to actual glass defect production data – in terms of number of bubbles per ton of glass – found at two process settings.

The simulation study is defined as Round Robin Test 5 (RRT5) by Technical Committee 21 (TC21) of the International Commission on Glass (ICG); TC21 is the ICG committee for Modeling of Melting Processes. Furnace geometry, process settings and validation data (measured data from furnace during its operation) are included in the RRT5 case definition.

The case study and parameter variation study has been carried out by use of GTM-X, a computer program for Computational Fluid Dynamics (CFD) owned, developed and licensed by TNO Glass Group.

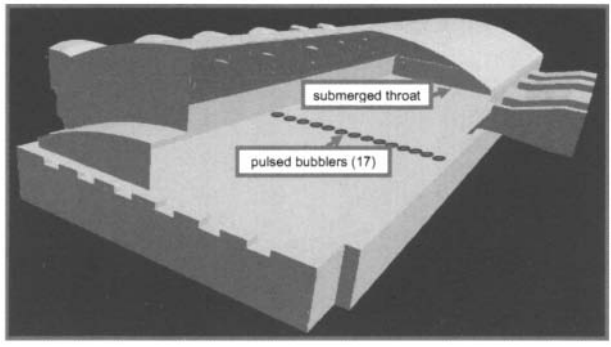

Figure 1. Geometry of melt tank and combustion space, with 2x6 ports.

Besides above-mentioned validation results of temperature profiles and glass quality, by mathematical modeling it is also possible to study the effects of process settings on soot formation, NO_x emission levels, specific energy consumption, NaOH evaporation rates or NaOH concentrations in the combustion atmosphere, together with the risk of carry-over, depletion and refractory corrosion.

DESCRIPTION OF THE ROUND ROBIN TEST 5

In the RRT5 of the ICG TC21, process settings and measurement data are used that apply to the operation of a TV-panel furnace that existed in Europe. The glass melt depth in the tank is 1.07 m, the melter length is 21.9 m and the furnace width is 7.3 m. Fig. 1 shows an overview of the furnace geometry.

Both in April 2002 and in March 2004, the operating conditions, temperature depth profiles, flue gas temperatures and glass defect data were recorded. Together with the furnace geometry and material properties (properties of combustion gas, batch, glass and refractory) this served as a basis to validate GTM-X. Important properties are heat conductivity, viscosity, thermal expansion, chemistry, surface tension, heat capacity, chemical activities and so forth, most of them are temperature dependent.

Table 1 shows the operating conditions that have been different between the two periods, which were firing rates, cullet fractions and pull. Other settings, like bubbling rates, were identical in 2002 and 2004. Only the burners of the first 4 out of 6 ports are actually firing in both cases. The last two ports operate with just pre-heated air flow; only estimates are available for the air flow rates through these ports.

		April 2002	**March 2004**	
Air preheat temp.	port #1	1172	1191	°C
	port #2	1219	1229	°C
	port #3	1205	1228	°C
	port #4	1171	1218	°C
	port #5	1018	1030	°C
	port #6	750	765	°C
Air excess		13 - 14	13 - 14	%
Nat. gas inlet temp.		30	30	°C
Natural gas amounts	port #1	451	561	Nm^3/hr
	port #2	351	353	Nm^3/hr
	port #3	434	425	Nm^3/hr
	port #4	434	471	Nm^3/hr
	port #5	0	0	Nm^3/hr
	port #6	0	0	Nm^3/hr
Total gas amount		1670	1810	Nm^3/hr
Net Calorific value gas		37.5228	37.5228	MJ/Nm^3
Cullet fraction		65	42.5	Mass % on glass basis
Pull		220	236	Metric tons/day

Table 1. Settings for firing rates, cullet fraction and pull (Nm^3 at 0°C and 1013 mbar).

In order to compensate for the increased pull and decreased cullet fraction (compared to 2002 settings) the firing rate on especially port #1 has been increased in 2004. This results in a batch blanket with approximately the same length as in 2002, preventing batch blanket

material to cross the bubbling line (forced bubbling is applied at x = 8.76 m from the back wall). The total firing rate was increased with about 8% in March 2004 as compared to April 2002. With a glass melt surface area (excl. doghouse) of 160 m^2, the specific pulls were resp. 1.38 and 1.48 metric tons/m^2/day, where a typical specific pull for a TV-panel (CRT) furnaces is 1.35 – 1.45 metric tons/m^2/day.

MATHEMATICAL MODELING WITH GTM-X

GTM-X is an industrially validated CFD program, developed and owned by the TNO Glass Group, which is used for and by the international glass industry [1][6]. CFD models define and solve conservation laws in order to calculate for instance fluid or gas velocities, temperatures and electrical voltages. For this, the space of interest is divided into small cells (volume elements) that form the grid. In each cell, conservation of basic quantities such as mass, momentum, energy or electric charge is demanded; this leads to a very large number of coupled equations (typically in the order of millions) that are solved by the program.

GTM-X is able to use grids that align with skew parts of the geometry (body-fitted), and cells can be divided in smaller sub-cells in regions where this is needed, while cells can remain larger in regions where this can be afforded (local grid refinement). This can reduce the total number of grid cells that are necessary to obtain an accurate solution. Also, GTM-X can use multiple processors to work on the same job (parallelisation), and it deals efficiently with physical phenomena that are not the same in all regions of the calculation domain (multi-physics), such as turbulence that is restricted to the combustion space, and electrical boosting that is restricted to the glass melt. These features reduce the turn-around simulation time, as compared to conventional CFD programs, significantly. The model can calculate for steady state conditions (if things do not change with time), or dynamic conditions/time transient circumstances, for instance during pull or glass colour changes.

A wide range of glass melt-dedicated sub-models is available, e.g. describing batch melting and conversion, electrical boosting [4], foam formation, mechanical stirring and forced bubbling. The main CFD model is linked to these sub-models and vice versa. Special models describe evaporation of volatile components (e.g. boron, sodium, lead, potassium species) from the glass melt, resulting in depletion of glass and risk for corrosion of superstructure (e.g. silica crown) refractory and dust emissions [8]. Glass melt level height and drawdown in forehearths can be determined as well with specific sub-models available.

For the combustion space, sub-models for turbulence, combustion of natural gas and fuel-oil with air and/or oxygen, with soot formation/oxidation and CO formation, and NO_x formation are available. Radiation heat transfer can be included in the domain of the glass melt (instead of Rosseland, effective conductivity approaches) as well as in the combustion space [5].

When the flow patterns and temperatures in all positions of a furnace have been calculated, glass quality parameters can be determined by the application of an accurate and fast so-called particle trace model. In fact particles are followed along their trajectories from doghouse to melter exit. Such particles represent just a small volume of melt, a bubble, sand grain or cord. When the particle has other properties than its direct environment, this has to be taken into account (e.g. a bubble has a different density compared to the surrounding melt and will experience buoyancy). By statistical analysis of the trajectories of many "particles" (in the order of 10^5- 10^6), residence time distributions, the minimum residence time and quality indices for melting, fining, temperature and homogeneity are obtained. In addition, it is possible to focus on the dissolution of sand grains or stones [9][10], and the growth and shrinkage of blisters [11][12], in order to localize the (potential) origin of defects or to study the effectiveness of the fining process to eliminate seeds coming from a certain source of these small bubbles.

All this makes GTM-X a practical tool that is used for realistic industrial cases like complete glass melting furnaces, forehearths and tin chambers of float furnaces. As sub-models are available for kinetic reactions and Chemical Vapour Deposition (CVD) processes, e.g. for tin oxide coatings on glass [7], GTM-X is also applied for coating systems. The tool is used for

trouble shooting, optimization of process settings and for design issues. Furthermore, GTM-X is a main component of TNO's online rigorous Model-based Predictive Control (rMPC) application [2][3].

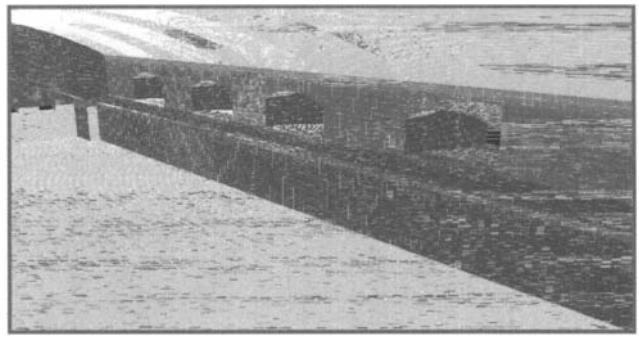

Figure 2. Inside view of the grid showing the local grid refinement at each port.

For the RRT5 a grid was used that consisted of 400,000 cells for the melt, 800,000 cells for the combustion space and 65,000 cells for the 3D refractories. Local grid refinement was used in the glass melt space near the bubbler row, where high velocity gradients occur, and in the combustion space between all opposite ports, surrounding the flames, see fig. 2. The switch in firing direction of this regenerative furnace took place every 20 minutes. Such a switch causes a transient, periodic behaviour of gas and glass melt flows and temperatures. This effect is large in the combustion space, but small in the glass melt, because of the long reaction times of the viscous glass flow and the large quantity of glass with a high heat capacity. In the calculation we choose an arbitrary, fixed firing direction, and average the exchange of heat fluxes and temperatures between combustion space and melt over 2 x 20 minutes total firing cycle; this allows for a steady calculation.

VALIDATION OF PREDICTED TEMPERATURES

In this paper, we focus on the validation of the simulation results for the March 2004 case. On 7 different locations on the centre line of the glass melt (and batch blanket), temperature depth profiles have been measured by lowering and submerging a water-cooled lance through crown thermocouple openings and moving the TC tip into the batch blanket or through the glass melt surface from the top.

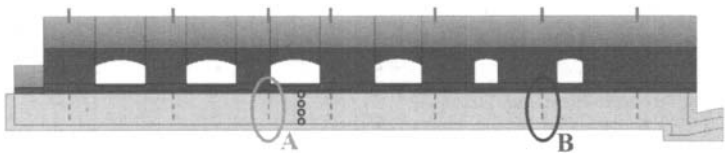

Figure 3. Measurement locations A and B.

For 2 of those lines (locations A and B, see fig. 3), the measured and calculated glass temperature profiles for March 2004 are plotted in fig. 4 and fig. 5.

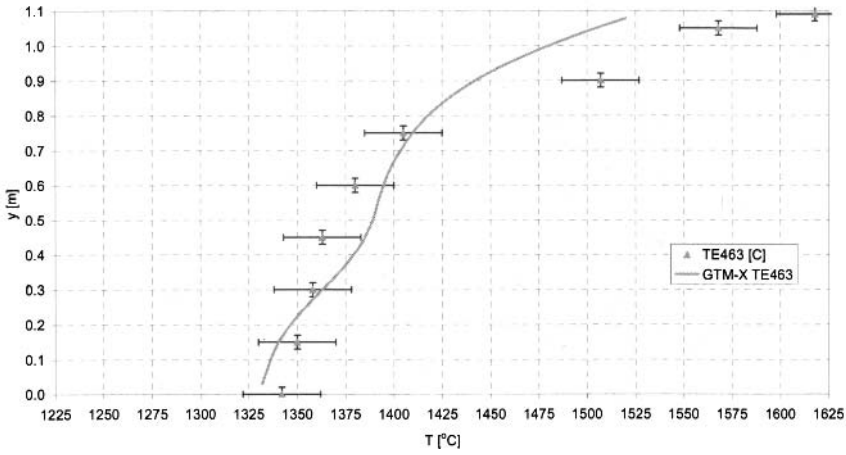

Figure 4. Measured (triangles) and calculated (line) temperatures on vertical line A. y = 0 is the tank bottom, y = 1.07 m is the melt surface.

In general, the agreement between calculated and measured temperatures is good. On most locations the differences are within the temperature and exact position measurement errors. Location A is just before the bubbler row, and the glass surface temperatures are somewhat underestimated by the model. Yet it is believed that the peak temperature in the measurement (1620 °C) can not be a glass melt temperature, but must be the temperature in the combustion space (probably the thermocouple was just outside the melt).

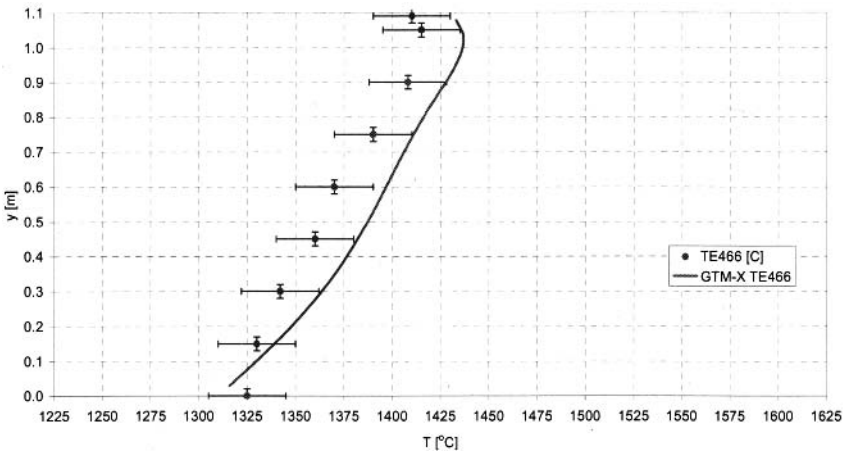

Figure 5. Measured (dots) and calculated (line) temperatures on line B.

On location B, the glass surface cooling effect by the non-fired ports is properly predicted by GTM-X, as is seen from the reversed temperature gradient in the top 10 cm of the glass.

Validation of temperatures in the combustion space is done by looking at

- flue gas temperatures in the 6 downstream ports (fig. 6)
- temperatures at the crown surface, in the 7 crown thermocouple openings (fig. 7)

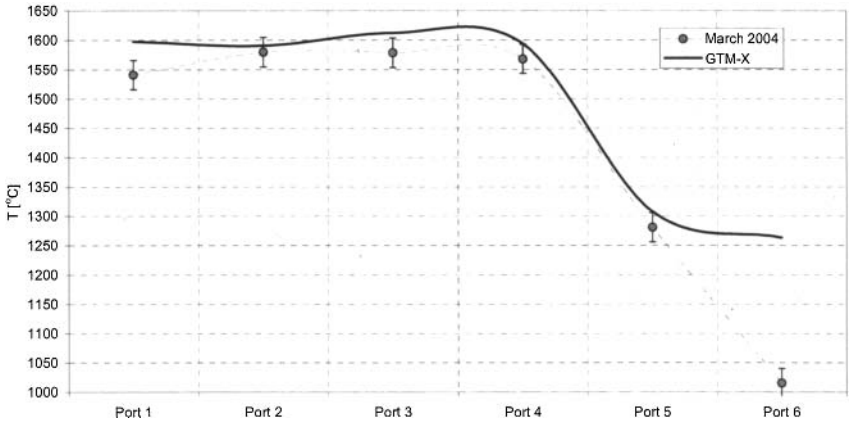

Figure 6. Measured (dots) and calculated (line) flue gas temperatures. Measurements by suction pyrometer.

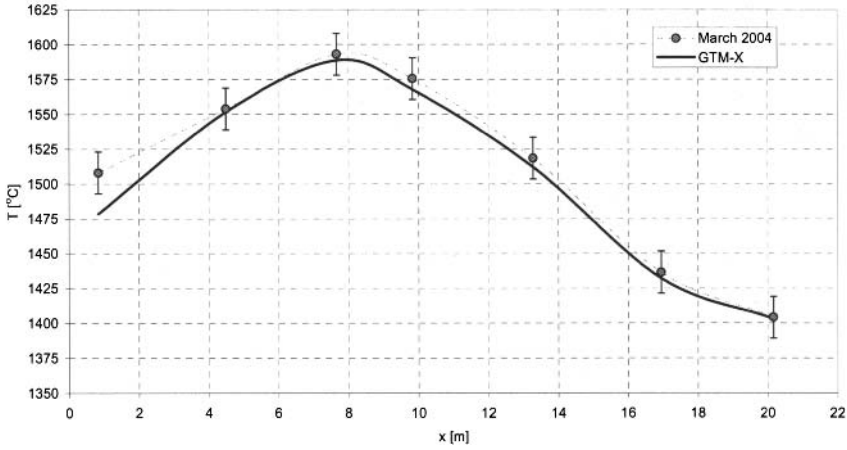

Figure 7. Measured (dots) and calculated (line) crown temperatures. Crown thermocouples exposed directly to the combustion space.

Both flue gas temperatures and crown temperatures are very well predicted by the model, and generally within the measurement errors. Only the flue gas temperature on the last (non-fired) port is strongly over-predicted by ~ 200 °C. This may indicate that the actual air flow rates on

port #5 and port #6 are higher than the estimated values that are supplied by the glass manufacturer.

GLASS QUALITY VALIDATION

Glass defect data are available in the form of the number of bubbles per metric ton of glass production, found after forming of the panels by pressing machines, that caused product rejection during both furnace campaigns, see fig. 8. The reject criterion for bubbles was 0.4 mm.

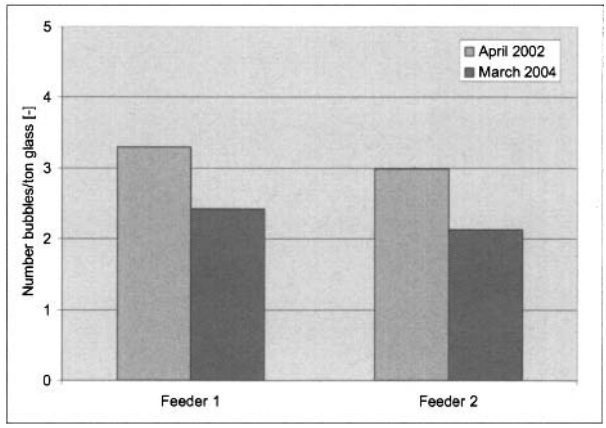

Figure 8. Number of bubbles that caused product rejection (bubbles > 0.4 mm).

It can be seen that there were extremely low defect levels, both at the 2002 and 2004 process conditions: only 2 – 3 bubbles/metric ton glass panels. In March 2004, the glass defect level reduced by ~ 25% as compared to April 2002. Over a period of a few months, many (> 1000) gas content bubble analyses for this panel furnace were performed by mass spectrometry. On the basis of analysis of the measured CO_2 content versus the ratio of Ar and N_2, the most likely location of origin (source) of the bubbles can be deduced. From these measurements, a detailed statistical analysis was performed by the TV panel glass manufacturer and the conclusion was made that around 35% of the bubbles originated from sources in the two feeders, and 60% originated from the melting tank (the remaining 5% had other sources). From the melting tank bubbles, 90% was believed to be caused by glass melt-tank refractory interaction (typical bubble compositions with 10-40% CO_2) and only 10% originated from batch melting (resulting in a high CO_2 content in the bubble; typical bubble compositions with 50-80% CO_2).

The applied side-wall refractory materials are fused cast AZS types from doghouse area till the bubbler row, and High density zirconia (HZ) downstream of the bubbler row. Bubbles are primarily released at the fused AZS-glass interface (due to the aluminosilicate-rich phases with some other components in it in AZS) and virtually no seeds are formed at HZ-glass interface. Therefore, to estimate the glass quality with the support of the CFD tool GTM-X, 50,000 bubbles have been traced with an initial diameter of 200 μm and with starting positions on the fused cast AZS-glass interface before the bubbler row. The trajectories in the glass obtained were statistically analysed, see table 2.

	April 2002	March 2004
% bubbles that arrived in throat	0.91	0.66
% bubbles escaped through glass surface melting tank	99.1	99.3

Table 2. Bubble trace results.

The results demonstrate that only a small number of bubbles end up in the product and that this number of bubbles is also lower in 2004 than in 2002. This corresponds qualitatively to the measurements. The calculated flow fields of 2002 and 2004 were very similar. But along the glass melt surface there is a stronger back-flow in March 2004, preventing slippage of bubbles in the direction of the throat.

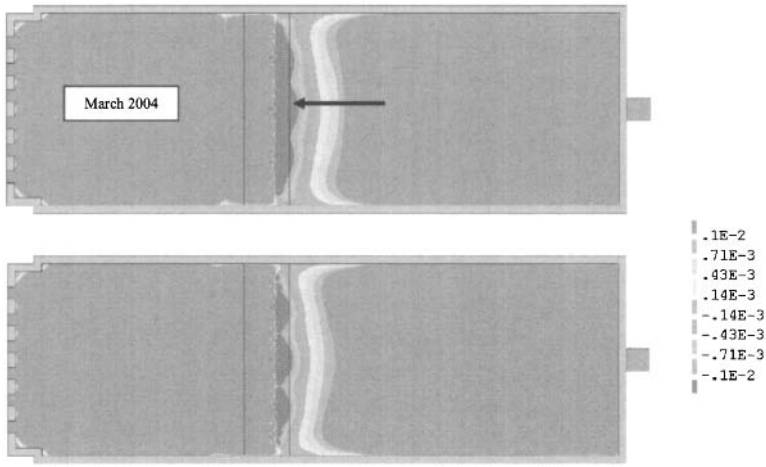

Figure 9. Forward flow distribution on glass surface (m/s).

FURNACE ANALYSIS

Based on the simulations, the performance of the furnace can be analyzed on various different aspects important for quality, production costs and lifetime or environmental performance (CO2, NOx, dust emissions). One can look at the major energy flows, and set up a global energy balance, but it is also possible to investigate some features in detail. Besides above-mentioned validation results of temperature profiles and glass quality, the effects of process settings on soot formation, NO_x emission levels, specific energy consumption and NaOH evaporation, together with the level of risk of carry-over, depletion of melt at the surface by evaporation processes and refractory corrosion can be studied as well.

As this is beyond the scope of this paper to present a detailed overview, only as an example the oxygen mass fraction on a horizontal plane through the burner nozzles is shown in fig. 10. The figure shows typical oxygen levels of the order of 2-4% in the exhaust ports opposite the firing ports. The exhaust ports opposite the non-fired inlet ports contain almost completely air, although some cross-over between port #4 and port #5 is observed.

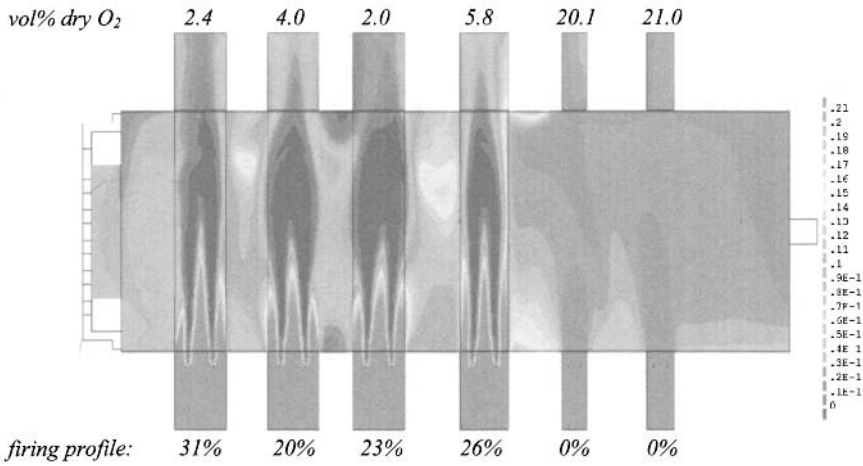

Figure 10. O_2 mass fraction distribution in plane through burner nozzles (-).

CONCLUSIONS

In this paper we have shown a successful validation of the simulation of an existing CRT TV panel glass furnace by using a CFD program: GTM-X. Temperature depth profiles in the glass, the crown temperature profile and flue gas temperatures that were calculated matched the measured values quite well; differences were within the measurement error ranges or could be attributed to unknown process conditions. The estimations of the bubble contents in the product for the settings of April 2002 and March 2004, using advanced particle tracing in GTM-X, matched the reported defect levels qualitatively. Modeling studies, like the one discussed in this paper, are a powerful means to investigate possibilities to improve glass quality and to reduce furnace energy consumption by changing process settings.

REFERENCES

[1] P. Simons, A. Twerda, R. Verweij, J. Wang, F. Simonis, A. Lankhorst, B. Paarhuis: X-stream: the most comprehensive glass furnace simulation tool. In: Glass Odyssey, 6th ESG Conference, Montpellier, July 2-6 2002

[2] J. Reijers, L. Huisman, A. Lankhorst: On-line Rigorous Model-based predictive control (RMPC) systems based on GTM-X simulation software. In: Proc. 10th International Seminar on Furnace Design - Operation & Process Simulation, June 16 - 19 2009, Velke Karlovice, Czech Republic

[3] Leo Huisman: Control of glass melting processes based on reduced CFD models (PhD thesis), Eindhoven, 2005

[4] P. Simons, K. Jochem, K. Aiuchi: A power consistent mathematical formulation for Joulean heat release, Glass Technol.: Eur. J. Glass Sci. Technol. A, June 2008, 49(3)

[5] Lankhorst, A.M., Faber, A.J.: Spectral Radiation Model for Simulation of Heat Transfer in Glass Melts, Glass Technol., Eur. J. Glass Sci. Technol. A, April 2008, 49(2), 73-82

[6] Adriaan Lankhorst, Luuk Thielen, Andries Habraken, Philip Simons, Dries Hegen: Modeling of Glass Melting Processes, Keynote paper at DGG Tagung - Glass Trend Workshop GLASS MELTING, 20/21 May 2008, Hameln, Germany

[7] Adriaan Lankhorst, Philip Simons, Karel Spee: Modeling of APCVD of tin oxide on float glass, 7th International Conference on Coatings on Glass and Plastics, June 15th-19th 2008, Eindhoven, The Netherlands

[8] A.J. Faber, R.G.C. Beerkens: Reduction of refractory corrosion in oxy-fuel glass furnaces, Proc. 18th Int. Congress on Glass, July 5-10, 1998, San Francisco (Am. Ceram. Soc., Westerville, OH 1998)

[9] M.K. Choudhary: The effect of free convection on the dissolution of a spherical particle in a viscous melt, Glass Technol. 29(3), 100-102 (1988)
[10] M.K. Choudhary: Dissolution of polydisperse silica grains in glass melt analysis, J. Am. Ceram. Soc. 73(10), 3053-3058 (1990)
[11] L. Nemeç: The behaviour of bubbles in glass melts. Part 1. Bubble size controlled by diffusion and chemical reaction, Glass Technol. 21(3), 134-138 (1980)
[12] F. Krämer: Mathematisches Modell der Veränderung von Glasblasen in Glasschmelzen, Glastechn. Ber. 52(2), 43-50 (1979)

PROCESS OPTIMIZATION OF THE GLASS FORMING PROCESS BY ADVANCED 3D FORMING MODELS

Erik Muijsenberg
Glass Service BV
Maastricht, The Netherlands

ABSTRACT

Production of glass bottles requires blowing of the glass after entrance of a gob of molten glass in the blank mould. The final shape of the bottle is highly dependent on the viscosity of the glass, the blow-pressure and the temperature distribution in the glass and the mould and simulation of this complicated process enables optimization of the process conditions. During simulation of blowing of the glass, the mesh has to be adapted due to the extreme deformations of the mesh. Using the existing ALE-technique for this kind of applications requires a lot of user-intervention and trial-and-error to create a mesh that suits both the initial and final topology of the glass. To reduce the user-time and to be able to run this kind of analyses automatically based on an arbitrary base-geometry, a completely automated remeshing/rezoning procedure is set-up. In this procedure the A/Explicit analysis is divided in a number of sub-analyses after each of which a new (3D) geometry of the glass is created based on the deformed mesh (using Galileo+CAE). Using a map-routine the solution from the previous analysis is mapped on the new mesh such that continuation of results is ensured. Using the automated remeshing capability, simulations of the glass bottle forming process have successfully been performed, enabling for example optimization of process settings. Due to the generic set-up of the remeshing procedure it can easily be used for other simulations that require adaptive meshing as well.

1. INTRODUCTION

Current container glass manufacturing is mainly driven by experience and craftsmanship rather than scientific knowledge. There is a lack of understanding of the complex glass forming process as well as of the application of (scientific) knowledge and tools. Troubleshooting at the design and production stages is based on experience and new container designs are introduced by trial and error. The trial & error stage is usually repeated several times over and can last several months. These stages are very expensive, as tests can only be carried out in a live production environment. Market demand however no longer allows for lengthy trial & error periods.

The glass industry is now forced to combine ever more physically complex designs with extremely tight production and delivery times. In order to meet these delivery times, insight into the process prior to the actual production phase is required. So a general approach is required for setting up analyses for glass forming processes.

1.1 The blow-blow process

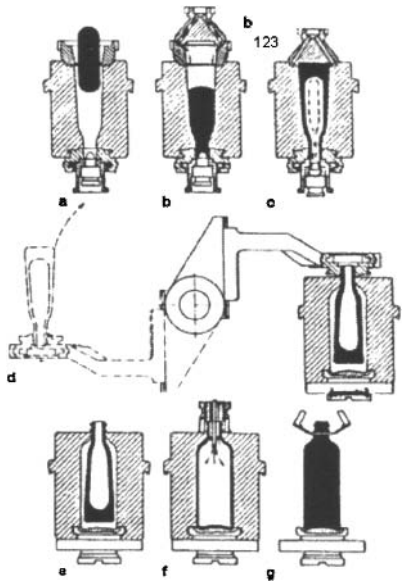

Figure 1. The blow-blow process.

The glass forming process that is studied in this paper is the blow-blow process as depicted in Figure 1. The total process consists of several stages among which are two forming stages which both incorporate a blowing of the glass. A gob of glass enters the first mold in step 'a'. The gob moves down in the tools and the neck is attached by a settle blow. After the proper creation of the neck, in step 'c' the first forming blow is performed, which is called the counterblow. This step induces a severe deformation of the glass. The product after the initial blow is called the parison. The parison is rotated in step 'd' into the final mold, held for some time in step 'e' to let it sag, and then in step 'f' it undergoes the final blow to attain the desired shape. The deformation in this step is less severe than that in the counterblow, but still the wall thickness can change significantly.

1.2 Organization

After this introduction, a short discussion on different remeshing strategies is discussed in Section 2. From this it can be seen that due to the radical geometry changes a full remeshing strategy is required. How to perform this remeshing is discussed in Section 3. Next in Section 4 an example is presented. Finally in Section 5, some conclusions are drawn.

2. REMESHING

Glass forming has not been done that often with a Finite Element Approach (FEM), since the material behavior lies somewhere between a fluid, which is the domain of Computational Fluid Dynamics (CFD) and a solid, which is the domain of FEM. The reason the glass industry has kept with the trial & error approach for so long is that there is no clear direct application of either technology to successfully simulate the glass forming problem.

The difficulty lies in the material behavior of the glass. It is feasible to do some forming of the glass as long as the deformation that occurs during the forming is not too drastic. Hence, a final blow of a parison to a bottle might be possible, making use of an adaptive remeshing technique. The counterblow from a gob to an initial shape however, incurs extreme deformation of the glass material. As a result the underlying mesh of the FEM solver will also distort severely, so much so that the original mesh topology can no longer represent the final shape.

2.1 Remeshing techniques

During the forming of the glass product, the deformation of the material is severe. This is because at high temperatures the glass behaves as a viscous fluid. Moreover, the geometry change that the gob needs to undergo is huge. The surface area will increase by a factor of 2 whereas the volume will remain the same. You can see this difference from studying phase 2 of the blow-blow process with phase 5, which are the respective start and end point. Thus, it is difficult for a given mesh topology to represent the two extremely differing geometries. A topology specifies how things are connected together logically: it does not consider shape. So if you take a sphere, and flatten it out to an ellipsoid they will have the same topology, but a different geometry. If however you take a sphere and a donut, these two objects also have a different topology: the sphere has no hole.

If we now would compare two meshes on two different geometries, and if you would be able to make a labeling on the nodes and elements, such that if element A shares a face with element B in both the first as well the second mesh for arbitrary A & B, then the two meshes have the same topology.

Based on this consideration, we can consider two types of remeshing algorithms: remeshing algorithms which retain the original mesh topology and those that do not. Galileo+ contains an implementation of the first technique in the form of ALE within the solvers. ALE stands for Arbitrary Lagrangian Eulerian. In the ALE algorithm, the mesh initially follows the motion of the material points. Then at a certain point in time, the mesh motion is decoupled from the material motion to optimize the element shape. The solution is then mapped using an advection scheme, and the analysis is continued. The ALE algorithm thus tries to optimize the original mesh topology onto the new geometry which arose due to deformation. However, as was already discussed before: In glass production the geometry changes in an extreme sense. This in turn means that the original mesh topology will not fit onto the new geometry without having distorted elements. It is for a finite element solver not possible to continue the calculation with distorted elements, and the analysis will thus end prematurely.

From this we can easily conclude that in order to analyze the glass forming problem and other problems that undergo such significant deformations, a full remeshing of the computation domain is to be performed. There is no such algorithm available by default in Galileo+, thus GS implemented a first order technique. To be usable by the typical design engineer working in the glass market, it also needs to be robust and fully automated.

Since it needs to be possible to mesh arbitrary geometries during the remeshing step, the model is set-up using modified formulation quadratic tetrahedral elements with both displacement and thermal

degrees of freedom. So that the glass will not exhibit volumetric locking, nor should it have problems with contact. Both temperature and displacement are required, since the viscosity of the glass changes strongly with temperature, and the temperature changes strongly if the glass touches the mold anywhere.

2.2 Remeshing simulation strategy

The counterblow and finalblow analyses will be set up using the following strategy:

1. A number of subjobs are chosen for the total analysis, let us say *n*, this will divide the total analysis history into *n* distinct jobs, which taken together form the complete job.
2. After each subjob, the quality of the mesh is checked. On the quadratic tetrahedral elements the face corner angle is checked as well as line angle on the midside edge nodes.
3. If the element quality is still ok, the next subjob is a restart of the current subjob.
4. If the element quality is poor, the analysis needs to be remeshed. The next subjob needs to have its solution then mapped as well.
5. Once all the subjobs are finished, the results need to be visualized in an easy way, so the results will need to be combined.

As can be seen there are already several ingredients here that need to be developed without even considering the remeshing yet:

- A driver script is required that runs the subjobs in sequence and decides what to do.
- An element check routine is necessary
- A remeshing routine is necessary
- A solution mapping scheme is necessary, since there is no equivalent *MAP SOLUTION capability in Galileo+.
- A script which performs similar the restartJoin script in Galileo+ is necessary, but this time based on remeshed instances.

All this has been implemented, and the discussion continues with how the remeshing itself is performed.

3. REMESHING USING GALILEO+/CAE

In order not to have to write a complete mesher and having to do the model set-up again in a different package, as much as possible of the technology in CAE that was available is re-used. This means that the model is kept, and all that is done is to replace the instance in the original model with the remeshed one. As soon as that is done, the new input file can be written out. In order to make the exchange of the old part with the new part as smooth as possible, the CAE model is required to be setup using only sets

and surfaces. Hence, the user should not pick anything in the viewport, but instead define all sets and surfaces on the part level. Everything in CAE is then referred to by name, and exchanging one part-instance with another having exactly the same sets and surfaces is then seamless.

The only issue to be solved is how to remesh the instance in the analysis. Moreover, the user should not have to define the sets and surfaces after every remesh increment, since this would be cumbersome; rather the sets and surfaces ought to be recreated from the deformed mesh piece. The remeshing strategy is thus as follows:

1. From the outside of the mesh a new geometry is created.
2. Using the original and the deformed mesh, along with the initial geometry of the instance with the mesh on it, all the topology regions are re-identified.
3. Using this topology map, the sets and surfaces can be reconstructed.
4. Finally the instance is replaced in the model, all boundary conditions are adapted to account for the time passed, amplitudes are fixed up, and the analysis is written out.

The total bookkeeping to get all this done is very complex, but quite efficiently automated. An application example is presented next.

4. EXAMPLE OF SIMULATING A BLOW-BLOW PROCESS

The automated remeshing capability as explained in the previous section has successfully been used in several bottle forming analyses. In this section an example of the Italian company 'Bormioli Luigi', known for it's manufacturing of glass containers for the perfumery and cosmetics industry, is presented.

Pictures of the final shape of the bottle of consideration are shown in Figure 2. From Figure 2, the complexity of the shape of the bottle and the variations in glass wall thickness are clearly visible.

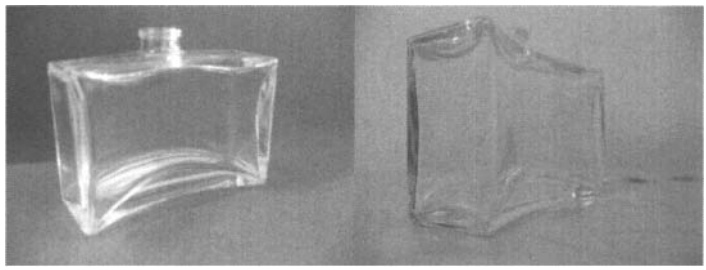

Figure 2. Pictures of final bottle

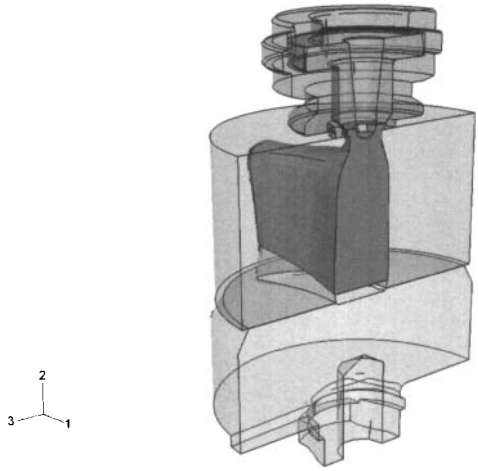

Figure 3. Shape of the gob in cavity of the tools

For a typical bottle, half of the assembly of the tools and the gob of glass prior to blowing is depicted in Figure 3. The translucent parts are the tools from which the shape of the cavity that has to be filled with glass becomes clear. The small spherical face on top of the gob is the face on which the blow-pressure is applied and because of the 'sticking' behavior of hot glass, contact between glass and tools is modeled as a no-separation contact with rough friction properties. Due to the complex geometry and to allow automated remeshing, the gob is meshed with quadratic tet-elements C3D10MT.

Glass at high temperatures is quite a difficult material to use in finite element analyses. The reason for that is quite simple: It behaves as a fluid, with a strong temperature dependent viscosity. The most direct approach to model glass in Galileo+ is to use an equation of state material model (EOS). However, using the glass material parameters in an equation of state material model in Galileo+/Explicit will give very small stable time increments, leading to long computation times. In order to reduce the calculation time, we have regularized the glass material model to a specific elasto-plastic material model such that it still gives accurate results, but also has a much larger stable time increment for the same element size. The actual details of the material model are out of the scope of this paper.

The simulation of the complete blow-blow process as described in paragraph 1.1 is simplified and consists in this example of the following stages:

1. Transient heat transfer analysis (A/Standard) from the moment the gob arrives in the mould till the start of the counterblow. This will result in the temperature distribution necessary for the next stage.
2. Coupled stress-displacement analysis (A/Explicit) of the counterblow. This will result in the shape of the parison and the temperature distribution during the process.
3. Cyclic transient heat transfer analyses (A/Standard) of the complete process to obtain the 'steady-state' temperature distribution in the tools and the glass. Starting with estimated initial temperatures, every subsequent analysis starts with the temperatures from the previous analysis. The complete cycle is assumed to be converged when the temperature distribution in all points during the analysis in two subsequent analyses differs not more than tolerance (in this example 1°).
4. Quasi-static analysis (A/Standard) of the 'elongation' of the parison. This will result in the shape of the glass and the temperature distribution necessary for the last stage.
5. Coupled stress-displacement analysis (A/Explicit) of the finalblow. This will result in the final shape of the bottle and the temperature distribution during the process.

The automated remeshing technique as explained in previous sections is used in the stages 2 and 5, the actual blow-simulations. Figure 4 illustrates one of the remesh operations during the counterblow analysis. The left picture shows the mesh of the gob at a certain moment, while the middle picture shows the same mesh after 4 [ms] of blowing with a pressure of 2 [bar]. Clearly visible is that some elements become too distorted and remeshing is required. The right picture shows the 'new' mesh of the gob after the remesh operation.

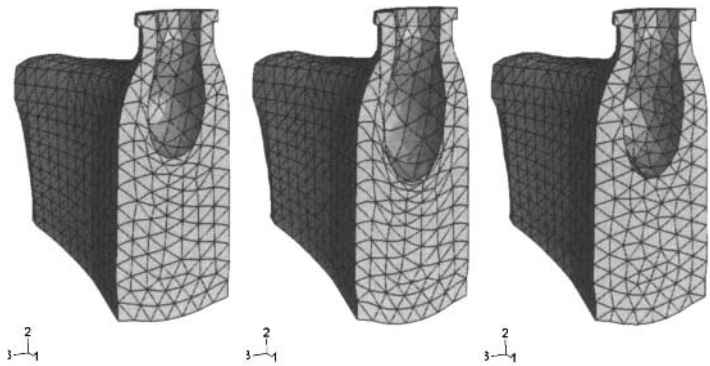

Figure 4. Mesh of the gob prior and after remeshing operation.

From Figure 4 it becomes obvious that without remeshing the analysis will abort quickly due to mesh distortion, even ignoring the effect that prior to the abort the stable time increment will drop drastically because of squeezing of elements. Including remeshing however allows the analysis to proceed easily.

With the specified tolerance on element quality, the complete counterblow analysis finished with 9 remesh-steps after which the cyclic thermal analyses start. The temperature distribution on the final shape of the parison and the tools is shown in Figure 5.

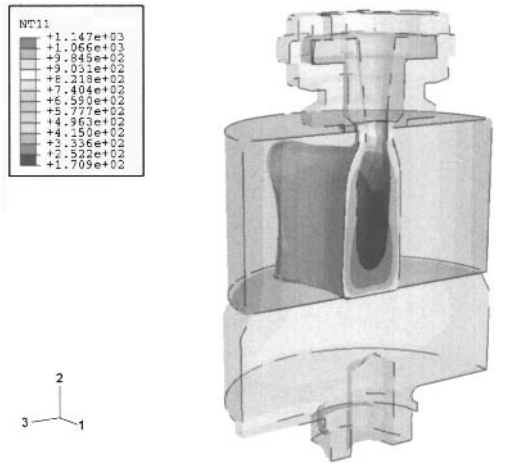

Figure 5. Temperature distribution on final shape of parison and tools.

The temperature distribution on the parison after the counterblow is validated with infra-red measurements on the real product. In Figure 6 these measured temperatures are given together with the results of the simulations. The continuous lines in Figure 6 indicate simulated temperatures after opening of the mould, where the 'path distance' as given on the horizontal axis is measured from the 'neck' to the bottom of the parison. Due to heat-redistribution from the inside of the parison, the temperature at the outside of the parison increases after opening of the mould, which is indicated by the two lines which are obtained at the moment of opening of the mould and some time afterwards. The markers in Figure 6 indicate the measured temperatures which are all in between the two curves and show the same trend over the length of the parison.

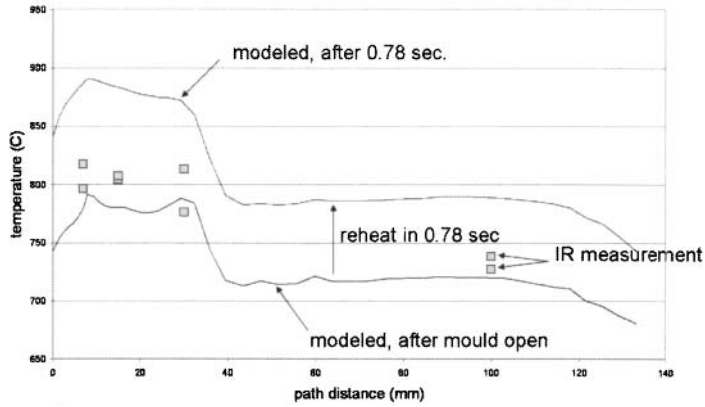

Figure 6. Simulated and measured temperature distribution on the parison after opening of the mould.

The final shape of the bottle is obtained in the last stage of the simulation sequence, the 'finalblow'. The cut-plot in Figure 7 shows the shape of the parison just before the start of the finalblow and the final shape of the bottle in the cavity of the final mold.

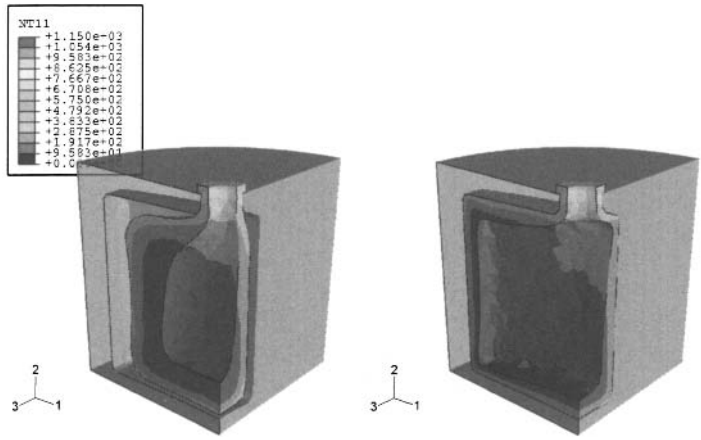

Figure 7. Shape of parison just before and after finalblow.

The need for remeshing becomes apparent again from Figure 7 although the deformation is less severe compared to the counterblow analysis. The finalblow analysis finished with 4 remesh steps and in Figure 8 finally the shape of the glass is displayed at different stages during the bottle forming process.

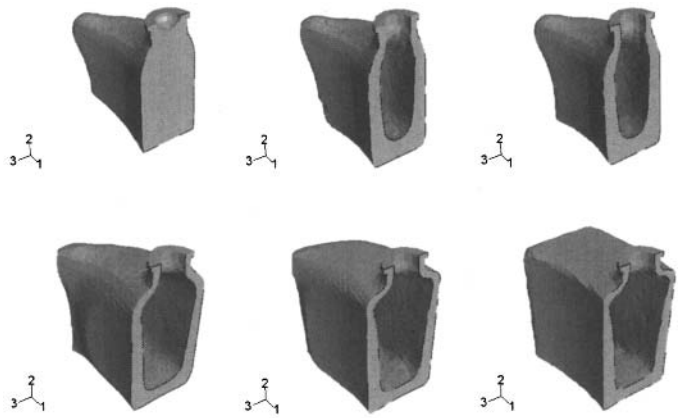

Figure 8. Shape of glass at different stages of the bottle forming process.

The complete analysis sequence took about 15 hours on an ordinary laptop using GALILEO+ V6.6. Being able to perform this kind of analyses without user-intervention now allows next steps to be taken such as optimization of the glass wall thickness distribution by modifying process conditions.

5. CONCLUSIONS

From the example we can see that even though the (Lagrangian) finite element method is not really laid out for the enormous deformations that occur during glass forming, it is still possible to simulate it using advanced remeshing techniques. The remeshing technique fully exploits the capabilities of Galileo+/CAE in terms of geometry handling and meshing.

The remesh technique is developed in close cooperation and successfully tested on complex shaped bottles in cooperation with GS. Due to the generic set-up the usage is not limited to glass forming problems. There are very likely other bulk-forming problems which are challenging and we hope in the future to use this technique also in those applications.

6. REFERENCES

1. Bird, R.B., W.E. Stewart, and E.N. Lightfoot, "Transport Phenomena", 2nd ed., John Wiley & Sons, New York, 2001
2. Kloosterman, G., and R.M.J. van Damme, "An orientation on surface reconstruction", Memorandum no 1478, University of Twente, Faculty of Mathematical Sciences, 1998.
3. Koch, H.J., "Optimization of mould design by mathematical modeling", Society of Glass Technology ESG2006, Sunderland, 2006

This Page Intentionally Left Blank

OPERATIONAL EXPERIENCE OF AN OXY-FUEL FIRED GLASS MELTER USING AN IMPROVED SILICA CROWN AND WIDE FLAME BURNERS

Alonso Gonzalez R., Grupo Pavisa, Naucalpan, MEX, México
Wladimir Sarmiento-Darkin, Praxair, Inc., Tonawanda, NY, USA
John T. Brown, GMIC, Corning, NY, USA
Len Switzer, Praxair, Inc., Burr Ridge, IL, USA
Euan Evenson, Praxair, Inc., Tonawanda, NY, USA
Sho Kobayashi, Praxair, Inc., Danbury, CT, USA
Cuauhtemoc Lagos, Praxair México S. de R.L. de C.V., México, D.F., México

ABSTRACT

The implementation of oxy-fuel firing technology in glass furnaces has become a technically feasible solution for producing glass over the last 2 decades. However, challenges do still exist concerning refractory corrosion and furnace life. It has been recognized that the high concentration of sodium species in an oxy-fuel fired furnace can lead to accelerated corrosion of the furnace crown. In this paper, the details of an operational campaign for an oxy-fuel fired container glass furnace are presented and discussed. The furnace crown was constructed with a low lime silica brick (0.8% CaO) which was expected to offer superior corrosion resistance to a conventional silica crown. The furnace also employed ultra low-momentum, Wide Flame burners to help minimize volatilization from the melt surface. The experience from this furnace campaign indicates that the crown material and burners both met performance expectations and should be considered as part of a robust operating solution for container glass manufacturers.

INTRODUCTION

The fundamental picture of a continuous glass melting operation has changed little in the past 150 years. Although the concept of an all refractory, reverberatory furnace with continual operation has not changed, great strides have been made in the materials of construction, maintenance and operation of these systems. One operational change which has greatly changed the operation and environmental footprint of glass production is the use of industrially pure oxygen in place of air. The conversion of typical air-fired glass furnaces to oxy-fuel firing has led to reductions in specific energy requirements, reduced emissions of air pollutants, increased specific pull rates, simplified furnace construction, and improved operational consistency and glass quality. However, oxy-fuel technology has also forced glass makers to consider alternative materials of construction, creative construction, operational changes and robust maintenance programs to address the challenges of using industrially pure oxygen.

The primary goal in optimizing the design, operation and maintenance of an oxy-fuel fired glass furnace has been extending the life of superstructure refractories, particularly the furnace crown. Traditional air-fired furnaces utilize silica brick for crown construction due to its relatively low density, thermal conductivity, corrosion characteristics, and moderate cost. However, silica crown bricks applied to oxy-fuel furnaces sometimes experience accelerated corrosion, , varying greatly with system design (e.g. burner choice and placement) and the operating conditions of the furnace (e.g. crown temperature). The mechanism of this accelerated corrosion is based on the formation of an alkali containing silicate or calcium silicate slag which is highly dependent on the concentration of Na species in the furnace atmosphere [1-5]. Water vapor in the atmosphere reacts with Na species to form NaOH, and the NaOH is present near the silica brick interface. The NaOH reacts with the silica and calcium in the brick to lower the equilibrium melting point, resulting in a Na_2O-CaO-SiO_2 slag which slowly "dissolves" the brick. The corrosion process is highly dependent on the temperature, NaOH concentration in the vapor phase, water content, gas velocity and calcium content in the brick.

Experimental evidence and theoretical calculations show that by maintaining sufficient temperature at the crown (e.g. >1450 °C) and minimizing Na species volatilization, corrosion of a silica brick crown can be sufficiently controlled to last the lifetime of the furnace under oxy-fuel firing conditions [6].

While the use of silica crowns in oxy-fuel fired furnaces has been demonstrated, substantial effort has been invested in alternate refractory materials of construction for the crown [7-8]. Bonded or fused cast alumina based refractories (e.g. α-β alumina or fused cast AZS) show excellent resistance to corrosion via Na species impregnation and slag formation. However, these refractory materials are substantially heavier than traditional silica brick (more steel infrastructure required) and are approximately an order of magnitude greater in cost to install. One tactic to address the less than optimal performance of silica while maintaining the cost advantages over other alternatives, has been to slightly adjust the composition of silica brick to minimize the CaO concentration. The presence of a CaO as a binder in the brick leads to the formation of a calcium silicate slag in which the calcium exacerbates the absorption of alkali species into the slag. The alkali results in further reduction in the melting point of the slag and a reduction in viscosity causing the slag to run. By reducing the CaO in the brick, this effect may be minimized, resulting in a larger, effective operating range (e.g. temperature and NaOH vapor concentration) compared to traditional silica [9].

In addition to effective use of refractory materials for oxy-fuel fired glass furnaces; construction, operation and maintenance also play a critical role in furnace integrity. Silica crown corrosion can be further controlled by using good construction practices to minimize joints and by the use of high quality materials to avoid joint expansion during the furnace campaign. Alkali vapors can penetrate these joints and reach lower temperature regimes in which slag develops and forms "ratholes" in the crown. Also, a good insulation package on the crown is critical to maintain sufficient temperature and avoid Na species penetration.

The combustion system and furnace design are also critical to reduce Na species volatilization from the glass melt. Volatilization of Na species from the melt is a function of temperature, gas velocity and gas composition near the surface. Thus, burners should be designed and positioned to result in low momentum flames while maintaining the proper temperature distribution throughout the furnace crown [11-14].

This paper reviews the performance of alternative materials, combustion technology and operational practices over the campaign lifetime of a modern, oxy-fuel fired container glass furnace.

OXY-FUEL GLASS FURNACE – BACKGROUND

In order to optimize the technical and economic operation of a soda-lime glass furnace, a number of objectives should be met. Gonzales *et al.* [10] suggested a number of goals or objectives that should be part of this analysis for crowns of oxy-fuel furnaces, and this list can be expanded for general furnace design and operation as outlined Table 1. While these goals are mostly common sense and good operating practice, it is worthwhile to reevaluate these items during any major change to a furnace system.

Table 1. Objectives for proper design and operation of an oxy-fuel glass melter

Design/Operating Consideration:	Goal:
Investment Cost	Minimize refractory costs relative to performance
Life Expectancy	Maintain or improve upon "typical" life compared to air-fuel
Materials	Investigate alternative materials or improvements on available materials
Construction and Heat-up	Utilize quality materials, stay true to fabrication drawings, minimize possibility of joint expansions
Operation	Maintain proper temperatures and utilize correct tools to optimize energy and environmental footprint (e.g. electric boost and burners)
Operating Cost	Improve competitiveness by designing system to minimize operating cost
Maintenance	Observe system carefully throughout operation, identify issues early and proactively repair
Burners and furnace layout	Utilize burners, burner positioning and flue positioning to minimize volatilization and maximize heat transfer

Grupo Pavisa in Naucalpan, Mexico, has worked to optimize these objectives on an oxy-fuel container furnace (Furnace 14) built in early 2000. This furnace was built to replace a smaller oxy-fuel glass melter. The furnace specifications are shown in Table 2. One of the major goals of this furnace design was to implement a potential improvement on typical silica crowns by utilizing a low lime silica brick which was specifically manufactured as a single production run for this furnace. The reduced CaO content (approximately 0.8%) was expected to reduce crown corrosion while maintaining a reasonable cost for the material and traditional silica crown construction practices. Table 3 shows a comparison of the basic properties of a conventional silica brick against the new, low-lime silica material used in Furnace 14.

Table 2. Operating and design specifications for Furnace 14 (Grupo Pavisa)

Parameter	Value
Glass:	Soda-lime, flint
Melter Area:	527 ft^2 (50 m^2)
Aspect Ratio:	2.2
Nominal Pull Rate:	165 tpd (150 t/d)
Electric Boost:	600 kW
Fuel:	Natural Gas
Oxidant:	Oxygen – Onsite VPSA
Nominal Cullet Ratio:	50%
Average	2779 °F (1530 °C)
Minimum	2712 °F (1489 °C)
Maximum	2835 °F (1557 °C)
Ave. Specific Energy*:	3.8 MM BTU/ston (952.2 kcal/kg)

Burners:	Wide Flame (6), opposed
Crown Material:	Low-Lime Silica (0.8% CaO)

*Average of HHV of natural gas and electric boost over furnace campaign

Table 3. Silica refractory properties

	Commercial Silica Low Flux Factor	**Low Lime Silica**
Bulk Density, kg/m^3	1794	1875
% Apparent Porosity	23.0	18.0
Modulus of Rupture At 21°C, MPa	6.2	4.3
Reheat Test at 1500°C % Linear Change	+0.2	+0.2
Chemical Analysis		
Silica	*95.9*	*98.4*
Alumina	*0.2*	*0.2*
Iron Oxide	*0.6*	*0.4*
Lime	*3.0*	*0.8*
Alkalies	*Tr*	*0.1*
Others	*0.2*	*0.1*
Silica Phases		
Quartz	*<1*	*<1*
Crist + Trid.	*75+*	*75+*
Amorphous	*N.D.*	*N.D.*

The combustion system was also designed to minimize refractory corrosion. The furnace utilized six (6) Praxair Wide Flame burners in an opposed arrangement. The burners were specifically designed to minimize gas momentum near the melt surface while maintaining good heat transfer characteristics and low NO_x emissions. With this combination of materials and combustion system, Grupo Pavisa hoped to maintain proper furnace life while optimizing operating costs.

The early results (first 45 months) of operation of this furnace have been previously described and the construction details outlined [10]. For business reasons, Grupo Pavisa made the decision to end the furnace campaign and complete a cold repair in April 2009, after 9 years and 4 months of operation. . A summary of this furnace campaign is presented below.

RESULTS: EXPERIENCE DURING SERVICE LIFE

FURNACE OPERATING SUMMARY

Furnace 14 started operation in late January 2000 and concluded operation in April of 2009, making approximately 440,000 tons of glass during the campaign. Figure 1 illustrates the pull rate and cullet ratio of the furnace over a 110 month period leading up to the shutdown and subsequent cold repair. Over the first 60 months of operation, production gradually increased to the nominal capacity of 150 t/d. Near the end of the campaign the pull rate exceeded the nominal capacity reaching a

maximum of 162 t/d and production remained high until the furnace shutdown. The cullet ratio of the furnace also varied significantly over the furnace life, mainly due to the availability of external cullet.

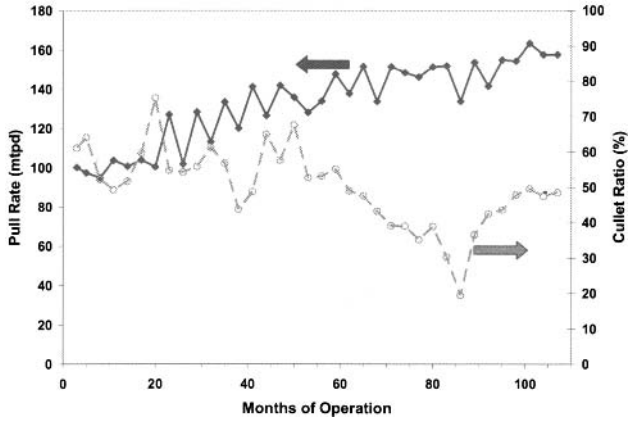

Figure 1. Furnace 14 Pull Rate and Cullet Ratio versus Month of Operation

Furnace operating conditions were adjusted during the campaign to satisfy requirements from the production lines and to respond to process variables changes. This included a general increase in electric boost during times of lower cullet input.

Figure 2 illustrates the energy input via fuel and electric boost over the life of the furnace. The electric boost was used somewhat sporadically through the furnace campaign to handle changing operational needs. Late in the campaign, a loss of cooling water to the electrodes resulted in a major malfunction and the permanent loss of the electric boost system. Hot work also had to be performed in the electrode area of the tank to avoid glass leaks and guarantee continued operability. Thus, the firing rate for the combustion system had to be increased to compensate which resulted in higher crown temperatures (up to 2900 °F or 1595 °C).

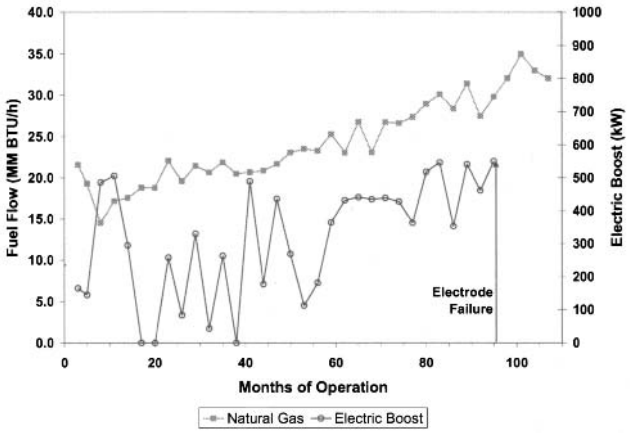

Figure 2. Furnace 14 Fuel Energy Input and Electric Boost versus Month of Operation

Analysis of the energy efficiency of the furnace over time requires normalization to compensate for changes in pull rate, cullet ratio and electric boosting.
Figure 3 illustrates the normalized specific energy consumption in MMBTU/short ton of glass and melting temperature versus the months of operation of the furnace. The normalization of the specific energy was based on a constant pull rate of 152 t/d, 50% of cullet ratio and no electric boosting. It was also necessary to correct for an increment observed in the glass temperatures at higher loads. After applying all corrections an increase of around 7 % in the specific energy consumption over the course of the furnace life was observed (or 0.77 %/y on linear bases). A careful review of the historic operating data of furnace 14 has revealed that most of the increment on the energy consumption is due to an increased amount of parasitic air leakages going into the furnace, which was calculated to be about 22% of the flue gas flow rate from the fuel and oxygen flow rates and the flue gas O2 concentration. Parasitic air leakages are typically less than 5 to10% of the flue gas flow rate for a new furnace or an old furnace with extensive sealing of open joints. If the specific energy consumption were corrected for the increment of parasitic air, the increase in the specific fuel consumption would be less than 1-2%, which would correspond to the furnace aging loss attributable to the increased wall heat losses.

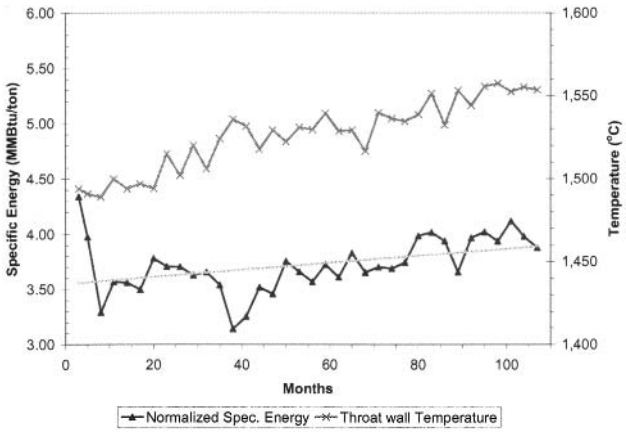

Figure 3. Furnace 14 Specific Energy Consumption and Melting Temperatures versus Month of Operation.

LOW LIME SILICA CROWN RESULTS

The plant expectations for using the low-lime silica brick as crown material were to have a crown that lasts a full campaign with minimal deterioration and few to no hot repairs. Based on the operating experience from the full furnace campaign, the performance of the new refractory material met or exceeded these expectations. Bricks showed minimum deterioration after more than 9 years of operation with oxy-fuel firing.

Figure 4 illustrates three brick samples taken from the crown from three different zones. Zone A was in the vicinity of the batch charge area, Zone B was near the hot spot and Zone C was near the glass discharge point. The dotted line near the top of the figure represents the original brick height of 15 inches. Examining the measured height of the remaining brick reveals corrosion of bewtween 1-1.3 inches (2.5-3.3 cm) of material, or a material loss rate of about 2.7 to 3.5 mm/year. This level of material loss (or less) was consistently observed throughout the crown.

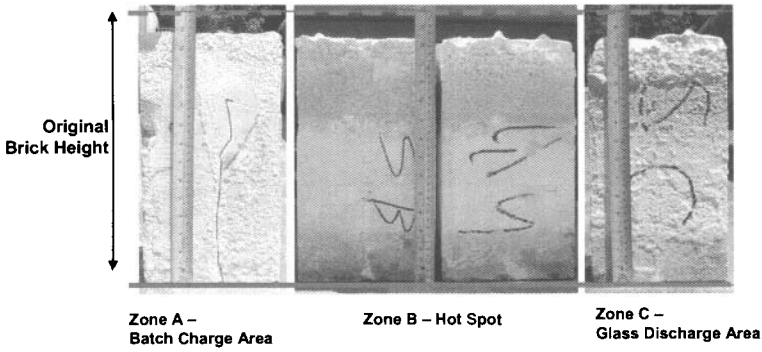

Figure 4. Crown Brick Samples taken from 3 Zones: A – Batch Charging Areas, B – Hot Spot, and C – Glass Discharge Area.

The temperature of the furnace crown was monitored throughout the campaign, and the profile along the length of the furnace varied with pull rate. Figure 5 illustrates the average crown temperature profile along the length of the furnace at varying pull rates. As might be expected, higher pull rates resulted in higher crown temperatures. However, in all operating conditions, the crown temperature was higher than 1450 C, which should minimize NaOH absorption into a calcium silicate slag [3].

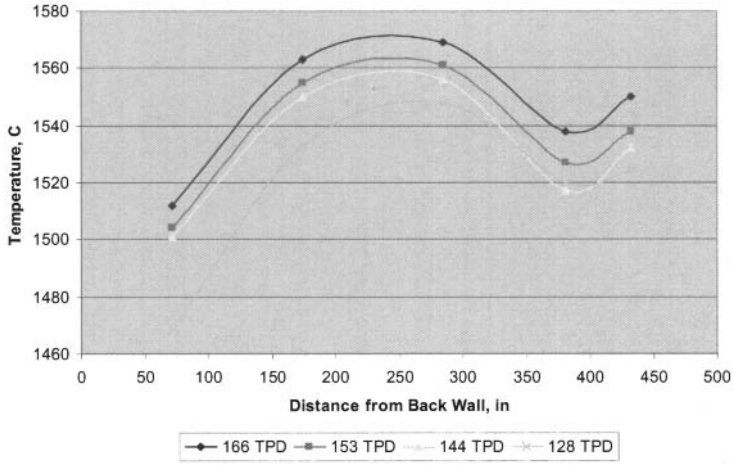

Figure 5. Average Crown Temperature as a Function of Distance from the Back Wall at Various Pull Rates

Maintenance of the crown was not a major issue during the course of the campaign and no repairs were required associated with the performance of the low lime brick. The only problem reported with the crown was in the expansion joint zones. Furnace 14 had two expansion joint zones, one close to the charging end and the other close to the refining area. Immediately after the furnace startup, sealing problems were detected at the expansion joints. However, at that time, the magnitude of the furnace gas leakage was not considered important and the issue was not immediately corrected. After a period of operation, alkali vapors started to penetrate the joint, absorb into a slag layer attacking the crown and causing damage to the nearby bricks. Hot repairs had to be made in these areas to avoid losing parts of the superstructure. No additional hot work was required after making this repair. Figure 6 and Figure 7 show images of the crown after cooling the furnace at the end of the campaign. The images illustrate consistent wear throughout the crown, and no significant points of deterioration.

The operations team at Grupo Pavisa felt that the furnace could have operated for at least 2 additional years under these conditions. However, the decision to rebuild the furnace after only 9+ years of operation was primarily due to market conditions and a desire to modify the furnace to enable the production of different product lines. With the current global economic downturn, this was an ideal time to take a furnace outage. Also, the tank refractory contained higher levels of chrome than desired for color requirements of certain product lines. Finally, the loss of electric boost resulted in an increase in furnace temperature due to increased gas firing, and the team felt it was important to restore electric boost capacity to properly balance furnace energy input. It should be noted, however, that even though a 40-50 °C increase in crown temperature occurred upon loss of electrodes, no deleterious effects were observed on the crown or other parts of the superstructure.

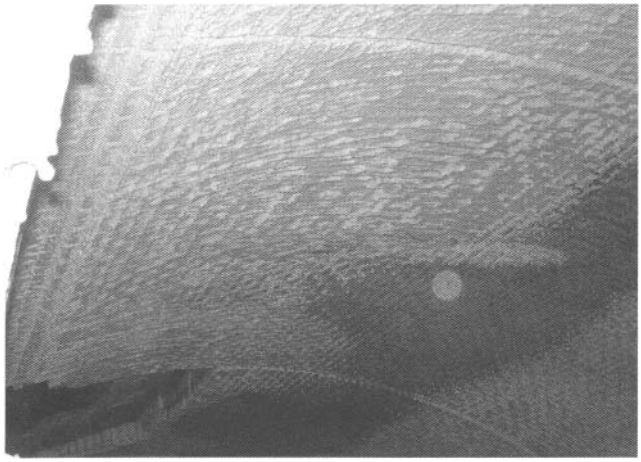

Figure 6. Furnace 14 Crown During Demolition – View 1

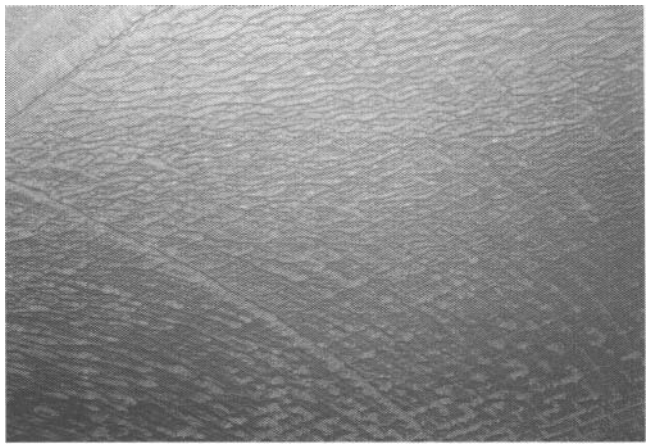

Figure 7. Furnace 14 Crown During Demolition – View 2

BURNERS

Grupo Pavisa furnace 14 is equipped with six of Praxair's first generation Wide Flame Burners installed in an opposed arrangement. These burners were designed to be a simple and flexible piece of combustion equipment and Grupo Pavisa selected this burner due to its unique attributes. The burner generates a wide flame pattern that covers up to 200% more of the glass surface than conventional oxy-fuel burners. In addition, the large, low velocity, luminous flame allows the burner to transfer heat more efficiently and prevent hot spots on the glass surface. Sufficiently high burner elevation together with low flame velocities and low momentum minimize alkali volatilization from the glass melt resulting in less furnace superstructure corrosion, longer furnace life, and reduced particulate formation. Figure 8 shows a schematic of the first generation burner. In order to minimize NOx formation, oxygen is staged through a separate set of nozzles under the fuel nozzles. The burners were fired between 2.5 to 6.5 MMBtu/hr (0.75 to 1.9 MW).

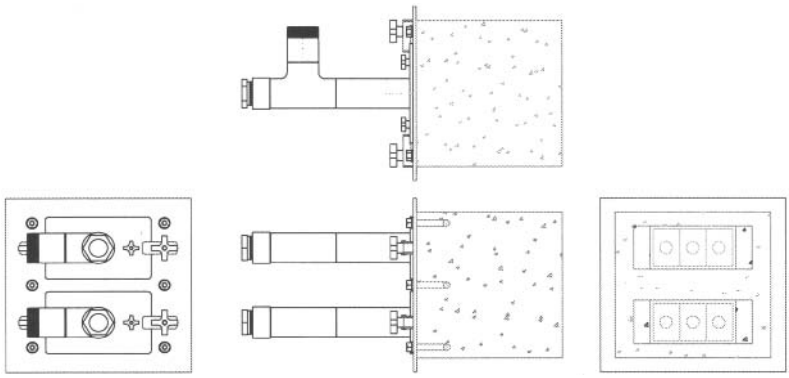

Figure 8. Praxair's Wide Flame Burner First Generation (From left to right: back, top & side and front)

A second generation of Wide Flame Burners was recently introduced to further improve burner performance and to minimize maintenance requirements. The new generation burner incorporates an evolution in Dilute Oxygen Combustion technology, including deeply staged oxygen injection and minimized gas velocities near the burner face. The result is a robust and durable burner with all the positive characteristics of the previous generation as well as the benefits of advanced flame dynamics. Figure 9 illustrates a schematic view of the second generation burner.

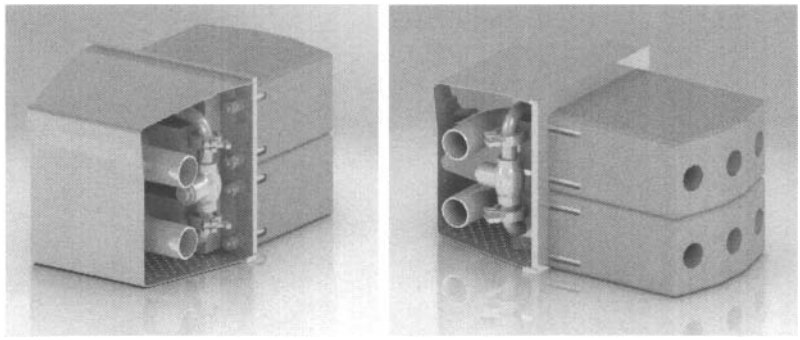

Figure 9. Praxair's Wide Flame Burner (Second Generation)

Grupo Pavisa tested two of the new generation burners in position 1 (Right and Left) of its furnace 14 from July 2008 to the furnace shut down in April 2009. Total evaluation time was approximately 9 months (37 weeks). During this time the burners were fired continuously at about 5 MMBtu/hr (1.5 MW) without needing any maintenance. Figure 10 illustrates the installed view outside the furnace (left) and the burner in operation from the interior view of the furnace through a viewport (right).

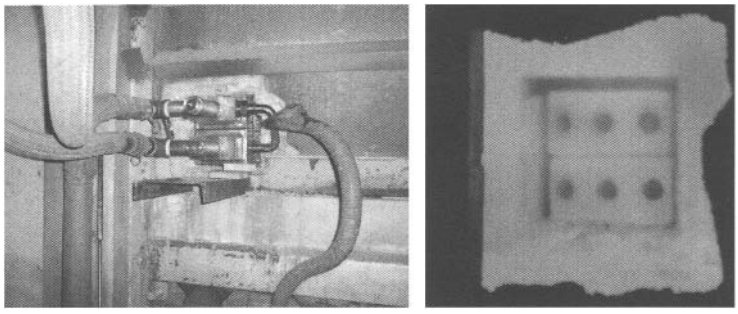

Figure 10. Wide Flame Burner Second Generation Prototype at Grupo Pavisa Furnace 14.

The flame shape and heat transfer characteristics were consistent with the first generation design, making substitution a seamless process. Both burners were carefully inspected after the shut down. The results of the inspection revealed that the burners were in excellent condition with no sign of deterioration in the burner blocks or other parts. These results indicate that the burners should be able to operate without maintenance for a much longer period of time. Grupo Pavisa was very pleased with the performance of the new burner design and plans to replace the existing burners with the new design in the near future. Another test of the next generation burner is currently underway on a container glass furnace at another site, with similar observations and results to date.

CONCLUSION

In this paper, the operational experience of an oxy-fuel container glass furnace has been presented including issues around material selection, construction practice, and operational practice. The operating campaign of Furnace 14 at Grupo Pavisa demonstrates the potential for a new type of silica brick to limit crown corrosion. This low-lime silica brick contained relatively low levels of CaO (~0.8%) while maintaining the general physical and thermodynamic attributes of standard silica brick. The furnace also untilized low-momentum Wide Flame burners to reduce volatilization off the melt, while maintaining good heat transfer and emissions characteristics. Implementation of these new

technologies led to excellent furnace performance and minimal crown deterioration over the course of the campaign.

ACKNOWLEDGMENTS

The authors of this work want to thank Dr. Ruud Beerkens (TNO) and Enrique Solorzano (PAVISA) for his valuable comments and contribution to this paper.

REFERENCES

1. M.D. Allendorf and K.E. Spear. "Thermodynamic Analysis of Silica Refractory Corrosion in Glass-Melting Furnaces." *Journal of the Electrochemical Society,* **148**(2) B59, 2001.
2. J. Brown, K.T. Wu, and H. Kobayahsi. "Alkali corrosion of superstructure refractory bricks in oxy-fuel fired glass furnaces." *The International Symposium on Glass Problems, September 4-6, 1996, Istanbul, Turkey*, Ed. R. Aksakaya.
3. R.G.C. Beerkens and O.S. Verheijen. "Reactions of alkali vapours with silica based refractory in glass furnaces, thermodynamics and mass transfer." *Glass Technology*, **46**(6) 371, 2005.
4. H. Kobayashi, K.T. Wu, and W. Richter. "Numerical modeling of alkali volatization in glass furnaces and applications for oxy-fuel fired furnace design." *Proceedings of the 4th International Conference on Advances in Fusion & Processing of Glass, 1995, Würzburg, Germany*, 1995.
5. H. Kobayashi and A. Tasca. "Oxy-fuel fired glass melting technology – Experience, evolution and expectation." *Presented at the International Commission on Glass, September 21-25, 2003, Campos do Jordão, Brazil*, 2003.
6. J.J. Schep. "Experiences with an oxygen-fired container glass furnace with silica crown – 14 years – A world record?" *69th Conference on Glass Problems*, Ed. C. H. Drummond III. Hoboken, NJ: John Wiley & Sons, Inc., 2009. 3-11.
7. M. Velez, M. Karakus, X. Liang, W.L. Headrick, R.E. Moore, J.G. Hemrick, and J.M. Almanza. "Evaluation of crown refractories under oxyfuel environment." *Proceedings of the 7th International Conference on Advances in Fusion & Processing of Glass, July 27-31, 2003, Rochester, New York USA*, Ed. J.R. Varner, T.P. Seward III, H.A. Schaeffer. Westerville, OH: The American Ceramic Society. 2004.
8. K. E. Spear and M. D. Allendorf. "Thermodynamic analysis of alumina refractory corrosion by sodium or potassium hydroxide in glass melting furnaces," *Journal of The Electrochemical Society*, **149**(12) B551, 2002.
9. J.T. Brown, R.F. Spaulding, D.S. Whittemore, and H.E. Wolfe. "New silica refractory for oxy/fuel glass melting." *International Glass Journal – A.T.I.V. Conference XV, Parma, Italy*, **102**, 120-124, 1999.
10. A. Gonzalez R., J.T. Brown, R.P. Weilacher, M.A. Nelson. "A review of improved silica crown refractory and practices for oxy-fuel fired glass melters." *64th Conference on Glass Problems*, Ed. C. H. Drummond III. Westerville, OH: American Ceramic Society, 33-42, 2004.
11. K.T. Wu and H. Kobayashi. "Three dimensional modeling of alkali volatilization/crown corrosion in oxy-fired glass furnaces." *98th Annual Meeting of the American Ceramic Society, Indianapolis, IN, April 14 to 17, 1996.*
12. H. Kobayashi and W. Richter. "Design considerations and modeling of the glass melter combustion space for oxy-fuel firing." *XVI International Congress on Glass,Madrid, Spain, October 4 to 9, 1992.*
13. W.J. Snyder, K.T. Wu, and R. Barbiero. "Reduction of alkali volatilization and refractory corrosion for oxy-fuel fired furnaces." *International Glass Journal – A.T.I.V. Conference XV, Parma, Italy*, **102**, 116-119, 1999.
14. W.J. Snyder. "Burner fulfills performance promise in service." *The Glass Industry*, **80**(8), 23-24, 1999.

C'MON, LEVEL WITH ME

Terry Berg
Sr. Pr. Process Engineer
CertainTeed Saint Gobain

ABSTRACT

There are many factors which affect glass level stability. Some of these include the type of charging system, the reliability and sensitivity of the level detector, the type of control logic loop and the stability of the process itself. This paper will only consider the various types glass level sensors and the pros and cons associated with each. A summary table is provided at the end.

When it comes to sensing changes in glass level, there are many different methods available from which to choose. They can be broken down into two basic categories, i.e. contact and non-contact. The contact types are oscillating probes, static conductivity probes and bubble pressure tubes. The non-contact types include nuclear, pneumatic, laser and optical. They vary in cost of installation and operation, frequency and cost of maintenance and system requirements. Since the various processes and glass compositions used in the industry have different requirements, this paper will look at the advantages and drawbacks of several techniques with the aim of helping you with the selection process. This information was derived where ever possible from interviewing engineers who have hands-on experience with these pieces of equipment installed in their plants. YMMV! (For non-texters, "Your mileage may vary")

Contact Level Sensors: Oscillating Probes

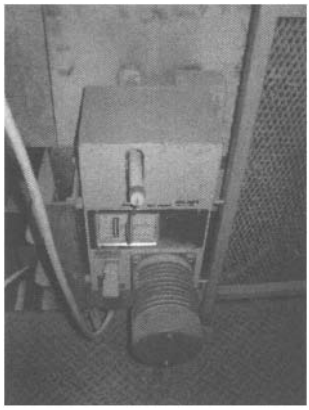

These are probably the most commonly used level sensing devices in use today and there are several different makes and installation methods. The one pictured here is installed directly into the forehearth through the breastwall. Some plants will have a separate alcove off to the side of the refiner or forehearth but the principle is the same. The oscillator moves a platinum-tipped probe down until contact with the glass is made. This completes an electric circuit telling the batch charger to speed up or slow down depending on the glass level and tells the oscillator to raise the probe to start another cycle. This process is very straightforward but not without its problems.

The unit shown here has a ceramic tube having a platinum tip. During a recent upset, the temperature in this section of the forehearth went up 200°F and the tube began droop. The batch charger interpreted this as a high level reading and stopped charging. The level dropped a couple of inches before the effects were seen in the process downstream. Fortunately, this was corrected before the electrodes became exposed. The same unit in the sister plant has a water-cooled probe which has never drooped.

If the temperature near the probe goes down and the glass becomes tacky, the probe will start to pull "stringers" or get a build up on it and again the batch charger will think the glass level is high and slow down or stop. To prevent this, the temperature in this zone should be monitored closely and the probe should be visually inspected periodically to make sure that no build up is occurring.

As with any unit that has moving parts, they eventually will wear out or break and require maintenance. Fortunately, the maintenance required is not costly and it can be handled by plant personnel.

Contact Level Sensors: Bubble Level Indicator Probes

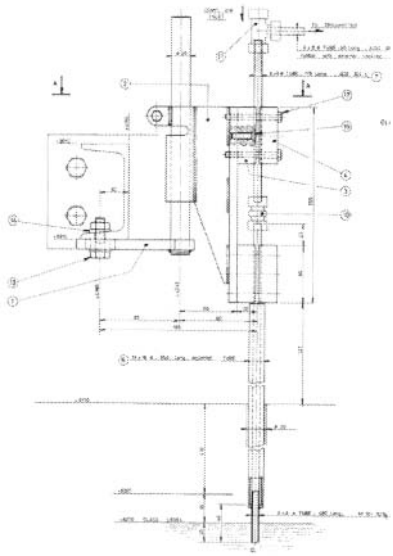

This indicator uses the bubbler tube principle, that is, it detects the air pressure required to bubble air into the molten glass. The end of a Platinum-10% Rhodium tube is inserted a nominal 20mm into the molten glass. As the glass level rises, the air pressure required to cause bubbles to form increases. Similarly when less of the end of the tube is covered, that is when the glass level falls, the air pressure is lower.

One thing to be aware of with this system is that the response can change with glass temperature (viscosity). A correctly damped system for normal melt rates can become a little erratic at low melt rates (i.e. during plant shut-downs) because the bubble release from the tip of the tube is much slower so we see the pressure building up and then releasing. This isn't normally a big problem because the control loop to the batch charger is fairly heavily damped so it doesn't chase the short term fluctuations in level signal.

The only maintenance required is maintaining a constant supply of air. If you lose the air to the probe, the end will fill with glass and it will have to be removed and cleaned out. Care must be taken to mark the exact position of the probe prior to pulling it out so that the immersion depth will be exactly the same when it goes back into the glass.

Contact Sensors: Static Conductivity Probes

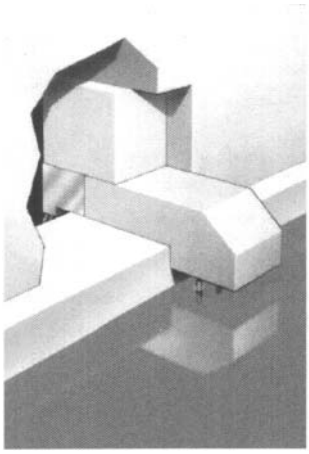

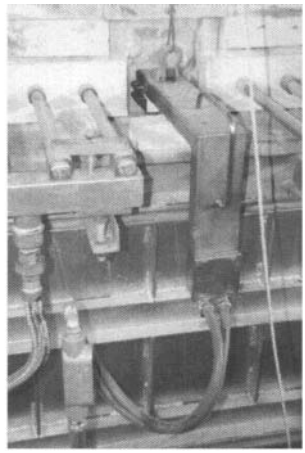

To me, the unit with the fewest adjustments or moving parts is the most desirable. The conductivity probe illustrated here is as simple as it gets. A refractory holder rests on the forehearth sidewall and two platinum probes stick down into the glass. As the level rises or falls, the probes detect changes in the apparent conductivity of the glass due to greater or lesser surface contact. This probe is a little less sensitive to changes in temperature than the bubble probe is but the more stable the temperature, the better the readings.

There is no maintenance or cooling required other than periodic replacement due to the deterioration of the refractory in the forehearth atmosphere. In a standard Soda-Lime glass the probe will last for years but in a more aggressive environment, like a Fluoride Opal, a year is the most one can reasonably expect.

Non - Contact Level Sensors: Nuclear Detectors

There are specific licensing and certification requirements for operating, maintaining and securing a detection system with a radioactive source. These regulations are not burdensome however and should not deter you from considering one of these units.

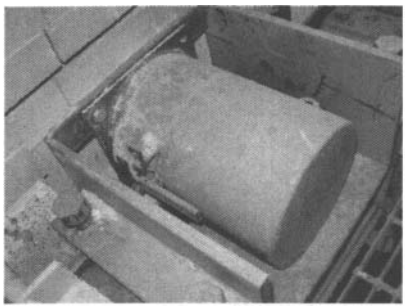

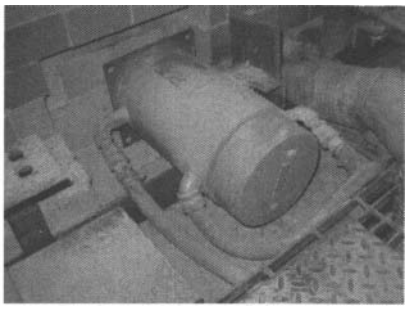

The principle, on which these operate, is simply measuring the amount of radiation hitting the detector. As the glass level goes up, more radiation is absorbed by the glass and as the level goes down more radiation reaches the sensor.

There are only a couple of maintenance items to watch with these units. The most important is being careful to maintain the cooling water to the detector as it houses all of the electronics. The second is to be aware that as the refractory in the forehearth erodes the reading will drift slightly. It may not be enough to bother your process depending what you are making but we typically have the units recalibrated every 5 years. Unfortunately, a service technician is needed for this job and chances are his travel expenses will be a large part of the service call.

Non - Contact Level Sensors: Pneumatic Probes

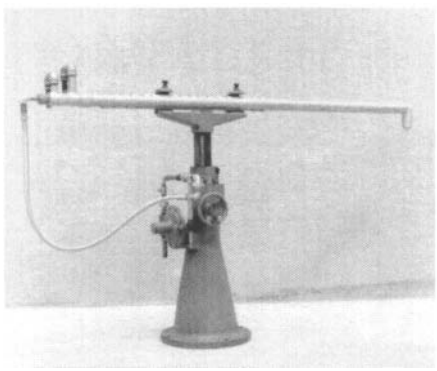

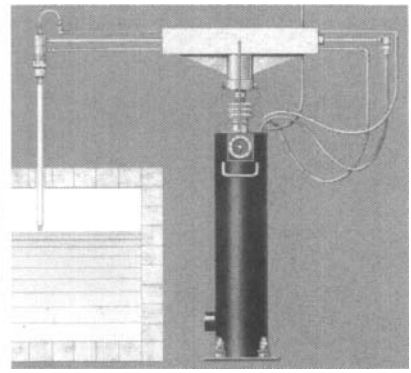

The water-cooled probes shown here are technically non-contact probes but the tips are over the glass so they are exposed to the heat and the atmosphere inside. Because of this exposure, one year is considered a reasonable life expectancy for the probe itself.

Air is blown out of the tip and changes in pressure are sensed as the glass level rises or falls. Although the unit has a bigger footprint than any of the other models, the ease of operation and low investment make this a practical choice for several segments of the glass industry, such as tableware.

Non - Contact Level Sensors: Laser Level Detectors

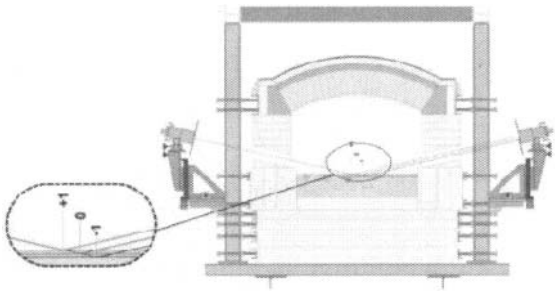

The development of lasers has revolutionized our approaches to everything from warfare to eye surgery. For our purposes, it is a simple matter, or at least it should be simple, to bounce a beam of light off the relatively smooth surface of glass flowing in a forehearth and then measure the amount of deflection. This deflection can then be correlated to a rise or fall in glass level.

A number of years ago, we trialed one of these units near the end of a furnace campaign ran into difficulties that were not the fault of the method but of the retro fit. The first problem was due to our having bubblers in our forehearth. The waves caused by the bubbling action and the bubbles themselves caused scattering of the beam which gave a very erratic signal. The second problem was

due to the volatile nature of our glass and the need to frequently clean the sight holes our operators hated it. I suspect that had we trialed this on one of our electric forehearths, our experience would have been very different.

Non - Contact Level Sensors: Optical Level Detectors

The latest method we have tried relies strictly on optics and the ability of a computer to sense changes in the pixels of an image being received by a camera mounted on the forehearth. The camera is focused on an object in the forehearth, in our case a platinum thermocouple sticking through the crown into the glass, and the increase or decrease in the number of pixels between the glass and reference point are measured.

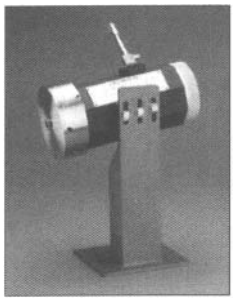

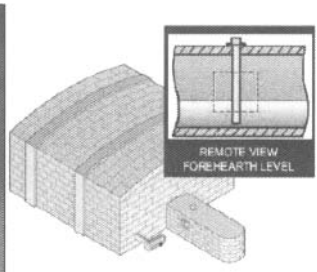

Again this trial involved a retro fit to a running forehearth and the results were not definitive. The problem was that thermocouple and the distance to the camera were such that we were unable to focus the image properly even after trying a lens with a longer focal length. We are going to continue to experiment with this method however as it appears to have potential.

Regardless of how reliable or accurate any of these sensors may be there are still going to be upsets in the glass level from time to time.

Conclusions: The table is a summary of the various level sensors discussed herein:

Type	Initial $	Operating $	Maintenance	Requirements
Oscillating Probe	Moderate	Moderate	Clean/replace probe & slide-wire (in-house)	Constant T
Bubbling Probe	Moderate	Moderate	Clean/replace probe (in-house)	Constant T & Pressure
Conductivity Probe	Moderate	Moderate	Replace probe (in-house)	Constant T& non-agressive glass
Pneumatic Probe	Low	Low	Clean probe (in-house)	Constant P & Cooling water
Nuclear Level	High	Low	Recalibrate @ 5 yrs (Service Technician)	Cooling water & Licensing
Laser Level	Moderate	Low	Clean lenses & sight path	Clean purge air & Cooling water
Optical Level	Low	Low	Clean lens & sight path	Clean purge air & Constant T

Most of the manufacturers claim similar tolerances of about +/- 0.1mm or better, which is tighter than anyone can set their "zero" point or span. Obviously, if you are making wide-mouth jars, you will need tighter level control than someone making insulation fiberglass but many of the above methods should do just fine if it fits with your type of glass and forehearth design.

Regardless of how reliable or sensitive your detector may be there are still going to be upsets in the glass level from time to time. How you handle these upsets can be a bigger issue than the upset itself. Consider the following example:

You are pulling 288 tons/day, almost maximum for this furnace, and your batch charger springs a leak. Even though it is caught right away, it still takes 10 minutes to change it out and begin charging again. If your furnace, refiner and forehearth hold 4 tons/inch at level, that means you have lost ½" of level during that time. If you leave your controllers in automatic mode to recover the level this may cause more problems than the leak and level loss have already.

Let's say that the level controller is left in auto and recovers the level back to "zero" in 30 minutes on its own. You have just filled you furnace with huge batch piles because your effective pull rate for the last half hour has been 384 tons/day.

(2 tons in 1/2hr = 4 t/hr x 24 hrs = 96 t/d + 288 t/d = 384 t/d)

Recovering the level is where your operators can make you or break you. Have they been properly trained in how to respond? Mistakes cost more than equipment.

For more information on these devices contact:

Oscillating probes – www.glassmech.cz www.haroldbeck.com www.acsitoledo.com
Bubbling probes – www.measurement-resources.com.au
Conductivity probes – www.electroglass.co.uk
Pneumatic probes – www.mtforni.com www.generalglassequipment.com
Nuclear level sensors – www.tn-technologies.com
Laser level sensors – www.hornglass.com/englisch/optibeam.php
Optical level sensors – www.jmcanty.com

Acknowledgements:

It is with deepest thanks that I acknowledge the following individuals who provided comments, pictures and the permissions necessary to publish this report:

- Robert Butler, Director of Process Development, CertainTeed Corp
- Mark Stahl, Senior Principal Process Engineer, CertainTeed Corp
- Dan Meger, Senior Project Engineer-Electrical, S-G Containers
- Phil Ross, Glass Industry Consultants Inc
- Francis Antoine, Senior Technologist, S-G Isover
- Keith DeMonstoy, Applications Engineer, JM Canty Inc.
- Richard Stormont, Managing Director, Electroglass
- Giuseppe Zanardo, MT Forni Industrial

The Future of the Glass Industry and Environmental Regulations

This Page Intentionally Left Blank

HOW BIG IS MY CARBON FOOTPRINT?

Todd J. Seifried, Christopher J. Hoyle and Douglas H. Davis
Toledo Engineering Co., Inc.
Toledo, Ohio

INTRODUCTION

Whether one agrees or disagrees with the science of global warming, it is apparent that sooner or later greenhouse gas emissions will be, at least, monitored and, most probably, limited by regulation. In Europe carbon dioxide emissions' limits and trading are already a fact of life, and here in the U.S.A. the current administration is actively pursuing similar legislation. The "American Clean Energy and Security Act of 2009" (HR 2454) was passed by the House of Representatives in June of this year. This act calls for the progressive reduction of greenhouse gases to 17% of their 2005 levels by 2050. If signed into law as it presently stands, the immediate effect would be a reduction to 97% of 2005 levels by 2012. The method of achieving these goals will first require an inventory of emissions, followed by the introduction of a cap and trade system, establishing a market for greenhouse gas emissions.

So what does this mean for the glass industry? It is obvious that in order to achieve an 83% reduction by 2050, dramatic changes will have to take place. The glass industry cannot continue to do what it has always done. To assess the challenge that lies ahead we must first establish where we are now. In the following comparisons we will look at the carbon dioxide emissions for three different furnace types producing 300 tons/day of soda-lime-silica glass for containers.

We will compare an end port regenerative, an oxy-gas and an all electric melter from both a micro level (which can be thought of as "inside the fence" of the glass plant) point of view and then from the wider macro viewpoint, which takes into account other sources "outside the fence" that result in the generation of carbon dioxide. For the purpose here, this can also be considered as the national level.

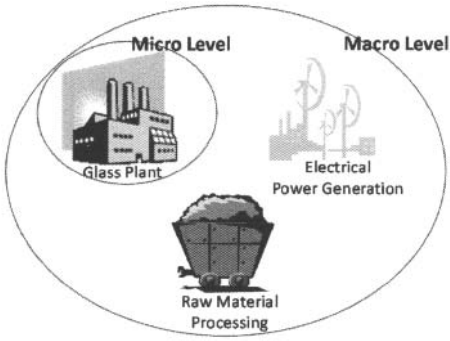

How does the U.S. glass industry fit into the national picture? In 2002, the last year for which all the data is available, the U.S. glass industry consumed about 250 trillion (1012) BTU of energy out of a total U.S. consumption of about 98 quadrillion (1015) BTU or 0.26%, and emitted about 17.9 million tons of carbon dioxide out of a total of 7,656 million tons or 0.23%. In terms of the U.S. manufacturing industry, the glass sector emits about 1.2% of that total. Glass is one of the top seven most energy intensive industries, so how we meet this challenge could well impact

other industries. Although we represent only a small fraction of the total emissions, we are a concentrated and easily targeted source. If glass is to remain in common use, we will have to consider large changes in how it is produced.

THE MICRO VIEW

For this study we have calculated the carbon dioxide emissions from three different types of melters producing 300 tons/day of soda-lime-silica glass for containers. We will establish a base case, look at the requirements to meet HR 2454, as well as some options to reduce carbon dioxide emissions and the cost implications of the cap and trade system. These comparisons will be made at a micro, or plant level, and at the wider macro, or national level.

In Table 1 the size, energy and utilities usage for the three furnace types are given. We assume they are producing a normal quality soda-lime-silica glass for container production from traditional carbonate batch materials with 20% cullet. For completeness we include the electricity for the end port combustion air fans and the oxy-gas oxygen separation plant. We will calculate the carbon dioxide evolved from the construction, the glass and the fuel. All the comparisons will be shown as the emission per ton of glass produced.

Table 1 - Base Case Furnace Data

	End Port	Oxy-Gas	Electric	
Pull	300	300	300	ton/day
Cullet	20	20	20	%
Melting Area	915	915	1152	ft2
Specific Energy	3.85	3.60	2.76	MBTU/ton
Gas Flow	51,410	48,030	0	scfh
Oxygen Flow	0	107,900	0	scfh
Electricity	22	1,471	10,100	kW

The carbon dioxide produced in the manufacture of the refractories, steel and other materials used in the construction of the furnaces is very small compared to that produced by the batch reactions and fuel. It is about 1.5 to 2.0 lb/ton of glass, depending on the assumptions made on furnace campaign length and the extent of a rebuild and can, therefore, be ignored in this comparison.

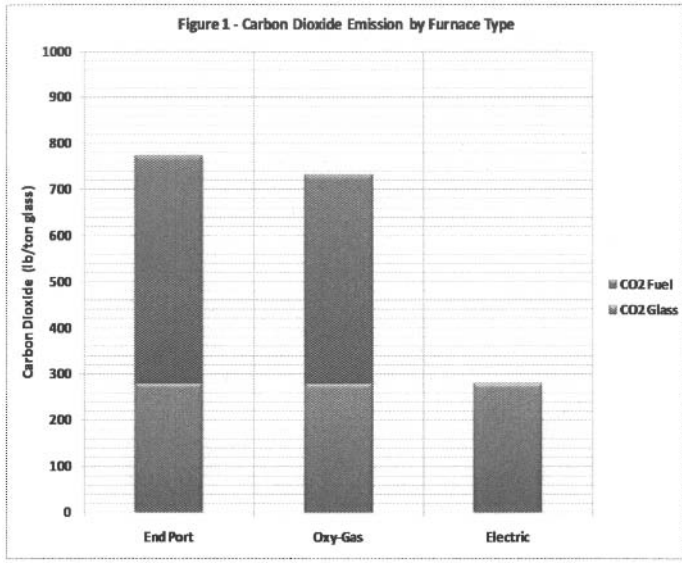

Figure 1 shows the carbon dioxide emissions for the three furnaces. The contribution from the batch reactions is independent of furnace type and is 281 lb/ton. The contribution from fuel depends on the energy efficiency and is 491 lb/ton for the end port and 451 lb/ton for the oxy-gas. This gives a total of 774 lb/ton for the end port, 731 lb/ton for the oxy-gas and 281 lb/ton for the all electric. As the electricity is generated off site there is no carbon dioxide emissions associated with it. The clear winner is the electric furnace.

So what are the implications of HR 2454 for the glass manufacturer? Greenhouse gas emissions are expressed in metric tonnes of carbon dioxide equivalents. We can not confirm as to the value of greenhouse gas emissions under the cap and trade system that will be implemented in the U.S., but we can look to the situation in Europe as a guide. The current (July, 2009) over-the-counter trading price in Europe is €14.30/tonne CO2 eq., or $18.44/ton CO2 eq. At these prices the additional cost to the glassmaker would be $7.14/ton of glass for the end port and $2.59/ ton of glass for the all electric furnace, if no adjustment to the carbon emissions were made, however, we also have to look at the long term reductions required by the cap. The purpose of the cap is to progressively reduce emissions over time, so whilst emissions can be traded, allowing plants which do not meet the targets to purchase additional emissions credits, the total amount of emissions is progressively reduced. The reductions will be implemented between now and 2050, although the act does not specify if the reductions will be implemented at a cold repair or not.

Figure 2 shows the reductions required by HR 2454. In 2020 these will be to 80% of the 2005 emission and can probably be met by changes in operation and melting practice. The reductions to

meet the 2030 and 2050 targets will require more fundamental changes. It can also be safely assumed that as the reductions in the cap get larger the price of greenhouse gas emissions will rise, thus, making it more attractive to invest in a plant and equipment with a lower carbon dioxide emission or move to a location where they are not limited.

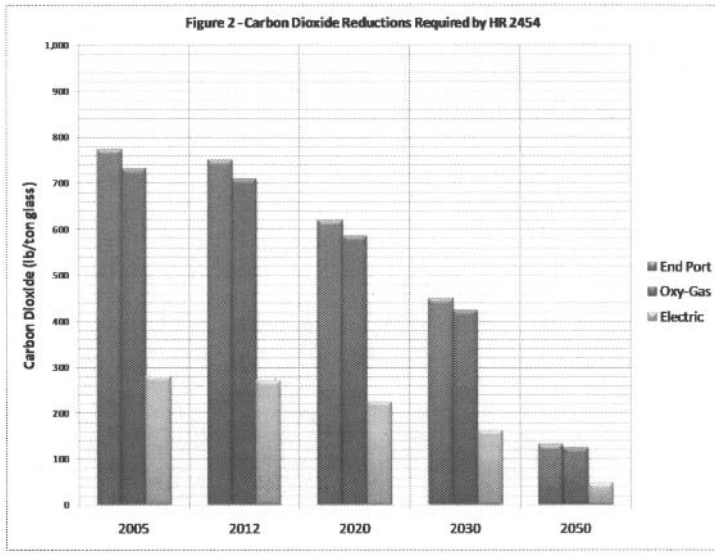

REDUCING CARBON DIOXIDE EMISSIONS

What are some options for reducing carbon dioxide emissions? There are a number of areas that can be attacked. In order of increasing capital cost, they are the batch and raw materials, furnace efficiency and melter type and design. Taking the batch and raw materials, the simplest means of reducing carbon dioxide emissions is to increase the use of cullet. Most plants already recycle all the in house cullet generated by their own manufacturing processes, so increasing cullet use will necessitate the use of external cullet from downstream processes or post consumer recycling. Increasing cullet use also reduces energy consumption as we do not need to supply energy for the endothermic batch reactions.

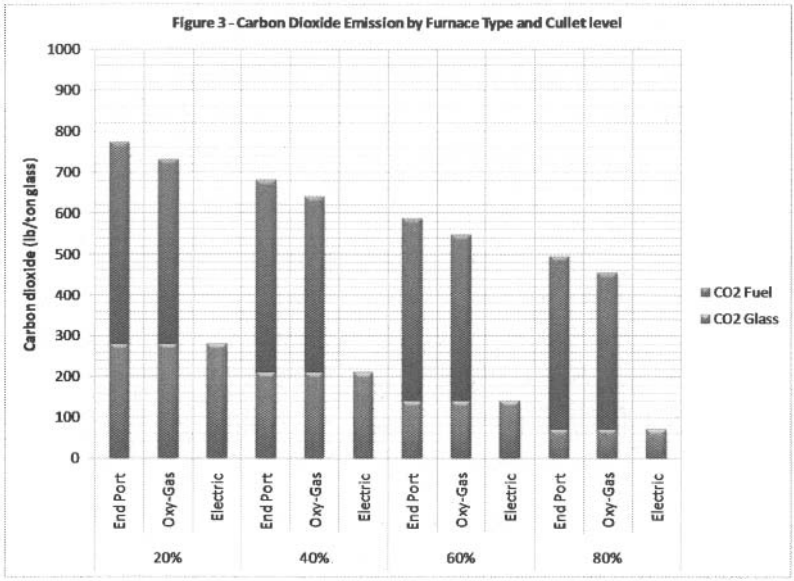

Figure 3 shows the reduction in carbon dioxide emissions by increased cullet use. On the face of it, simply increasing cullet levels to 80% will go a long way to meeting the targets for 2030. However, as is often the case, this is easier said than done. Using cullet at these levels will mean the quality of the cullet will have to closely match the glass composition of the product. Present methods of post consumer recycling will not deliver either the quantity or quality of cullet required. Some major investment will be required to improve current cullet recycling systems to the necessary level.

The other means of reducing carbon dioxide emissions from batch is to reduce or eliminate the use of carbonates. The use of burnt lime or dolomite is already proven, especially in textile fiberglass production, but both these materials are more costly and have handling problems that will require batch plant modifications. Soda ash can be replaced with sodium hydroxide, but again, this is more expensive and will also require batch plant modifications and increased maintenance due to its corrosive nature. The use of pelletized batch could eliminate some of these handling problems, but this may require major modifications to the batch plant. However, applying both increased cullet use and eliminating carbonates from the batch will allow us to just about meet the 2030 emissions target.

Improvements or changes in operation and furnace efficiency will also reduce greenhouse gas emissions. Switching to natural gas from heavy fuel oil will immediately reduce CO2 emissions by 30%, but most, if not all, furnaces in the U.S. burn natural gas already. Improved furnace efficiency by increasing insulation, improvements in regeneration, improved port and burner design and better control and monitoring will all help but they will not significantly improve a modern, well designed and operating furnace. For older designs there will have to be some thought given to these types of

improvements when furnace cold repairs are carried out, especially if significant improvements can be implemented.

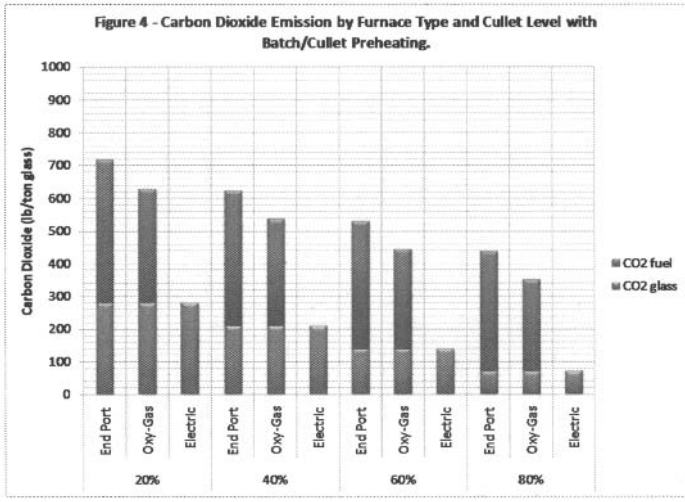

One technically proven method of significantly improving energy efficiency for regenerative and oxy-gas furnaces is batch and cullet preheating. This is especially true for oxy-gas furnaces where a significant quantity of high grade energy is currently most often thrown away. Up to now the return on investment of this technology has not been good, hence the very small number, less than ten, of installations worldwide. Including the price of carbon dioxide emissions may tip the balance in its favor. Figure 4 shows the effect batch and cullet preheating has on furnace efficiency. We have assumed that the maximum preheat temperature for the end port case is 550 °F and for the oxy-gas is 1150 °F. The reduction for the end port ranges from 11% to 15% and 23% to 27%, depending on cullet fraction, for the oxy-gas.

Another technically proven method of improving energy efficiency is to take advantage of the waste heat using a waste heat boiler that in turn drives a steam turbine. It is also possible to use this energy more directly in any application where the heat can be used directly, such as preheating for other processes. It can also be used to provide cooling when used in conjunction with an absorption chiller.

It should be noted that these forms of waste heat recovery have not generally proven to be economically feasible. Payback for these types of projects currently can range from 6 to 20 years or more, depending on a large number of variables; however, they will become more attractive as energy and carbon credits become more valuable.

Combining the use of increased cullet, no carbonates in the batch and batch and cullet preheating allows us to meet the 2030 targets but we are still short of meeting those for 2050. So far the only proven method of meeting the 2050 target would be to convert to all electric melting, in addition to modified batch and high levels of cullet. Whilst this is feasible for some types of glasses, it certainly does not apply to all; the production of high quality float glass, for example, has up to now proved impossible with electric melting.

THE MACRO VIEW

The comparisons made so far have all been at the micro plant level; if we look at the wider macro view, a different picture emerges. The aim of the bill is to reduce carbon dioxide emissions nationally, but looking nationally we have to include the production of electricity and pre-processing of raw materials. Merely shifting the emissions from one place to another does not help the nation advance towards the goal of carbon dioxide reductions. Figure 5 shows the generating mix for the U.S.A. for 2008. We see that 70% of our electricity is generated from fossil fuels with about 50% from coal. Current DOE projections to 2030, both for the U.S.A. and the world, do not forecast a significant change in this mix (see figures 6 and 7).

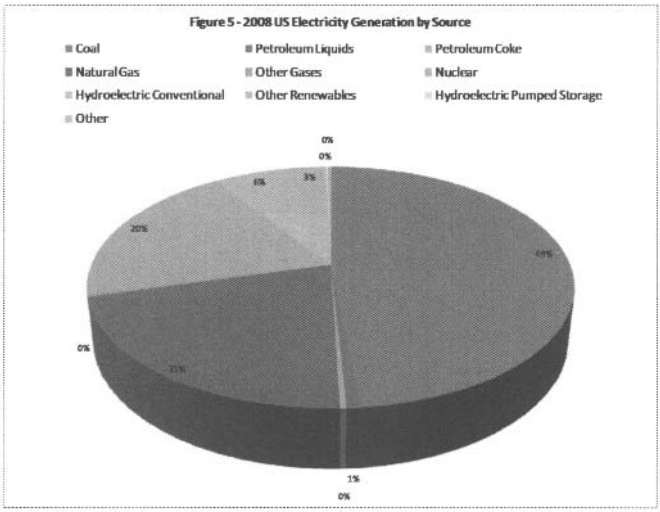

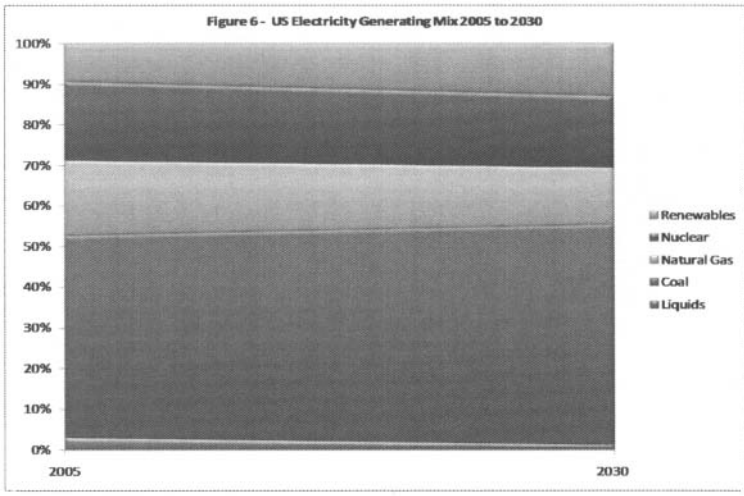
Figure 6 - US Electricity Generating Mix 2005 to 2030
100%
90%
80%
70%
60%
50%
40%
30%
20%
10%
0%
2005
2030
Renewables
Nuclear
Natural Gas
Coal
Liquids

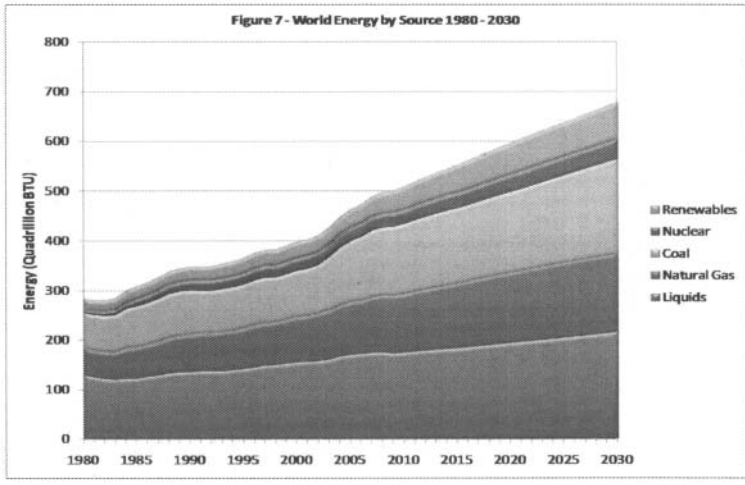
Figure 7 - World Energy by Source 1980 - 2030
Energy (Quadrillion BTU)
800
700
600
500
400
300
200
100
0
1980
1985
1990
1995
2000
2005
2010
2015
2020
2025
2030
Renewables
Nuclear
Coal
Natural Gas
Liquids

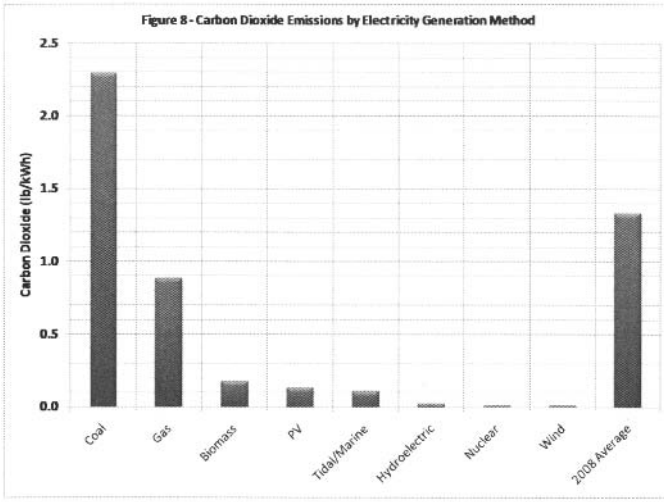
Figure 8 - Carbon Dioxide Emissions by Electricity Generation Method
Carbon Dioxide (lb/kWh)
2.5
2.0
1.5
1.0
0.5
0.0
Coal
Gas
Biomass
PV
Tidal/Marine
Hydroelectric
Nuclear
Wind
2008 Average

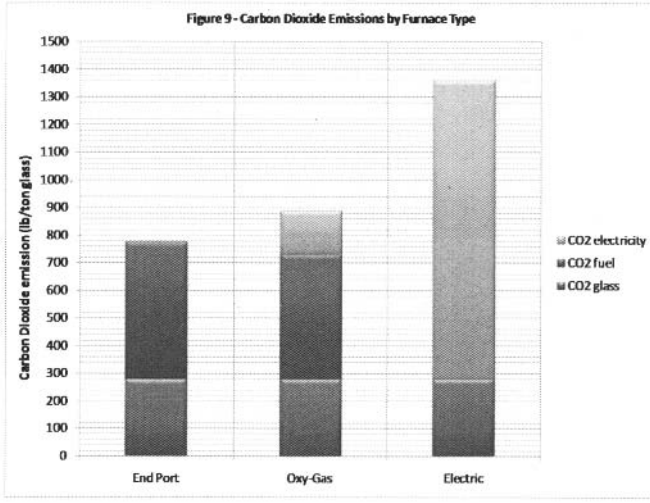
Figure 9 - Carbon Dioxide Emissions by Furnace Type
Carbon Dioxide emission (lb/ton glass)
1500
1400
1300
1200
1100
1000
900
800
700
600
500
400
300
200
100
0
End Port
Oxy-Gas
Electric
CO2 electricity
CO2 fuel
CO2 glass

Taking the electricity generation mix into account produces a very different picture and conclusion. The average carbon dioxide emission based on the 2008 generating mix is 1.34 lb/kWh, although as can be seen from Figure 8, this varies from 2.3 lb/kWh, for coal to almost zero for nuclear or wind generation. If we recalculate the carbon dioxide emissions, including the average emission for electricity generation, a very different picture emerges (see Figures 9 through 12).

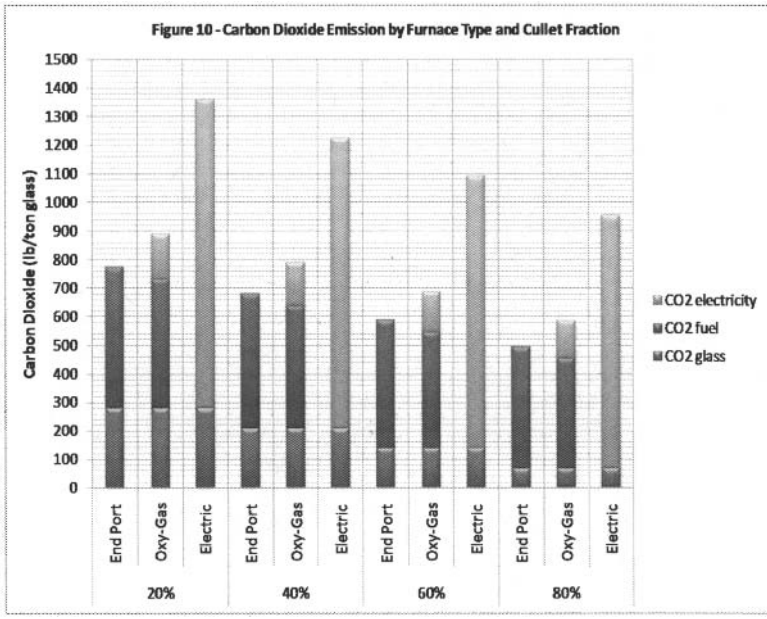

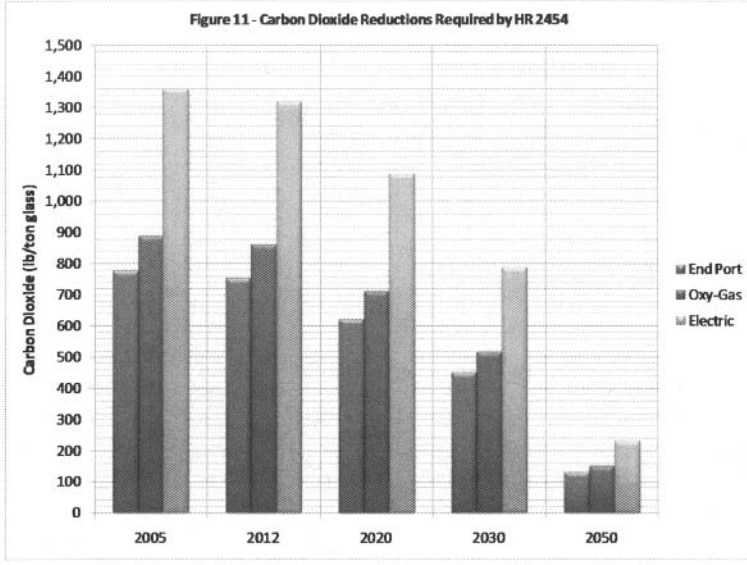
Figure 11 - Carbon Dioxide Reductions Required by HR 2454
Carbon Dioxide (lb/ton glass)
1,500
1,400
1,300
1,200
1,100
1,000
900
800
700
600
500
400
300
200
100
0
2005
2012
2020
2030
2050
End Port
Oxy-Gas
Electric

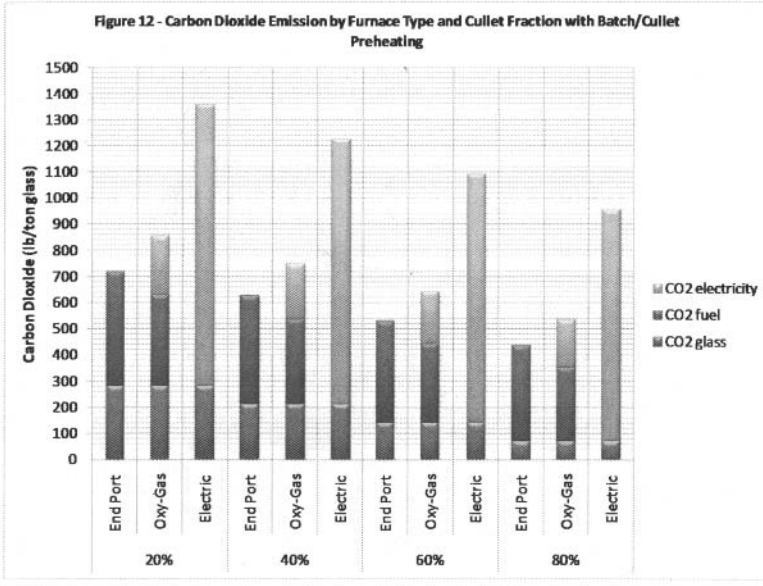
Figure 12 - Carbon Dioxide Emission by Furnace Type and Cullet Fraction with Batch/Cullet Preheating
Carbon Dioxide (lb/ton glass)
1500
1400
1300
1200
1100
1000
900
800
700
600
500
400
300
200
100
0
End Port
Oxy-Gas
Electric
20%
40%
60%
80%
CO2 electricity
CO2 fuel
CO2 glass

In this scenario the conclusion is that efficient, well-regenerated air-fuel furnaces with batch/cullet preheating using modified batch and high levels of cullet appears to be the most practical approach. Glass manufacturers will have to be concerned about how their electricity is generated as this will have a big impact on their carbon emissions and hence operating costs.

ELECTRICITY GENERATION

We have seen from Figure 8 that carbon emissions for electricity generation vary widely depending on how it is produced. Electricity from renewable, nuclear and fossil fuel with carbon capture and sequestration (CCS) will dramatically lower carbon dioxide emissions. At present, only 30% of our electricity is generated from low carbon sources and current projections to 2030 do not forecast much change. The effect of HR 2454 will be to increase the price of electricity generated from fossil fuels, bringing closer the time when electricity generated from renewable or nuclear sources is equal or cheaper in price. This is a significant milestone of the renewable industry, i.e., "grid parity", and is closer than many think, predicted to be around 2015 in the U.S.A. However, to have a significant impact on national emissions, a massive investment in both renewable and fossil fuel with CCS technology will be necessary. Installed total generating capacity in the U.S.A. is about 1 million MW. To increase the percentage generated by wind or solar to 50% from the present 3% would require the installation of 7,250 million solar panels, or about 100,000 5MW wind turbines. What do we do when the sun doesn't shine or the wind blow?

There is a lot of discussion and research in progress on carbon capture and sequestration, seen by many in the coal industry as the white knight coming to the rescue of fossil fuel electricity generation. In principal, the carbon dioxide produced from burning fossil fuels is somehow separated from the waste gas stream and then pumped into an underground storage facility so that it cannot be released into the atmosphere. To date there have been no successful demonstration projects, but recently the EU earmarked €1.25 billion for 11 CCS demonstration projects and the U.S. economic stimulus package included $1 billion for research into clean coal. However, we do not know if these technologies can become practicable nor can we know the long term viability or implications of storing vast quantities of carbon dioxide underground. To give some idea of the scale of the problem some experts believe that to capture just 10% of the carbon dioxide from existing coal fired generating plants and transport it to a storage facility would require a pipeline system with capacity equivalent to transporting all the present day's oil flow. To make CCS viable it has been estimated that the European carbon dioxide emissions trading price would have to increase by three to five times the current level. Based on our earlier calculations, this will cost the glass manufacturer between $8 and $36/ton of glass produced depending on furnace type.

CONCLUSIONS

The size of your carbon footprint depends on whether we draw the circle at a micro or macro level. In any case, the effect of any legislated reduction in carbon emissions should aim to benefit the whole planet not merely move emissions from one place to another.

At the macro level an efficient air fuel regenerative furnace has the lowest carbon emission. In order to prepare for a carbon emission limit this is the technology of choice, particularly given the average furnace campaign is 10 to 12 years for containers, 15 to 20 years for float glass and spans more than one step change in carbon emissions, and that the currently predicted electricity generation mix will not significantly change.

If the carbon cap and trade system does bring about a change in the generating mix away from fossil fuels, then the glass industry should focus now on developing electric melting technologies to produce better quality glass in larger quantities.

Under either scenario increased use of cullet will be necessary to reduce carbon dioxide emissions. Present post-consumer recycling systems are incapable of supplying the quantity and quality of cullet required. We need to address this problem urgently due to the time required to set up the infrastructure.

If the use of burnt raw materials, sodium hydroxide and preheating is adopted more widely, batch pelletization will become more desirable to offset some of the problems associated with using these materials.

This Page Intentionally Left Blank

ICG: A GLOBAL COOPERATION IN THE CHALLENGING WORLD OF GLASS

Fabiano Nicoletti
Stevanato Group
Piombino Deve, Italy

René Vacher
University of Montpellier and CNRS
Montepellier, France

COOPERATİON WİTHİN COMPETİTİON

The ICG is not only a society of scientists, technologists, artists, or businessmen of glass, but also a body, where we share knowledge and experience, as it is best described in the words of Prof. W.E.S. Turner in 1951, which is still valid in our days of global challenges.

Competition develops the powers of hard thinking, ingenuity and resourcefulness, and can thus be salutary. But there are many ways in life in which we can carry on competition and yet be helpful to one another. There can, I feel sure, be many occasions, even in business, when mutual giving and mutual taking help both parties to the exchange. The International Commission is a body in which its distinguished members can talk with one another and be mutually helpful...

W. E. S. Turner, 1951


International Commission on Glass (ICG)
ICG Mission
... to be more innovative and to get more value
"TO CARRY FORWARD THE WORK OF INTERNATIONAL COLLABORATION BETWEEN GLASS TECHNOLOGISTS & SCIENTISTS OF THE WORLD"
"TO IDENTIFY FUTURE DIRECTIONS FOR RESEARCH AND DEVELOPMENT"
will contribute
to the achievement of more glass usage
within many more different areas.

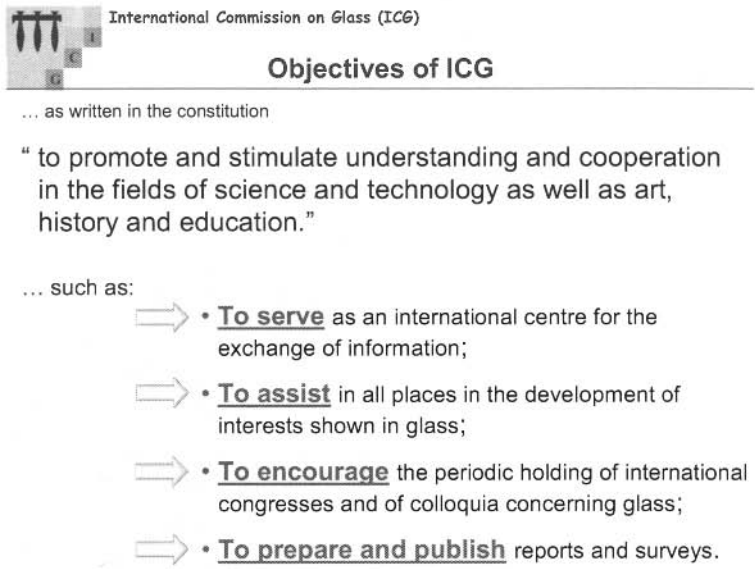
International Commission on Glass (ICG)
Objectives of ICG
... as written in the constitution
" to promote and stimulate understanding and cooperation in the fields of science and technology as well as art, history and education."
... such as:
• To serve as an international centre for the exchange of information;
• To assist in all places in the development of interests shown in glass;
• To encourage the periodic holding of international congresses and of colloquia concerning glass;
• To prepare and publish reports and surveys.

International Commission on Glass (ICG)

Objectives of ICG

ICG promotes the organization of expert meetings as starting point of developing R&D roadmaps in important fields of glass science and technology such as:

- **Glass melting**
- **Bio-active glassy materials**
- **Glass-ceramics**
- **Basics of glass**
- **Nanomechanical aspects of glass**

International Commission on Glass (ICG)

Member Countries

Argentina	France	Netherlands	Thailand
Australia	Germany	Philippines	Turkey
Belgium	Greece	Poland	United Kingdom
Brazil	Hungary	Portugal	Usa
Bulgaria	India	Rumania	
Canada	Italy	Russia	
China	Japan	Serbia	
Czech Republic	Korea	Slovakia	
Denmark	Liechtenstein	Spain	
Finland	Mexico	Sweden	

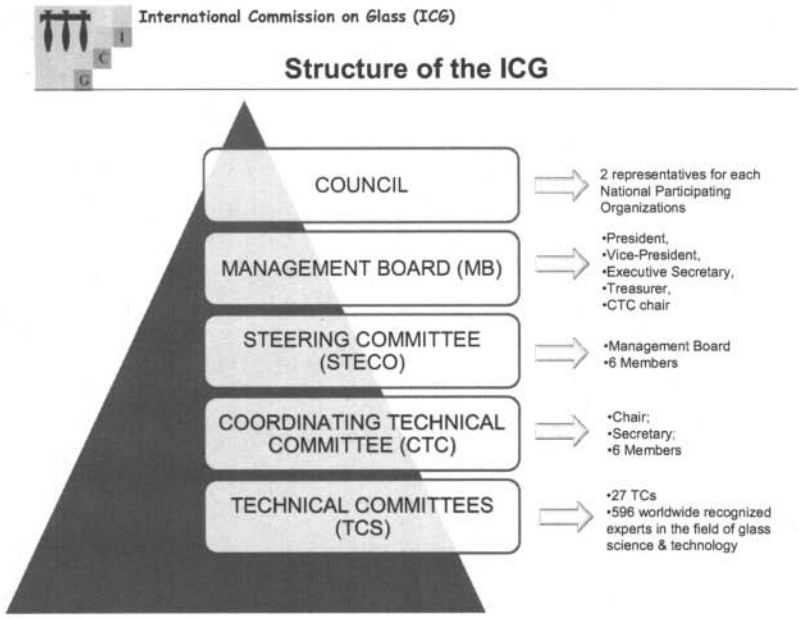
International Commission on Glass (ICG)
Structure of the ICG
COUNCIL
2 representatives for each National Participating Organizations
MANAGEMENT BOARD (MB)
•President,
•Vice-President,
•Executive Secretary,
•Treasurer,
•CTC chair
STEERING COMMITTEE (STECO)
•Management Board
•6 Members
COORDINATING TECHNICAL COMMITTEE (CTC)
•Chair;
•Secretary;
•6 Members
TECHNICAL COMMITTEES (TCS)
•27 TCs
•596 worldwide recognized experts in the field of glass science & technology

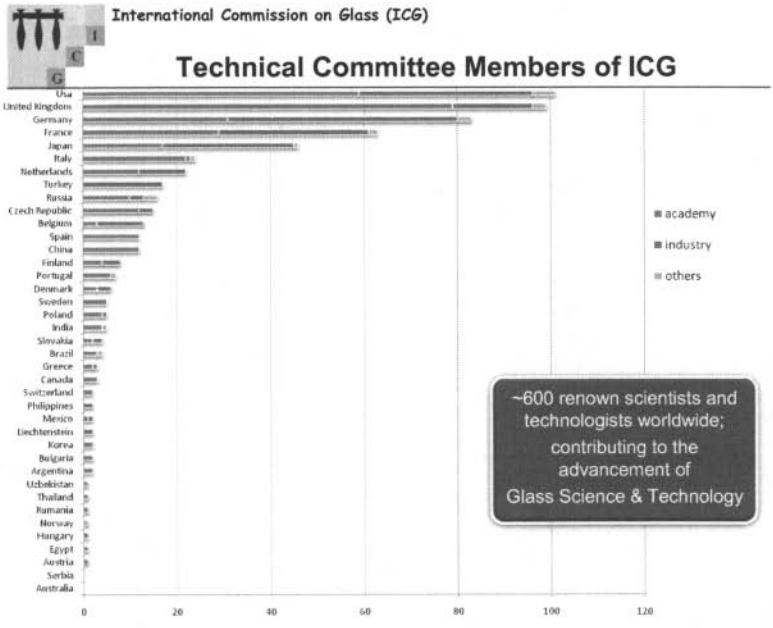
International Commission on Glass (ICG)
Technical Committee Members of ICG
Usa
United Kingdom
Germany
France
Japan
Italy
Netherlands
Turkey
Russia
Czech Republic
Belgium
Spain
China
Finland
Portugal
Denmark
Sweden
Poland
India
Slovakia
Brazil
Greece
Canada
Switzerland
Philippines
Mexico
Liechtenstein
Korea
Bulgaria
Argentina
Uzbekistan
Thailand
Rumania
Norway
Hungary
Egypt
Austria
Serbia
Australia
0
20
40
60
80
100
120
academy
industry
others
~600 renown scientists and technologists worldwide; contributing to the advancement of Glass Science & Technology

International Commission on Glass (ICG)

Tc Members Sources

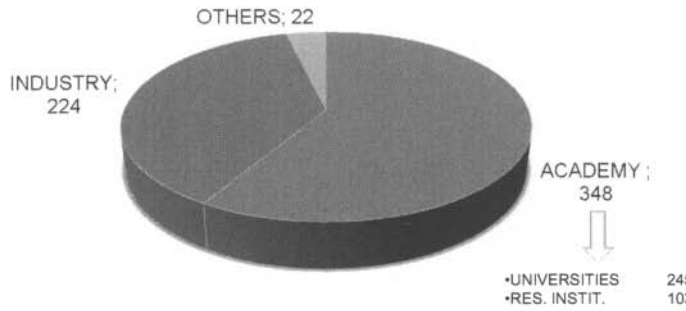

International Commission on Glass (ICG)

Glass Application Areas

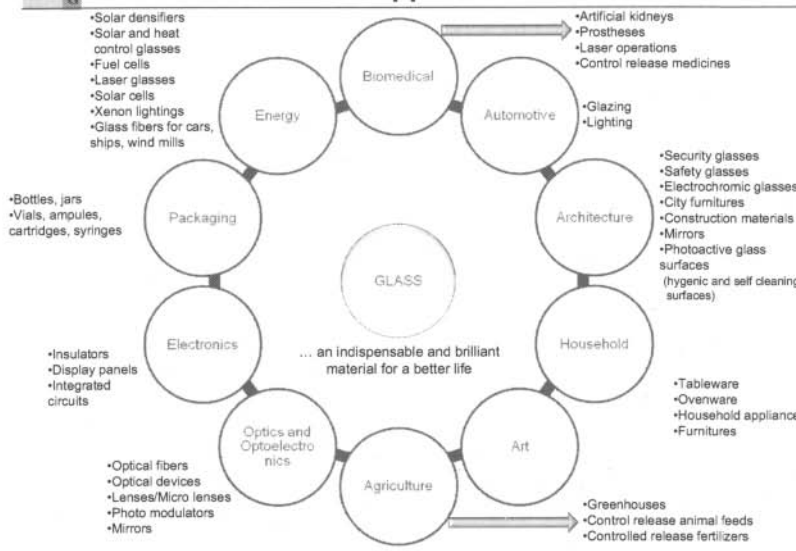

International Commission on Glass (ICG)

The ICG „World"

... to be more innovative and to get more value

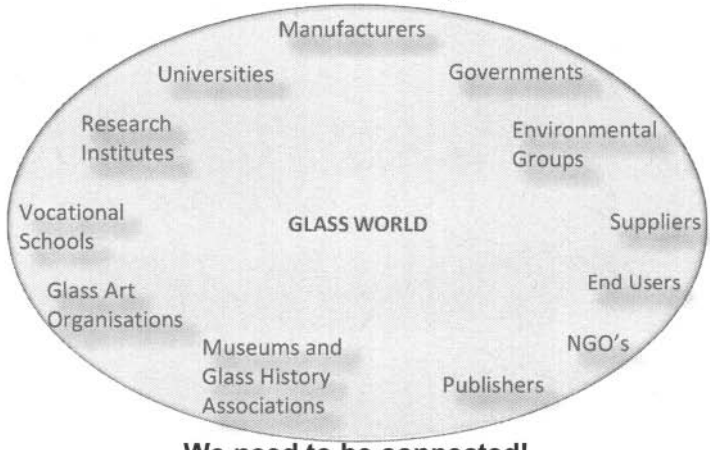

We need to be connected!

International Commission on Glass (ICG)

R&D activity fields in the ICG

... the Technical Committees (TC) are the backbone for international cooperation

... the work of the Technical Committees is organized in the following

- R&D activity fields
- Basics & Properties
- Glass Production
- Surfaces & Interfaces
- New Applications
- Information, Communication, Education, History

International Commission on Glass (ICG)

R&D activity fields & TCs

Basics & Properties

Basic Glass Science (TC03)
J. Zwanziger, Dalhousie University, Canada

Glass Transition (TC08)
L. Wondraczek, Universität Erlangen-Nürnberg, Germany

Nucleation, Crystallisation & Glass Ceramics (TC07)
E. Zanotto, University of Sao Carlos, Brazil

Nanomechanics (TC09)
M. Ciccotti, CNRS – Université Montpellier 2, France

Mechanical Properties of Glass (TC06)
R. Hand, Sheffield University, UK

Optical Properties of Glass (TC10)
C. Anderson, Saint-Gobain, France

Chemical Durability & Analysis (TC02)
D. Brochot, Corning, France

Structure – Properties Relations (TC22)
G.Calas, Université de Paris, France

Vibrations & Structure (TC 26)
B.Hehlen, Université Montpellier 2, France

Atomistic Simulation (TC 27)
J.Mauro, Corning, USA

Glass Production

Properties of Glass Forming Melts (TC18)
R. Beerkens, TNO, The Netherlands

Modelling of Glass Melting Processes (TC21)
E. Muijsenberg, Glass Service B.V., The Netherlands

Modelling of Glass-Forming Processes (TC25)
C. Berndhäuser, Schott AG, Germany

Materials for Glass Manufacturing (TC11)
M. Dunkl, Dunkl Consulting, Germany

Sensors & Advanced Control Systems (TC15)
W. Linz, Schott AG, Germany

Gases in Glass (TC14)
D. Köpsel, Schott AG, Germany

Environment (TC13)
G.Van Marcke, Glaverbel, Belgium

International Commission on Glass (ICG)

R&D activity fields & TCs

Surfaces & Interfaces

Nanostructured Glasses (TC16)
R. Almeida, Instituto Superior Technico, Lisboa, Portugal

Coatings on Glass (TC24)
K. Sanderson, Pilkington European Technical Centre, UK

Glass Surface Diagnostics (TC19)
V. Rupertus, Schott AG, Germany

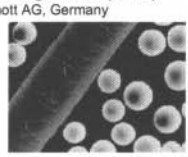

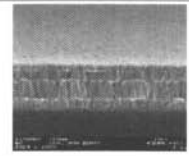

New Application Fields

Glass for Medicine & Biotechnology (TC04)
J. Jones, Imperial College, UK

Hazardous & Nuclear Waste Vitrification (TC05)
J. Marra, Savannah River Nat. Lab., USA

Glasses for Optoelectronics (TC20)
S. Tanabe, Kyoto University, Japan

Information, Communication, Education, History

Information & Communication (TC01)
J.M. Parker, Sheffield University, UK

Glass, Society & Environment (TC 12)
J. Stockdale, British Glass Manufacturers Confederation, UK

Education & Training in Glass Science and Engineering (TC 23)
R. Conradt, RWTH Aachen, Germany

Archeometry of Glass (TC17)
S.P. Koob, Corning Museum, USA

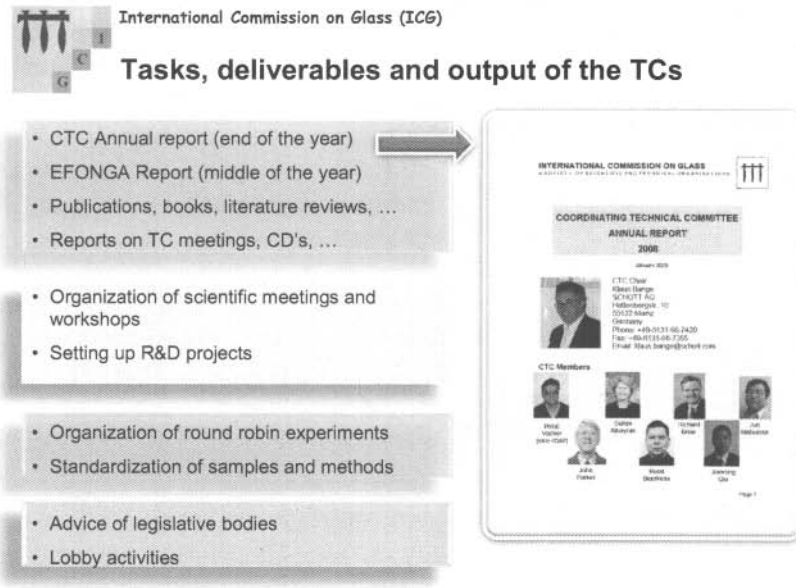

For additional information on ICG, visit www.icglass.org

PARTICLE SIZE MEASUREMENTS IN THE FLUE GAS OF GLASS MELTING FURNACES

Andreas Kasper*, Simon Slade**, Dilek Bolcan***, and Guy van Marcke de Lummen****

*Saint Gobain, Germany, speaker
**Pilkington GLC, England
*** Şişeçam, Turkey
**** Asahi Glass Company, Belgium

SUMMARY

Particulate emissions make part of the classical air polluting matters. Especially the respiratory fraction (commonly „fine dust"), i.e. dust with aerodynamic diameter Ø up to 10 micrometers, is frequently subject of discussion in the last years. Four main European flat glass producers have therefore made a common research project, in the frame of their collaboration in ICG-TC13 (Technical Committee of the International Commission on Glass on the subject: environment), using ANDERSON MARK III impactors to measure for several flat glass furnaces their fine dust emissions before and after the waste gas scrubbing & filter system, in most cases: an electrostatic precipitator with an upstream scrubbing system. Different conditions were researched, such as natural gas, mixed and pure fuel oil fired furnaces and waste gas filters working at high and low temperature. The results are:

Fine dust and coarser dust levels in the flue gas are reduced by the same degree by the filter system, the particle size distribution in raw and clean gas are measured to be very similar in nearly every case. Only the total level is much lower in the clean gas. Electrostatic precipitators are therefore adequate to reduce homogeneously the fine dust for all relevant sizes observed.

The chemical composition of the clean gas dust resembles the raw gas dust composition (before injecting the absorption agent), but it is significantly different from that of the collected ESP dust.

Most of the fine raw gas particles are ad/absorbed, even before filtration by the ESP, on the bigger particles of the upstream injected scrubbing reagent powder.

Consequently, a big part of the dust slipping through the ESP system is un-absorbed raw gas dust, only a smaller fraction is coming from the fines of the scrubbing reagent. This indicates that an electrostatic precipitator is capable of reducing dust emissions for all particle sizes

observed to comply with the emission limits and while doing so, does not preferentially remove any particular size of particles.

INTRODUCTION

Particulate emissions by stationary (industry, households) or mobile (cars) sources make part of the classical air polluting matters. Especially, the respiratory fraction (commonly „fine dust"), i.e. dust with aerodynamic diameter Ø up to 10 micrometers, is frequently subject to discussion in the last years. In Europe, the transmission of EU guideline 1999/30/EG into national regulations of the different countries has lead to limitation of dust immission (or particulate concentration level in ambient air) in every member state of the EU, and the limits are frequently stepped over, mainly in big towns. Also the emission levels of particulate matter of stationary sources is controlled by national regulations in all EU member states. Today the IPPC guidelines (1) per sector are applied to determine these limits ("Glass BREF").

Figure 1:
Principle of the impactor: one nozzle
→ not a filter! (except last stage)

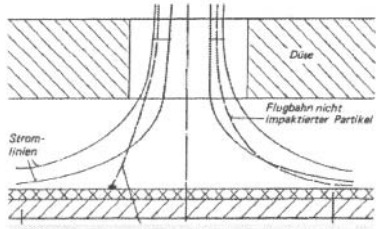

Particles fly on different trajectories following their individual mass.

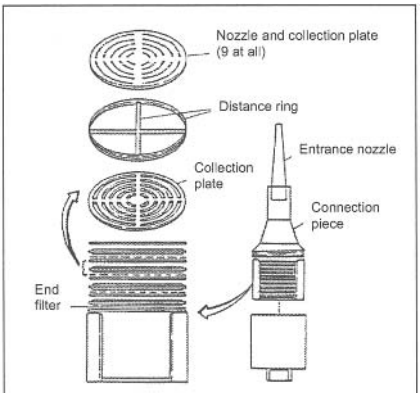

Figure 2: Assembly of the impactor
(Typ M III, Andersen Inc., Atlanta, Georgia 30220, USA)

Following the current regulation, the glass industry is emitting "mainly" fine dust. In this context, a differentiation is actually made between PM10 ($Ø \leq 10\ \mu m$) and PM2.5 ($Ø \leq 2.5\ \mu m$). From the discussion about respirable crystalline SiO2 particulate matter (cristobalite, quartz, but not tridymite) a PM4 ($Ø \leq 4\ \mu m$) limit, and even smaller ("ultra-fine") particles ($< 1\ \mu m$) are under discussion to be limited, but in the present study, we didn't address the latter. The limit values always refer to „aerodynamic" diameter, i.e. (citation[2]) „Particles passing through a size selective inlet of aerodynamic diameter x □m, with an abatement efficiency of 50%".

The particle diameter distribution is measured gravimetrically by impaction, see figures 1 and 2. At waste gas temperature, the gas containing the dust particles passes trough a series of "nozzles" with decreasing diameter, and is forced to fly a curve after every nozzle. Particles coarser then the aerodynamic diameter of the actual stage touch the "substrate" (quartz fiber material used by the participants of the study) and are impacted. Aerodynamically smaller particles are flushed away with the gas flow. From stage to stage, the impacted particles are smaller and smaller. The last stage of the impactor is a quartz fiber filter with high filtration efficiency, absorbing also the very finest particles quantitatively.

The upper and lower particle size limits of the given impactor are controlled by the choice of the right entrance nozzle and the drawing velocity of the gas pump. Also the waste gas temperature, humidity and density have to be taken into account. In the actual study an eight-stage round nozzle impactor Mark III of ANDERSON inc. (USA) was used by the participants of the ICG-TC13 study(3). The time needed for one measurement may vary largely, from 15 minutes in a raw (i.e. un-cleaned) gas, up to 24 hours in a very clean gas downstream a new electrostatic precipitator (ESP). The following table 1 shows an example for the raw results such a measurement in clean gas.

Table 1: Example for a raw measuring result, size intervals and collected masses

Stage	Size interval		$d_{ae\,50}$	Mass of plates		Mass impacted
Nr.	from µm	to µm	µm	before g	after g	mg
1	10,99	ad infinitum	---	0,4474	0,4482	0,8
2	7,24	10,99	9,1148	0,4725	0,4735	1
3	4,64	7,24	5,9382	0,403	0,4041	1,1
4	3,23	4,64	3,9342	0,3994	0,4004	1
5	1,76	3,23	2,4954	0,4589	0,4592	0,3
6	0,77	1,76	1,2651	0,3888	0,3898	1
7	0,41	0,77	0,5866	0,4063	0,4175	11,2
8	0,27	0,41	0,3400	0,3657	0,3784	12,7
F	**0,00**	0,27	0,1368	0,4347	0,4428	8,1

F: Final filter

Also without computing, a size distribution including two maxima is easily identified on this list. A high concentration peak is seen on stage 7/8 (0.27-0.77 micrometer) and a smaller one on stage 3 (4.64 to 7.24 micrometer). The exact evaluation is made using a computer program called WINCIDRS, included in the purchased measurement equipment. It calculates a 40 point size distribution curve, taking into account the kind of impactor (apparently the program is used for other impactor types as well), the masses impacted on the different stages, the pump rate, the entrance nozzle diameter, the gas density and the gas temperature. Unfortunately there is no literature available for this calculation proposed by the instrument's provider, but the procedure is exactly the same for every measurement, so that the results are at least comparable, e.g. between raw and clean waste gas. But the results are also qualitatively plausible, i.e. the two maxima size distribution seen in table 1 is reflected in a reasonable way in the calculated curve.

Example: Line n°.8		
Tonnage	575	t/day
Glass kind	clear	
Waste gas temperature		
Channel	458	°C
Stack	250	°C
Firing		
Fuel oil	---	kg/h
Natural gas	ca. 4000	Nm^3/h
Electrostatic precipitator		
Number of fields	3	
Absorbant	bicarbonate	
Flow of abs.	45	kg/h

In the following, the results obtained in both raw and clean gas are illustrated by an example (see table: Example: Line n°.8, and figure 3). Particle size distribution is given on the basis of differential mass. In every point, the measurement was carried out three times, but we never found significant differences comparing successive measurements. It becomes clear that indeed mainly fine dust is emitted (lists besides diagrams) also in the clean gas. In the example, the removal rate of the ESP is very high: 99.4% with respect to the primary dust content upstream of the air pollution control system, but in other cases also smaller absorption rates down to 90% have been measured.

The extreme example is chosen here to show that, in spite of the great difference between the absolute concentrations, and in spite of the very different temperatures in the channel (458°C, un-cleaned flue gas measurement) and the stack (250°C, clean flue gas measurement) respectively, the results are very similar. The following figure 4 compares both curves in the same scales, the clean gas result is marked in red, because otherwise it would be invisible.

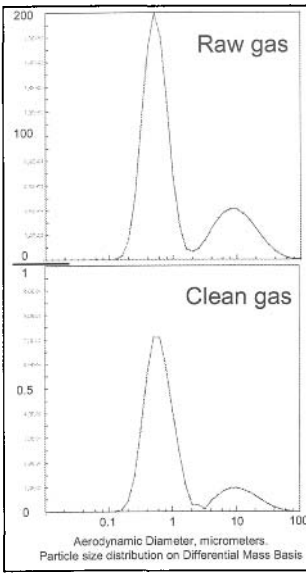

Figure 3:
Particle size distribution calculated for the example (Line n°.8)

	<10 µm	< 4µm	< 2,5 µm
Raw gas	**87,9 %**	**76.7 %**	**74.2 %**

	<10 µm	< 4µm	< 2,5 µm
Clean gas	**91,4 %**	**84,5 %**	**83,9 %**

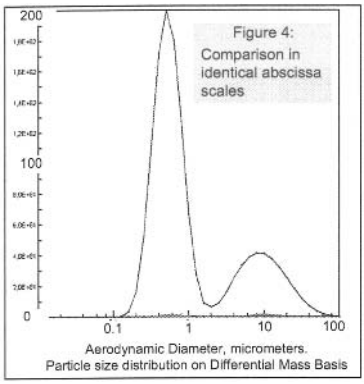

Figure 4:
Comparison in identical abscissa scales

The comparison with quantitative (total) dust measurements following VDI 2066(4) (a German standard for quantitative in-stack dust measurement using quartz fiber filters) did not show significant differences, but a remarkably higher scattering of the total concentrations obtained by the Mark III Impactor. The following diagrams of figure 4, and table 3, resume all measurements obtained in the study by our institute. Numbers from 1 to 8 signify different production lines with different operating conditions, as mentioned above; in every line, a series of measurements were taken, and the average values obtained are represented in the diagrams of figure 5.

The other ICG-TC13 member's results are very similar, but actually not yet ready for publication. The publication will be filed in Autumn this year (2009).

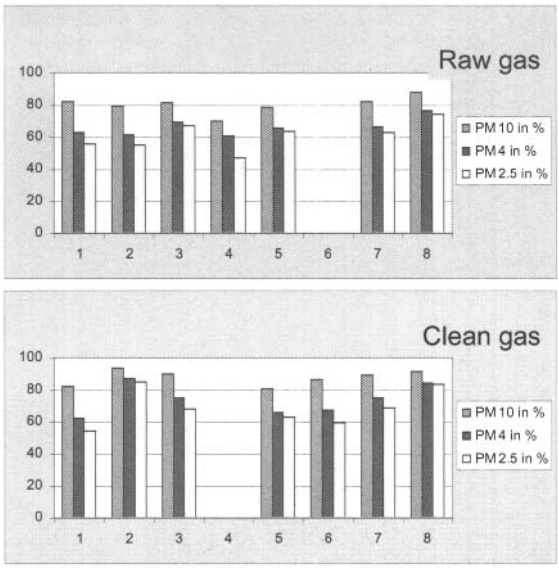

Figure 5:
Compilation of the results obtained (SG only)

PM10
ca. (80 ± 10)%

PM2,5
ca. (60 ± 10)%

Table 3: Compilation of results obtained (SG only)

Furnace	Fuel	ESP	Conc.(mg/Nm³)		MMD (µm)	
			Before	After	Before	After
1	Gas/Oil	Yes	203	1	1	1.9
2	Gas/Oil	Yes	168	13	1.6	0.6
3	Gas	Yes	157	6	1.22	0.52
4	Gas	No	112		2.4	
5	Oil	Yes	149	0.7	1.25	1.19
6	Gas	Yes		5		1.57
7	Oil	Yes	140	1	1.2	1.1
8	Gas	Yes	164	2.4	0.64	0.67
		Averages	156	4.2	1.3	1.1
		Standard deviations	±27.9	±4.4	±0.6	±0.5

Empty field: not analyzed / ESP not available

INTERPRETATION

There is not a significant difference in the shape of the size distribution curves of the particulate matter between raw and clean gas (but well in the concentrations);

There is also not a significant difference of size distribution shapes of dust particles between the different production lines, in spite of their different parameters (kind of fuel, pull rate, cullet percentage, temperature of the ESP and the measuring points a.s.o.).

The chemical analysis (done by microanalysis, see example of figure 6) of the particles absorbed on the different stages of the impactor instrument is – within the precision of the EDX used – the same, but with different scrubbing reagents we find different compositions. Using bicarbonate, nearly no calcium can be seen, but using lime hydrate, the latter's peak is clearly visible in the EDX spectrum.

Figure 6:
Example (Electron microscope / EDX spectrum) of dust collected in clean gas:

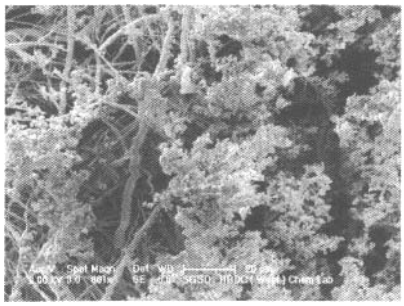

Gas fired float furnace
Absorbent = $Ca(OH)_2$
Plate n°.5

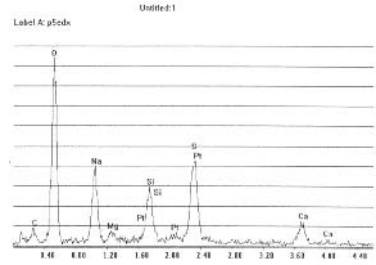

The Si peak in the spectrum is caused by the impaction material (pure SiO_2 fibers).

Additionally, the chemical analyses of clean gas dust sampled following VDI 2066, and the collected ESP dust appear to be significantly different. In the example of table 4, the furnace was fired with heavy fuel oil, and 15 kg/h lime hydrate was added to the flue gas for scrubbing.

Obviously, the clean gas dust mainly consists of unabated primary raw gas dust (the primary dust already contains ca. 2.4 wt.-% CaO !), and only in a low amount of fines from the (reacted) scrubbing reagent.

Table 4: Dust analysis in (wt.-%) / (standard deviation)

Analysis of **clean gas dust** captured following VDI 2066			Analysis of dust collected in the **electrostatic precipitator**		
11+Na2O	35.44 % ±	0.17	11+Na2O	16.68 % ±	0.13
12+MgO	1.88	0.04	12+MgO	0.582	0.023
13+Al2O3	1.74	0.04	13+Al2O3	0.261	0.015
16+SO3	54.10	0.48	16+SO3	34.05	0.59
			17+Cl	0.539	0.022
19+K2O	1.14	0.02	19+K2O	0.369	0.013
20+CaO	3.63	0.21	20+CaO	30.05	0.60
22+TiO2	0.0801	0.0074	22+TiO2	0.0134	0.0011
23+V2O5	0.463	0.017	23+V2O5	0.204	0.003
28+NiO	0.089	0.019	28+NiO	0.0315	0.0008

CONCLUSIONS AND SUMMARY

Because the calculation method of the dust size distribution curves (the software is supplied by the company that sells these instruments) is unknown, its algorithm cannot be checked, but the method is the same with every measurement, and the results obtained with the ANDERSON MARK III impactor are plausible.

Ca. (80 ±10)% of both the raw and clean gas dust is PM10,
ca. (60 ± 10)% is PM2,5 .

Fine dust and coarser dust in the flue gas are reduced by the same degree comparing the flue gas upstream of the scrubber with the flue gas downstream the ESP, the particle size distribution shapes in raw and clean gas are very similar in nearly every case.

The chemical composition of the clean gas dust resembles the raw gas dust, but it is significantly different from that of the collected ESP dust in our cases (float gas furnaces, using both bi-carbonate and hydrated lime dry-scrubbing).

Most of the fine raw gas particles are ad/absorbed, before filtration by the ESP, on the bigger particles of the scrubbing reagent (5). This mechanism is very important for the abatement of fine and finest particles.
→ The biggest part of the dust passing through the ESP is un-absorbed raw gas dust, only a little fraction is coming from the fines of the scrubbing reagent.

(1) http://www.ipcc-nggip.iges.or.jp/public/gl/invs1.html

(2) http:/ /www.epa.ie/downloads/legislation/air/quality/EU_Directive_Air_99-30-EC.pdf; p.2

(3) Instruction manual, Mark ii and iii particle sizing stack samplers, Thermo electron company, 27 Forge Parkway, Franklin, Massachusetts.

(4) German VDI 2066 "Particulate matter measurement - Dust measurement in flowing gases - Gravimetric determination of dust load". Beuth Verlag GmbH, Burggrafenstraße 6, 10787 Berlin, Germany, Nov. 2006

(5) Kasper, A., Carduck, E., Manges, M., Stadelmann, H., Klinkers, J.: Particulate emissions in the flue gas of flat glass furnaces after electrostatic precipitators. Glass Sci. Technol. 77(2004)n°4 pp.177-185.

This Page Intentionally Left Blank

CERAMIC FILTER ELEMENTS FOR EMISSION CONTROL ON GLASS FURNACES – EFFICIENT MULTI-POLLUTANT TREATMENT IN A SINGLE STEP

Gary Elliott and Andrew Startin
Clear Edge Filtration GmbH. Cerafil Division
Salzgitter, Germany

ABSTRACT

Glass furnace off gases are at elevated temperature and carry a cocktail of pollutants. The pollutants in glass furnace off gases are dust particles, oxides of sulphur and oxides of nitrogen. Well established techniques exist for treating these pollutants, either individually or in combination notably electro-static precipitators, fabric filters and Selective Catalytic Reduction (SCR). Each technique has its limitations to effectively and economically clean up the mixture of pollutants present in the gas stream.

An emerging technology for glass furnace off gas clean up is the employment of low density ceramic filter elements. Ceramic filter elements are extremely efficient and work well in combination with a dry scrubbing agent for acid gas removal. Furthermore the filtration temperature can be maintained at a suitable level for catalytic treatment of NOx.

The Clear Edge catalytic ceramic filter element, registered trade name Cerafil TopKat, offers deNOx functionality as well as efficient particulate and acid gas removal. Thus the major pollutants emitted by a glass furnace can be treated in a single piece of equipment. The technology, apart from major environmental performance benefits, offers the possibility of substantial savings both in monetary terms and space utilisation. The issue of available space is of paramount importance for many existing glass manufacturing sites.

The use of ceramic filter technology also offers the potential for phased implementation of pollution abatement equipment and the ability to meet abatement requirements without unnecessary or premature expense.

1. INTRODUCTION

Gas filtration employing rigid low density ceramic filter elements, also known as ceramic candles, is now a well established technique for cleaning off gases from industrial processes. The product was initially developed in the mid 1980's in response to the need to clean hot dirty gas from coal gasifiers down to levels of particulate matter sufficiently low provide a clean fuel gas to a turbine.

The earliest commercial applications for the product were rather specialised but application soon broadened out to a wide variety of duties where the benefits of the product could be exploited. This process was accelerated by the introduction of monolithic filter elements in the early 1990's and large robust filters in the mid 90's which made ceramic filters user friendly and compatible with techniques used in fabric filtration.

The benefits of ceramic filters are focussed on the need to filter gas, either process or off gas, at a high or variable temperature while delivering high particulate removal efficiency. Key applications therefore include waste incineration and gasification, metals processing, mineral processing and glass melting. The majority of duties are air pollution control (APC) however there is also now an increasing uptake of ceramic filters for process filtration and product recovery duties.

In recent years the demands on gas filtration media have strengthened in parallel as legislative emission limits have tightened. These trends have precipitated an ongoing development program aimed at providing a range of ceramic elements tailored to meet the demands of industrial end users. Cerafil TopKat (patent granted 2007) represents a revolutionary development in the technology. The filter element, jointly developed with Haldor Topsøe A/S, incorporates an integral catalyst capable of significantly reducing dioxin, NOx and volatile organic compound (VOC) emissions and still is able to remove particulates and acid gas emissions at the same time.

2. CHARACTERISTICS, BENEFITS AND APPLICATION

Low density ceramic elements (ceramic elements) are produced in a variety of sizes from 60mm outside diameter and 1 meter long up to 150mm outside diameter and 3 meters long (2.4" diameter and 39" long up to 6" diameter and 120" long). The larger sizes can be employed like fabric bags in new equipment and can also be retrofitted into existing plant.

Ceramic elements are manufactured from ceramic or mineral fibres, which are bonded together with a combination of organic and inorganic binders. Elements are formed into a shape which incorporates an integral mounting flange resulting in a rigid, self supporting structure. Ceramic elements take the benefits of fabric bag filtration a stage further by offering excellent filtration efficiency coupled with the ability to operate at elevated temperatures. This latter benefit is utilised across a broad spectrum of industrial applications where there is a requirement to filter gases which are at a high or variable temperature or where temperature surges can occur. This is at temperatures above 250° C (480° F) or where temperature surges are above this temperature. An otherwise stable operation can suffer from temperature surges, which can be very damaging to conventional fabric media. When such events occur it is not just the cost of the media which has to be taken into account; the costs associated with an unscheduled filter plant shutdown can also be high. These benefits can be directly applied to the glass furnace operator to realise a more forgiving reliable and robust pollution control system as well as a more efficient and better performing system.

The benefits to the end user of high or elevated temperature filtration include-

- Move away from the temperature limitations imposed by fabric bags
- Reduced requirement for gas dilution results in smaller plant
- Acid and water dew points can be avoided thus minimising plant corrosion
- The gas temperature can be maintained for optimal deNOx without the need to re-heat gases
- More efficient acid gas scrubbing at elevated temperatures to remove SOx
- Elevated temperature gas cleaning gives the potential for heat recovery from clean gas
- Higher stack exit temperatures increase gas buoyancy, decrease plume visibility and reduce the risk of plume grounding

The rigidity of ceramic elements further promotes cake filtration since the protective dust layer is not compromised during cleaning. Ceramic elements are employed on duties where the benefits, described earlier, of the medium can be effectively utilised. This is typically duties where high capture efficiency is required in combination with temperature resistance. However it is worthwhile stressing that ceramic elements are not simply a "hot gas filter". Although ceramic elements can be and are applied in high temperature filtration duties they are equally applicable where the filtration temperature regime is variable or subject to surges which could damage conventional fabric media.

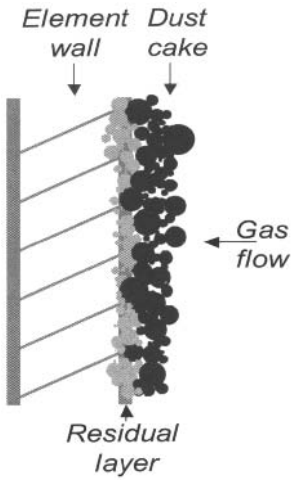

High filtration efficiency is a key benefit associated with ceramic filter elements. This results from the development, during the early stages of operation, of a protective dust layer on the element surface which promotes cake filtration. Cake filtration is essential to long term performance of a barrier filter medium. Even after cleaning with a pulse of air there is a residual dust cake on the surface of the element ensuring continuity of filtration efficiency and acid gas treatment.

3. CATALYTIC CERAMIC FILTER ELEMENT DEVELOPMENT

Clear Edge, in collaboration with catalyst experts Haldor Topsøe A/S of Denmark have developed a catalytically active ceramic filter element which is patent protected. The filter element incorporates an integrated catalyst formulated to oxidise dioxins and reduce NOx, the latter in combination with ammonia or urea injection. The catalyst is also effective at oxidising VOC's where the operating temperature regime is sufficiently high for instance above 220° C.

The catalyst material is a proprietary mixture of oxides which is incorporated into the body of a filter element in such a way as to ensure even distribution. The SEM below shows the distribution of catalyst within the filter and EDAX plots confirm an excellent distribution of catalyst within the filter thickness in turn maximising the time for the catalytic reaction to take place as the gases pass through the catalyst distributed throughout the 20mm (3/4") thick element wall

As can be seen, in the SEM below, the mixed oxide catalyst materials are distributed throughout the depth of the filter body thus ensuring maximum possible residence time. Catalyst efficiency is further enhanced by virtue of the fine nano sized particles of the material employed. This application of nano technology ensures that the diffusion restrictions associated with conventional catalyst technology are eliminated thus ensuring optimal removal efficiencies.

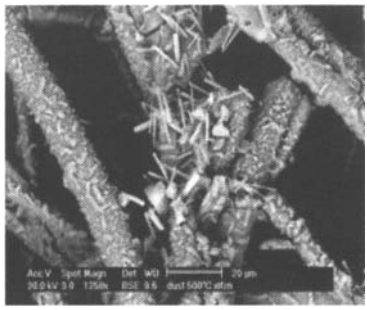

This photo shows an SEM image of a portion of filter body. The catalyst particles can be clearly seen as needle like particles bonded into the fibre matrix

4. PERFORMANCE

The catalytic filter builds on the efficiency and temperature capability of ceramic elements by adding the ability to dramatically reduce dioxin, NOx and VOC emissions. As these species increasingly become the focus of environmental legislation technically and economically effective means of controlling them need to be developed. Selective catalytic reduction (SCR) can be employed for glass furnace off gas NOx reduction, particularly where primary controls are unable to meet local legislative requirements. The technology is effective but there are drawbacks. SCR catalysts can be poisoned by particulate matter carried over from upstream abatement plant. This is especially critical where electrostatic precipitators (ESP's) are employed since emissions of the order of 20 – 30 mg/Nm3 (0.008-0.012 grains per scfm) are typical, and can be significantly higher during upset conditions. The use of catalytic filter elements is a potential solution providing the necessary removal efficiency through a filter plant with the minimum of ancillary components. The dust poisons are prevented from contacting the catalyst particles and the dust collected accumulates on the surface of the filter. This leaves a cleaned gas to pass through the filter element ensuring close and intimate contact with the catalyst. The catalytic reaction is enhanced compared with standard SCR technology, as the contact time is not reduced by diffusion of gases in and out of the catalyst pores. This diffusion slows the reaction and can lead to slippage of untreated gases with SCR systems.

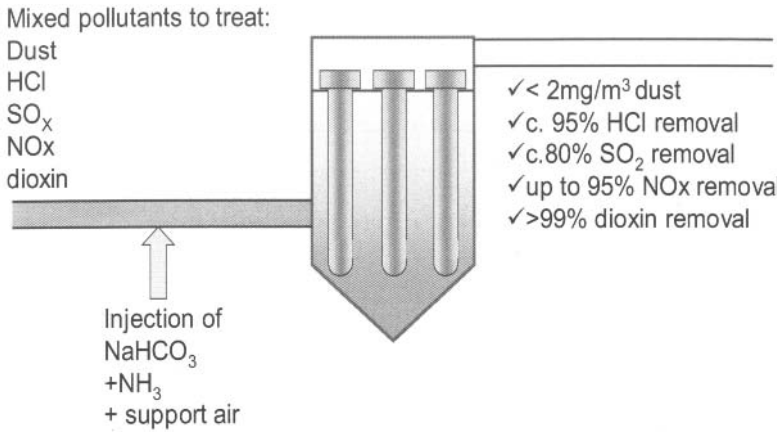

This simple schematic demonstrates how a single piece of equipment can be utilized to eliminate and destroy a combination of pollutants. Dry acid scrubbing requires a sorbent such as sodium bicarbonate and the destruction of NOx requires the addition of ammonia or urea and the catalyst acts to break down NOx at relatively low temperatures to form nitrogen and water.

$$NO + NH3 + 0.25O2 = N2 + 1.5H2O$$

Dust emissions are below 2mg/m3 or 0.0008 gr/scfm.

5. IMPLEMENTATION AND TECHNOLOGY OPTIONS

There are currently three options available for reducing emissions from glass melting furnaces. Where particulates are the only pollutant to be controlled then electrostatic precipitators or bag filters have been widely applied in Europe. Electrostatic precipitators operate at high temperatures and have a low pressure drop but are limited to efficiencies around 20mg/m3 (0.008gr/scfm) of dust with 3 or field units and cannot cope very well with surges in gas volumes or particulate levels. Where higher efficiencies are required bag filters have been used and emissions can be reduced to around 5mg/m3 (0.002gr/scfm). The drawback with bags is that they are limited to use below 200° C or if special fabrics are used then 250° C (392°F or up to 480°F) can be attained.

The filtration mechanism exhibited by ceramic filters is essentially a surface filtration phenomenon. This results from the development, during the early stages of operation, of a dust layer on the element surface which promotes cake filtration. The dust layer is a mixture of dust from the furnace and sorbent added to react with and control acid gas emissions. Cake filtration is essential to long term performance of a barrier filter medium. Even after cleaning with a pulse of air there is a residual dust cake on the surface of the element ensuring continuity of filtration efficiency and acid gas treatment. The presence of the dust cake firstly prevents very fine particles from penetrating the filter medium giving a steady pressure drop and long term stability and secondly presents an active cake of sorbent

ensuring intimate contact with acid gases as they pass through the depth of the cake. This ensures a high removal efficiency of acid gases as well as extremely low particulate emissions.

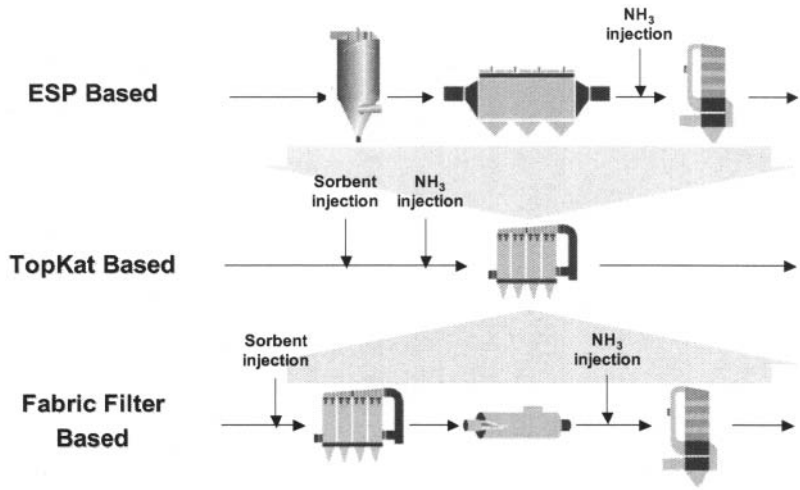

If acid gases have to be controlled then a dry scrubbing agent has to be injected into the gas stream. Dry scrubbing of acid gases is widely applied across many industry sectors and is an effective way to remove gaseous acids converting them into a solid by-product that can then be easily collected by the filtration system. Clearly barrier filtration systems such as bags and ceramic filters have an advantage here over electrostatic precipitators as efficiency of removal is very high and consumption of sorbent is kept to a minimum. Sodium bicarbonate or lime are the common sorbents used. Often an extra stage of equipment is needed and a scrubbing tower is inserted into the equipment line ahead of the precipitator to ensure intimate mixing of acids and sorbent and this is not necessary with barrier filters. Dry scrubbing has an advantage over wet scrubbing technology as the by-product is collected dry and requires no further treatment before disposal.

The reactions showing conversion of a gaseous pollutant to a solid are shown below;

$$Ca(OH)2_{solid} + SO2_{gas} + 1/2O2 = CaSO4_{solid} + H2O$$

$$2NaHCO3_{solid} + SO2_{gas} + 1/2O2 = Na2SO4_{solid} + H2O + 2CO2.$$

Where deNOx is required and the limits are so low that SNCR cannot be employed then an SCR is used and a catalyst is employed to increase the reaction rate to reduce NOx emissions.

The dust particles from a glass furnace can contain sodium salts and unfortunately this acts as a poison on the catalysts used in this process so even with emissions as low as 20mg/m3 (0.008gr/scfm) of dust there can be a significant effect over time on the SCR catalyst. Bag filters are efficient enough

to remove this threat of catalyst poisoning but at the low temperatures enforced on the filtration system by the limitations of the fabric itself then a re-heat of the flue gases is needed to increase the temperature to that where the SCR catalyst can work efficiently.

It can be seen that the ceramic filter option is an elegant solution to these technical issues. The filter and the catalyst can comfortably and efficiently operate at the same temperature and of course the dry scrubbing operation can also be accommodated therefore removing the need to cool gas and reheat. An added advantage is that the catalyst is buried within the filter element and allied with the highly effective surface filter the catalyst is protected from poisoning which will enhance both the effectiveness and the lifetime of the catalyst.

Ceramic filters offer the potential for phased implementation of pollution abatement equipment. In the first instance a filter based around standard filter elements can be installed. This phase provides particulate abatement, acid gas removal (with a sorbent) and sufficient temperature for future NOx control. At the point when NOx control is required the end user has the choice to opt for selective catalytic reduction (SCR) technology or retrofit the ceramic filter with Cerafil TopKat catalytic filter elements. The most appropriate choice can be made on the basis of economic and technical considerations. The attractions of phased introduction are the ability to meet abatement requirements without unnecessary or premature expense. The catalytic filter is well suited to the glass industry as it can handle the mixture of dust acid gases and NOx

	ESP + SCR	Bag filter + SCR	Cerafil TopKat
High temp ability	Good	Poor	Good
Footprint	Poor	Average	Good
Dust removal	Average	Good	Excellent
Pressure drop	Average	Average	Average
DeNOx capability	Good	Average	Excellent
Upset resistance	Poor	Average	Excellent
Suitable for small plant	Poor	Average	Good
References	Many	Growing	Small but growing
Capital cost	Lowest	Highest	Average
Operating cost	Average	Highest	Potential for lowest

Table showing a comparison between the different technology choices for pollution control in the glass industry.

6. CASE STUDY

A trial has been carried out in two European float glass lines in order to demonstrate the technology. The trials ran for several months and data was collected under different operating conditions to establish to optimum operation of the plant.

Exhaust gases exiting the furnace first pass through a boiler plant which drops the gas temperature to between 400°C and 470°C (750° F and 880° F). The filtration temperature was controlled by the addition of quench air. Volume flow through the plant was adjusted by means of a frequency inverter on the fan which in turn was controlled by the orifice plate flow measurement. The purpose of the trial was to determine the flow/pressure drop/temperature characteristics of the filter media along with NOx reduction efficiency. The SOx removal efficiency was also measured. The trial

result has allowed for the future scaling of full scale plants while a NOx reduction in excess of 80%, down to target levels, was easily achieved.

The pilot trial used a slipstream of gases from a producing furnace and demonstrated very clearly the effectiveness and the potential for the application of this technology within the glass industry. The effectiveness of gas acid scrubbing was excellent and deNOx was achieved by the addition of ammonia solution upstream of the filter plant.

Pilot unit details

Element type TopKat-3000
Quantity 40
Filter Surface area 56m2 /560ft2
Filtration temperature. 350°C /660° F
Gas flow Nm3/h 1800 /1060 scfm
NOx inlet concentration mg/Nm3 ~1200
NOx outlet concentration mg/Nm3 <200
NH3 used
Dust outlet less than 1mg/m3 0.0004gr/scfm
Face velocity m/s 0.02 /4ft/min
Pressure drop KPa ~1.75 / 7" wg

This graph shows the close correlation between actual and theoretical acid gas removal using sodium bicarbonate as a dry scrubbing agent at 350°C/660° F

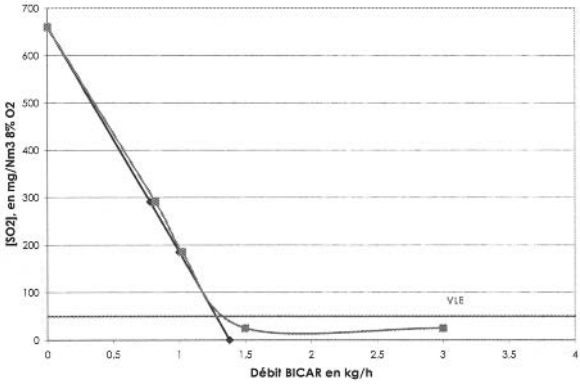

Lime can also be used to dry scrub acid gases from glass furnaces

This graph details the deNOx efficiency at 300°C/570°F again demonstrating the close correlation between actual and theoretical values.

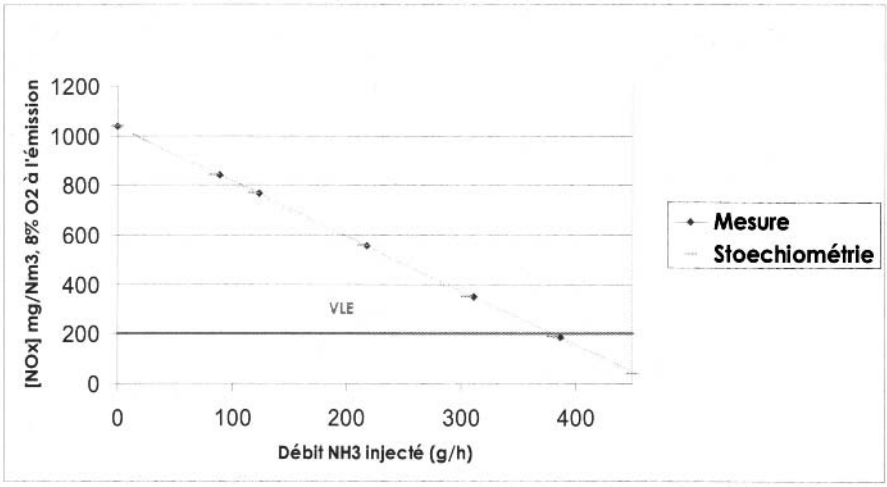

Following these successful trials two orders for the catalytic ceramic filter have been received. Both are for full sized units, one for a float glass line and the other for a container glass furnace.

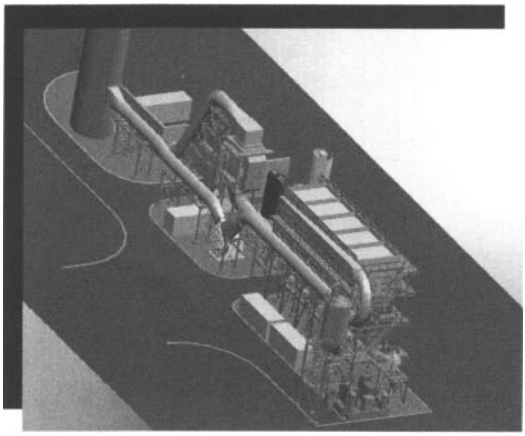

A schematic showing the first commercial plant in the glass industry using catalytic ceramic filter technology.

The first plant was commissioned in early September 2009 and the second is scheduled for November 2009.

7. CONCLUSIONS

The employment of low density ceramic filter elements for pollution control and product recovery applications is now well established. The principal benefits of ceramic elements are high filtration efficiency and high temperature capability now allied with a catalyst capable of removing NOx. These benefits can most effectively be utilised to treat the gases associated with glass furnaces.

Pollutants	Units	Filter inlet	Filter Outlet	Efficiency %	Limit
Dust	mg/Nm3	1,500	0.5	99.97	10
N0x	mg/Nm3	1,000	150	85.00	200
SO2	mg/Nm3	850	25	97.10	50
HCI	mg/Nm3	600	5	99.20	10

The above table shows actual results from a glass furnace measured over a two month period on a filter plant containing catalytic filters.

Cerafil TopKat represents a revolutionary advance in ceramic filter technology. This system offers the highest efficiency for particulate removal even with very fine particles and the new catalytic element extends ceramic filter capability by incorporating an integral catalyst for dioxin, NOx and VOC removal. The product has already exhibited excellent NOx removal ability both in pilot and full scale plants. Empirical data collected to date has demonstrated that it is possible to effectively combine filtration capability with catalytic activity.

Following the successful trials at two major glass companies in Europe two orders were received for this new catalytic filter element system. One was for a float unit for the treatment of a gas volume of 80,000Nm3/h at 540°C/1000°F. The other was for treatment of a gas volume of 33,000Nm3/h at 350°C/660°F for a furnace producing glass for tableware.

The European Union BREF for the glass industry was published in draft form in July 2009. The latest reference document (BREF) generally gives information on a specific industrial sector in the EU, techniques and processes used in this sector, current emission and consumption levels, techniques to consider in the determination of BAT, the best available techniques (BAT) and some emerging techniques. The document stated that;

"The use of ceramic filter elements represents an emerging technique for treating flues gases generated by glass melting furnaces. Ceramic filters are very efficient for the separation of dust and will work well in combination with a dry scrubbing stage for acid gas removal. Furthermore given the refractory nature of the filter medium and the favourable filtration temperature the catalytic reduction of NOx emissions is possible with this technique by applying catalytic ceramic filters where the catalyst is incorporated into the ceramic filter elements. Thus the major pollutants can be treated simultaneously in a single piece of equipment"

"Ceramic filters offer the potential for phased implementation of the pollutant abatement equipment. In the first phase a filter based on standard filter elements can be installed for particulate abatement and acid gas removal maintaining sufficient temperature for future NOx control. In a second stage the filter may be retrofitted with catalytic filter elements for NOx reduction or a SCR system can be installed. The most appropriate choice can be made on the basis of economic and technical considerations. The phased introduction would avoid unnecessary or premature expenses. The initial costs of the catalytic ceramic filter can be substantially lower than traditional alternatives. When annualised operating costs are calculated the costs of energy, adsorbent, replacement of filter media, labour and other factors

should be considered. Cost calculations suggest that the lifetime ownership cost of a catalytic ceramic filter system is favourable when compared with other technologies"

ACKNOWLEDGEMENTS

Maguin sas 2, rue Pierre Sémard - 02800 Charmes - France - Tel 33 (0)3 23 56 63 00 www.maguin.com in particular David Gambier and Raoul Garcia. Maguin design and build filtration systems under the Cercat name, utilizing Cerafil Topkat, and ran the pilot tests detailed in this article. Maguin and Clear Edge Filtration subsequently received the first commercial orders from St Gobain and ARC for this new technological breakthrough.

This Page Intentionally Left Blank

REQUIREMENTS FOR GLASS COMPOSITIONS FOR SOLAR APPLICATIONS

A. Ganjoo, L. J. Shelestak, J. W. McCamy and M. Arbab
PPG Industries, Inc., Glass Business & Discovery Center
Cheswick, PA 15024

ABSTRACT

Glass substrates and cover plates form an integral part in harvesting solar energy, e.g., glass substrates for thin film solar cells, cover plates for c-Si solar cells, substrates for solar mirrors, and various other components. Since the cell efficiencies and performance of a solar harvesting device are directly related to the number of absorbed photons, the first and foremost demand for glass to be used in solar application is to have a very high transmission in the visible region of the electromagnetic spectrum. This makes the glass composition a very critical parameter as various additives to normal (clear) glass, which act as absorbing centers for photons in the visible region, need to be taken out of the glass compositions. In addition, one of the biggest requirements for solar glass is its chemical durability. Most of the harvesting devices/techniques involve exposing the device, and thus the glass, to outdoor environments. The glass needs to be durable to withstand sudden and drastic changes in temperature and humidity among other things for prolonged and effective use. Furthermore, the glass needs to be mechanically strong as it is exposed to harsh weather conditions, which include, rain, snow, sleet, hail, etc. In this paper, we will take a look at the various issues facing the glass selection in various solar related applications and will discuss the importance of glass composition in addressing these issues.

1-INTRODUCTION

New markets can increase the demand for glass products. The predicted growth of the solar energy industry is one such area, which has taken on even more importance with the recent concern with global warming from green house gas (GHG) emissions [1-2]. The requirements for glass compositions for solar applications vary depending on the end use, which can range from arrays of roof-top photovoltaic (PV) panels and concentrated photovoltaic (CPV) devices to massive solar power plants (SPP) generating up to 100 MW of electricity annually. Other growing markets include the use of glass in building integrated photovoltaic (BIPV) devices. Flat glass products for use in solar industry applications are manufactured today basically in only two forms for economic reasons to provide either improved solar light transmission or aesthetics. These include pattern glass used mainly as cover plates for photovoltaic solar cells, and float glass commonly used in new thin film photovoltaic applications, often in combination with transparent conductive oxide (TCO) coatings, antireflective (AR) coatings or mirror coatings on glass substrates.

Several flat glass producers have investigated methods to further improve light transmittance [3-5]. Innovative technical approaches are currently being explored to identify potential solutions when making float glass for solar applications. Newer applications need improved glass properties to satisfy solar power customer needs and expected performance specifications. This imposes several challenges to the glass manufacturer while targeting for the successful design of new solar glass products. The necessary R&D expertise is essential to identify possible new glass compositions that are compatible with current glass production processes and capabilities while still also complying with more strict environmental regulations. This paper will further investigate the key issues facing the glass selection in various solar related applications and will discuss the importance of glass composition in addressing these issues.

2- GLASS REQUIREMENTS FOR SOLAR APPLICATIONS

Recently, there has been increased interest in achieving better solar glass properties while still maintaining a very high glass transmittance. For certain applications, solar glass should have a total solar light transmittance of >90.2%. This generally requires the development of low iron containing glass compositions that also have low iron redox ratios (highly oxidized) to minimize the degrading visible and infrared light absorbing properties associated with greater Fe^{+2} contents. The iron redox ratio is defined as the wt. % FeO to total iron oxide wt. % as Fe_2O_3.

There are many factors that can affect the total iron content and glass redox during glass melting, including batching considerations such as the type and availability of raw materials employed, the addition of either oxidizing (such as sodium nitrate, salt cake, etc.) or reducing agents (coal, silicon, etc.) to the glass batch, and cullet percent. Steps must also be taken to remove any iron contamination when recycling cullet. Furnace operating conditions can also affect glass redox and include total residence times, furnace temperatures, and the partial pressure of oxygen in the furnace combustion atmosphere.

Besides high light transmittance, there are several other critical glass property requirements. One of the biggest requirements for solar glass is its chemical durability. Most solar applications expose the device, and thus the glass, to outdoor environments. The glass needs to be durable to withstand sudden and drastic changes in temperature and humidity among other things for prolonged and effective use. As a consequence of the forming process, the bottom surface of float glass is enriched in tin compared to the interior bulk glass composition. This can impact certain surface dependent glass properties including durability. It is well known that the bottom tin surface is more durable than the top air surface, which can necessitate proper surface orientation for end usage in solar applications [6]. Figure 1 compares the behavior of two commercial solar glass compositions after an exposure of 5.5 weeks in an accelerated durability test at 85°C and 85% relative humidity, which is a widely used qualification test for PV modules [7]. This severe test requires that the PV modules must pass 1000 hours exposure in the damp heat environment. The surface corrosion is mainly due to a water induced ion-exchange reaction with sodium found in the glass composition [3]. Both samples showed similarly acceptable corrosion behavior even though the two glasses had significant differences in composition. Therefore, the first main challenge is to improve the resistance to water/moisture attack as well as other chemical environments, while still being able to readily melt the glass.

The glass also must be resistant to solarization, which is the loss of light transmittance after prolonged exposure to sunlight [8], and thus resulting in darkening of the glass (or increasing the absorption coefficient). Therefore, the number of photons available to the PV cell decreases resulting in a lower power output. Of course, this is of great importance for solar energy applications. Two possible causes of solarization are 1) certain additives (such as Cerium) present in the glass composition, and 2) non-bridging oxygen (NBO) ions found in the glass structure which can generate intrinsic hole (h^+) color centers from the interaction between UV light and the glass. Figure 2 shows the loss in light transmittance for *Solarphire*™ glass, which is a cerium containing glass composition after exposure to sunlight for 28 days. Certain solarization reactions involve a redox reaction where one species is oxidized (loss of electron, e^-) by solar radiation (hv) as follows

$$(1) \quad X^{+2} + hv \leftrightarrow X^{+3} + e^-$$

and another species is reduced (gain of e^-)

(2) $Y^{+3} + e^- \leftrightarrow Y^{+2}$.

For example, two known solarization reactions are

(3) $4MnO + As_2O_5 \leftrightarrow 2Mn_2O_3 + As_2O_3$
(4) $Fe_2O_3 + Ce_2O_3 \leftrightarrow 2FeO + 2CeO_2$.

It is therefore important to avoid certain additives that are prone to solarization. Similarly, production of electron-hole pairs can be formed from UV radiation as follows

(5) $NBO + hv \leftrightarrow h^+ + e^-$

and thus generate hole centers localized at NBO sites [9]. These color centers also absorb visible light and decrease the number of photons reaching the PV cell. Therefore, the second main challenge is to identify solar glass compositions that have good resistance to solarization.

Furthermore, the glass needs to be mechanically strong as it is exposed to harsh weather conditions, which include rain, snow, sleet, hail, sand, etc. Good impact resistance is a further requirement. During manufacturing there is an obvious need to maintain pristine glass surfaces and to avoid creating any damaging surface flaws that can lower glass strength. Therefore, good scratch resistance is imperative. Often, thermally tempered glass is required to further strengthen the glass sheet for use in PV modules [10]. The trend is towards using even thinner glass to maximize light transmittance and give lighter weight devices, but glass strength can not be compromised. However, as the glass gets thinner it becomes more difficult to strengthen by thermally tempering. Therefore, the third challenge is to maintain high glass strength while producing thin glass plates.

The glass composition also must have certain other properties (see Table I) that are compatible with the glass melting process, including glass viscosity at log 2 (low melting temperature), liquidus temperature (good working range), low density (light weight), and acceptable softening point, anneal point and thermal expansion. In general, Figure 3 illustrates the relative functions of commonly used glass oxides in determining various glass properties [11]. The use of computer modeling to accurately predict glass properties can quickly identify possible new glass formulations. However, in order to maintain relative consistency in the physical properties of glass supplied from various manufacturers, a basic soda lime silicate composition has been maintained for use in solar glass markets.

3- SOLAR GLASS MANUFACTURING

A discussion of solar glass manufacturing can identify issues with production costs of low iron glass compositions. Figure 4 schematically depicts the float glass melting and forming process. The primary source of energy in glass melting is overhead heating by natural gas combustion with air as the oxidizing gas. More recently, oxy-fuel technology has been used where pure oxygen has replaced air. This has improved the energy efficiency of the furnace while drastically decreasing air emissions including GHG such as CO_2, as well as NO_x, SO_x, particulate matter, etc. Therefore, the production of solar glass can comply with "Green Engineering" principles in the glass manufacturing process.

There are several issues of significance that impact production costs. First, since heat is primarily delivered to the top layer of the glass melt, the spectral properties of the final product have a huge impact on the heat transfer efficiency throughout the depth of the glass melt, convective flows and refining of glass. Therefore, generally speaking, melting a "lighter" glass becomes more challenging. This in turn can influence the cost of homogenizing the glass and refining it, since these have to meet

strict quality requirements. Here, the use of CFD modeling can be useful in better understanding changes in glass flow patterns and temperature gradients in the furnace. In addition, the glass composition also influences the chemical reactions occurring in the glass batch, its melting rate, and the concentration of refining gases, e.g., SO_3, in the melt. Considering all of these parameters is critical to the design of a cost-effective solar glass product.

A final important factor to consider is the suitability of the furnace for product change. A float tank can hold up to several thousand tons of molten glass with a throughput of several hundred tons per day. If the tank is considered as a perfect mixer, then the time required for completing a product change can be long, e.g., seven to ten days in extreme cases, and costly. Depending on customer specifications, the comparatively minor modifications in glass composition for solar glasses may still result in long product changes; this requires careful attention to product sequencing. Here again, computer modeling of product changes has been helpful in better understanding ways to minimize product change times.

4- SOLAR GLASS COMPOSITIONS

Three examples of solar glass compositions and their key physical properties are listed in Table I. Glass 1 contains added Al_2O_3 and Glass 3 contains added MgO, while Glass 2 contains no deliberate addition of either Al_2O_3 or MgO. For comparison, the spectral transmission curves for two solar glass products (*Solarphire*™ glass and *Solarphire*™ PV glass, which are low iron float glasses made by PPG Industries, Inc.) are compared to clear float glass in Figure 2. A low total Fe_2O_3 content is very important in producing solar glass since Fe^{+3} contributes UV absorption, while Fe^{+2} supplies visible and IR absorption. Through proper control of the total Fe_2O_3 content and the glass redox ratio the glass color can be changed from yellow (when most of the iron oxide is present as Fe^{+3}) to blue (when most of the iron oxide is found in the Fe^{+2} state). Typical clear float glass contains about 0.10 wt. % Fe_2O_3 and has a redox ratio of about 0.27-0.34, and therefore has its familiar greenish edge color.

Of course, in very high transmittance glasses, all colorants, including iron oxide, need to be avoided. As shown in Table I, solar glasses typically have very low total Fe_2O_3 levels of about 0.01 wt. % or less. Other colorants (such as chrome, cobalt, nickel, selenium, manganese, cerium, etc.) should be below ppm levels. By using very high purity raw materials commercial float glasses have been produced in thicknesses ranging from 2 mm to 19 mm. The ability to accurately control the glass redox ratio and the glass colorant impurity levels has led to the production of a variety of new glass products with a wide range of aesthetics to meet the market demands for solar glass. As the ongoing development of new glass products continues at an even more rapid pace, the flexibility of the glass melting process will likely provide even greater benefits in the years to come.

Certain solar glass products are now routinely made at throughput levels of 550-650 T/D. Several process related advantages are achieved, such as 1) the ability to adjust iron redox ratios for enhanced product attributes, 2) lower environmental emissions, 3) shorter product transition times, 4) increased production flexibility, and 5) the ability to supply lower volume glass products for niche markets (shorter production runs now become economical). Product applications include cover plates for solar cells, thin film photovoltaic glass substrates, and solar mirrors for power plants, etc.

In designing the solar glass product, the glass manufacturer can choose from several options of glass compositions and coatings, or a combination thereof. This choice is driven by several critical customer requirements: aesthetics or appearance, solar transmittance requirements, end use performance, and material cost, among others. The glass supplier must be sensitive to all these needs while offering a product portfolio that agrees with its own business goals. During its fabrication glass usually

undergoes such process steps as cutting, edging, washing, coating, tempering or bending, and laminating. The overall process must be economically acceptable to both the supplier and the customer. Thus, the product has to be process robust. For example, it must be mechanically durable and amenable to glass tempering or bending. Thus, compromises are necessary in the ability to choose the product with the right performance for a given end use at an acceptable price, and the ability to process it economically and without unnecessary dependence on the production schedule of the glass supplier. Glass 3 as given in Table I is currently being produced for solar glass applications.

5- TRANSPARENT CONDUCTING OXIDE (TCO) COATINGS ON GLASS

In the case of thin film PV modules, another important part of the total stack is a transparent conducting oxide (TCO) layer deposited on the glass. The commonly used TCO material used for various solar applications is SnO_2 doped with Fluorine. This material is less expensive and with precursors readily available, SnO_2:F can be easily deposited by on-line and off-line atmospheric pressure chemical vapor deposition (APCVD). Fluorine is added to increase the conductivity of SnO_2. The main criteria for TCO coatings on glass for solar applications are high transmission, low sheet resistance (high conductivity) and high chemical durability. Generally, another layer(s) is deposited between the glass and the TCO layer which serves as a barrier layer against alkali diffusion from the glass. Further, the composition of this underlayer can also be tailored to reduce optical losses caused by the difference in refractive index values between the TCO (n~1.9) and glass superstrate (n~1.5).

Another important property for the TCO layer is the magnitude and direction of the forward scattering of light (i.e., haze). For those thin film modules where the physical thickness of the PV active layer is shorter than the 1/e absorption length of the material, the scattering can provide for an increase in the path length the photons travel through that layer. For example, in the case of a-Si modules the active layer thickness is typically less than 1μm and a high haze TCO is preferred. This is ironic in that glass manufacturers have spent decades developing and producing coatings that minimize the level of haze.

6- CONCLUSION

The main challenges to the design of new glass compositions that meet solar glass customer's requirements calls for compromises in performance and manufacturing while still controlling costs. In the future, as the solar market demand grows for low iron float glass products with even better solar transmission properties, further research and development efforts will continue to strive to better understand the relationships between glass composition, iron content, glass redox and glass properties. It is expected that computer modeling will play a much larger role in the further development of glass compositions. Therefore, glass manufacturers will ensure that new glasses will continue to be commercially available over a broad range of compositions and properties.

7- ACKNOWLEDGEMENTS

We thank our co-workers at PPG Industries, Inc. especially Mike Buchanan, Dave Haskins, Kevin Hill and Pam Snyder for their help.

REFERENCES

1. J. Deubener et al., *J. Eur. Cer. Soc.,* Vol. 29, 2009, pg. 1203-1210, "Glasses for Solar Energy Conversion Systems."
2. *Ceramic Industry*, Vol. 158, Dec. 2008, pg. 16-19, "Harnessing the Sun."
3. N. G. Dhere et al., *Proc. of 29th IEEE Photovoltaic Specialists Conference*, May 19-24, 2002, New Orleans, LA, pg. 231-234, "Effect of Glass Na Content on Adhesional Strength of PV Modules."
4. T. Doege et al., *Glass Researcher,* Vol. 12, Nos. 1 & 2, Fall 2002 & Spring 2003, pg. 5-7, "Textured Glass Increases Light Transmission in Solar Modules."
5. S. V. Thomsen et al., U.S. Patent Application Publication No. 2006/0249199 A1, published 11/9/06, "Solar Cell Using Low Iron High Transmission Glass with Antimony and Corresponding Method."
6. M. Feldmann et al., *J. Non-Cryst. Solids,* Vol. 218, 1997, pg. 205-209, "Initial stages of Float Glass Corrosion."
7. International Standard IEC 61215, "Crystalline Silicon Terrestrial Photovoltaic (PV) Modules – Design Qualification and Type Approval," International Electrotechnical Commission, Geneva, Switzerland, 2005.
8. D. E. King et al., *Proc. of 26th IEEE Photovoltaic Specialists Conference*, Sept. 29-Oct. 3, 1997, Anaheim, CA, pg. 1117-1120, "Optical Changes in Cerium-Containing Glass as a Result of Accelerated Exposure Testing."
9. K. Bermuth et al., *Glastechn. Ber.,* Vol. 58, No. 3, 1985, pg. 52-58, "Solarization Phenomena in Soda-Lime-Silica Glasses Containing Cerium and Arsenic."
10. T. M. Shimpi et al., *J. Testing & Evaluation,* Vol. 36, No. 2, 2008, pg. 207-212, "Effect of Hail Impact on Thermally Tempered Glass Substrates Used for Processing CdTe PV Modules."
11. S. R. Scholes, Modern Glass Practice, Industrial Publications, Inc., Chicago, IL, 1952, pg 17-18.

Table I. Comparison of Low Iron Glass Compositions

Glass composition, wt. %	Glass 1	Glass 2	Glass 3
SiO_2	73.2	73.3	72.5
Na_2O	14.5	15.0	13.9
CaO	10.2	11.1	10.2
MgO	0.1	0.1	3.0
Al_2O_3	1.6	0.04	0.04
Fe_2O_3	0.01	0.01	0.01
Other (K_2O, SrO, SO_3, etc.)	0.39	0.45	0.35
Total	100.0	100.0	100.0
Glass Properties:			
Viscosity Log 2 (°F)	2622	2554	2570
Liquidus temp., TL (°F)	1807	1819	1857
Working Range, log 3.5 - TL (°F)	194	123	112
Softening Pt. (°F)	1341	1310	1329
Anneal Pt. (°F)	1022	1015	1014
Density (gm/cc)	2.49	2.51	2.50
Thermal exp., 25-300°C (10^{-6}/°C)	8.8	9.1	8.7
Tensile strength, MOR (psi)	6000	6000	6000
Durability: 85°C/85% RH test	marginal	poor	good

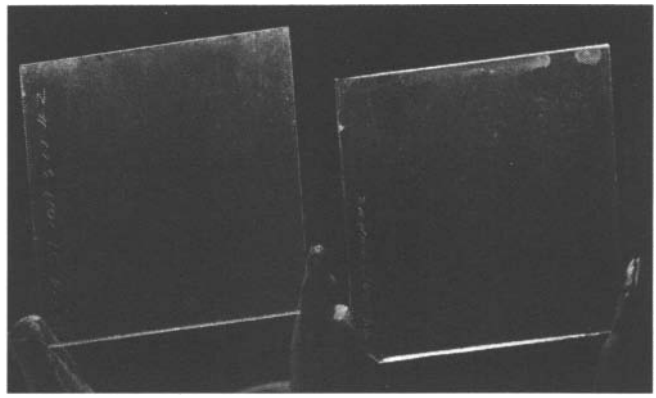

Figure 1. Comparison of performance for two commercial low iron float glass compositions in accelerated durability test after 5.5 weeks at 85°C and 85% RH.

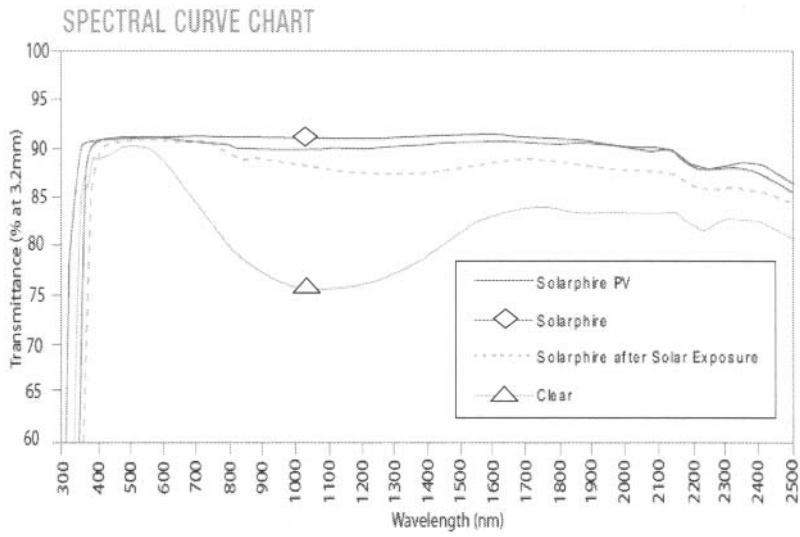

Figure 2. Transmittance curves of clear glass and two different low iron glass compositions. Also shown is the transmittance curve for *Solarphire*™ glass after solar exposure.

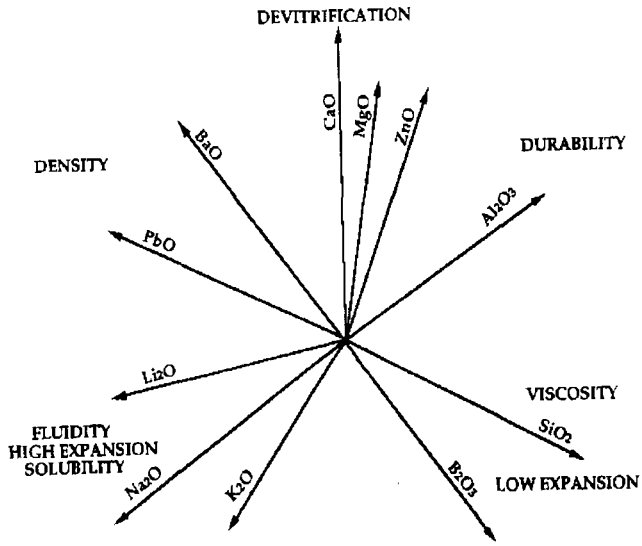

Figure 3. Relative Functions of the Glass-Making Oxides.

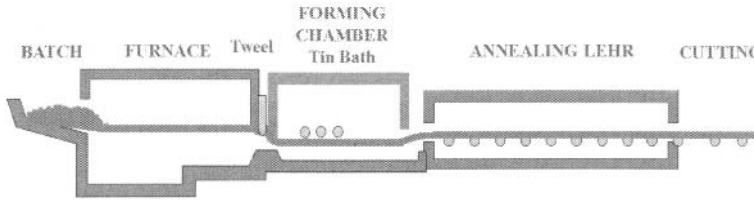

Figure 4. The float glass manufacturing process.

This Page Intentionally Left Blank

STRATEGIC MATERIALS: STRATEGIC PLANNING, GEOPOLITICAL FORCES AND RISK MANAGEMENT

Peter E. Wray
The American Ceramic Society
Westerville, OH 43082 USA
pwray@ceramics.org

ABSTRACT

Scientific and technical developments coupled with a surge in demand in emerging markets for industrial and consumer goods have begun to accentuate current and potential problems with sourcing strategic minerals and metals. This includes materials already in broad usage in major industries (e.g., bauxite) and materials whose usage is expected to grow geometrically and that are linked to significant progressive societal developments (lithium and rare earths). While, in theory, the amount of reserves of these special raw materials may be adequate, their location and ownership, often in underdeveloped nations, is transforming the bargaining powers and interests of various owners, businesses and governments. Some nations and enterprises appear to be grasping the significance of the materials problems and are taking aggressive geopolitical steps to manage their long-terms risks. Other nations, such as the United States, appear more lackadaisical and disorganized in their approach and arguably are increasing the risk of negative outcomes to their economic, scientific and diplomatic standings. Nations that will be in the best position are those that are making sober and multipronged assessments of the risks posed by materials shortages and are willing to move apace to take methodical multilateral steps to address these risks.

INTRODUCTION

Interest in strategic materials isn't necessarily new. Consider, for example, the attention that was once placed on natural rubber supplies as industrialization was getting underway in the West,[i] or the attention paid to uranium after Lise Meitner and Otto Robert Frisch identified the process of nuclear fission in 1939.[ii]

Concern about strategic materials is seldom static and often is linked to emergencies and discontinuities in technology. In the example of rubber, Brazil and its neighbors initially were the only exporters of the natural material. However, growing demand and shifts in international politics triggered the establishment of vast rubber plantations in Asia. Further disruptions in the supply and demand for rubber occurred frequently in the 20th century because of world wars, anticolonialism and developments in the transportation industry, beginning with the bicycle, the automobile and, more recently, advances in tire production. Additional disruptions occurred with the invention of synthetic rubber. Throughout this process, the relative economic and political strengths of nations and businesses were often in flux, shifting from stability to jeopardy.

At times the stakes were very high, such as in World War II when viable synthetic rubber production suddenly presented new opportunities for the Allied Nations. The United States approach to rubber supplies pre-World War II illustrates something of a positive example of strategic planning in regard to

an essential material. There were significant national risks at the time: risks of war in general; risks of war, in particular, with rubber-producing regions; risks of having a the military crippled by lack of tires and engine components; risks of having American agriculture and transportation businesses struggling to survive the Depression, cut off from essential raw materials; and risks that German scientists would be the first to succeed in developing a new and inexpensive rubber substitute.

U.S. officials eventually understood to a large extent that rubber supplies weren't just an industrial problem but a national problem. Many branches of the government and U.S. private sector were mobilized to stockpile rubber[iii], to identify new rubber sources and to increase the productivity of existing reliable sources. At the same time, the government launched a secret effort to perfect synthetic rubber production, in part leading to the successful efforts of B.F. Goodrich scientist Waldo Semon in 1940.

Did U.S. planning efforts succeed? Indeed they did, according Army historian Maj. Paul Wakefield:

> "Both the military and the industrial base needed rubber for vehicle tires, engine components and other machine parts, so this invention would prove critical to the Allied Forces during World War II. Even though the Japanese controlled virtually all of the world's rubber-producing regions in 1942, 50 U.S. factories were manufacturing synthetic rubber by 1944, producing a volume twice that of the entire world's natural rubber production before the beginning of the war."[iv]

Similar events occurred with U.S. concerns about silk supplies.

MODERN MATERIALS SHORTAGES

The worlds of science, business and technology recently faced the threat of shortage – if not real shortages – of several key materials: bauxite, lithium and rare earths.

Bauxite

Bauxite is an important material. It is a central raw ingredient in aluminum production and a major ingredient for the manufacture of refractory materials that make oven and ladle linings in the steel industry and kiln hardware used in the sintering of basic and advanced specialty materials, such as advanced ceramics.

The boom in steel production in the mid-2000s should have been a boom time for refractory makers, but they began to be stymied by the unavailability of bauxite, in large part because of booming aluminum manufacturing by China. China has become the world's largest smelter of aluminum, responsible for almost one-third of the world's production – and its share is growing. In 2007, its production increased 33.8 percent. Even with forced smelter cutbacks because of energy shortages and Olympics-related pollution concerns, Chinese aluminum production in June 2008 was up 20.2 percent year-on-year. Its domestic aluminum consumption grew by 22 percent. Worldwide, aluminum production increased by more than 10 percent in 2007. Consequently, world bauxite supplies are under extreme pressures, resulting in price surges and spot shortages.[v]

According to *Industrial Minerals*, the shortages have been immediately reflected in prices. In

January 2008, prices of refractory-grade, round and rotary-kiln bauxite was $245 – $265 per ton (FOB). By mid-June, these prices had almost doubled to $440 – $465 per ton. At one point in 2008, bauxite peaked at $550 per ton.

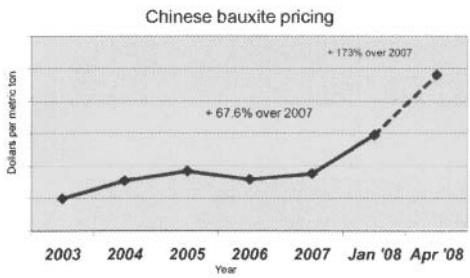

"All commodity prices have been increasing, but what's happening with bauxite is beyond simple increases," said William K. Brown, CEO of Pittsburgh-based refractory maker Resco Products. "Chinese bauxite has increased in price 600 percent to 700 percent in three years and has more than doubled since January. We can't get prices to stay firm beyond 30 or 60 days."

Although refractory makers in India and other countries have responded by developing internal raw-material resources, U.S.-based bauxite suppliers and refractory businesses are in a different situation altogether. Because the nation has few domestic sources or reserves and is entirely dependent on imports, suppliers and manufacturers are uniquely vulnerable to bauxite shortages.

The interests of manufacturers and suppliers are not necessarily identical: manufacturers are primarily concerned with risks related to volatility of bauxite prices. On the other hand, the actual suppliers are concerned with counterparty risks, volatility in governmental stabilities, currency valuations and transportation cost volatility, just to name a few.

The bauxite shortage may last indefinitely. Long term, there are a number of new bauxite mines being developed in Australia and Africa, but a significant increase in world mining is several years off. But even these may not be sufficient to return prices to previous levels. A recent report by consulting firm McKinsey warned that the best-case development of new bauxite mines would leave capacity well under the 70 percent increase in supplies expected to be required by 2015. A McKinsey researcher warned a Reuters reporter that, "The aluminum industry faces a paradigm shift, from an abundance of resources to scarcity of supply."

The giant in the supply and manufacturing marketplaces is China. Native supplies of bauxite, although significant, have not kept up with domestic needs and even declined when Chinese officials closed several unsafe mines that previously operated with little regulation.

Many consumers of bauxite have been increasingly looking for salvation in Africa. The African continent is believed to hold some of the largest and best-quality bauxite reserves in the world. Guinea, alone, is thought to hold 30 percent of the world's bauxite reserves and is already Africa's largest exporter of the material. However, any strategy that depends on Africa carries significant risks. Political turmoil, infrastructure weaknesses and energy shortages make some buyers in the market place very nervous about the long-term dependability of these sources.

China, on the other hand, has taken a long-term view in general toward Africa and has been developing political and economic ties for at least four decades. Russia, relatively speaking, has been a latecomer to Guinea and the rest of West Africa. Despite dangling an offer of $5 billion in investments for the region, the Russians have not had easy going, and its bauxite mining concessions have been

challenged by Guinean officials.

As the dust settles, insiders believe China virtually has locked up Guinean bauxite-mining rights.

However, China is also developing strategic partnerships in Asia. *News Trak International* reported last summer that the China Aluminum International Engineering Corporation signed an agreement valued at about $460 million to build a 600,000-ton aluminum smelter and related bauxite mines in Vietnam, which has bauxite deposits of up to 8.3 billion tons, the world's third largest amount after Guinea and Australia.

What are some of the key components of China's success?

- A long-term, material-independent strategy in countries with abundant resources based on relative independence and initiative of the partnering countries;
- A willingness to mobilize governmental and nongovernmental agencies in developing foreign-aid projects that develop the overall infrastructure of the countries;
- A willingness to share some intellectual capital (i.e., mining and smelting techniques); and
- A willingness to risk signing long-term agreements and contracts.

Lithium

The situation with lithium is intriguing, uncertain and one that may have higher risks than those being faced with the bauxite shortage.[vi]

Concern about lithium supplies has been building for several years, but the issue has gotten "hot" because of the world's recent emphasis on developing energy-storage technologies that could unleash a new generation of renewable energy sources and transportation solutions. One particular event that has clouded the lithium picture is President Barack Obama's announced goal of having one million 150-mile-per-gallon plug-in hybrid electric vehicles on the road in the U.S. by 2015 – something that would require millions of new lithium-based batteries.

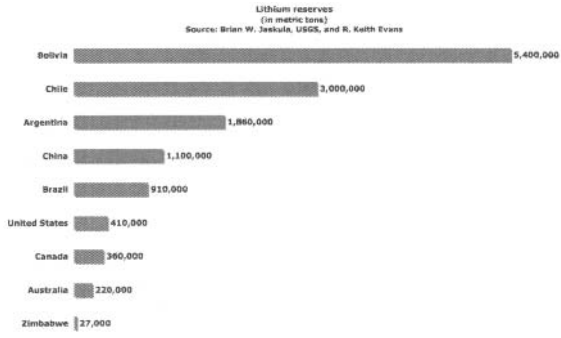

In early August 2009, the Obama administration issued approximately $2 billion in grants to do the nuts-to-soup production of third-generation lithium battery systems for U.S. consumer and commercial vehicles. Billions more are being spent for federal lab and university research for fourth- and fifth-generation battery systems. Although these next-gen systems won't necessarily be lithium based, lithium cannot be ruled out. Regardless, for environmental and economic development reasons, numerous countries have determined that it is in their national interest to be a player in this worldwide competition/cooperation, and the grab for lithium has begun.

Given this situation, whether the demand for lithium translates into an actual lithium shortage is an

extremely important question.

Before looking further at lithium, it's worth acknowledging two reasons why there are big differences between lithium supplies and bauxite supplies. The first is that, generally speaking, bauxite is connected to the production of commodity products, such as aluminum and steel, whereas lithium is linked to what currently are considered to be proprietary technologies that could (at least in theory) lead to transformational changes in the environment, transportation, energy usage patterns, etc. The relative importance of strategic materials is often debatable: I argue that lithium is likely to be of greater strategic significance than bauxite for the U.S. and other nations. Another significant difference is that the actual market for bauxite provides important information about future prices, supplies and trends, whereas the concerns about lithium are centered on a largely theoretical marketplace that likely will be different from current lithium mining and processing levels.

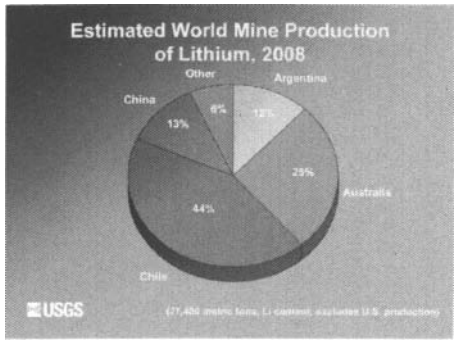

Although my research suggests that there are enormous questions related to how much lithium ultimately will be needed in the future, it is important to start with current lithium reserves. In this regard, the U.S., Canada, Europe and other developed nations currently are at a distinct competitive disadvantage because – as of today – they lack plentiful domestic lithium reserves, according the U.S. Geological Survey. Very little lithium mining occurs in the U.S., and the nation has only a very small portion – less than 3 percent – of the total world's reserves.

Conversely, abundant reserves lie in China and other emerging-market countries, such as Brazil, Argentina and Chile. By far, the largest lithium reserves are in Bolivia, a nation locked in such deep levels of poverty and economic polarization that it barely rises to the level of being a "developing country." But, Bolivian mining operations are nearly nonexistent.

In terms of actual production, Chile is the largest lithium supplier in the world and supplies the U.S. with 61 percent of its needs.

Two people are currently getting a lot of attention in regard to lithium supplies, and they are at opposite ends of the "lithium shortage" spectrum. William Tahil thinks there will be a lithium shortage. He operates an "independent strategy research and technology consultancy" firm, Meridian International Research. Tahil raised eyebrows with his widely read report, *The Trouble With Lithium.* His asserts:

> Analysis of Lithium's geological resource base shows that there are insufficient economically recoverable Lithium resources available to sustain Electrified Vehicle manufacture in the volumes required, based solely on Li-Ion batteries. Depletion rates would exceed current oil depletion rates and switch dependency from one diminishing resource to another. Concentration of supply would create new geopolitical tensions, not reduce them. Reliance on other hypothetical, unproven potential sources of lithium,

> such as seawater, is not a realistic or practical strategy on which to base a technology revolution in the automotive industry.[vii]

If Tahil is the supreme doubter when it comes to lithium supplies, R. Keith Evans is the supreme believer. According to his website, Evans is a geologist who lives in San Diego, Calif., who has a history of working on several international lithium-mining projects. Evans has drafted another widely circulated report titled, *Lithium Abundance – World Lithium Reserve*. In this report, he compares known worldwide reserves with demand predictions, and he concludes:

> In 1976 a National Research Council Panel estimated that Western World lithium reserves and resources totaled 10.6 million tonnes as elemental lithium. Subsequent discoveries, particularly in brines in the southern Andes and the plateaus of western China and Tibet have increased the tonnages significantly. Geothermal brines and lithium bearing clays add to the total. This current estimate totals 28.4 million tonnes Li equivalent to more than 150.0 million tonnes of lithium carbonate of which nearly 14.0 million tonnes lithium (about 74.0 million tonnes of carbonate) are at active or proposed operations. This can be compared with current demand for lithium chemicals which approximates to 84,000 tonnes as lithium carbonate equivalents (16,000 tonnes Li). Concerns regarding lithium availability for hybrid or electric vehicle batteries or other foreseeable applications are unfounded.

Complicating matters, somewhat, is that Evans has a disciple in Brian W. Jaskula, a lithium specialist working for the USGS. In conducting interviews for my research, I came across many key figures in U.S. science and industry who have attended presentations or read PowerPoint presentations by Jaskula. Jaskula has assembled an interesting fact base that is an interesting amalgam of USGS reserves and trade data, information from Evans and information from research groups, including SQM, Rockwood/Chemetall and Deutsch Bank Securities.

Several scientists and lithium manufacturers were nonchalant about the shortage issue when I interviewed them. Several repeated an anecdote (attributed to Jaskula) regarding the feared shortages of lead at the dawn of the lead–acid battery age and used this as an example of how market forces and recycling technology made lead shortages a nonissue.

Several also displayed marked reluctance to engage potential suppliers like Bolivia. Bolivia's president Evo Morales caused some international concerns and gained a bad reputation in some circles when he nationalized his country's oil and gas business, reportedly because the income was going entirely to a few gentrified families that own much of the nation's natural resources.

How much lithium is required for an electric vehicle?

Power requirements	16 kilowatt hours (specified for Chevy Volt)
Lithium estimate per kWh	0.431 kg (U.S. Department of Transportation estimate)
Total lithium for one Chevy Volt	6.896 kg
Total Li_2CO_3 for one Chevy Volt	36.5 kg
Total Li_2CO_3 one million PHEVs	36,500 metric tons

However, Bolivia's consul in Washington, D.C., Osvaldo Cuevas, told me that Bolivia is eager to see its lithium put to use. "Yes, lithium is a huge deal for Bolivia. Everything is open now. All discussions are open. We are meeting with representatives from many nations, including the

United States," he says. Cuevas would not provide names of the U.S. contacts.

According to press reports and other interviews I conducted, there is a large reluctance to work with Bolivia because – in exchange for the lithium – Bolivia wants to retain some long-term benefits. In particular, Morales has mentioned that he wants Bolivia to gain expertise in mining techniques, lithium processing and some aspects of battery manufacturing. "Even before gas and oil, Bolivians had a long, dark history with silver and tin," he says. "Silver and tin were taken from Bolivia and we really received nothing for it. We are not going to give away our raw materials again."

Still another viewpoint was expressed by Bob Kanode, CEO of battery-maker Valence Technologies, who told me he isn't losing any sleep worrying about where the U.S. is going to get its lithium supplies:

> I am not concerned because of a couple of trends. The demand is still small and small mining companies that are not well established or well organized are filling it. Right now, there is just not enough money involved to bring the major players in. When the major mining companies enter the picture, they will bring new efficiencies. I think the market will balance supply and demand, and create strong competitive drivers that will mediate the situation … . I think the official numbers underestimate the sources of lithium. We reopen old U.S. mines. We can extract lithium from oil potash, from rivers and from the ocean. Those market dynamics will continue to be played out … . There's lots of noise about reserves in countries that may not be friendly. But Australia has reserves, China has reserves and South Africa may have reserves well beyond anything that's been reported."

Kanode, however, did concede an important point:

> We are in our infancy. Lots of people are throwing around estimates that the auto battery business could be worth as much as $33 billion. But we don't know. The truth is that until we show consumers how great [electric vehicles] are – and I think EVs provide an amazingly great driving experience – we have no idea how fast or how large the demand will be.

And that starts to get at the crux of the problem. Like the story of the blind men trying to describe an elephant, Tahil, Evans, Jaskula and Kanode all describe conflicting, but not necessarily false aspects of the same issue. They are each person's best guesses about a very hazy subject that, as yet, refuses to come into focus.

The reality is that, right now, no one currently can

- Accurately predict overall lithium demand;
- Accurately predict when lithium demand will peak;
- Accurately predict what quality of lithium will be required in final technologies;
- Know how to manage the full supply chain of lithium battery manufacturing;

- Know what regions, nations, technologies or countries have a sustainable competitive advantage in any steps of the lithium battery supply chain;
- Know if natural market forces will mitigate lithium shortages and turn lithium into a commodity (like lead), or be unresponsive, leaving lithium as a scarce material (like bauxite);
- Know how willing China and Chile may be to share lithium with the rest of the world in future years;
- Know, outside of their proprietors, the extent and quality of U.S. lithium reserves, including reserves that are considered to be currently unprofitable; and
- Know what technologies and/or price points replacement technologies become viable.

Rare earths and other rare metals

Although I have only done some preliminary research on the topic of supplies of rare-earth materials, a quick survey of recent news stories suggests that another real or created strategic shortage may be in the making, particularly in regard to other rare metals and rare-earth oxides and metals.

Although rare-earth elements are relatively abundant (in amounts similar to chromium, nickel, copper, zinc, molybdenum, tin, tungsten or lead), REEs are subject to a unique problem in that they tend not to accumulate in ore deposits. The few sites where REEs are concentrated are highly valued. Consequently, nations and industries that require REEs are very vulnerable to disruptions in their supply chains because of the scarcity of suppliers.

The following is an incomplete list of applications for REEs and related yttrium compounds: automotive catalytic converters; color televisions and flat-panel displays; permanent magnets; electronic thermometers; fiber optics; lasers; oxygen sensors; fluorescent lights; pigments; superconductors; X-ray-intensifying screens; armaments; base-metal alloys; pyrophoric alloys; and superalloys. REEs are also especially important for rechargeable batteries for electric and hybrid vehicles.[viii]

The U.S. appears to have fairly large REE reserves but mines only one deposit located in California. Other significant reserves are limited to a small list of countries: Australia; China; the Commonwealth of Independent States; and India.

China's reserves may be 60 percent of the world's total. Thus, shock waves were sent around the world this summer when China's Ministry of Industry and Information Technology suggested a national policy that would sharply limit or end the export of five rare-earth metals. Chinese officials said the moves are aimed at building a region of Inner Mongolia into a world rare-earth mining and processing center, but others speculated that China's plans also represent an effort to create leverage for companies to expand TV and battery manufacturing within its borders.

The question for many countries, and potentially for the U.S., is whether the complete supply chain can exist outside of China. Japan, for example, is entirely dependent on outside suppliers and seems to be willing to develop and act on a national strategic plan in regard to REEs. In response to the developments in China (or at least as "last straw" events), Japan's public and private sectors have moved quickly. For example, following satellite-based surveying, Japan's Economy, Trade and Industry ministry has signed contracts with Zambia and may soon have agreements with Mozambique

and Namibia to develop these countries' rare-metal sourcing capabilities. The Japan Oil, Gas and Metals National Corporation started a rare-metals project in Botswana in July, the Sumitomo Corporation has an agreement to extract rare earths from a Kazakhstan uranium mine and Toyota just gained drilling rights in India and a purchase agreement with Vietnam. Japan is also making strides in developing "urban mines" by recycling rare metals from old electronics.[ix]

Chinese development efforts in South America

The contrast between the national strategies of the U.S. and China seem to be clear in the case of the approach to the South America continent. The U.S. appears to have little in the way of an apparent strategy for relations with Latin American countries and also appears to be doing little to dissuade categorization of these nations (a habit fed by many U.S. media outlets) into either a "friendly" or "unfriendly" status. Financially speaking, targeted U.S. aid to South America primarily is funneled through either the U.S. Agency for International Development or the Inter-American Development Bank. USAID has provided small amounts to Peru and Bolivia in the past, but these have been connected with controversial programs.[x] However, IADB is controlled by various nations that act as shareholders, with the U.S. controlling a 30 percent share of the institution. Most of the cash reserves of the IADB already have been allocated, and, despite pleas for a $100 - $200 billion capital increase,[xi] new funding for the IADB appears to be a low priority for the U.S. government.

In the meantime, China's strategic efforts in South America seem to be accelerating. Hugo Restall, editor of the *Far Eastern Economic Review*, recently wrote that, "Latin America is the most important arena for China's investments."[xii] If Restall is accurate, from a worldwide point of view, that outlook truly is remarkable. In steep contrast to the poverty of the IADB and USAID programs, the China Development Bank is flush with U.S. dollar reserves. As Restell notes, " At a time when capital is in short supply, especially in emerging markets, Chinese institutions can make a critical difference in financing new projects."

Relative to aid offers from the U.S., Chinese aid appears to have few strings attached. China has reached out to some of the largest nations in South America – Argentina and Brazil – and others – Venezuela and Bolivia – whose leaders are not seen in favorable light in the U.S. Although some of this economic activity may be attributed to ideology and opening new markets for Chinese goods, the cooperative economic agreements also have overt strategic considerations if Restall is correct about the combination of long-term loan rates and guarantees of supplies of certain commodities.

CONCLUSION

The bauxite shortage continues to be a real concern, but it is primarily being played out in a company-by-company, market-by-market situation. The only new development is that one refractory manufacture, Resco Refractories, has taken the issue to the International Trade Commission, arguing that Chinese bauxite producers and traders have conspired to fix prices and supplies.

Regarding lithium, I think the most accurate, comprehensive thing that can be said is that, unlike bauxite, it is far to early to know if there will be a lithium shortage.

But, after looking at these two materials and the emerging situation with rare earths/rare metals, three general recommendations seem obvious:

- Establish multidisciplinary responsibility for strategic materials at the national level;
- Develop risk management approaches and tools to evaluate potential outcomes; and
- Develop long-term international economic, political and diplomatic strategies that will augment a specific material strategy.

National responsibilities

One thing that the bauxite and lithium situations have in common is that it is not clear who within the U.S. – outside of the obvious stakeholders – is thinking about these supplies in a comprehensive manner. This goes beyond the simple question of reserves and trading activity. Who, if anyone, is responsible for considering the myriad of scientific, political, business and geological questions that affect supply and demand? Which agencies are responsible for transcending the natural biases of the various stakeholders or synthesizing the variety of science and politic data streams? And this goes beyond a specific material. What experts, for example, are empowered to identify and monitor the broad materials markets and to develop appropriate response proposals for implementation at the national level?

As noted earlier, the USGS does some of this work, but it lacks the ability and authority to integrate a multicomponent analysis required to adequately develop a functional national strategy. Furthermore, tasking USGS with these responsibilities would likely detract from its core mission.

A better situation, I think, would be for many of these duties to be shouldered by existing intelligence agencies, which would prepare reports for teams of national advisors comprised of undersecretaries from key agencies, such as DOD, DOE, NSF and State plus science and business appointees from academia and the private sector.

Of course, it is possible that some of this is occurring "under the radar," but there is little public evidence that this is the case. On the contrary, the U.S.'s lack of initiatives on the materials supplies front seems startling compared with, say, the involvement of Chinese governmental officials with bauxite supplies or the Japanese government with rare-metals supplies.

Risk management

Conceptually, too much of the discussion of strategic materials gets stuck into "black-or-white" thinking. Although risk evaluation is also applicable to bauxite, it is, in fact, evident from the situation with lithium that there are many "gray" areas and risk factors that will ultimately determine if there will ever be a lithium shortage.

In the business world, there are three major components to cumulative risk analysis. The first component is a dynamic framework that models – as best can be determined at any given point – the relative interaction and correlations among the risk factors. The second component is a dynamic method for assigning a probabilistic metric to each risk factor. The third component is a system for evaluating and testing the framework, including stress tests and "fat-tail" (high-risk low-probability) outcomes analysis. Although initially challenging, these techniques have been perfected and demonstrated in such areas as Monte Carlo simulations and Value-At-Risk determinations.

The corollary to understanding the multiple risks is to develop multiple strategies that hedge the various risks. Put simply, even if one is 75 percent certain that one outcome is likely, one probably

should still have a contingency plan for the other possibilities that fall within the remaining 25 percent.

As discussed in one important new book[xiii] on risk management, the starting point in all this is an effort to define five key questions:

- What's the problem?
- For whom is something a problem?
- Who is the decision-maker?
- Do we already know what to do?
- How will we be better off because of risk assessment?

Develop long-term augmenting international strategies

This is the most difficult area to prescribe a solution, in part because of my lack of expertise. However, I suggest here that the U.S. – and other developed countries – establish a positive base for all of its future dealings with developing nations. My empirical experience is that the U.S. suffers from a lack of efforts to offer long-term "untied" support in South America, Africa and other regions. Such unencumbered aid establishes mutual trust, cross-cultural knowledge and expertise, and, hopefully, economic growth for the recipient nations.

Although many South American and African citizens have something of a personal affinity for the people, culture and economic opportunities of the developed world, they are also wary and often repulsed by international efforts that they perceive as being self-serving. In South America, my business contacts often mention the history of colonialism and neocolonialism as being a subtext to much of their analysis of foreign relations. The common outlook is one that U.S. foreign policy is totally self-serving and is associated with past support for nondemocratic regimes and pressure to agree to asymmetrical trade and environmental pacts.

Regardless of the reality, I believe that the U.S. remains at a considerable disadvantage compared with other great economic powers, such as China or Japan. Unfortunately, this situation cannot be reversed quickly, but the longer a nation delays such steps, the longer it cedes a continuing advantage to other countries.

Likewise, the U.S. and other nations should examine to what extent they play a zero-sum game in foreign relations. In the long term, the U.S.'s loss isn't always another country's gain, and vice versa. For example, from the vantage point of today, I find that Bolivia's request for being taught mining techniques as not an unreasonable sine qua non in exchange for an agreement regarding long-term access to lithium. Ten years from now, even Bolivia's demand for manufacturing capabilities may seem like an incredibly small price to pay to retain the U.S.'s standing in the transportation and energy industries.

I do not seek any specific support for the suggestions I put forward. I certainly lack the experience and know-how to draft recommendations in a meaningful and comprehensive way. However, I increasingly worry that members of the materials community often operate with their heads in the ground and naively assume that the fancy materials they play with in the lab will always be available at cheap prices and in plentiful supplies. A healthy dose of geopolitical reality is needed, and, hopefully, this paper serves to stimulate what I think is a long-missing debate and discussion among the

appropriate scientific, governmental and industrial groups.

---

[i] Zephyr Frank, Stanford University, and Aldo Musacchio, Ibmec Sao Paulo, "The International Natural Rubber Market, 1870–1930," www.eh.net/encyclopedia/article/frank.international.rubber.market

[ii] L. Meitner and O. Frisch (1939), "Disintegration of Uranium by Neutrons: a New Type of Nuclear Reaction." *Nature*, **143**, 239–40, www.atomicarchive.com/Docs/Begin/Nature_Meitner.shtml.

[iii] William M. Tuttle Jr., "The Birth of an Industry: The Synthetic Rubber 'Mess' in World War II." *Technology and Culture*, Society for the History of Technology, 1981.

[iv] Major Paul Wakefield, "Polymer Advances in the Interwar Period: The Impact of Science on World War II," *Army Logitician*, **39** [2] March 2007, www.almc.army.mil/alog/issues/Mar-Apr07/polymer_advan.html

[v] Peter Wray, "Battling for Bauxite," *American Ceramic Society Bulletin*, 87 [8] 26–28 August 2008.

[vi] Peter Wray, "Lithium Lowdown," *American Ceramic Society Bulletin*, 88 [7] 17–24 August 2009.

[vii] William Tahil, "The Trouble With Lithium," 2007, www.meridian-int-res.com/Projects/Lithium.htm

[viii] *U.S. Geological Survey, Mineral Commodity Summaries*, January 2009

[ix] "Japan Accelerates Moves to Secure Rare Metals," *The Yomiuri Shimbun*, Sept. 9, 2009, www.istockanalyst.com/article/viewiStockNews/articleid/3468633

[x] Andean Information Network. "Bolivian Coca Growers Cut Ties with USAID," www.ain-bolivia.org/index.php?option=com_content&task=view&id=128&Itemid=28

[xi] Bank Information Center. "Civil Society Organizations Challenge IDB Commitments to Development Results and Sustainability," June 30, 2009, www.bicusa.org/en/Article.11274.aspx

[xii] Hugo Restall. "China's Latin Economic Gambit," *Wall Street Journal*, Aug. 24, 2009

[xiii] "Science and Decisions: Advancing Risk Management," National Research Council, National Academies Press, Washington, DC, 2009, www.nap.edu/catalog.php?record_id=12209.

Energy

This Page Intentionally Left Blank

RED LION BIO-ENERGY—SYNGAS PRODUCTION FROM A NOVEL THERMAL CONVERSION PROCESS OF COAL/BIOMASS

Doug Struble
Red Lion Bio-Energy
Maumee, Ohio, USA

INTRODUCTION:

The world is facing rapid growth in energy demand, volatile and high-energy prices, and a challenge to reduce green house gas emissions. Red Lion's unique thermal conversion process relies on existing feedstocks, typically from waste streams or by-products, to create a clean source of energy - Syngas - while generating fewer air emissions than traditional technologies.

Whether used for power generation or for production of gaseous or liquid fuels, Red Lion's thermal conversion process has significant environmental benefits over conventional technologies, including:

Feature	**Benefit**
Uses waste products as feedstock	Reduces the environmental impact of waste disposal
The bi-products from this process are non-hazardous	The Bi-products are readily marketable
Patented water clean-up technology designed to recycle process water	No discharge of water to the surrounding environment

The unique Red Lion thermal conversion process offers a clean, effective means of converting coal to energy and carbon dioxide reduction. These benefits can further be enhanced using biomass as the feedstock.

Biomass is a renewable energy source. The energy it contains comes from the sun. Through the process of photosynthesis, plants capture the sun's energy by converting CO_2, air and water into carbohydrates (complex compounds composed of C, H and O). When these carbohydrates are burned, they turn back into CO_2 and H_2O and release the sun's energy; therefore, the entire process may be considered "carbon neutral."

Red Lion uses a patented process to produce a biofuel that is cost efficient and eco friendly. Since there is no feedstock combustion in the Red Lion Syngas process, there are very low CO_2, NO_X and SO_X emissions. The Red Lion Syngas process focuses on pollution prevention because it recycles products back in to the system. Ash and other solid waste can be separated and sold to other markets. Designed as an intermediate sized plant, syngas output is in the 100-mmbtu/hr range.

FOSSIL FUEL CO_2 EMISSION LEVELS (Pounds per Billion Btu Energy)	
COAL	208,000
NATURAL GAS	117,000
SYNGAS, COAL FEEDSTOCK	117,000
SYNGAS, BIOMASS FEEDSTOCK	117,000

Source: EIA – Natural gas issues and Trends, Syngas estimates based on Red Lion Bio-Energy Syngas Composition

TECHNOLOGY:

Unlike conventional conversion processes, Red Lion's patented Waste to Energy (W2E) technology involves feedstock pyrolysis in the absence of oxygen, followed by "non-catalytic" steam reforming which produces syngas with energy content ranging from 300-450 BTU/SCF. This technology can be manipulated to produce syngas with different H_2 to CO ratios. In addition, this novel technology focuses on emission prevention, reducing greenhouse gas emissions, and the capture of sulfur, mercury and other contaminants as a solid bi-product.

REACTION CHEMISTRY:

STEP ONE: PYROLYSIS

Pryolysis is the thermal decomposition of organic materials by heating in the absence of oxygen. This process is done at operating temperatures of about 800°F.

Devolatilization of feedstock $\longrightarrow$ $CH_4 + CO + CO_2$ + char + tar + hydrocarbons

STEP TWO: STEAM REFORMATION

The solid and gaseous products from step one react with steam at high temperatures of about 1700-1800°F and pressure of about 25-50 psi to produce syngas, which is mainly a mixture of H_2 and CO.

PROCESS DESCRIPTION:

The feedstock is prepared and fed in dry form into a sealed reactor chamber called the pyrolytic chamber. It is subjected to high temperature and pressure (>800°F @ 25psig) in an oxygen free environment. An outside fuel source is used to generate initial heat to begin this process. Once the reactor is producing syngas, a portion of this fuel is used to sustain the ongoing reaction.

Devolatilization of the feed occurs as the material heats up. Volatiles are released and char is produced at the end of the pyrolysis step. The degree of decomposition is dependent on the properties of the carbonaceous material used for the feedstock. This determines the structure and composition of the char that will then undergo gasification reactions. Steam is fed into the reactor coils at rates relative to the amount of carbon in feedstock. The steam reformation reactions, which are carried out at high temperature of about 1700-1800°F, convert the pyrolysis products into smaller gas molecules, primarily consisting H_2, CO, CH_4 and CO_2. The gases exiting the steam reforming coils are at a temperature of about 1750°F. The ash produced after processing of feedstock is removed using a cyclone removal system. The syngas is then sent into a wet scrubber for further removal of contaminants. Clean syngas is then sent into condensing tanks where moisture drops out and clean dry syngas produced can be used either as a gaseous fuel source for power generation, or, with additional refining, can be converted to liquid fuels such as methanol and ethanol, among others.

PERFORMANCE:

Red Lion's thermal conversion process is approximately 70% energy efficient because it has a very low BTU input requirement, which is supplied from the process itself. The result of Red Lion's proprietary process is a 30 – 80% reduction in your carbon footprint.

The composition of the gas can be varied with different operating conditions for temperature, pressure, feedstock composition, feed input rate, and amount of steam used. Therefore, the syngas heat content changes depending upon the composition of syngas. Typically Red Lion Syngas heat content ranges from about 300-450 BTU/SCF.

RED LION SYNGAS COMPOSITION (vol%)			
	COAL	RICE HULLS	PETROLIUM COKE
HYDROGEN	63 %	53%	75%
CARBON DIOXIDE	20 %	20%	5%
METHANE	4%	14%	14%
CARBON DIOXIDE	12%	12%	5%
HYDROGEN SULFIDE	< 1%	<1%	<1%

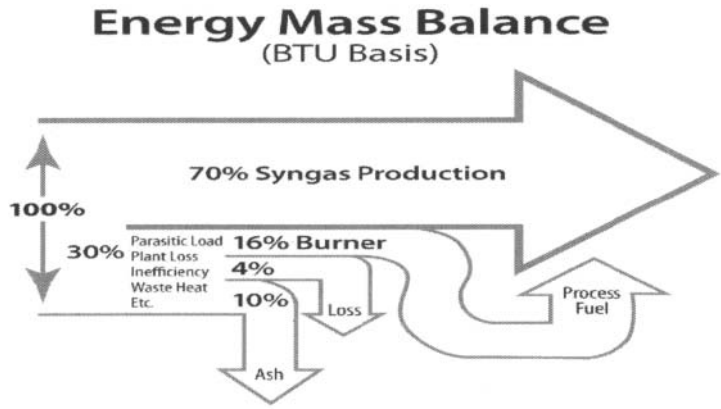

FIRST RED LION UNIT ALREADY IN SERVICE – SIGNIFICANT MILESTONE ACHIEVED

Red Lion launched its operations in August 2006 and has built a commercial scale pilot plant. The plant was initially commissioned in November 2007 and moved to Toledo, Ohio in February 2008.

The move took place in conjunction with a unique partnership established with the University of Toledo. This partnership provides Red Lion access to the UT faculty and various research tools that are used to analyze progress and results. UT's support to date has been institution-wide, ranging from Trustee and Presidential levels, through the College of Engineering and the Chemical Engineering Departments, to the Facilities and Physical Plant Department. This location allows the technology to operate on a commercial scale by selling the syngas directly to the University of Toledo's boiler system.

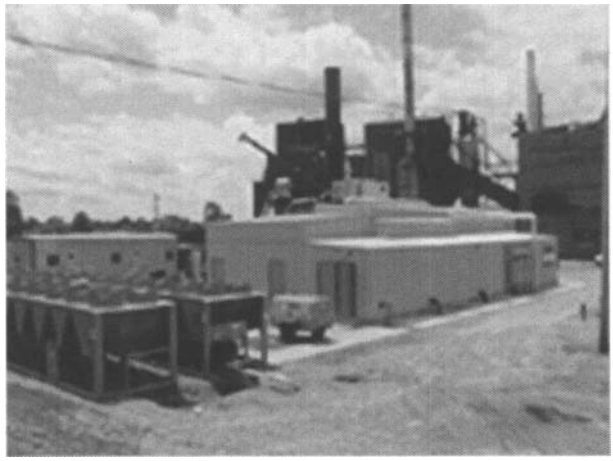

RED LION 100 FT x 100FT PORTABLE GASIFICATION UNIT
ON THE UNIVERSITY OF TOLEDO CAMPUS, TOLEDO, OHIO

NEXT STEPS:

Red Lion is presently working towards two additional significant milestones for operational and commercial advancement.

PRODUCTION OF DIESEL FUEL FROM SYNGAS

In July 2009, Red Lion and The Renewable Energy Institute International (REII), a nonprofit organization, announced the formation of an alliance of industry, academic, and government organizations. This alliance will operate a pilot plant in Toledo, Ohio to demonstrate the efficient and economical conversion of waste biomass to clean, diesel fuel. This new alliance includes organizations from around the United States including Red Lion Bio-Energy, Pacific Renewable Fuels, Grace Davison, PACCAR, Solar Turbines/Caterpillar, National Renewable Energy Laboratory (NREL), Desert Research Institute, Quanta Services, Worley Parsons, University of Toledo, Midwest Terminals/Port of Toledo, and other leading partners. In December 2009 Red Lion received Department of Energy Stimulus Funding of 20million dollars toward the development of a 25million dollar Bio diesel refinery to be constructed near the University of Toledo's Health Science Campus.

This demonstration plant, will integrate both existing and next generation conversion processes that have been operated at test sites in Sacramento, California and Toledo, Ohio during the past two years (Red Lion's existing gasification unit and Pacific Renewable Fuels' gas to liquids unit). This demonstration plant will produce 350,000 gallons of no sulfur, high-cetane, clean diesel fuel per year with a high biomass to fuel energy conversion efficiency of 44%. Based upon a comprehensive lifecycle analysis using Argonne National Labs' computer models, this production of diesel from biomass will reduce greenhouse gas emissions by 89%, compared to petroleum-derived fuels.

Red Lion's understanding is that this operation would be the first in North America to produce diesel fuel from biomass.

POWER PURCHASE AGREEMENT WITH UNIVERSITY OF TOLEDO

Red Lion is negotiating with the University of Toledo to supply fuel to generate electric power from a combination of its existing gasifier facility plus an additional new unit. Syngas from these units would be used to generate approximately 10 megawatts of electric power via turbine generator. Additionally this operation would generate steam quantities that are adequate to meet the University's steam needs throughout its Health Science Campus

CONCLUSION:

Red Lion's proprietary technology offers an attractive alternative energy by processing low-value, secondary materials to produce a cleaner form of energy - syngas. The synthetic gas produced has wide variety of applications such as power generation, liquid or gaseous fuel production, or various other chemical manufacturing processes. The bi-products, like sulfur and metal-bearing slag, are marketable. Therefore, waste streams are minimized and emissions associated with the waste streams are also reduced.

This Page Intentionally Left Blank

MACRO ENERGY BALANCES

John Brown
GMIC
brownjt@gmic.org

John Nelson
Corning Inc. retired
jwnelson@stny.rr.com

Between 1975 and 1990, perhaps 120 full Furnace Energy balances were completed on sixty large Corning Incorporated furnaces, both US and off shore, plus many contracted non-Corning furnaces. The cost of a full furnace audit in the 1980's was $20,000+, and included a five person crew collecting the data for a week, plus a second week by one engineer completing the calculations and writing a report that was reviewed within a month by representatives of Corporate Melting Technology and representatives of the plant. At this review, recommendations from the recent Furnace Energy Balance were incorporated into the capital planning for the next repair.

Included were at least 23 complete heat transfer calculations to determine the heat loss from the furnace crown, usually two sections, the back and front wall, breast walls, bottom of furnace, port necks, regenerator crowns, regenerator inside and outside walls, and end walls. Each regenerator chamber measured with a suction pyrometer for a complete pre-heat and exhaust cycle temperature measurement. The refiner, in most cases was treated for wall losses as well. We contacted the local natural gas supply company to install turbine meters to confirm accuracy of our fuel meters and asked systems controls to confirm all remaining furnace metering. Outside labs analyzed sample bottles of the natural gas taken during the Energy Balance for quantitative analysis of constituents, stoichiometric ratio and thermal value.

Rewards for the effort and cost came in the form of a reduction in total energy and improved glass quality to produce a ton of good product by 54% over the four years from 1978 through 1982. These were the years when we were responding to the oil embargo of 1974.

Cycle forward 30 years and we face similar threats to our glass production in unpredictable energy cost. Perhaps a new gorilla is the question of carbon costs from combustion and from carbonate containing raw materials. All are tied to total energy and to use Doug Davis (TECO) words, we must not miss picking the low hanging fruit.

What is presented today is a lower cost and easier method to pick this low hanging fruit.

Over the past three years John Nelson has stuck with me in trying come up with a universal and single program for all glass furnaces. We now realize that one universal program is too much to However, we are pretty close with three programs for the above type furnaces.

Some hand holding is recommended for the first application of this program to a new furnace, and perhaps some special programming to fit the use intended.

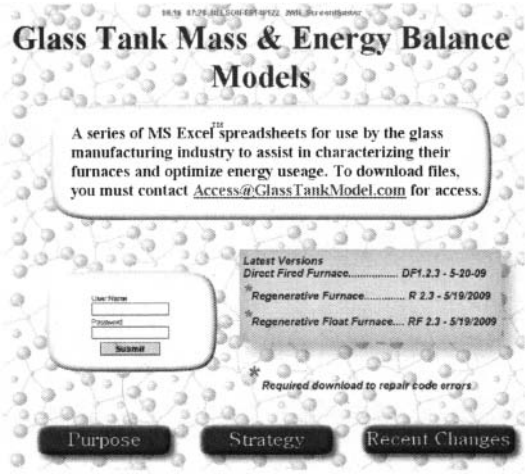

to

ask.

of

GMIC will include on their web page, access to the program through a protected user password. After receiving the software, all data entered will remain on the individuals laptop or plant computer. There is no provision to share data on the secure web page. All users may down load updates from the website as beneficial modifications, agreed upon by John Nelson and users, become available. As important upgrades are generated, e-mails will notify subscribers.

We began testing at the Pittsburgh-Corning site in Port Allegheny, PA. This was the old method with some short cuts to predict preheated air temperatures. Following that analysis, John Nelson volunteered to see if he could simplify my calculations for sensible heats of gases and fuel, cullet and batch plus heats of reactions, into several excel sheets. We applied this first effort to the Sedalia, Missouri P-C plant and John Nelson operated remotely with Rodney Snell for that analysis. Since then, GMIC has by board action opened membership to the world and Vitro (Roberto Cabrera) and Pavisa (Alonso Gonzales, speaking today, both from Mexico) became early users of the software. Zeledyne in two visits has completed balances on two float furnaces and recently World Kitchen used the software in Charleroi. Longhorn is planned for December, so with that completed we will have covered two float furnaces, three regenerative furnaces (end and side port), plus three oxy-fuel furnaces. This will complete our beta testing.

The cover page for each of the three types of furnaces will have one of the above figures. Included are suggested methods of taking certain optical readings, location of bubblers, electrodes and fuel for the intended furnace. Some furnace require a little pre-work and with this completed a complete energy balance can happen in as little as one and a half days, if in the case of regenerative furnaces the pre-work of special opticals can happen the evening prior to the full day effort.

We will take pre-meditated short cuts in the determination of heats of mixing of the raw materials, pre-heated air measurements and for structural heat loss which we determine by difference. That is the total energy purchased less stack loss (measured) and heats to melt the glass and cullet (measured, and from earlier sources). The remainder is the structural heat loss. If additional precision is required, opticals of the cold face and hot face plus the known materials, thickness and k values can be used to predict heat loss. Or, with some confidence thickness, if the hot face thickness is left as the unknown.

The old analysis was felt to be accurate to +/- 3% and originally we were targeting the Macro Energy Balance for +/- 10%. However, we feel we are better and more in the +/- 5% range.

Let's practice entering data for a regenerative furnace.

We will use this time to provide you, as possible users, some experience in using the Macro Energy Balance. Here, you will learn where your energy is being consumed in your furnace. We will pretend to fill in the data on an imaginary furnace. No data will represent any furnace and some will be obviously out of the normal experience.

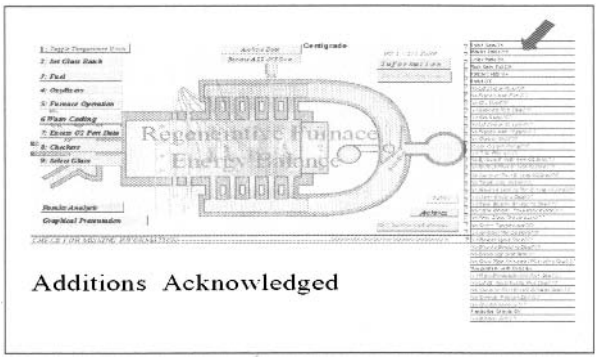

When opening the program the home page offers an opportunity to choose the temperature units that will be used through out the exercise for data entry and display. Of course, nearly all calculations are completed in absolute temperature and converted to either Fahrenheit or Centigrade, as chosen in this exercise.

On the right side are all the areas where data can be filled in to execute a furnace energy and mass balance. All areas in red are incomplete and when changed to blue indicate completion of that task.

After selecting centigrade as the temperature scale, this task block is now blue, indicating completion of this task.

The second program selects the raw materials, including cullet and batch that will be entered in an excel sheet that has more information than can be displayed on a power point slide. There are a number of raw materials that you can choose from or you can enter your own personal list of materials. Water associated with cullet and raw materials is entered as well as any batched water to control dusting. We are primarily interested in capturing all the carbonates and water that will be driven off in

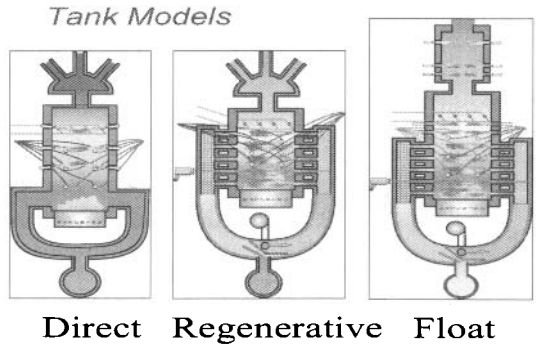

the melting process. Water has latent heats that are significant and there are the sensible heats of both the water and carbon dioxide that need to be calculated. Carbon dioxide and water result from combustion as well as from the batched raw materials and we must capture both for a complete energy balance.

The total carbon dioxide and water as percentages of the total batched weight is reported in percentages in the accumulated batch page.

At this point, as shown in the figure, eight of the possible tasks have been fulfilled.

Total energy from all sources is entered in the Energy page. Fuel for each port, total electric boost and cost of each of these energy sources is entered. If you have either the calorific value, provided by your natural gas supplier or the gross thermal energy, the other will be calculated. Also, the stoichiometric air to gas ratio as well as thermal value per standard cubic foot is calculated. Cost of electric and natural gas or what ever fuel is used can be entered for a financial balance as well as energy and mass balances.

Air, in the case of regenerative furnaces is entered on this page. If oxygen is used as a boost it can be entered here as well and the cost and purity.

If individual port air measurements are not available, and this is the rule rather than the exception in most regenerative furnaces, we only have the entering air from either of the two firing directions. Your case may require a direction like North and South or perhaps you use the convention of right or left when facing the same direction as the flow of the glass through the furnace. Choice of direction labels is your choice and can be tailored to the application.

Peak glass temperature, generally just before the throat, determines the total invested energy in melting glass and cullet for this exercise. This energy number is the numerator in determining furnace efficiency, with total purchased energy as the denominator.

Peak crown temperature will determine the energy invested in exhausting products of combustion and gas released from the melting of the glass raw materials and any water that was entrained in the batch.

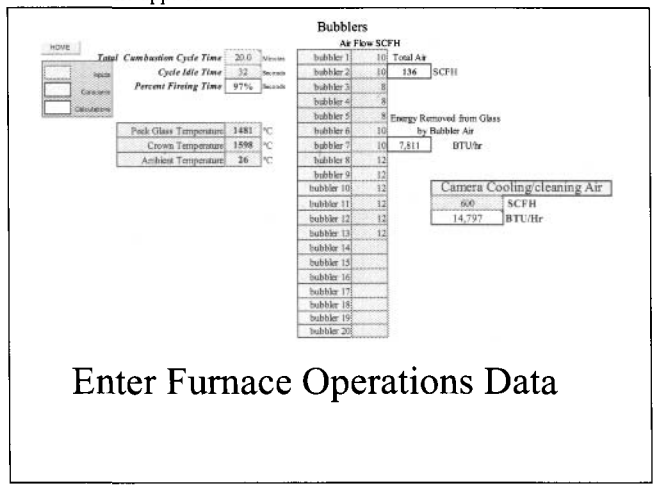

All air/gas sources are captured in this example excel sheet, including bubblers, and any cooling air that enters the furnace.

For more accuracy in total energy invested, we measure the seconds that fires are off during each reversal, or no fuel is entering the furnace.

Water cooling can be a large drain on total energy required to melt. Here we have the entering temperature and exiting temperature of water cooling and mass of water per unit of time for all known sources of water cooling. Total cooling water, including batch feeder cooling, throat cooling, any burner cooling and all bubblers and electrodes are captured. While the total heat seems large, it is really larger by the reciprocal of the furnace efficiency. In the case provided in the subject lecture, 1.2 million Btu per hour was determined as the total heat removed from the furnace via water cooling. However, the real energy is what had to be invested in the furnace to remove this heat. If the efficiency is 33%, then the true cost of energy for cooling is three times this number, or three million six hundred thousand Btu's per hour.

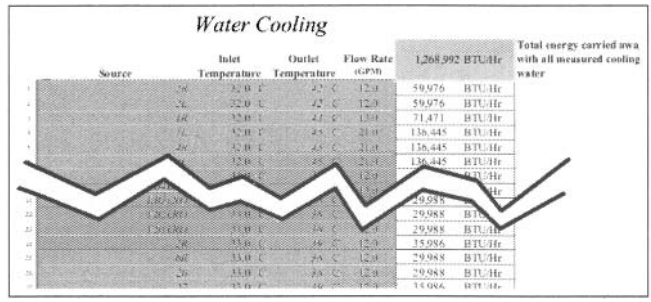

Now we are in an area where parasitic air can be calculated. We do this with oxygen sensors and assume that the increase in excess oxygen is due to inspirited air. A number of options are available to the furnace operators to determine total inspirited air. If possible, we recommend beginning with a global measurement for total parasitic air. For example if the fan air can be blocked by placing a large piece of plywood, a comparison with no fan air can be made with oxygen sensors and there is no potential damage to belts driving the large fan. Alternatively, the fan intake may be controlled by louvers, and by closing the louvers you will accomplish the same result. This is an example of going after the larger causes of parasitic air first. Learn to divide and conquer by incremental pieces, large to small. After seeing the value of the inspirited air and looking at costs to seal these sources, an analysis of cost to eliminate or reduce these parasitic air sources can be presented.

For example, at the top of the regenerator on the exhaust side the excess oxygen can be compared to the excess oxygen at the bottom of the chamber. Because the chambers are common in most regenerators this is best done if all top chambers are read and then the combination effect at the lower common exhaust is compared.

Superstructure and substructure block cooling air fans are predictable sources of inspirited air into the furnace. Blast gates providing air cooling to tuck stone areas and superstructure air can be marked with a felt pen at the normal operating position. Then after excess oxygen measurements are made, in normal operating positions, the blast gates can be closed and another excess oxygen measurement made. For confirmation, the gates can be returned to the original marked positions and a third set of

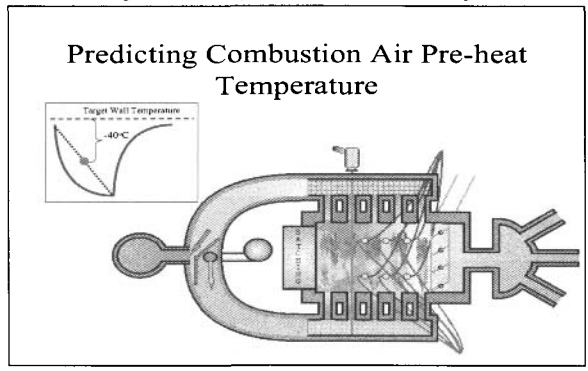

excess oxygen measurement taken.

One of the most difficult tasks is to determine the heat contribution from the regenerators. Going back over the 120+ full furnace energy balances, I could find nothing that came close to the measured suction pyrometer values. We did some checking and found that if we took the target wall temperatures immediately after fires off, on the in-go side, which is opposite what is normally done, that we got a pretty good estimate of the actual measured value. It was always high by about 40°C and we have since explained this as the effect of radiation from the furnace back to the cooler regenerator target wall. We normalize each port target wall temperature by the percentage of fuel in that port and add these normalized numbers to get the predicted temperature on each side. Average the two sides and then subtract the correction factor of 40°C. The figure, "Predicting Combustion Air Pre-heat Temperature", has an insert figure beside the regenerative model showing a typical suction pyrometer reading of the preheat air and then the reversal and the higher exhaust temperatures. Our goal is to find a number that matches the mid preheat combustion air temperature and we need to subtract 40°C to match this number.

We ask operators to take these reverse optical pyrometer measurements over the night shift and in the morning enter the numbers measured to obtain our estimate of the preheated air temperature. This contribution should equal at least 40% of the purchased energy, if the investment in regenerators is paying for itself.

Total combustion gases include all the products of combustion plus all gases liberated from the incoming batch materials, including water and carbon dioxide from carbonates. Each gas type has its own thermal properties and the Gas Table equations for enthalpy have been included such that if the volume converted to mass of the gases is established and the peak temperature of the gases, or the temperature where they leave the furnace, then the total energy invested is easily presented. Entering the temperature of interest plus the mass of the gas and you have the total energy.

The change of temperature in exhaust gases over the reversal period speaks to the robustness of the checker or heat exchange refractory material. If the slope is too high the refractories are corroded and worn away such that much of the heat capturing materials capacity has been lost. This is subjective, but having the graph makes decisions as to length of time for each reversal cycle and scheduling future repairs a bit more predictable.

Leaking reversing valves can rob the furnace of measured combustion air. If metered combustion air is greater than can be explained by the exhausting ports excess oxygen and fuel, there may be leakage at the reversing valve. Or the piping carrying the combustion air from the fan to the in coming flue has holes or leaks.

Another difficult determination is the heats of mixing or melting of the raw materials that make up the glass. This has been determined for a wide range of glasses and we have included in a short table three compositions that have covered all the glasses we have encountered, to date.

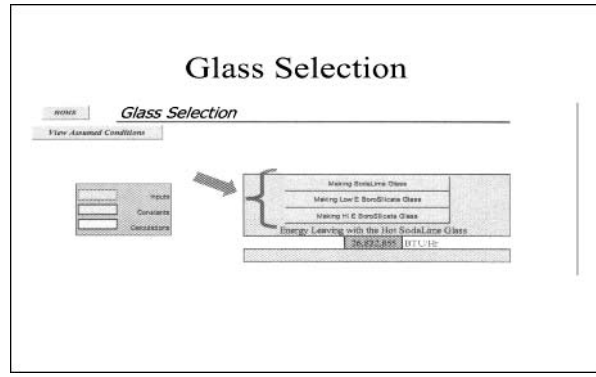

Selecting soda-lime glass, for example, determines the energy required to convert the soda ash,

sand and limestone to glass at 25 °C. While this is not what happens, it is how we handle the numbers. Then, after selecting the peak temperature of the glass bath, the sensible heat to raise the raw materials, and cullet to this temperature is calculated. In addition, the sensible and latent heats of the water vapor and sensible heat of carbon dioxide raised to the crown temperature is calculated.

This activity determines the numerator in defining the furnace efficiency.

CONCLUSIONS AND RESULTS:

Here is where you can become creative.

Find ways to graphically present your results in forms that will impress your boss.

As an example we have presented all the energy uses as Btu's and percentages of the total purchased energy. Knowing the cost of energy, the annual costs of these different uses of energy are presented in another financial balance. In addition, the same uses of energy are shown on a bar graph.

Some additional conclusions would be to identify areas that could be improved.

The energy returned to the furnace as preheated air, I've said earlier, should be in the neighborhood of 40% to be performing as regenerators are expected to perform. We didn't do too good a job in our make believe furnace as we only had 26% of the purchased energy being returned as preheated air.

We have not discussed the rational of determining air infiltration into the exhaust gases but it comes as a ratio to the measured in-go/out-go pressure of the regenerator chamber and the measured air infiltration determined on the exhaust side. Generally, the parasitic air on the preheated air side is about 2/3rds the value that is measured on the exhaust side, due to pressure differences.

If you decide you wish to be trained in use of the Macro Energy Balance, there are a lot of areas that have been investigated in previous furnaces that may have value for your furnace.

Rarely would anyone think to ask the cost of cooling electrodes, bubblers, throat coils or filling machines. Once the data is presented, most are amazed by how much these relative mundane furnace melting tools cost in terms of energy. Each of the measured cost of energy lost has to be increased by the reciprocal of the furnace efficiency. This particular slide has had the boost in cost due to furnace efficiency incorporated in the numbers presented.

Mass balance is a good way to show that for most glass furnaces, the first product is preheated nitrogen—not glass. In this case, the mass of nitrogen in the exhaust is 37,999 pounds per hour. Or, nearly 20 tons of nitrogen per hour. There only 12.5 tons of glass produced per hour. The nitrogen represents 46.3% of the mass of all materials going through the furnace. Again, graphical representation will have a large effect on your controller and plant manager.

Use data to make the furnace interesting to your decision making financial controllers and plant management. Perhaps, making you more valuable as a plant team member.

We are out of time, but there are so many additional experiments you can plan with the basic data available after your first Macro Energy Balance. Always remember, the true value is in the delta (**Δ**), that is, the change in the results of several energy balances. Each one done with some particular change you have made to the process. Maybe insulating the crown, or, insulating the regenerator walls and sealing against any parasitic air. Due to the difficulty of sealing and keeping sealed the tuck stone to flux block, consider re-sealing the tuck stone to flux block area against block cooling air entering the furnace.

The more you use the tool, the more you will learn about your furnace and the better your furnace will perform.

ACKNOWLEDGEMENT:

George Boettner, in 1975 introduced me to Sankey Diagrams, gross heat balance, air flow and distribution, and a program he developed on his 9830 Hewlett Packard mini computer which enabled a heat balance to be made simultaneously around the melt zone, distributor, regenerator—and, the total system. This was following the oil embargo and was the first reaction to learning where our formerly inexpensive energy was going and how we could better operate regenerative furnaces. I was infected by the elegance of the mathematical approach to understanding furnaces. I thank George Boettner for the exposure to this marvelous approach to glass furnaces and hope George, who is 95, can appreciate where we are today, even though it has taken 34 years since the original exposure.

GLASS FURNACE STACK GAS CALCULATION ISSUES

C. Philip Ross
Creative Opportunities, Inc.
Laguna Niguel, CA

ABSTRACT
Exhaust gases from glass melting furnaces require quantification for a variety of purposes. These include potential waste heat recovery system design and optimization, engineering for "add-on" pollution control equipment, and air emission compliance calculations. This "tutorial" paper will review aspects of performing exhaust volume calculations, as well as identifying all process sources to be considered.

PRESENTATION

Glass producing furnaces are typically quantified by their production output, operating temperatures and energy consumption values. This paper will review aspects on process gases resulting from combustion, gaseous evolution from the melt's raw materials, and a variety of sources of air infiltration. Common calculations using gas volumes include:

- Stack Gas Volumes and Draft Potential
- Stack Emission Compliance (mass vs. concentrations)
- Gas Velocities (burners, Ports, Checkers, Flues)
- Thermal Content and Heat Recovery Potential
- Combustion Efficiency
- Greenhouse Gas Emissions

Air emission regulations in the U.S. are most typically stated on a weight basis (such as pounds of pollutant per ton of glass melted). However, actual stack measurements are determined on a dry concentration basis (ppmv, or mg/m^3). To convert these concentration measurements into weights it is necessary to know the total volume and water content of exhaust gases exiting through the stack.

Mass Rate (lb. / hr.) = Concentration (mass / volume in ppmv, or mg/m^3) * Volume (cu. ft. / hr.)

For furnaces with Continuous Emission Measurement Systems (CEMS), the actual volume of gases passing a specific location (typically in the stack) is calculated by:

Quantity (acfm) = Area (sq. ft.) * Velocity (ft./min)

The accuracy of this method is dependent upon determining the true average velocity, having a well defined cross sectional area, and accurately measuring the average temperature of the gases. The velocity measurement is most typically taken with a Pitot Tube or Optical Flow Sensors (Scintillation) at a single location and applying a correction factor to represent the average velocity across the defined area. The correction factor comes from EPA's Velocity traverse procedure (Method 2).

Each gas species had it's own specific gravity (lb. / ft^3). Consequently it is necessary to convert between mass and volume for gas species. For glass furnaces more than 99 % of the furnace exhaust volume is made up of CO_2, H_2O. O_2 and N_2. Criteria gaseous pollutants, such as NO_X, CO and SO_X, seldom exceed totals of 2,000 ppm (or < 0.1 %).

Air pollution gases are measured in volume concentration of the furnace exhaust gases. Since the measurements are taken typically at ambient temperatures, the water from combustion has condensed out and we are consequently dealing with a "dry" volumes. Again EPA defines procedures for determining the moisture level of exhaust gases and converts the sampled gas volumes to a dry basis (using their Method 4). Since the "dry" gases are essentially CO_2, N_2 and O_2, EPA Method 3 determines the average molecular weight for mass concentration conversion calculations.

To better understand all sources of furnace exhaust gases, the following section will review how quantify the mass and volume from each source. The sources of the exhaust gases from the melter can be categorized as follows:

Products of Stochiometric Fuel Combustion
Excess Combustion Air or Oxygen
Process Emissions from Raw Material Calcination or Dehydration
Batch Moisture
Air Infiltration (Cooling Air, CCTV, Bubblers, etc.)

Straight forward calculations can be made for each of these components to determine the volume and chemistry of each of these categories. For dealing with actual volumes of gases at elevated temperatures, the "wet" volumes are used. For converting from concentration measurements made below 212 ^{o}F, the "dry" volumes (excluding water) must be used.

Products of Stochiometric Fuel Combustion - Fossil fuel combustion results in all of the hydrocarbons converted to CO_2 and H_2O gases. Nitrogen in the air, natural gas or oxygen source pass through the combustion process. Natural gas chemistry includes varying percentages of Methane, Ethane, Propane which results in the caloric value of heat released in the combustion process. It is possible to precisely calculate the products of combustion gases [Spreadsheet]. More typically, a "Fuel Factor" is applied to the fuel consumption quantity which yields the amount of products of combustion.

Process Emissions from Raw Material Calcination or Dehydration - Fusion losses typically occur from the major carbonate and hydrated raw materials. Raw material batches are typically described with a :fusion loss" factor, which relates to the weight percent loss of the batch contributing mass to the furnace exhaust. The typical weigh losses which significantly contribute to the furnace exhaust volume are:

Limestone	44.8 % CO_2
Dolomite	46.8 % CO_2
Soda Ash	41.9 % CO_2
Borax	30.0 % H_2O
Boric Acid	43.5 % H_2O

Batch Moisture - Soda Lime glasses, batch wetting levels of 3 - 3.5 % are very typical. These measurements are made by direct measurements of batch as it enters the furnace. Depending upon whether the measurement includes or excludes cullet, the weight of water per hour or unit of production can be directly calculated.

Excess Combustion Air or Oxygen / Air Infiltration - For air combustion, measurements of the level of excess O_2 can be used a variety of EPA factors. The scfm volume of stochiometric combustion products is calculated with the following factor for the fossil fuel input and level of O_2 in the exhaust gas:

Scfm Exhaust = (8710 * scfh * (mmbtu/mcf)/1000/60 - O_2 scfm Boost * 79.1/60/20.9) * 20.9/(20.9 - Stack $\%O_2$)

Unfortunately, these factors are based upon products of combustion only, and do not take into consideration the significant amount of CO_2 and H_2O evolution from the glass making raw materials and batch moisture. To more accurately calculate the total exhaust gases, it is necessary to begin with the natural gas chemistry, and specific information regarding the raw material chemistries. The following calculation for two 300 ton/day soda lime furnaces (Conventional air and Oxy-gas) shows how gas volumes can be calculated, using typical natural gas:

	Air Combustion	Oxy-Gas
Fossil Fuel Energy Efficiency	4.2 mmBTU/Ton	3.6 mmBTU/Ton
Natural Gas Consumption (@1040 BTU/Ft^3)	50.5 mcfh	45 mcfh
Batch Fusion Loss	17 %	17 %
Percent Cullet	40 %	40 %
Batch Wetting	3.5 %	3.5 %
Products of Combustion		
Stochiometry Combustion Factor	10.3	2.05
Stochiometry Comb. Products Factor	11.36	3.17
Combustion Products	573,680 scfh	142,650 scfh
N_2 @ 8.20 scf/ft^3	414,100 scfh	450 scfh
CO_2 @ 1.09 scf/ft^3	55,045 scfh	49,050 scfh
H_2O @ 2.07 scf/ft^3	104,535 scfh	93,150 scfh
Excess O_2	@ 1 %	@ 0.5 %
N_2	4,114 scfh	0 scfh
O_2	1,087 scfh	461 scfh
Process Gases		
Glass From Raw Materials	180 ton/day	180 ton/day
Dry Batch Requirements	217 ton/day	217 ton/day
Batch CO_2	37 ton/day	37 ton/day
CO_2 @ 0.1167 / scf	26,421 scfh	26,421 scfh
Batch Moisture @ 3.5 %	7.9 ton/day	7.9 ton/day
H_2O @ 0.0466 / scf	14,127 scfh	14,127 scfh
Total Gas Volumes	scfh	scfh
N_2	418,214	450
CO_2	81,466	75,471
H_2O	118,662	107,277
O_2	1,087	461
TOTAL	**619,429 scfh (wet)**	**183,659 scfh (wet)**
	500,767 scfh (dry)	**76,382 scfh (dry)**

@ 2800 °F	(2800+460)/(60+460) = 6.27 X	3,883,820 acfh	1,151,540 acfh
@ 800 °F	(800+460)/(60+460) = 2.42 X	1,499,020 acfh	444,455 acfh

Total Gas Weights		Tons / Day	Tons / Day
N_2	@ 0.0738 / scf	370.4	0.4
CO_2	@ 0.1167 / scf	114.1	105.7
H_2O	@ 0.0466 / scf	66.4	60.0
O_2	@ 0.0843 / scf	1.1	0.5
	TOTAL	**552.0 tons/day**	**166.6 tons/day**

When dealing with the weight of each gas species, the heat content (enthalpy) in BTU's can be calculated ad specific temperatures for a variety of purposes. For basic calculations, the following factors can be considered for common gases between 800 to 2900 °F:

Gas	MWT	lb./ft^3	BTU/lb/°F	BTU/lb @ 800 °F
Air	28.88	0.0749	0.282	179.0
N_2	28.02	0.0738	0.290	188.8
CO_2	44.01	0.1167	0.304	176.5
H_2O	18.02	0.0466	0.586	1327.7
O_2	32.00	0.0843	0.263	172.1

POLLUTANT CONCENTRATION TO MASS CONVERSION

Portable chemical cell analyzers are often used to obtain representative concentrations of a variety of gaseous components of a furnace exhaust. These can include O_2, CO, NO, SO_2. For converting a pollutant concentration (PPMV) into a mass emission, the application of a "Fuel Factor" is typically employed. A detailed determination can be calculates from the nature of the fuel being combusted.

(scf / mmBTU) = (3.64 * % H +1.53% % C + 0.57 * % S + 0.14 * % N -0.46 * % O) * (scf / lb.) / (HHV BTU/lb)

The typical fuel factor (on a dry basis or F_d) varies between Air and Oxygen combustion:

	F_d
Air Combustion	8,710 scf/mmBTU
O_2 Combustion (100 % Purity)	1,048 " "
O_2 Combustion (90 % Purity)	1,291 " "

Knowing the molecular weight of the criteria pollutant being measured, the following equation can then be used to complete the conversion calculation.

E = C * (mwt / (385.1 * 10^6)) * [(Fuel Energy * Fd * PFC) * (20.9 / (20.9 - %O2)) + A/(1 - 4.78 * %O2 / 100)]

Where:

E	=	**Pollutant's Pound per Hour**
C	=	**Concentration in parts per million (dry)**
mwt	=	**Molecular Weight of Pollutant**
Fuel Energy	=	**Million BTU per hour from Combustion**
Fd	=	**Fuel Factor**
PFC	=	**Stack Flow Correction Factor**

A = scfh of Process CO_2 (from Batch fusion loss calculation)
% O_2 = % Oxygen where pollutant gas is measured

For comparing these "informal" emission measurements relative to regulatory compliance, the emission in pounds per hour can be divided by the furnace output (in tons/hour) to determine the pound per ton emission estimate. Obviously the use of a certified CEM's or certified stack emission test (using procedures specified by the appropriate agency) will be the only official determinant for legal compliance.

GHG REPORTING

Beginning in 2009, glass industry has been required to report Green House Gas emissions in California, and proposed Federal reporting requirements are expected shortly. Essentially all of the CO_2 emissions from glass container manufacturing is the result of natural gas combustion and calcination of two major raw materials in the soda-lime glass batch recipe - Soda Ash (Sodium Carbonate or Na_2CO_3) and Limestone (Calcium Carbonate or $CaCO_3$). (Some facilities may emit CO_2 from acid gas scrubber operations.) The following CO_2 emission factors were used for the Container industry's 1990 California inventory analysis:

Natural Gas - 0.05305 mTonnes CO_2/mmBTU's *(Per CARB)*
Soda Ash - 0.4152 mTonnes CO_2/mTonne Soda Ash *(Na_2CO_3 to $Na_2O + CO_2$)*
Limestone - 0.4397 mTonnes CO_2/mTonne Limestone *($CaCO_3$ to $CaO + CO_2$)*

CALCULATION REMINDERS

In dealing with gas calculations it is important to recognize that calculations must take into account the wide range of temperatures experienced in glass furnaces, as they have a significant impact upon the actual volume of gases. Most gas volumes are corrected to standard temperature and pressure conditions. Pressure is corrected to atmospheric conditions at sea level, while pressure may be defined at different temperatures. In English units the standard temperature is usually 60 °F, while in normalized Metric it is 0 °C. This sometimes leads to errors in converting between English and Metric units.

	Metric	English
Standard Pressure	101.325 kPa or *760 mmHg*	14.7 psi or 29.92" Hg
Standard Temperature	0 °C	60 °F (15.6 °C)
Absolute Temperature	273.15 °K + °C	459.67 °R
Gas Volume Equivalent	1 nM^3	37.326 scf [1]
	1 scf	0.0269 nM^3

Calculating total gas volumes under different temperature or pressure conditions is easily performed with the use of "Boyles Law".

PV = nRT

Where: P = Pressure psia (absolute)
V = Volume ft^3

[1] 1 cubic meter's volume is $(3.28083 \text{ ft.})^3 = 35.314$ cubic ft

n = Number of moles

R = Gas Constant 1073 psia · ft^3 / lb. Mole · °R

T = Absolute Temperature, °R

For converting between different temperature and pressure conditions, the equation is simplified to:

$$P_1V_1/T_1 = P_2V_2/T_2$$ where the temperature and pressures are in Absolute units

When dealing with the chemistry of gas mixtures, the molecular weight of each gas must be considered. For the simple combustion of Methane with Air, the following chemical equation is used:

$$CH_4 + 2O_2 + 8\,N_2 \rightarrow CO_2 + 2H_2O + 8N_2$$

This means that each scf of Methane requires 2 scf of Oxygen (or 10 scf of Air) and results in one scf of CO_2 and 2 scf of H_2O. Having the precise chemistry of natural gas (a mixture of Methane, Ethane, Propane, and other gases) and the actual level of excess air (or Oxygen) allows a specific calculation of the actual products of combustion. Of course the products of combustion gases are at elevated temperatures (but the same atmospheric pressure) and their actual volumes would have to be corrected with a modified Boyles Equation:

$$V_2 = V_1 * T_2/T_1$$ where the temperatures are in Absolute units

The T_2/T_1 would be a volumetric expansion factor, and as example for "actual" combustion volumes to 2800 °F would be:

(2800 + 460) / (60 + 460) = 6.27 times the standard volume

Specific Gravity and Molecular Weight Conversion:

$S = M / M_{air}$,

where S = gas specific gravity, MWT = gas molecular weight, MWT_{air} = 28.96443 g/mole

At 70 °F and 14.696 Pisa, dry air has a density of 0.074887 lb/ft^3. For the density (D) of any gas at standard conditions:

Gas Species Density = 0.074887 lb/ft^3 * MWT / 28.96443 = MWT * 0.002586 lb/ft^3

Glass melting with natural gas combustion involves metering of both the natural gas and the combustion air. The actual products of combustion gases are calculated based upon the natural gas chemistry. This is because it can contain various proportions of CH_4, C_2H_6, C_3H_8, C_4H_{10}, CO, etc. For typical natural gas chemistry a simplified factor can be applied to calculate the products of combustion under stochiometric conditions.

scfh nat. Gas * 10.3 = scfh combustion air, and yields 11.3 scfh of products of combustion

or scfh nat. Gas * 2.05 = scfh oxygen, and yields 3.05 scfh of products of combustion

Of course the actual volume must be calculated for the actual temperature of the gases by Boyles Law.

In actual furnace operations, the volume of products of combustion also included certain levels of excess oxygen (air). In fact, most furnaces operate with target levels of excess O_2 - as measured with combustion analyzers. For air combustion, the use of a "F" (or fuel) factor is used to calculate the volume of combustion products:

Absolute pressure is measured relative to the absolute zero pressure. *Gauge Pressure* is often used to measure the pressure difference between a system and the surrounding atmosphere. This pressure is often called the gauge pressure and can be expressed as $p_g = p_s - p_a$

where:

p_g = gauge pressure
p_s = system pressure
p_a = atmospheric pressure

Some calculations can also generate errors when the proper atmospheric pressure is not corrected for elevation above sea level, and even unusual weather conditions.

This Page Intentionally Left Blank

INCREASE OF GLASS PRODUCTION EFFICIENCY AND ENERGY EFFICIENCY WITH MODEL-BASED PREDICTIVE CONTROL

Erik Muijsenberg and Menno Eisenga
Glass Service B.V.
Maastricht, The Netherlands
HQ Glass Service Inc., Vsetin Czech Republic
info@gsl.cz - www.gsl.cz

Jörg Buchmayer
Gerresheimer Lohr
Lohr, Germany

ABSTRACT

In the past decade, advanced multiple input/multiple output (MIMO) process control systems have found their way into the glass industry. Today a growing number of glass furnaces and forehearths have been equipped with a supervisory control system. Daily regulation of fossil fuel firing and electric energy supply to stabilize temperatures is no longer in the hands of the operator, but fully taken over automatically by the ES III™ MPC controller, which provides consistent process control, 24 hours per day, focused to operate the entire glass production process in the most efficient way.

INTRODUCTION

Expert System, either version *ESII*™ or *ESIII*™, provides supervisory multi-variable model based predictive control in time and space This definition is not very understandable to people who are not familiar with advanced process control, thus let's try to explain it word by word.

Word *supervisory* means that the *Expert System* implementation preserves the primary control level: all devices (PLCs, internal switches) as well as up to date control mechanisms (PID loops, availability to change inputs manually). *ES III*™ can even use primary control level elements as part of the advanced process control.

Next word, *multi-variable,* means that multiple inputs can be handled at the same time to affect multiple outputs. This property is very important for supervisory control of the glass melting and conditioning processes. For example, in a float furnace the total amount of gas is only one of the inputs that affect the crown temperatures. The next one is batch feed rate. And batch composition (the next one) is maybe even more important. An ambient temperature also correlates with crown temperatures. So it can be concluded that crown temperatures are affected not only by one variable (total gas), but by many more. On the other hand, there are usually several crown temperatures with different importance for process control. And we have not discussed yet the effects of glass level, canal temperatures, oxy-boosting, etc. All of them affect (or are affected by) process control too.

Overall, the process control is a complex problem where multiple inputs and outputs play strongly together at various levels of importance.

Next important portion of *Expert System* definition is the word *model* (*model based predictive control*). It refers to the control techniques that are mostly used. Model based control uses information about the process variables history and a mathematical approximation of the process behavior: the *model*. Model knowledge is important for process control and the predicted future behavior. At each moment the next control actions are planned as well as the estimated future behavior of temperatures and other controlled variables. The models can be derived in 4 ways:

1. From dynamic step response testing on the real process.
2. From step response tests on a mathematical model (computer fluid dynamics, also called white models).
3. By a combination of the above or by estimating models based on the behaviour of the process
4. Or from a historical database.

The remaining words from the definition seem to be understandable. On top of this there are properties not mentioned in the definition above that are implemented in *ES III*™ too.

- Safety. Every system you are going to use for continuous glass production has to be safe. At first, it is necessary to return automatically to the basic control level in case the communication between systems (*ES III*™ and DCS) fails. Next, *ES III*™ contains fault detection logic that refuses to react on variable values that are out of specified intervals or changes abruptly (typical for thermocouple failure).

  An off-line simulator can be included into safe tools too. Would you like to know how the process will react with different process control settings? Or even would you like to try it but you don't want to violate your valuable glass production? The off-line simulator offers you to experiment with these settings off-line, in simulation mode. Thus you can look for best-fitting solution that fully matches your ideas about precise process control while you are producing high-quality glass. The final solution can be applied as settings on real process control then. You also can store these settings through the Process Settings Manager. This manager contains recipes for various glass production types so these settings are always ready to be applied on the process – it eliminates the potential mistakes caused by hand made inputs.

- Flexibility coming especially from the entire package of algorithms devoted to process control. It can happen that some variables affecting process behavior are not predictable – you can estimate the future behavior only with limited reliability. As a consequence, the model based predictive controller (MPC) cannot consider these variables as known inputs. So it is necessary to find out alternative ways how to get such variables back to the game. Except for MPC controllers there are fuzzy logic controllers and classic rules based systems available for use. These tools are very powerful and can work either

separately or together. It gives the process control designer a big chance to choose the strategy that fits optimally.

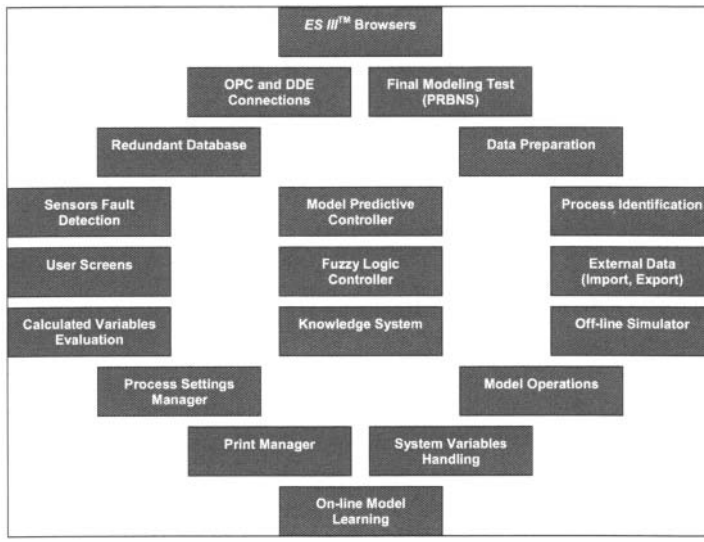

Figure 1: Summary of ES III™ system features

- Control System Enhancements. Beside all properties mentioned above there are several tools that belong more to the plant information. Among those tools can be included internal database (gathers and stores data in requested form and timing), user screens (serves for visualization of all available data including data from database) and reports (either printed out at specified time of the day or stored as PDF document), etc.

ES III™ is the trademark of the advanced process control system developed by Glass Service, especially for applications in the glass production industry. The glass melting process is characterized by slow process changes in the melting tank with extremely long reaction times, but on the other hand short timescales in combustion process changes . Typically, glass resides 24 hours or longer in the melting-end and any change in the furnace heat input can easily take 4 till 8 hours before the impact on the glass melt throat or bottom temperature is observed. This makes it difficult for operators to run the furnace stable in their limited 8 hour shifts, and also conventional automatic controllers without process knowledge or predictive response models are not suitable to handle such long term process changes and slow response (e.g. change of melt temperatures by changing fuel input) either.

The Model-based Predictive Controller (MPC) is the main controller engine inside *ES III*™. Unique process models (identified from a 3-4 weeks historical data sample) These models are so called black models and can be derived in different ways as described earlier. Inform the controller about the actual response of the furnace, including dead times between heat input and change in glass melt temperature, at different positions important for glass quality, over time. *ES III*™ continuously monitors the actual situation in the furnace and forehearth and predicts future trends based on the process models and recent control actions. If a new temperature set-point is required, the *ES III*™ system predicts the necessary changes in firing to achieve the new temperature in a fast and optimal way taking into consideration constraints (e.g. maximum temperatures or maximum acceptable fuel injection rates), just like a car navigation system optimizes the directions to a new destination. Despite a good process model, the glass melting process is unfortunately not 100% predictable because of disturbances that cannot be measured nor predicted, so (just like the weather forecast) a continuous adjustment of the long term prediction is inevitably necessary. For glass melting and conditioning, the prediction update of the process every couple of minutes is sufficient and the operator is informed by clear trend lines in the *ES III*™ graphical user interface (see figure 1).

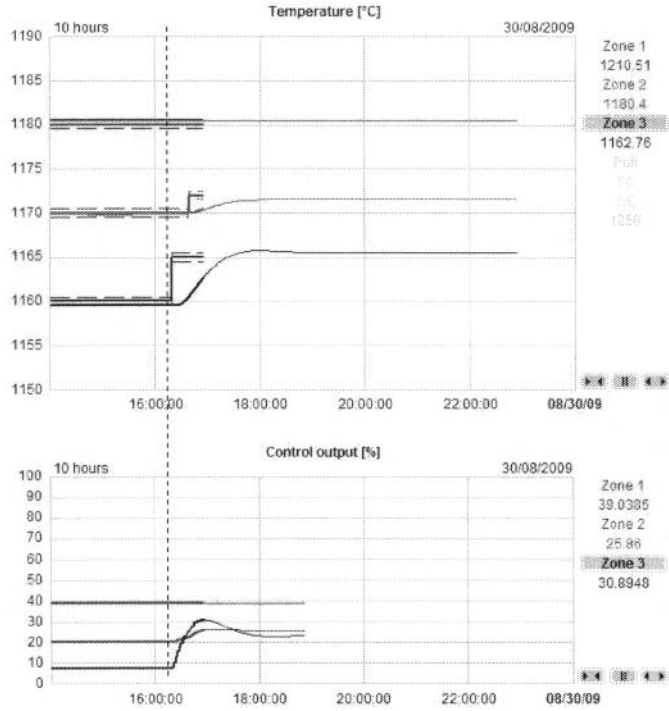

Figure 1: Example of ES III™ Predictive Control. Thin solid trend lines show the predictions of the temperatures (top) and planned firing changes (control output, bottom picture) in a forehearth with 3 conditioning zones. The dashed vertical line denotes the actual time. The solid thick lines show historical behaviour and actions and the dashed lines are the zones of the controlled variable (also can be called a setpoint with a zone)

ABOUT CONTROL AND STABILITY

The primary objective of the *ES III*™ controller is to control the temperatures of the entire glass melting process and improve the stability of temperatures, glass melt level and the final melt temperatures delivered into the forming process (e.g. gob temperature or glass outflow), firing and cooling conditions, etc. More stable production conditions obviously yields better conditions for glass forming, thus increasing the production line yield and minimizing the amount of rejects. Customers even report reduction of common repairs and thus a positive impact on the furnace lifetime, however it is not easy to proof that this is directly related to the better control only.

In order to take over the entire temperature control of a glass furnace, the advanced controller should be able to control multiple temperatures at the same time. Typically, the furnace crown temperature and temperature profile should be controlled to prevent crown overheating (or to prevent too low temperatures where silica reacts with sodium vapors) and to obtain the minimum required bottom glass temperature to melt the glass with best quality. Usually, there is more than a single burner in the furnace, and usually additional electric boosting is directly applied into the glass melt. All these heat sources should operate together in the most efficient and stable conditions. The *ES III*™ MPC controller has been designed to handle such Multiple Input Multiple Output (MIMO) process changes that takes into account all possible correlations between the various inputs (firing, boosting, valves, cullet ratio?, pull? etc) and control outputs (temperatures, glass melt level, and sometimes pressure).

HOW TO SAVE ENERGY?

Improving the stability of the melting process is the first step towards saving energy. A continuous monitoring of the process helps to prevent glass temperatures to slowly drift and excessive reactions of the operators in firing may then be necessary. The *ES III*™ system watches the furnace the entire day and collects all relevant furnace data to update predictions of future trend lines. Only smooth changes are applied in the firing and furnace setup, unless a major step change is required (e.g. at a sudden job change). It is important for energy efficiency that throat temperatures are not higher than really necessary for a certain glass product, higher temperatures result in extra energy consumption in the glass furnaces and requires additional cooling in the forehearths, working-end or feeders. However, on a long term basis, the expected savings in terms of heat input often turn out to be marginal typically: 1-4 %, though most traditional glass furnaces are operated by experienced operators that are able to control the process without excesses most of the time. This situation can be different in completely new plants as the new operating people do not have so much experience yet and need to learn from their mistakes. Enhanced stability of the glass melting and conditioning process is often most profitable for the subsequent glass forming, hence more and better quality of final products and higher pack-to-melt levels.

The figure below shows how temperature control and stability can really be used to save energy. Most glass furnaces are operated at an average glass temperature that is hot enough to prevent fining problems and seeds and blisters in the final product. The more the glass temperature varies, the hotter the average furnace glass melt temperature is chosen to prevent glass quality issues. With a controlled and stable glass temperature, the furnace manager is able to explore the limits for his glass production. By lowering the set-point of the operating temperature he can save a considerable amount of energy, up to 3% or sometimes even more. But this depends also on how the customer uses the tool most effectively.

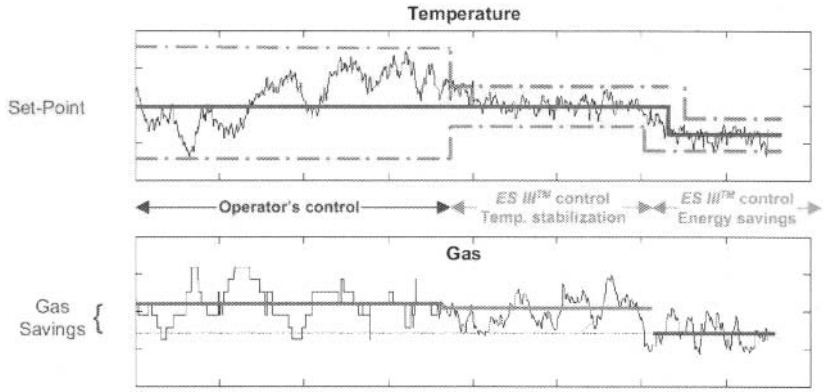

Figure 2: Energy savings by temperature control and stability. The step down in the set-point of the glass temperature saves directly on average gas consumption. Use the reduction in temperature variation to explore the actual limits of the melting process and keep the desired glass quality. The vertical scale on the top picture shows temperature in °C and on the bottom picture gas consumption in m3/hr. For customer confidentiality the real levels are not show.

As a third example of how to save energy, using an advanced control system, let's comment on the conventional forehearth control. Usually each conditioning zone is controlled by a PID controller with the temperature set-point selected by an operator. As the zones are controlled individually, the firing in each zone can be completely different. Often the heating in one zone is followed by cooling in the next zone and again strong heating in the next. A smooth reduction in the forehearth temperature with more uniform heating or cooling is considered to be ideal and this can only be accomplished with the advanced *ES III*™ MIMO controller that is able to handle all zones of the entire forehearth at once. Cooling valves are only opened after firing is reduced to the minimum and, oppositely, are properly closed before heating starts. The MIMO controller can also help to make the glass melt temperatures close to the spout (e.g. at the 9 grid if available) more homogeneous, but practical experience has shown us that keeping the glass melt temperature of the 9 grid bottom measurement constant is more important than small homogeneity variations. Also the model based control can help to

change these temperatures faster than operators can do for a job change (typically twice as fast).

The last example mentioned here applies to fossil fuel fired glass furnaces that are equipped with an additional electric boosting system. The electric boosting systems are usually very efficient as the heat is supplied directly to the glass. However, the actual high price of electric energy often forces the furnace manager to find an optimal balance between energy efficiency and cost efficiency. Using the *ES III*™ Minimal Cost Strategy, the MPC controller takes into account the prices of the various heat sources as well as their efficiency to control the furnace temperature. So the required glass temperature is obtained at minimum costs. The same strategy can even be used to find the optimal balance with 2 or more electric boosting systems. It's almost impossible to find such a balance without a supervisory control system.

The *ES III*™ advanced control system is a tool that helps the operator in their daily operation of the furnace, as well as the furnace manager being able to reach his targets for producing glass of the highest quality with minimum energy and costs.

To give you some example of energy savings we are pleased that Gerresheimer Glass agreed to participate on this paper and share their experience. In their factory in Lohr we have achieved energy savings on annual comparison of 4.3% at a production of 130 TPD. During the slide presentation we will show more of their results.

REFERENCES

[1] Josef Müller, Robert Bódi, Josef Chmelař: How to Make Glass Furnace Control Easier: Advanced Optimal Control by Expert System *ES III*™, Proceedings of the VIII. International seminar on mathematical simulation in glass melting, Velké Karlovice 2005, p. 200
[2] Josef Müller, Josef Chmelař, Robert Bódi, Erik Muysenberg: Aspects of Glass Production Optimal Control, Proceedings of the VII. International seminar on mathematical simulation in glass melting, Velké Karlovice 2003, p. 157
[3] Josef Müller, Robert Bódi, František Matuštík: Expert System ES III - A System for Optimal Glass Furnace Control, Glass - Monthly Journal (Vol. 81, No. 9, October 2004)
[4] Josef Chmelař, Erik Muysenberg, Robert Bódi: Optimizing Glass Production with Expert System ES-II, Proceedings of the VI. International seminar on mathematical simulation in glass melting, Velké Karlovice 2001, p. 101
[5] Erik Muysenberg, Josef Chmelař, Robert Bódi: Supervisory Advanced Control of Glass Melters by GS Expert System ES-II, Proceedings of the V. International seminar on mathematical simulation in glass melting, Horní Bečva 1999, p. 162
[6] Peter Mikulecký, Robert Bódi, Josef Chmelař: Towards Total Glass Quality Management, Proceedings of the IV. International seminar on mathematical simulation in glass melting, Horní Bečva 1997, p. 172

This Page Intentionally Left Blank

TEMPERATURE DISTRIBUTIONS IN GLASS GOBS BETWEEN SHEARS AND BLANK MOLD: CALCULATIONS AND MEASUREMENTS

Hayo Müller-Simon, Gesine Bergmann, and Kristina Kessler
Research Association of the German Glass Industry (HVG)
Offenbach, Germany

ABSTRACT

In IS machines in container glass production between the shears and the blank mould the glass gob is in contact with the cold delivery system which induces considerable temperature gradients in the gob surface. Because of the strong dependence of the viscosity on temperature this often causes problems such as hot cracks or an unfavorable glass distribution. In a current research project temperature distributions in glass gobs are measured by means of pyrometers using different wavelengths. Finite element method calculations are used in order to reconstruct the internal temperature profiles from the measured data as well as to relate them to the influence of the delivery system. The temperature decrease at the surface of the gob can be explained as a function of heat loss by radiation and by contact with scoop, trough and deflector. There is evidence that the heat transfer coefficient in the trough decreases as the gob travels through the trough.

INTRODUCTION

In IS machines for container glass production the glass gob is in contact with the cold delivery system between the shears and the blank mould which induces considerable temperature gradients in the gob surface. Because of the strong dependence of the viscosity on temperature this often causes problems such as hot cracks or an unfavorable glass distribution. In a current research project temperature distributions in glass gobs are measured by means of pyrometers using different wavelengths. Finite element method calculations are used in order to reconstruct the internal temperature profiles from the measured data as well as to relate them to the influence of the delivery system.

MEASUREMENTS

Measurements have been carried out at an IS-machine of Saint-Gobain Oberland at work Bad Wurzach. Temperatures have been measured by means of fast operating pyrometers at wavelengths of 1.46 µm, 3.9 µm und 5.14 µm. Figure 1 shows a sketch of the delivery system. The temperatures have been measured 0.6 m below the shears during the free fall of the gob through the view field of the pyrometers. When the gob passes the view field of the pyrometer the temperature increases not only due to the reaction time of the detector, but also a linear increase of the temperature along the length of the gob is measured. The higher temperature at the top and the lower temperature at the bottom of the gob can be assigned to the heat loss by radiation during the extrusion of the glass from the feeder before the gob is cut. Figure 2 shows the maximum temperatures which have been detected when the gob passes the pyrometer. The circumferential temperature distribution was only accessible from one side. According to figure 2 the gob has already a distinct radial temperature profile. The measured temperature gradient is much to large to be explained only by heat loss by radiation. Obviously the gob carries the temperature profile already out of the feeder. A second temperature measurement has been carried out looking into the deflector about 0.8 m above the blank mould. These results are shown in figure 3. Provided that the gob does not rotate when it is transferred into the deflector, the surface which is observed with the pyrometer is the one which was in contact with the trough.

Additionally, the lengths and the velocities of the gobs have been measured by means of a speed gob. These measurements have been carried out 0,6 m below the shears and 0.8 m above the blank mould in the deflector as well as at a few points in the trough where it is accessible.

MODEL BASED INTERPOLATION

In recent years mathematical modeling has made large progress not only in glass melting but also in forming of glass [1]. Also the delivery system of container glass machines has been subject to modeling activities in the last years [2, 3]. These advances were mainly possible by the use of increasingly larger computers and increasingly sophisticated software. However, these models require a very great effort of material, manpower and time, which is not always available. On the other hand the significance of mathematical modeling is restricted by the possibilities of practical verification, which is extremely difficult especially under industrial conditions. Thus, in many cases it is sufficient to use comparatively simple models in order to meet the accuracy of the measured control data. Thus, for this research project a very basic approach has been chosen. The main purpose of the fem calculations was the connection of the measured values, which is achieved by adjusting free parameters like for instance the heat transfer coefficient α between glassmelt and trough material. Thus, the calculation can be denoted as a model based interpolation.
The temperature field inside a body can be calculated by solving the heat transfer equation. In case of semi-transparent materials this equation is extended by the portion of absorbed and emitted radiation:

$$c_p \cdot \rho \cdot \frac{\partial T}{\partial t} = k \cdot \nabla^2 T + W_{abs} - W_{emis} = k_{eff} \cdot \nabla^2 T \qquad (1)$$

with temperature T, time t, heat conductivity k, specific heat capacity c_p, density ρ, absorbed heat flux W_{abs} and emitted heat flux W_{emis}. In the simplest case the fraction of radiation can be regarded as effective heat conductivity k_{eff}. Equation 1 yields for optical thick media. Therefore, the investigations have been carried out on amber glass, which fulfills the requirements of an optic thick medium best. Further the boundary conditions for the heat loss are required. Heat loss occurs via radiation:

$$q = \varepsilon\sigma\left(T^4 - T_0^4\right) \qquad (2)$$

or via contact:

$$q = \alpha(T - T_0) \qquad (3)$$

with heat flux q, emissivity ε, Stefan-Boltzmann constant σ, the environment temperature T_0 and heat transfer coefficient α. Heat loss by means of convection is not considered in this paper.
The heat transfer calculations have been carried out by means of free fem software [4]. The material data required in the heat transfer equation have been taken from literature: specific heat capacity c_p (T) [5], density ρ (T) [6, 7, 8] and heat conductivity for an amber glass [9]. The emissivity can be assumed to be 0,96 because approximately 4 % of the radiation from the inside is reflected at the surface. The heat transfer coefficient α is a result of the calculations.

MODELLING THE GOB HISTORY

The development of the gob's heat content shows four phases:

1. extrusion of the glass melt out of the feeder: the part of the gob which already left the feeder loses heat by radiation,

2. free fall between the shears and the scoop: during this phase the gob loses further heat by radiation,
3. passage through the scoop and the trough: the part of the gob which is in contact with metal loses heat by heat transfer, the upper side loses heat by radiation,
4. passage through the deflector: the surface which is in contact with the deflector loser heat by heat transfer, the opposite surface loses heat by radiation.

In order to couple the measured and the calculated data the path of the gob between shears and blank must be formulated in order to gain all relevant quantities as functions of time. Motion in the gravity field of earth can be described by the equations of motion for the case of free fall

$$m\frac{ds^2}{dt^2} = mg \tag{4}$$

with mass m, distance s, time t and gravity g and the case of inclined plane

$$m\frac{ds}{dt^2} = m \cdot \sin(\beta) \cdot g - \mu_R \cdot m \cdot \cos(\beta) \tag{5}$$

with the slope of the plane β and the coefficient of friction μ_R, which is assumed to be negligible in this investigation. Solving the equations of motion to time yields

$$t = \frac{-v_o + \sqrt{v_o^2 - 2bs}}{b}$$

for every section of the gob path with the starting velocity, the acceleration b and the position s inside the section. It is b = g for free fall and b = sin (β) g in the trough. The curve in fig. 4 shows the calculated velocities as a function of drop height.

A basic quantity in order to couple temperature calculations and measurements is the visibility depth of the optical temperature measurement. According to the approximation of Eddington-Barbier [1] the visibility depth is the reciprocal of absorption $1/\kappa$, which is 4 mm at 1.46 µm and 2,5 mm at 3.9 µm. The result at 5.14 µm refers to the surface.

Up to now the gob is described as a rigid cylinder and plastic deformation is not part of the model. In order to account for the elongation of the cylinder length and radius have been adapted to the results of the speed gob measurements for the phases 2, 3 and 4.

Results

Figure 5 shows the relations between measurements and calculations. In a first step the starting temperature profile which has been induced by the feeder must be estimated. Therefore, a rectangular temperature profile at starting time is assumed in such a way that the temperatures fit the results of the temperature measurements below the shears. Figure 6 shows the calculated temperature development when the gob passes the trough and deflector. The calculations have been carried out with a constant heat transfer coefficient of 1200 W/m^{2}K. When the gob has passed the trough the surface temperature increases due to reheating from the inside of the gob.

Based on the measured temperatures it is possible to calculate the heat transfer coefficient between the gob and the trough. The adjustion has been carried out separately for the surface temperature and the temperature of 2 mm depth. The results are shown in figure 7. Although, there is a large variation between the series of measurements the variations over the sections show a clear pattern. Especially, the lowest heat transfer coefficients at the center sections 6 and 7 are surely caused by the larger slope of the trough.

The heat transfer coefficient based on the surface temperature is lower than the heat transfer coefficient based on the inside temperatures. If one considers that the temperature changes much faster at the surface in case of external influences than inside the gob, the heat transfer coefficient connected with the temperature at 2 mm depth refers to an earlier point in time than the heat transfer coefficient connected with the surface temperature. It seems that the heat transfer coefficient decreases during the travel through the trough possibly due to the increasing velocity. This behavior agrees with the behavior of the trough temperatures. The temperature of the trough can be estimated by the heat loss of the gob. This heat must be released by the trough. If mainly heat loss by radiation is assumed the temperature distribution in figure 8 is calculated for the trough, which has a much smaller slope than the measured temperatures. There are still several influences which are not considered like convection of the surrounding air and exchange of heat radiation with the environment. But it seems evident that the heat transfer coefficient decreases as the gob travels through the trough.

***

The investigations were conducted with the kind support of the Arbeitsgemeinschaft industrieller Forschungsvereinigungen (AiF), Köln, (AiF-No. 15223 N), by agency of the Hüttentechnische Vereinigung der Deutschen Glasindustrie (HVG), Offenbach/M., utilizing resources provided by the Bundesminister für Wirtschaft und Arbeit. Thanks are due to all these institutions. The authors wish to thank also Saint-Gobain Oberland for the possibility to carry out the experiments and the colleagues at Bad Wurzach for their kind support.

REFERENCES

[1] Loch, H.; Krause, D.: Mathematical Simulation in Glass Technology. Springer-Verlag: Berlin Heidelberg 2002

[2] Hyre, M.: Numerical Simulation of Glass Forming and Conditioning. Journal Glass and Optical Materials (2002), S. 1047

[3] Liu, X. J.; Hyre, M. R.; Frost, G. S.; Austin, S. A.: Numerical simulation of heat transfer for the gob delivery system in glass container production. Proceedings of IMECE2008, ASME (2008)

[4] Dhondt, G.: The finite element method for three-dimensional thermomechanical applications. Chichester: John Wiley, 2004

[5] NEDO-Projekt-Report des New Glass Forum.

[6] Stebbins, J. F.; Carmichael, I. S. E.; Moret, L. K.: Contribution to Mineralogy and Petrology (1984) S. 131.

[7] Coenen, M.: Dichtemessungen an Boratgläsern. Glastechn. Ber. 35 (1962) S. 14 – 21.

[8] Coenen, M.: Dichte von "Scherbengläsern" bei hohen Temperaturen. Glastechn. Ber. 39 (1966) S. 81 – 89.

[9] Endrys, J.; Blazek, A.; Ederova, J.: Experimental determination of the effective thermal conductivity of glass by steady-state method. Glastech. Ber. 66 (1993), S. 151.

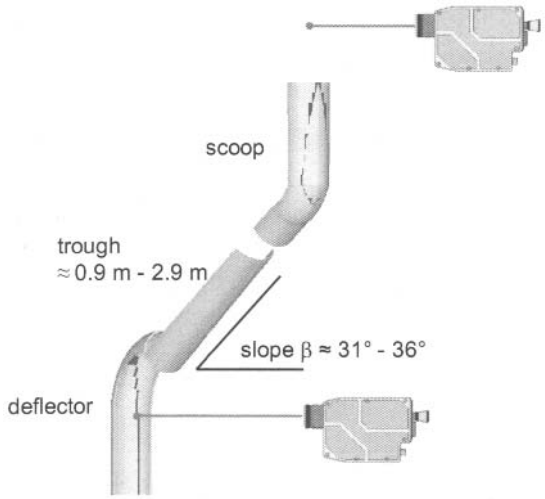

Fig. 1: Sketch of the delivery system and positions of temperature measurement.

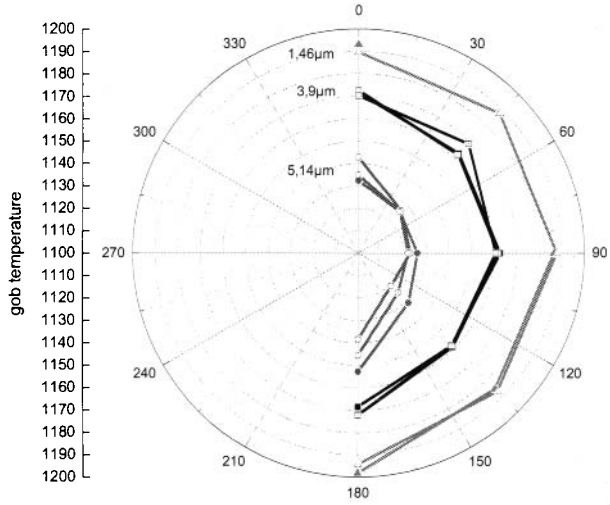

Fig. 2: Temperature distribution of the gob measured 0.6 m below the shears.

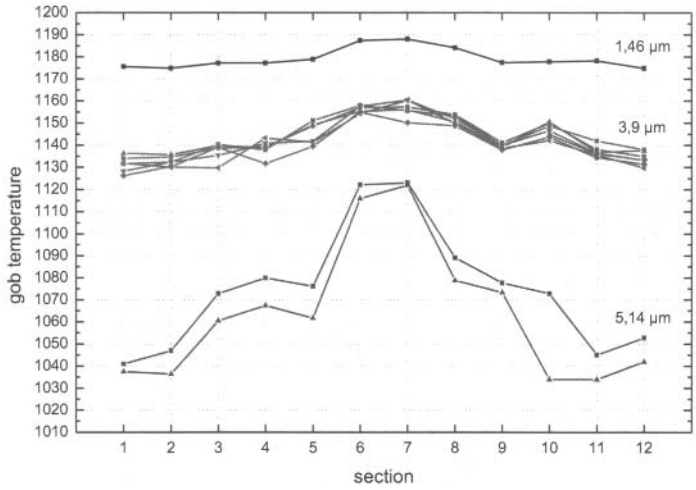

Fig. 3: Temperature distribution over all sections looking in the direction of the deflector.

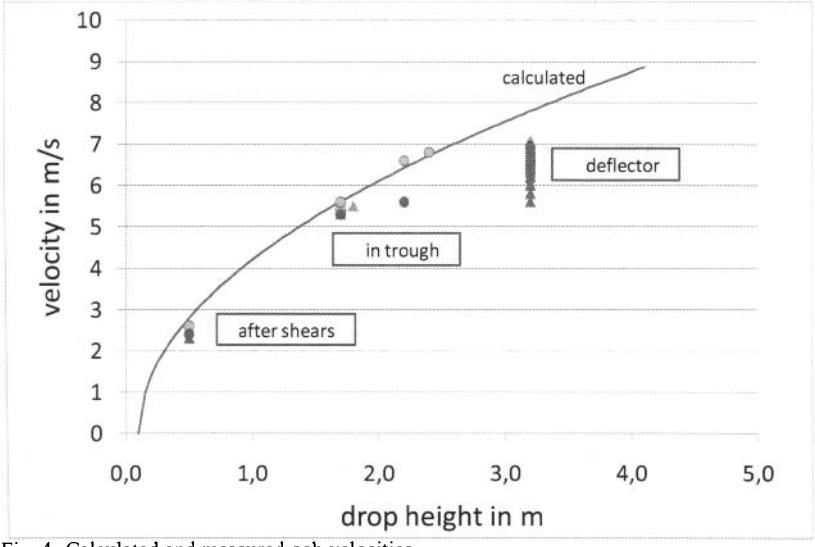

Fig. 4: Calculated and measured gob velocities.

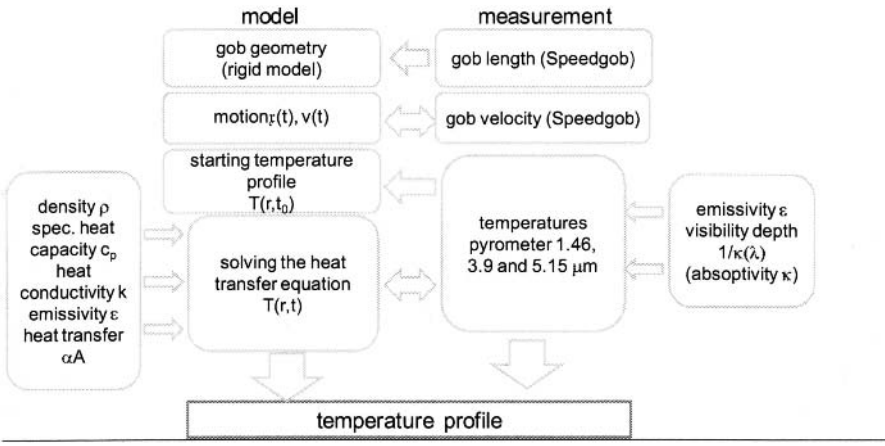

Fig. 5: Connection of measurement and calculation.

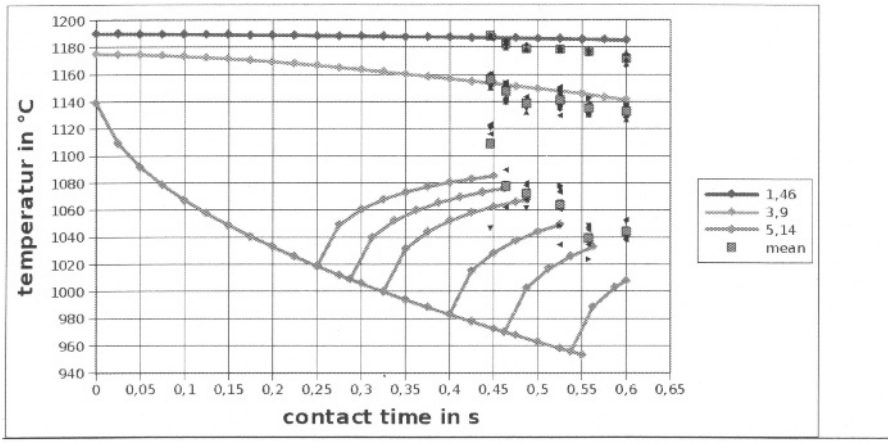

Fig. 6: Temperature development in contact with the trough, fitted to data measured at 1.46 µm corresponding to 4 mm depth, 3.9 µm corresponding to 2.5 mm depth and 5.14 µm corresponding to the surface.

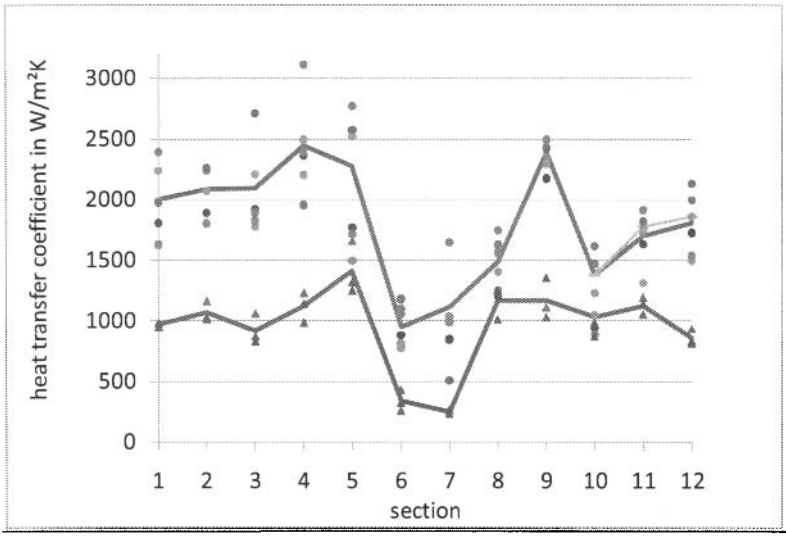

Fig. 7: Heat transfer coefficients, 1) based on use of 3,9 µm pyrometer, 2) based on use of 5,14 µm pyrometer.

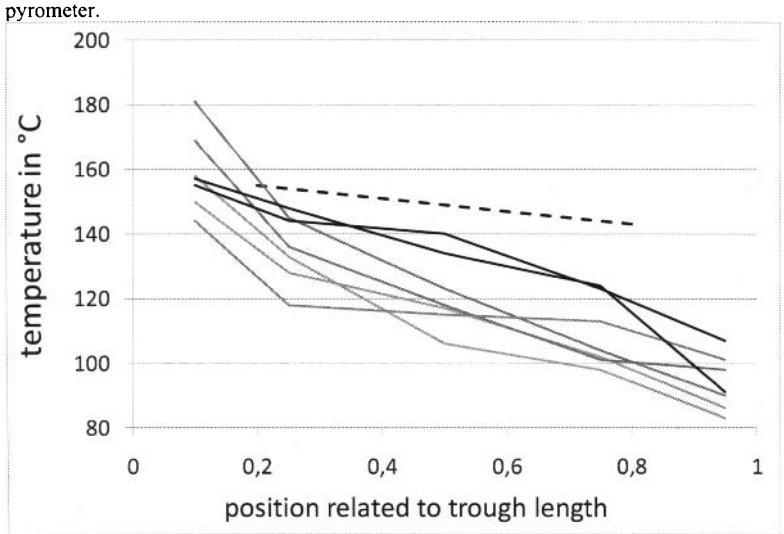

Fig. 8: Surface temperatures of the troughs and temperatures estimated by a heat balance (dotted line).

Refractories

This Page Intentionally Left Blank

POSTMORTEM OF A CONVENTIONAL SILICA BRICK FROM A SODA-LIME FLOAT GLASS FURNACE CROWN

Warren Curtis
PPG Industries
Cheswick, PA

ABSTRACT

In the 1990s, a silica brick retrieved from a conventional air-fired float glass furnace was analyzed to determine its alteration in service. Changes in its crystallinity, thermal expansion, chemistry, bulk density, porosity and physical appearance were determined at 6 different locations, going from its hot face to its cold face. Testing results and physical observations showed it to be completely altered from its original state. Considerably differences were also noted between the six different locations, going from its hot face towards its cold face. Such extensive alterations are attributed to its reaction with the alkali present in the furnace atmosphere and also the temperature and thermal gradient in which it operated.

INTRODUCTION

When this work was undertaken nearly 11-years ago, there had already been several reports issued on the rapid corrosion and poor performance of silica brick used in the crowns of oxy-fuel-fired soda-lime-silica glass furnaces, due to the corrosive nature of those furnace's atmosphere. There were also reports issued, suggesting ways to improve the performance of silica brick, and also heroic hot repair methods that could be used to extend the furnace campaign length when using silica. At this time, fused cast suppliers were also extolling the virtues of their AZS, and alpha-beta or beta alumina products for use as oxy-fuel furnace crown materials and there was also some work being done by bonded refractory suppliers on improving their silica brick to be less reactive in the oxy-fuel furnace environment. With such work ongoing, it was decided to investigate how badly standard silica brick would become altered in one of our conventional air-fired soda lime float glass furnace over the length of a typical campaign.

SAMPLE SELECTION

The silica brick evaluated in this study was a Type A superduty silica brand of domestic source. The term superduty means that the sum of alumina, titania and alkali impurities is <0.5%, whereas Type A, per ASTM C416-97 means that its alumina content plus twice its alkali content is less than 0.5%; those particular impurities are known to be by themselves, severe fluxes of silica brick.

This brick had been in service for nearly 11-years over which time this furnace had produced clear and also green and light-bronze tinted soda-lime-silica float glass. The crown had been insulated with a slurry coat of zircon cement seal layer, followed by a course of insulating silica brick and ceramic fiber blanket.

The brick analyzed was believed to be from near the hot spot of the furnace. The original thickness of this crown's silica brick was 18". This particular brick and nearby brick, however, were only approximately 17-1/2"-tall. This is because sometime during this furnace's campaign, this area experienced some distress, as it appeared that the hot face was shrinking-up to some degree and also appeared to have been molten at some time during its history.

Figure 1 shows the brick from which samples were taken and also their location in that brick. The left side is the cold face, while the right side is the hot face. The area that is missing from the hot face in the lower right of Figure 1 was due to this portion of the brick breaking off when the crown was dropped during demolition.

To obtain samples for evaluation, a 1" slice was removed from the brick on its 3" x 17-1/2" surface, which is parallel to the thermal gradient in this brick. From this slice, additional slices approximately ½"-thick perpendicular to this bricks' thermal gradient, were then taken for analysis. Those samples were located at approximately 17-3/8", 16", 11-1/2", 8", 5-1/2" and 2" from the cold face, and they are the missing slices as shown in Figure 1.

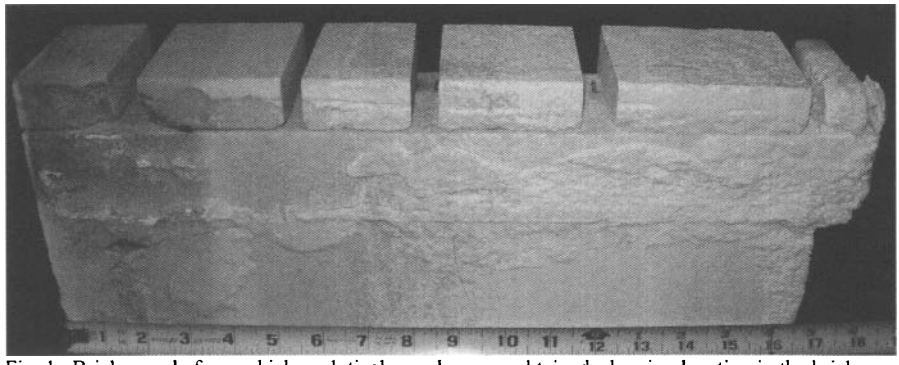

Fig. 1. Brick sample from which analytical samples were obtained, showing location in the brick.

ANALYTICAL TESTS PERFORMED

To determine how the chemistry, crystallographic and physical properties changed from near the hot face to near the cold face due to this brick being in service, XRF, XRD, thermal expansion, and physical property data were obtained from PPG's Analytical Laboratory. The XRF analysis was by the "pressed pellet" method using a Rigaku 3371, the thermal expansion was determined using a Harrop automatic recording dilatometer, the crystalline phases present were determined by using a Philips X'Pert MPD Diffractometer and the porosity, bulk density and apparent specific gravity were determined by Archimedes' Principle.

TEST RESULTS

XRD Analyses

Figure 2 shows the relative peak intensity of the crystalline species present in the samples, along with a sample from the cold face and also for comparison, the peaks for pure cristobalite and pure tridymite. The typical zoning (1, 2, 3) that occurs with silica brick in a thermal gradient, with cristobalite being found at the hot face and tridymite being stable towards the cold face was also observed in this brick. Per typical silica phase diagrams, cristobalite is the stable phase above 1470°C (2678°F), whereas tridymite is stable below that temperature.

From this work, it appears that from the hot face to a distance 11-1/2" from the cold face, only cristobalite was present. At 8" from the cold face, a mixture of tridymite and cristobablite was then present, while at 5-1/2" from the cold face, there is only a trace of cristobalite, with the major phase being tridymite. At 2" from the cold face, only tridymite exists; there appears to be no cristobalite peaks present. At the cold face, there is again some cristobalite present but tridymite is predominant which implies that recrystallization was also occurring even at the cold face. Per A. Wereszczak (4), this particular brand of silica brick, should contain about 1.4 times more cristobalite than tridymite.

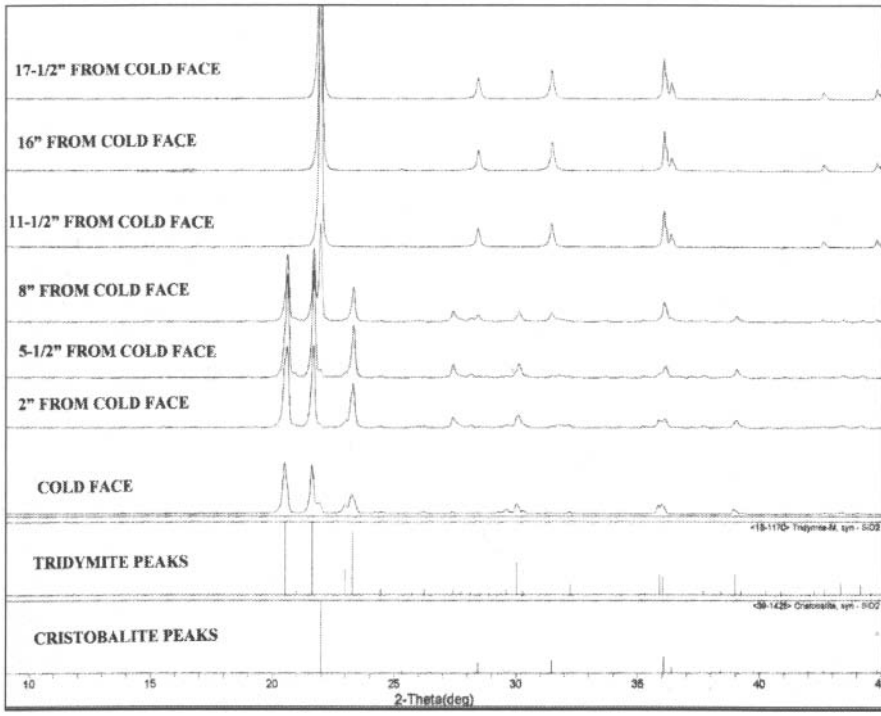

Figure 2. XRD Analyses of Samples, from Hot Face, to and Including Cold Face.

Thermal Expansion

Having seen the different crystalline forms of silica present in these samples from the XRD results, one would expect such differences to be reflected in their thermal expansions and they are. Figure 3 presents their thermal expansions and please note, especially if the legend is not legible, that the sample with the highest thermal expansion and likely the greatest percentage of cristobalite, is the hot face sample at ~17-1/2" from the cold face. It expanded 1.67% at 1800°F (982°C).

The sample with the next highest expansion, 1.57% at 1800°F, is the one 16" from the cold face, while the third highest at 1.52% at 1800°F is the one 11-1/2" from the cold face. This decrease in thermal expansion of the samples going towards the cold face, is likely due to an increase in the glassy phase that is present.

Those three 100%-cristobalite-containing samples – no tridymite was evident per XRD – have grouped themselves together in Figure 3, per their characteristic cristobalite-inversion thermal expansion. Please note the sharpness of the transition from the low-temperature form of cristobalite to its high-temperature form, as over a span of only a few degrees Centigrade, a 1% change in length occurs. It is no wonder why silica brick that have been used at temperatures >1470°C (2678°F), where cristobalite is the stable phase, crack so badly upon furnace cool-down.

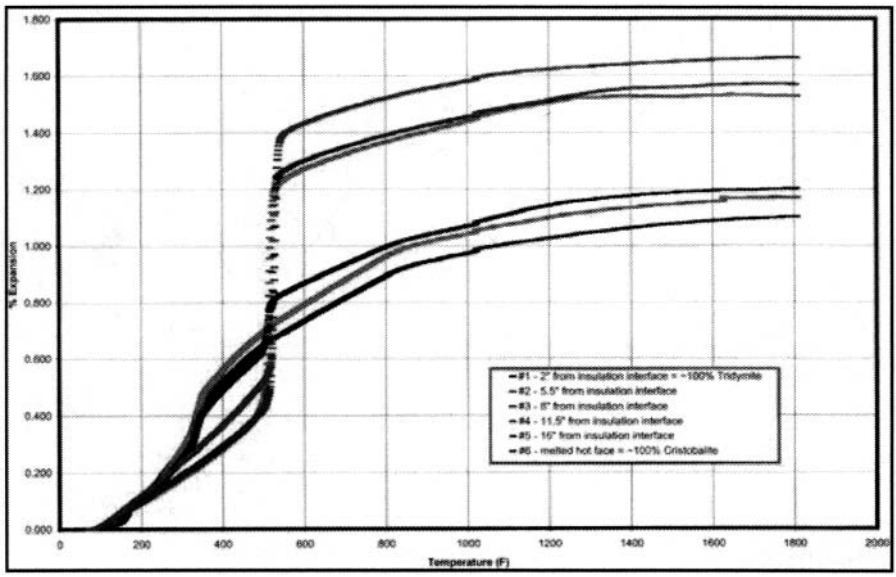

Figure 3. Thermal Expansion of Samples. Please note, the Hot Face sample has the highest expansion.

The next three samples, which have a considerably lower thermal expansion than the first 3 due to the latter's lower or nonexistent cristobalite content and higher tridymite content, also have grouped themselves together due to their characteristic tridymite-shaped thermal expansion curve and the low-tridymite-to-high tridymite transition that occurs more gently than does the cristobalite transition.

Of note, as with the 3 samples containing predominantly cristobalite, these samples keep the same ranking with a decreasing overall thermal expansion as one goes towards the cold face. The sample 8" from the cold face expanded 1.20% at 1800°F (982°C), the sample 5.5" from the cold face expanded 1.17% at 1800°F, and the sample 2" from the cold face, comprised of only tridymite (and a glassy phase), expanded the least, to 1.10% at 1800°F.

It is unfortunate that these samples were not examined petrographically to better ascertain the amount of glassy phase that is present as a function of location in the thermal gradient and the local composition. Such microstructure characterization work, however, can be found in the literature (5).

For reference, Figure 4 presents the thermal expansion of a sample of new silica brick, that was the same brand and from the same vintage as when this furnace was constructed. It expanded 1.41% upon heating to 1800°F (982°C). Please also note that this combination of crisobalite and tridymite in this unaltered sample is readily reflected in the shape of its thermal expansion curve. And please also note the difference in scale [°C vs. °F] between those graphs and that this expansion of this unaltered material was obtained using an Orton Automatic Recording Dilatometer.

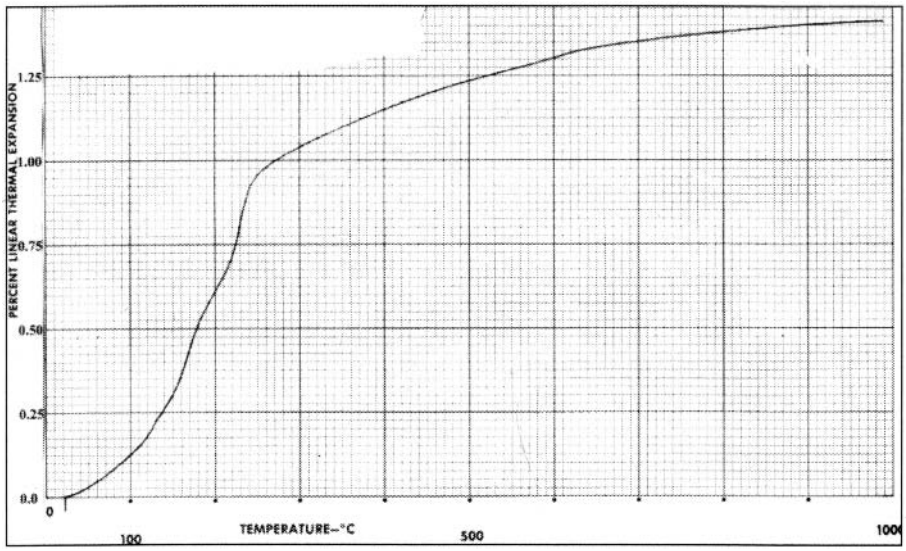

Figure 4. Thermal Expansion of New Crown Brick Sample from Same Vintage as the Crown

Changes in Chemistry

From the excellent work that has been done in the past investigating the corrosion of silica brick in air-fuel fired soda-lime-glass furnaces (1, 2), while I have a theoretical appreciation of how glass-forming-fluxing-oxides react, melt and are reported to migrate towards the silica brick's cold face during which time the silica itself is being partly dissolved and is recrystallizing and changing phases, one derives a greater comprehension and appreciation by observing firsthand, the changes that have occurred in one's own silica brick. Table I presents the chemistry of the samples from the dissected brick. It appears that the known-silica-fluxing oxides such as Al_2O_3, TiO_2 and in-situ alkali melt and react at temperature, which then allows additional alkali to be absorbed into this glassy phase from the furnace atmosphere. This increase in alkali increases this melt's reactiveness and it readily reacts with and consumes other glass-forming oxide phase(s) present, including the alkaline earths, and also ferric oxide.

Please note that while in the classic sense of silica brick chemistry, CaO and Fe_2O_3 are not fluxing oxides due to their immiscibility plateaus (6) and CaO is used as the bonding phase of traditional silica brick, all such oxides in the presence of alkali are depleted from the hot face of the silica brick and at least a portion of this glass-forming-fluxing oxide melt, migrates towards the cold face. This apparent migration is especially evident in the region beginning about 11.5" from the cold face, and going to the sample 2" from the cold face. This is shown graphically in Figure 5. The hot face is depleted of the glass-forming-fluxing oxides and by default becomes enriched in silica, whereas going towards the cold face, the percentage of silica decreases due to the migration of this melt of glass-forming-fluxing oxides towards the cold face.

Regarding the extent of this reaction and migration and the fact that NaOH at standard air-gas-fired furnace atmosphere concentrations is too low to react with silica at typical glass furnace crown temperatures (7, 8), it is interesting to note how pure the hot faces is, at 99.8% SiO_2. The second highest oxide in the hot face sample, is CaO at 0.14%, and the third highest are the alkalis, at 0.04%.

It was also interesting to note that despite the purity of the hot face and the absence of fluxing oxides, the hot face definitely had an appearance of being molten at one time. So to help ascertain if the analysis of the hot face was correct, another sample was tested from a similar-appearing brick taken from the same location in the furnace, to verify. Those results are shown in Column G of Table 1, at 99.7% silica, so this confirms the accuracy of first sample's results in Column F.

Table I. Chemistry of Dissected Brick (w/melted hot face) & Melted Hot Face of 2nd Brick.

NOTE: Columns A, B, C, D, E, and F are cut from same brick. Column G is from a similar-appearing brick.								
		A	B	C	D	E	F	G
	New Brick	2" From Cold Face	5.5" From Cold Face	8" From Cold Face	11.5" From Cold Face	16" From Cold Face	Hot Face 17.5" From Cold Face	Hot Face of Like Brick (At ~ 17.5")
SiO_2	95.7	94.4	96.1	94.7	96.8	98.2	99.8	99.7
Na_2O+K_2O	0.06	0.39	0.42	0.71	0.43	0.25	0.04	0.04
CaO	3.2	3.9	2.4	3.1	1.9	1.3	0.14	0.16
Al_2O_3	0.4	0.43	0.41	0.49	0.33	0.13	0.03	0.03
Fe_2O_3	0.6	0.70	0.59	0.81	0.47	0.11	0.005	0.004
MgO	0.1	0.03	0.03	0.05	0.03	0.05	0.02	0.02
TiO_2	Tr.	0.06	0.07	0.09	0.05	0.01	0.008	
P_2O_5	*(data)*	0.03	0.01	0.01	0.01			
SO_3	*(sheet)*	0.007	0.004	0.005	0.004			
ZrO_2		0.02	0.02	0.03	0.02	0.003	<0.001	<0.001

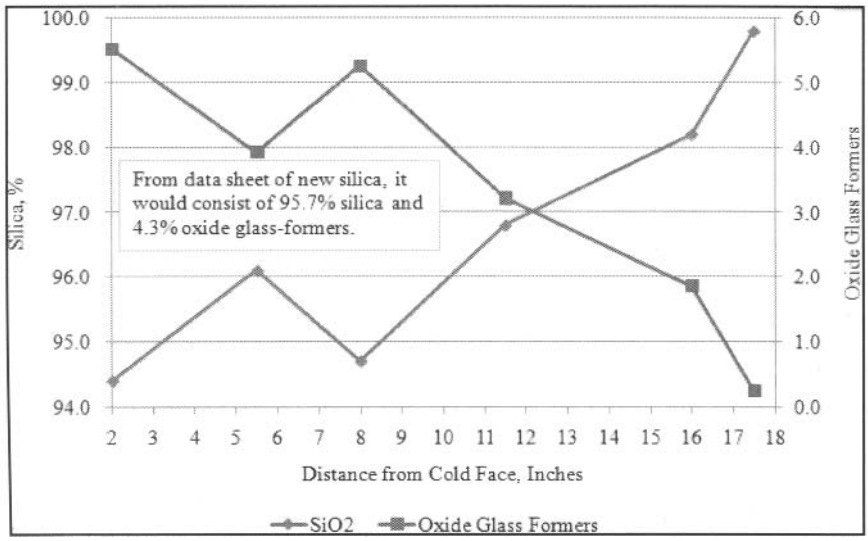

Figure 5. Silica and Oxide Glass Formers (Ca, Al, Ti, Na, K, Mg, Fe) Vs. Location in Brick.

While we know empirically and from thermodynamic studies (7, 8), that the alkali concentration in the atmosphere of a standard air-fired soda-lime-glass furnaces is sufficiently low and the hot face of its silica crown brick is sufficiently hot so that NaOH will not react with silica on the hot face of the crown, it is interesting to note how the brick was enriched in alkali at every location except for the immediate hot face. Other than the hot face which contained only 0.04% total alkali, at 16" from the cold face the alkali content had increased to 0.25% and at every other location it was ≥0.4%, with a high of 0.71% in the sample at 8" from the cold face. This is presented graphically in Figure 6, which shows the CaO, alkali, alkaline-earths, alumina plus titania, and ferric oxide content of the six samples as a function of their location.

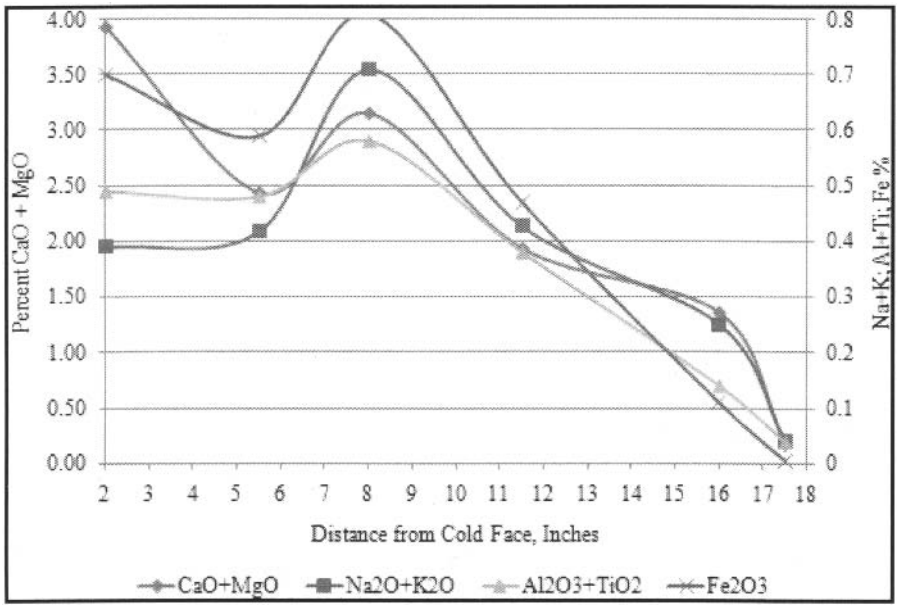

Figure 6. Distribution of Alkali, Alkaline Earths, Alumina, Titania and Ferric Oxide

While this liquid-oxide flux phase appears to migrate to some degree towards the cold face due to it wetting the host silica and capillary action, looking at the silica brick composition from a mass-balance viewpoint, there appears to be a net loss of some of the components. This is most easily noted by looking at CaO, since the only place that the CaO is higher than the data sheet's 3.2%, is at 2" from the cold face at 3.9% and furthermore, CaO is especially depleted at 11-1/2" from the cold face at 1.9%, decreasing down to 0.14% at the hot face. To ascertain how much material was actually lost from this brick would require looking at the whole brick instead of just 6 areas, but this loss appears to start at somewhere between 8" to 11-1/2" from the cold face, going towards the hot face.

With the CaO content of standard silica brick now being recognized as contributing to the corrosion of silica brick in the highly-alkaline atmosphere of soda-lime oxy-gas furnaces (9) due to it being a glass former (Na-Ca-Si) and contributing to alkali pick-up (and what I call self-digestion of the brick), the depletion of lime and other fluxing ingredients beginning at a location somewhere greater than 8" from the cold face and going towards the hot face, should not be surprising. It appears that

even in air-gas-fired soda-lime glass furnaces at relatively low NaOH concentrations, the resultant soda-lime-silica glass phase that forms in the brick, is leached from the hot face of the brick in service and likely falls as minute droplets onto the production glass. Being of a soda-lime-silica composition, they would be readily assimilated by the production glass and never be noticed in the final product.

Changes in Porosity, Bulk Density, and Apparent Specific Gravity

Table II presents the porosity, bulk density and apparent specific gravity of the six samples and Figure 7 presents that information graphically. Of note, the hot face sample, 17-1/2" from the cold face had the least porosity at 4.3% and the greatest bulk density at 2.23 gm/cc, whereas the sample 16" from the cold face was the least dense at 1.67 gm/cc and it also had the greatest porosity at 29.6%.

Table II. Porosity, Bulk Density and App. Specific Gravity of Dissected Brick & "Melted" Hot Face.

			(2 samples tested per location)					Hot Face
	New Brick *1		2" From Cold Face	5.5" From Cold Face	8" From Cold Face	11.5" From Cold Face	16" From Cold Face	17.5" From Cold Face
Porosity, %	19.4		15.8	18.7	13.5	15.8	29.6	4.3
Bulk Density, gm/cc	1.88		1.94	1.86	2.00	1.98	1.67	2.23
App. Spec. Gravity	2.34		2.31	2.29	2.32	2.36	2.37	2.33
*1 "Preshipment" Q/C data of the brick used for this crown.								

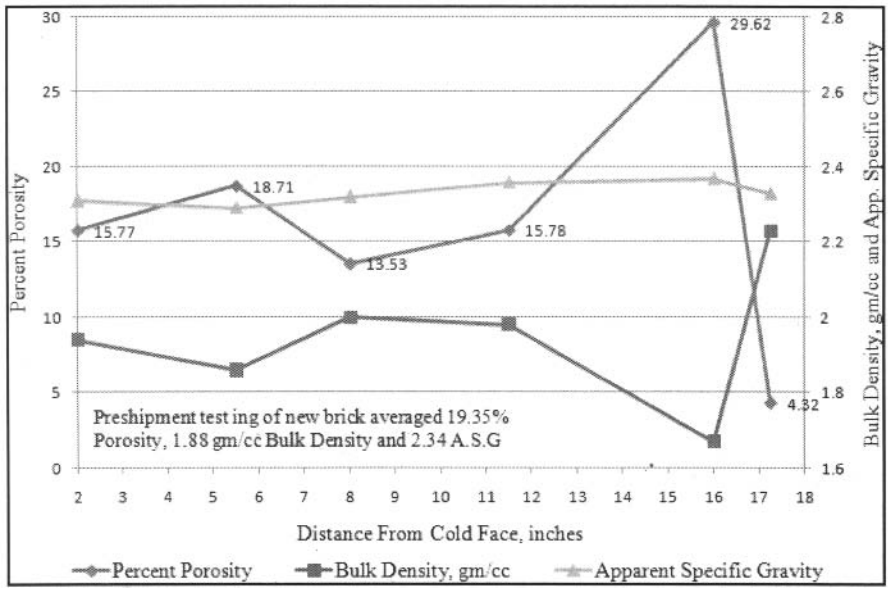

Figure 7. Percent Porosity, Bulk Density and Apparent Specific Gravity Vs. Sample Location.

From the sample 16" from the cold face, to the sample 2" from the cold face, all samples had a lower porosity than did the pre-shipment Q/C lot of the brick that was used in this crown, which was

19.4%. This lower porosity in this area is due to the pick-up of Na_2O and migration of the fluxing oxide glass formers that both altered and filled in some of the original porosity.

MACROSCOPIC APPEARANCE / POROSITY / STRUCTURE / MORTAR / MELTING

Hot Face Surface vs. Internal Porosity Alignment and Columnar Structure Appearance

What is most impressive regarding porosity is that the hot face has a porosity of only 4%, while less than 1-1/2" away, the porosity was nearly 30%. The Figure 8 photograph, shows on its left side, the hot face that appears to have melted with no visible, open porosity, while to the right is the saw-cut surface of the sample less than 1-1/2"-away that had gross, open and continuous porosity, with this porosity being aligned in a vertical direction, from the hot face to the cold face.

While such columnar porosity and crystal growth orientation is to be expected due to: the presence of a liquid phase; the dissolution and recrystallization of the silica; and the thermal gradient (1, 2), the amount of porosity and the extent of this columnar feature was impressive. This columnar appearance was still present on the sample 5-1/2" from the cold face and this feature also went from where cristobalite was the single phase, to where tridymite was the predominant phase.

Regarding the amount of columnar porosity and its alignment from the hot face-to-cold face, it was easily observed that it was also continuous. To get an indication on the amount and nature of this porosity, a simple, subjective comparative test was devised to diffuse a gas through the ½"-thick samples from each location, along with a subjective visual rating of the nature of the porosity, from it being very coarse, to being fine (very small in size) porosity. This is summarized in Table III, which is a photograph of the postmortem brick, onto which the distance from the cold face is labeled, along with structure/appearance (columnar or random); ease or difficulty with which gas diffused through the sample, the relative nature of the porosity (coarse or fine), and also the percent porosity, crystalline phases present and the percent total alkali.

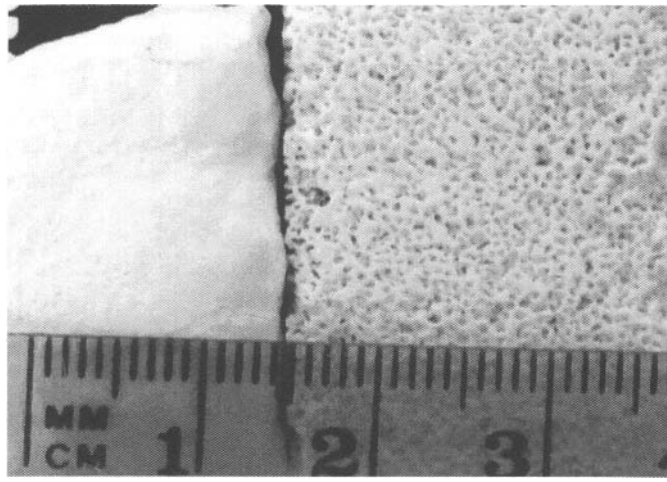

Figure 8 Hot Face Appearance of Hot Face Sample (left) and Saw-Cut Sample 1-1/2" Away (right).

Table III. Appearance of the Brick, Nature of Porosity and Percent and Crystalline Phases & Alkali

Cold Face		Structure/ Appearnce	Diffusion of Gas in Vertical Direction	Porosity	Crystalline Phase(s)	Total Alkali
2"	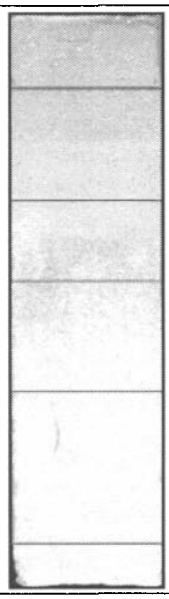	Random	Difficult (random porosity)	15.8%	Tridymite	0.39%
5.5"		Columnar	Easy (fine porosity)	18.7%	Tridymite Tr. Cristobalite	0.42%
8"		Columnar	More Difficult (finer porosity)	13.5%	Cristobalite & Tridymite	0.71%
11.5"		Columnar	Easy (coarse porosity)	15.8%	Cristobalite	0.43%
16"		Columnar	Very Easy (very coarse por.)	29.6%	Cristobalite	0.25%
17.5"		Fused	Air-tight	4.3%	Cristobalite	0.04%

Consumption, Recrystallization of Mortar / Intergrowth of Silica from Brick-to-Brick

Regarding the fluxing glassy phase and its migration and the impact that it has on altering the brick, via the dissolution and recrystallization of the silica phase(s) present, macroscopically it appeared that where there was mortar present, this mortar had been converted to be of a similar composition and structure as the brick and that there was some intergrowth of phases from brick-to-brick. The evidence of this is shown in Figure 1 on the brick's 6" x 18" face, where there are "pull-outs" from the adjacent bricks that is well-bonded to the sample brick.

Melting of Hot Face

Despite every furnace being operated with a crown temperature limit in place and utilizing modern process control schemes and systems, it is evident that process problems can occur which may result in the hot face of the crown accidentally becoming overheated and melting to some degree. One might ask, how could that happen, but we all know that such accidents can and do occur.

The question then becomes, given the composition of the hot face of the brick at 99.8% SiO_2, at what temperature would the hot face become molten? Figure 9 (10), shows the calculated percent liquid in a superduty silica brick containing 1.2% and 0.4% fluxing oxides, and even if the fluxing oxides would remain at the hot face, at 3000°F (1649°F) in a glass furnace environment and not migrate away, the brick containing 0.4% fluxing oxides, would contain less than 10% liquid. This reference also claimed that in the absence of outside fluxing agents, a superduty silica brick may begin to show evidence of surface melting at about 3105°F (1707°C).

One additional major observation to draw from Figure 9, is how rapidly the amount of liquid phase may increase, especially once the temperature exceeds 3000°F. The brick could appear solid one moment, and then with a relatively small increase in temperature, its hot face could be molten.

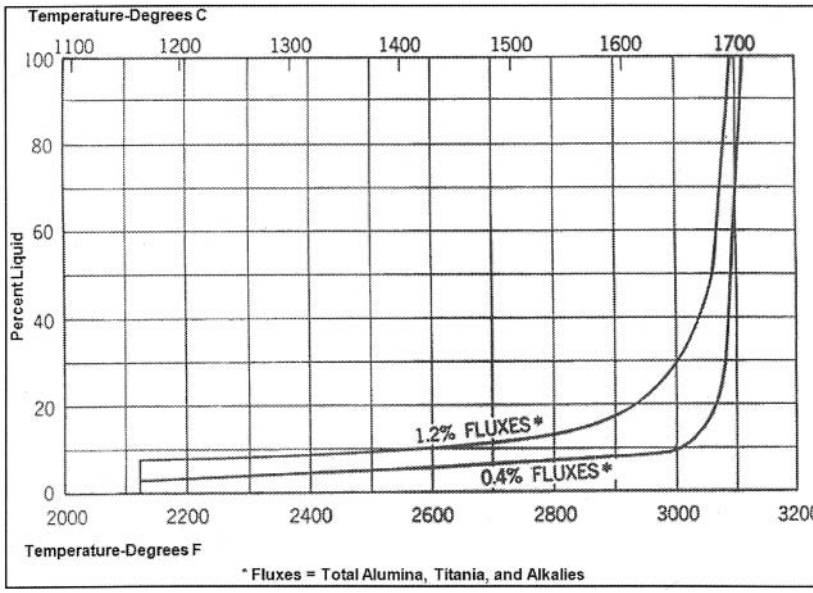

Figure 9. Melting Behavior of Silica Brick (10)

With the hot face being 99.8% SiO_2 and the remaining 0.2% being a mixture of fluxing impurities, the impact of this 0.2% material on the melting behavior of the hot face is not accurately known. With CaO at 0.14% being the major component of this 0.2% mixture, if we assumes that it behaves as CaO, per one SiO_2–CaO phase diagram (11) there would only be 2% liquid present at just below 3088°F (1698°C). (Above 3088°F the amount of liquid would change greatly as there is a eutectic melt occurring at that temperature which has a composition of 0.6% CaO and 99.4% SiO_2.)

If we assume this 0.2% flux mixture to be as aggressive as Na_2O, per a Na_2O-SiO_2 phase diagram (11), even at 3050°F (1677°C) only 20% liquid would be present. Thus in any case, one would assume that the hot face of this silica brick saw an errant temperature excursion that likely exceeded 3050°F and was probably closer to 3100°F (1704°C).

SUMMARY / CONCLUSIONS / RECOMMENDATIONS

1. This brick was 100% altered and it was altered differently, going from its hot face to its cold face.
2. From the extent of alteration, one concludes that in a more aggressive, highly-alkaline oxy-gas atmosphere its performance would have been considerably poorer.
3. Despite alteration, it successfully fulfilled its function as a low cost, light weight crown refractory.
4. Upgrading to the new low- or no-lime silica brick composition for a conventional air-gas furnace would be difficult to justify.
5. Due to the great difference in crystallinity and corresponding thermal expansion going from the brick's hot face to its cold face, increases the likelihood for a shear plane to develop during cool-down, and makes the seemingly-attractive practice of reusing good-appearing crown sections and suspended walls for a second campaign, a dubious practice. (Nearly every brick in one section cleaved in-two after the crown was dropped during demolition.)

6. Na_2O was absorbed into the brick's oxide glassy phase at concentrations higher than new brick, at all locations tested except for the hot face.
7. This glassy phase and its mobility is why silica refractory suppliers recommend against insulating a previously uninsulated crown, or increasing the insulation on a marginally-insulated crown.
8. This glassy phase also:
    a. Assists in the dissolution and recrystallization of the silica phase(s) present
    b. Results in the brick developing a columnar appearance with continuous porosity extending from near the hot face, going towards the cold face.
    c. Alters the mortar to be similar to the brick in appearance and structure.
9. This absorption of alkali, the presence and migration of the glassy phase towards the cold face and the columnar structural and continuous porosity towards the hot face, would cause an increase in the thermal conductivity of the brick from its pristine, new state.
10. While migration of the glassy phase components towards the cold face was evident, from a mass-balance viewpoint there appeared to be a depletion of the glassy phase components, in particular CaO, beginning ~11" from the cold face and extending towards the hot face.
11. The loss of material from this refractory as evidenced by the leaching out of the glassy phase and the 30% porosity near the hot face, indicates that considerable alkali corrosion even occurs in a relatively low-NaOH-concentration air-fired furnace.
12. The hot face, was purified at 99.8% SiO2, 0.14% CaO and only 0.04% total alkali.
13. The melting (or puddling) of the hot face likely occurred at a temperature >3050°F and approaching 3100°F. To prevent such incidents from occurring in the future, trained, quick and proper response to process upsets is a requirement and to minimize those upsets, there should also be sufficiently-frequent maintenance of the temperature monitoring systems, combustion system including burners, batch/cullet feed system, and the process control system.

ACKNOWLEDGEMENT: PPG Analytical Department

REFERENCES:

1. Several Studies of Silica Bricks from the Crowns of Glass Tanks at Different Working Temperatures, by Heinz Friedich Reich, Glastechnische Berechte. V. 34 (1961), No. 1, p. 15-27
2. Zonal Endurance Strength of Used Silica Crown Bricks, by Klause Schulte, Glastechnische Berechte V. 39 (1966); No. 2, p. 41-45.
3. The Effect of Heat on Ceramics W. Ford Mclaren and Sons LTD. London England, 1967, p. 95-96.
4. Compressive Creep Performance and High Temperature Dimensional Stability of Conventional Silica Refractories, by A. A. Wereszczak, et. al. ORNL. reference ORNIJTM-13757 http://www.osti.gov/bridge/servlets/purl/4204-dnvjix/webviewable/4204.pdf (March 1999)
5. A. Wereszczak, H. Wang, M. Karakus, et. al., Postmortem Analyses of Salvaged Conventional Silica Bricks from Glass Production Furnaces, Glastech. Ber. Glass Sci. Technol. V. 73 (2000), No. 6: p. 165–174.
6. Phase-Equilibria Data in the Manufacture of Refractories, by Raymond E. Birch, Journal of the American Ceramic Society, V. 29 (1941), No. 9. p. 241-280.
7. Report NCNG Project: Reduction of Refractory Corrosion -Phase 1, TNO Institute of Applied Physics, HAM-RPT-96396, August 1996.
8. Thermodynamic Analysis of Refractory Corrosion in Glass Melting Furnaces by M. D. Allendorf, K. E. Spear J. Electrochem. Soc., 148, B59 (2001).
9. New Silica Refractory for Oxy/Fuel Glass Melting, by J. T. Brown, R. F. Spaulding, et. al., A.T.I.V Conference N° 15, Parma, Italy (15/09/1999) 1999 N° 102 (175 p.) (bibl.:dissem.), pp 120-124.

10. Modern Refractory Practice, Copyright 1961 by Harbison-Walker Refractories Co., p. 298-299.
11. Melting Relations of the Common Rock-Forming Oxides by J. F. Schairer, Journal of the American Ceramic Society, V. 40 (1957), No. 7, p. 215-235.

This Page Intentionally Left Blank

REFRACTORY CERAMIC FIBERS

Joe Ventura and Daniel M. Wood
Safety Controls Technology, Inc.
Bedford Heights, OH

ABSTRACT

The intent of this presentation is to provide a forum for the attendees to share their experiences in controlling respirable Refractory Ceramic Fibers (RFC) exposures during installation, repair and after service demolition.

This presentation will include: a brief background of RCF; exposure and current occupational exposure limits (OEL); air monitoring; hazard control methods including PPE recommendations.
This presentation is not intended to present new laboratory findings or address exposures of RCF;s in the manufacturing process.

BACKGROUND

Production of ceramic fibers began in the 1940's. The Commercial exploitation did not occur until the early 1970's – primarily as the result of on-going pressure to limit the use of friable asbestos materials in high temperature applications. By the early to mid 1980's it was estimated that the United States, alone, produced between 77 and 88 million pounds of ceramic fibers.

Ceramic fibers are produced by blowing and spinning. Colloidal evaporation, continuous filamentation and whisker-making technologies are also used, to a lesser extent. RCF is less durable than the least durable form of asbestos (chrysotile) but more durable than fibrous glass.

Ceramic fibers are used as insulation material, primarily for lining furnaces. Products produced are in the form of blankets, boards, felts, bulk fibers, vacuum-formed or cast shapes, paper and textile products. The light-weight, thermal shock resistance and strength of the ceramic fibers make them useful in a number of industries. High-temperature resistant boards are used in combination with blankets for insulation of furnaces designed to produce temperatures up to approximately 1400° C. Ceramic blankets are also used in Lears.

The American Conference of Governmental Industrial Hygienists (ACGIH) and EPA designations are consistent with that of the International Agency for Research on Cancer (IARC), which classified ceramic fibers, including RCF, as "possibly carcinogenic to humans (Group 2B)"[IARC 1988, 2002].

The IARC characterization was based on "sufficient evidence for the carcinogenicity of ceramic fibers in experimental animals" and a lack of data on the carcinogenicity of ceramic fibers to humans [IARC 1988, 2002].

EXPOSURE

The primary route of potential human exposure to ceramic fibers is by inhalation, mainly during installation and during removal on glass furnace projects. Exposure to the fibers by occupants would be minimal as these products are generally encapsulated, minimizing exposure potential if any exists. The upper diameter of limit of respirable fibers is considered to be 3 μm to 3.5 μm.

*Note: Fibers in this size range remain airborne for extended periods of time.

In 2002, the Refractory Ceramic Fibers Coalition (RCFC) established a Product Stewardship Program (PSP), that was endorsed by OSHA as a 5-year voluntary program. Contained in the PSP was a recommendation to limit worker exposures to 0.5 f/cm3 based on the contention that most industries that manufactured or used RCF could achieve these levels.

NIOSH supported the intent of the PSP and concurred the recommended exposure level of 0.5 f/cm3 measured according to the NIOSH 7400 B rules would lower worker risk. It would also reduce the risk of irritation of the eyes and upper respiratory system. NIOSH further recommended the reduction of the occupational exposure limit (OEL) to 0.2 f/cm3 as a method of further reducing the estimated risk of lung cancer.

In 2000 the ACGIH had already reduced their Threshold Limit Value (TLV) guideline to 0.2 f/cm3. An Action Level (AL) is typically defined as one-half the OEL or in this case 0.1 f/cm3 and is used to determine when additional engineering controls, PPE and monitoring are required.

Controlling airborne exposures to RCF below an OEL of 0.2 f/cm3 and preferably below an AL of 0.1 f/cm3 during installation and after service demolition requires a comprehensive safety and health program that includes provisions for personal exposure monitoring, use and routine maintenance of engineering control, and training of workers in good work practices.

AIR MONITORING

Air monitoring is required for the proper selection of worker respiratory protection. Periodic sampling, at least annually, and whenever a major process change takes place or any other conditions change. Collect all air samples in the worker's breathing zone. If concentrations exceed the OEL, then more frequent monitoring is recommended and engineering controls need to be implemented until at least two consecutive samples indicate that exposures no longer exceed the OEL. Notify all workers of air monitoring results and any actions taken to reduce their exposures.

In most cases the use of a focused sampling strategy rather than a random strategy is recommended due to budget constraints. A focused strategy targets workers perceived to be exposed to the highest concentrations and is most efficient at identifying exposures above the OEL if they are accurately identified. Area Sampling is useful to determine if engineering controls are effective but can not be used as a substitute for the personal sampling required by OSHA.

HAZARD PREVENTION AND CONTROLS

Consistent with the Occupational safety and Health Administration, (OSHA) Hierarchy of Controls and with the recommendations of the National Institute of Occupational Safety and Health control measures should begin with Engineering Controls combined with Administrative Controls and finally Personal Protective Equipment, (PPE). Respirators are a significant component to the PPE component. However OSHA requires employers to employ respirator protection as a last line of defense. A few examples of these control measures include:

Engineering Controls

- Use local exhaust ventilation as opposed to dilution ventilation.
- Power tools equipped with HEPA filtered local exhaust ventilation.
- Wet down methods during demolition of refractory and RCF board effective.
- Frequently clean the work area with HEPA filtered vacuum or wet sweeping (during demolition) to minimize the accumulation of debris.
- Provide showers and changing areas free from contamination where workers can store clothes and change into street clothes before leaving the work site.
- Provide services for laundering work clothes.

Administrative Controls

- Do not allow smoking, eating, or drinking in areas where workers may contact RCFs.
- Consistent documented training of the health risks and review of good work practices to minimize personal exposure.
- Preferential use hand tools where appropriate.
- Do not use compressed air for clean-up.

Personal Protective Equipment (PPE)

- Respiratory Protection includes: ½ and full face negative pressure respirators with N-P100 cartridges/filters.
- Respirator protection supplements engineering controls it does not replace such control methods. Proper training, medical evaluation and fit testing required prior to use of a respirator.

This Page Intentionally Left Blank

REFRACTORY SOLUTIONS FOR EXTRA WHITE GLASSES

M. Blackburn [1], L. Massard [2], M.Gaubil [2]
[1]*Saint-Gobain SEFPro, Louisville, United States*
[2]*Saint-Gobain CREE, Cavaillon, France*

ABSTRACT

Extra clear glasses are widely used for solar applications. The extra clear glass properties and especially the higher transmission coefficient induce an evolution of glass furnace running conditions. After discussing the consequences on refractories in terms of corrosion, a new bottom paving solution is proposed. This solution consists of optimally machined fused cast AZS tiles and a new formulation of AZS mortar layer.

1. INTRODUCTION

Extra white glasses are widely used in industry as substrate or support for many solar applications such as photovoltaic panel, thermal solar or solar concentration (cf. figure 1).

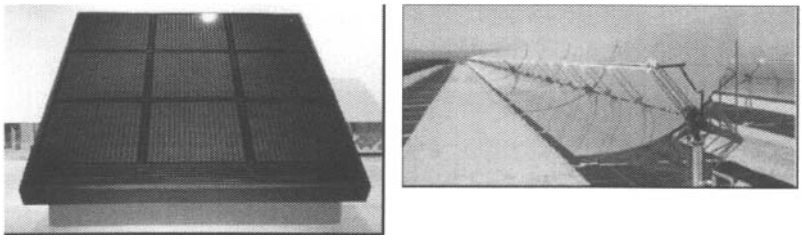

Figure 1: Few examples of applications using extra clear glass

The extra clear glass is characterized by lower iron content and redox values. In terms of properties, theses characteristics give better optical characteristics for the solar application which means a higher transmission coefficient. This evolution is not without consequence on glass furnace running conditions especially due to the increase of heat transfer into the glass furnace.

2. EXTRA WHITE GLASS EFFECT ON REFRACTORIES

The higher transmission coefficient of extra clear glass will modify glass furnace running conditions. At first, due to the increase of heat transfer into the glass, the refractory interface temperature may increase. This is especially true for the bottom of the soldier block and the pavement. The impact at the metal line should be lower. The glass flow rate (i.e. glass thermal convection) should also increase. Finally, the glass will be less capable of dissolving oxygen bubbles which could result in a source of increased glass defects.

From the refractory point of view, these conditions may imply corrosion highly enhanced due to temperature and convection. The increase of corrosion could impact the glass quality by increasing stones and cords defects.

3. REFRACTORY CORROSION ISSUE

Reminder on corrosion mechanism

For refractory block, we can find two kind of corrosion: the metal line corrosion and the corrosion at submerged zone.

The corrosion at the submerged zone corresponds to a frontal dissolution process that involved oxides solubility and diffusion coefficient [1]. The equation below resumes the typical corrosion law:

Corrosion speed $\approx$ D.S.(Csat – Cx)/ δ in stationary condition hypothesis

We can note that the corrosion rate is highly dependant on interface temperature, interface layer thickness associated with the dissolution layer (glass flow rate) and chemical analysis distribution in the block.

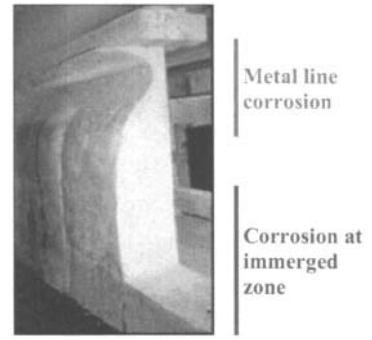

Figure 2: AZS refractory corrosion location

Concerning the metal line corrosion [2-5], the mechanism is more complicated. It is associated with an accelerated corrosion due to the effect of the triple point and glass surface tension. The mechanism is the association between the dissolution (static aspect) and the dissolution layer evacuation (dynamic aspect, Marangoni fluxes).

Consequences of glass furnace running condition

As we mentioned before, the extra clear glass melting will influence the refractory temperature interface and the glass flow rate. Regarding the refractory, it will induce a real impact on corrosion speed.

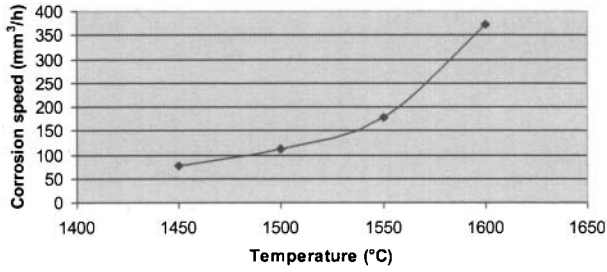

Figure 3: Corrosion speed vs. Temperature for AZS refractory

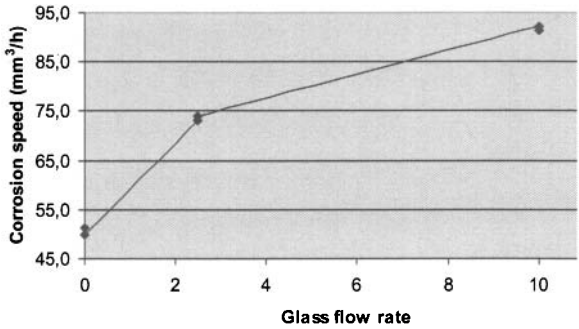

Figure 4: Corrosion speed vs. Glass flow rate for AZS refractory

As we can see on figure 3 & 4, temperature remains the main factor of corrosion with an exponential dependence of corrosion speed to the temperature and corrosion speed is proportional to square root of glass flow.

Refractory corrosion evaluation

Various means have been developed to evaluate the refractory corrosion resistance for the corrosion at and below the metal line.

To evaluate the corrosion below metal line, we use a dynamic test, called MGR. This test consists in dipping a sample in melted glass at high temperature. The results consist in measurements of volumetric refractory loss and the associated calculation of the corrosion index.

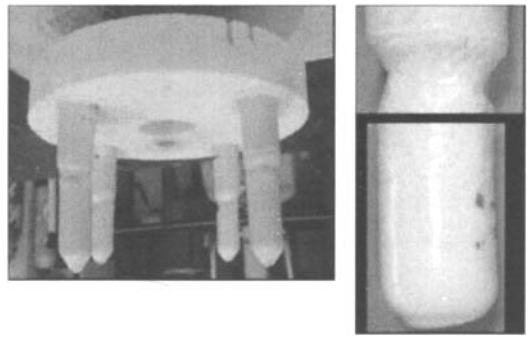

Figure 5: MGR test

To evaluate the corrosion at the metal line, two tests could be used. An electrical furnace test, for static conditions which reproduces the glass furnace geometry. A second test in a gas furnace can be used in dynamic conditions. Theses two tests are illustrated in figures 6 and 7.

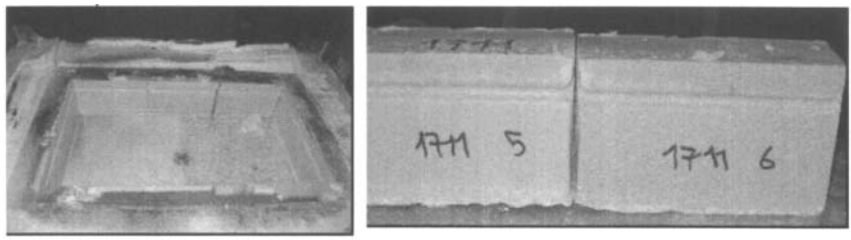

Figure 6: Electrical furnace test

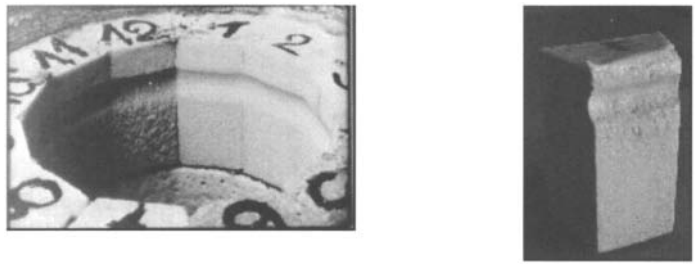

Figure 7: Gas furnace test

The corrosion resistance evaluation (volume, corrosion depth profile ...) can be made on tested refractory by image analysis, as illustrated on figure 8.

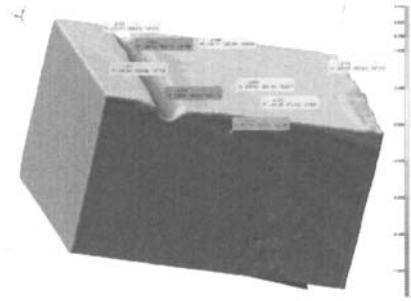

Figure 8: Corrosion evaluation

4. BOTTOM PAVING SOLUTION

Basic solution

Typically the bottom paving solution for a glass furnace consists of :

- Bonded or Fused cast AZS refractory tiles
- A layer of AZS Mortar
- A layer of bonded AZS
- An insulation

Due to new glass furnace running conditions, the bottom paving solution needs to be optimized, especially for the tile's refractory material and the mortar layer.

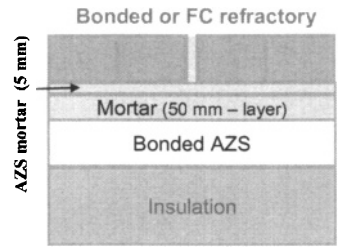

Figure 9: Current bottom paving solution for glass furnace

Tile's refractory materials optimization

We need to improve the material's corrosion resistance due to the increase in temperature and glass flow rate. Compared to bonded AZS material, fused cast AZS materials seems to be the best solution for extra clear glass. The figures 10 and 11 compare corrosion resistance in dynamic conditions of bonded and fused cast refractories.

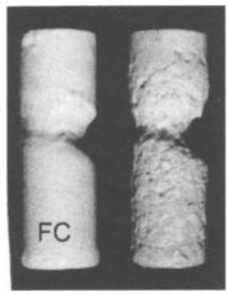

Low rate (50cm/mn)

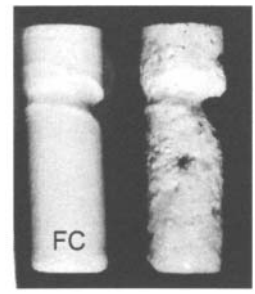

High rate (300cm/mn)

Figure 10: MGR results at 1450°C during 48 hours

	Low speed rate (50 cm/mn)		High speed rate (300cm/mn)	
	Corroded volume (cm3)	Index	Corroded volume (cm3)	Index
A.Z.S FC	1.37	100	1.80	100
AZS Bonded	2.74	50	3.64	49

Table 1: MGR results at 1450°C during 48 hours

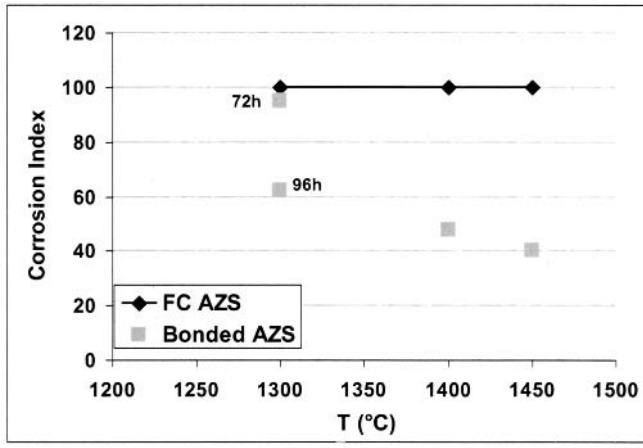

Figure 11: Evolution on corrosion resistance versus temperature (MGR test)

The fused cast AZS refractory solution can be improved by an optimized machining process. These tiles, called FC AZS TJ have tight joints (TJ) between adjacent tiles. This means joints between tiles less than 0.5 mm compared to the traditional joint thickness of 1.5 to 2 mm. The tighter joints limit glass penetration in the sub layer which prevents upward drilling phenomenon. This could lead to improved glass quality.

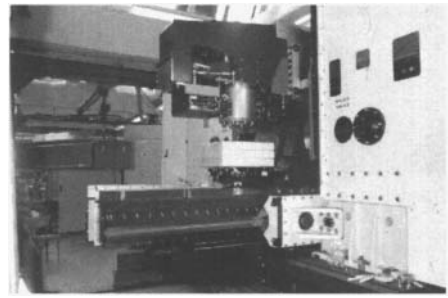

Figure 12: New machining device for FC AZS TJ tiles manufacturing

Mortar layer improvement

A new AZS mortar has been developed to improve the installation and overall bottom paving solution.

In terms of implementation, the new AZS mortar (cf. figure 13) is characterized by a uniformity of setting time and a self leveling behavior. This allows reduction or elimination of the vibration operation and also simplifies installation.

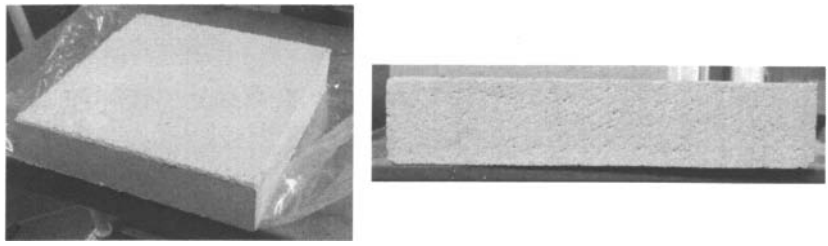

Figure 13: New AZS mortar

Moreover, the new formulation will allow a safer bottom paving solution by reducing the thermal expansion joint and an higher glass contact corrosion resistance.

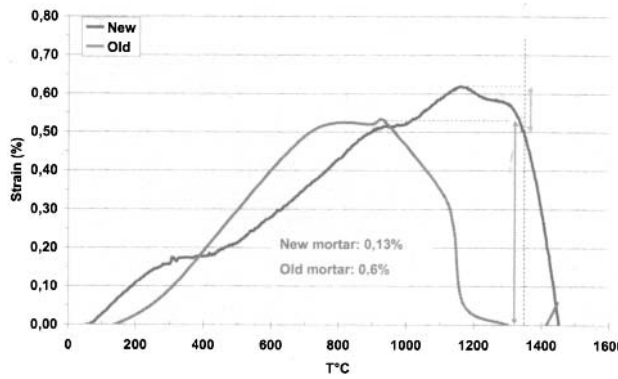

Figure 14: Thermal expansion of AZS mortar: old and new

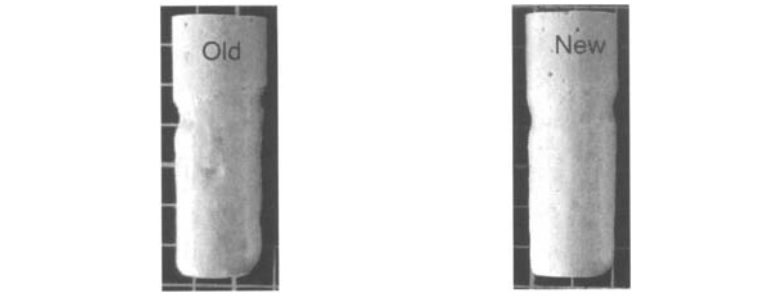

Figure 15: MGR results at 1400°C during 72h in sodalime glass

Finally, to really optimize the bottom solution, two layers of AZS mortar are recommended to prevent cracks in the upper layer after heating up. As a consequence, after heat up, we develop a monolithic layer in order to prevent glass penetration and damage to the sub-layers.

As a conclusion, the bottom paving optimization for extra clear glass can be summarized in figure 16.

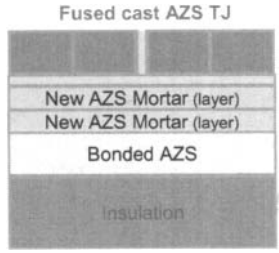

Figure 16: New bottom paving conception for extra clear glass

5. CONCLUSION

Extra clear glasses are widely used for solar applications. The extra clear glass properties and especially the higher transmission coefficient induce an evolution of glass furnace running conditions: the refractory interface temperature and glass flow rate will increase.
As a consequence, bottom furnace refractory corrosion (bottom soldier block and pavement) are increased.

In this paper, SEFPRO present an optimized solution for bottom paving that consist of using:

- fused cast AZS tiles with a optimized joint machining (TJ) in glass contact,
- and a new AZS mortar layer that allow to close the thermal expansion join after heating up and present a better corrosion resistance.

6. REFERENCES

[1] Löffler, Physikalische und chemische reaktionen, die in glaswannen zur Ausbildung von Spülfugen oder zum LochfraB führen, 1965

[2] E. D. Hondros (Editor), M. McLean (Editor), K. C. Mills (Editor) Marangoni and Interfacial Phenomena in Materials Processing: Originating from Contributions to a Discussion of the Royal Society of London

[3] K. Mukai, Marangoni Flows and Corrosion of Refractory Walls', pp1015-1026, 1998 Philosophical Transactions of The Royal Society of London A, 356,

[4] R. Beerkens, Refractory wear of glass melt tanks, Technische Universiteit Eindhoven.

[5] R. Beerkens, Reactions and Interactions between Tank Refractory and Glass melt, Norbert Kreidl Memorial conference, 23-26 juin 2004.

This Page Intentionally Left Blank

TESTING AND PERFORMANCE OF FUSION-CAST REFRACTORIES

Amul Gupta, Kevin Selkregg: RHI Monofrax, Falconer, NY, USA
Roland Heidrich: RHI Refel, San Vito al Tagliamento, Italy

ABSTRACT

Fusion-cast AZS refractory was invented more than 70 years ago. Up until the early 1990s, there were only a handful of companies producing and delivering AZS refractories to the glass industry in North America and Europe. Due to the economic development in the BRIC region, today, there are well over 20 companies worldwide that produce AZS refractories for use in the lining of glass melting furnaces. A large number of these companies are located in Asia. In the last decade, we have seen a greater willingness on part of the glass industry in N. America and, increasingly, in Europe to import lower-cost refractories from Asia.

The basic manufacturing process for making fusion-cast AZS refractories consists of raw material selection, mold making, arc melting, casting, annealing, finishing, inspection and set-up. Though all AZS manufacturers use these process steps, there can be rather significant differences in the actual practice of each process step between different companies.

This paper deals with several topics pertaining to the testing and selection of fusion-cast AZS refractories for use in glass melting furnaces. First, the impact of manufacturing process on AZS chemistry, microstructure, properties and performance is discussed. Next, the performance of lower-cost AZS refractories is compared with AZS produced in N. America and Europe. Finally, some suggestions are provided for more reliable testing of AZS refractories.

1) FUSION-CAST AZS REFRACTORY DESCRIPTION

Fusion-cast AZS refractory is made up of 3 main phases, namely, alumina, zirconia and glass. These phases can be seen the micrograph shown as Figure 1 below.

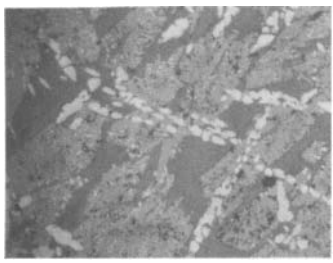

Figure 1: The bright nodular shaped grains are Zirconia; light gray color elongated / blocky grains are alumina (with very fine zirconia crystals embedded); the dark matrix phase is glass.

The most common Fusion-cast AZS refractory products are differentiated on the basis of their Zirconia content, i.e. 32 – 34%, 36%, and 38 – 41%. As the Zirconia content of the AZS increases, the glassy phase content decreases. Higher Zirconia and lower glassy phase allows greater corrosion resistance against molten glass.

The grain size of the phases can be affected by the cooling conditions during manufacturing. Generally, the outer region of AZS blocks tends to have a finer microstructure, whereas towards the center the microstructure becomes coarse.

2) EFFECT OF AZS SAMPLE LOCATION ON CHEMISTRY

A common feature of fusion-cast AZS refractories is chemical segregation within a block. This results from different densities[1] and solidification temperature of the 3 main phases of AZS. For example, Zirconia phase solidifies ahead of the other two phases and settles near the bottom of the blocks owing to its higher density.

Figure 2 shows natural chemistry variation in a large Monofrax CS3 (34% ZrO_2) AZS sidewall block. It is clear that near the as-cast surface, Zirconia content does not fluctuate much along the height of the block, whereas considerable variation is observed a few inches inside the block. A ZrO_2 rich region can be found in the bottom 12" of the sidewall block (refer to cores A, B and C in fig. 2).

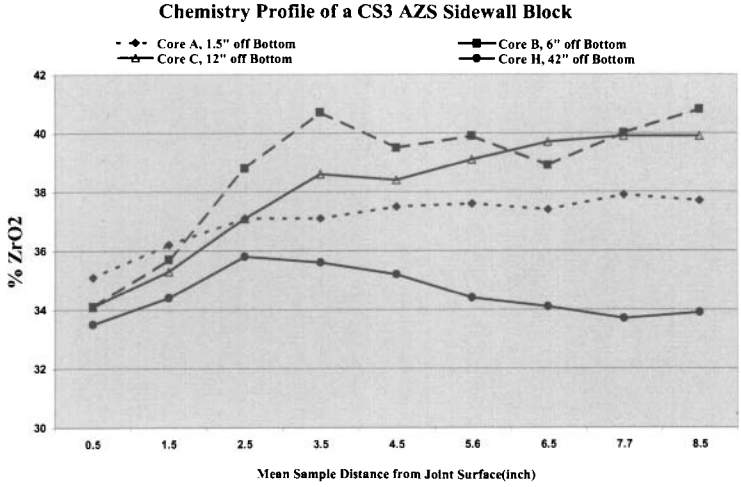

Figure 2: Variability in the ZrO_2 content of a 34% AZS Sidewall Block

In addition to the chemistry segregation, there are variations in the grain size (as mentioned above), and apparent porosity. The consequence of the chemical and physical segregation in a large AZS block can be profound on the testing of AZS samples in a laboratory. Since short-term tests typically require small samples, the sample location becomes very important, when AZS refractories made by different companies are compared.

3) TEST METHODS USED FOR CORROSION TESTING

Figure 3 shows the arrangement of refractory sample and platinum crucible used in the static finger corrosion test, as described in the ASTM C-621 method and ICG TC-11 method. These methods are used commonly to select refractory materials for glass melting furnaces.

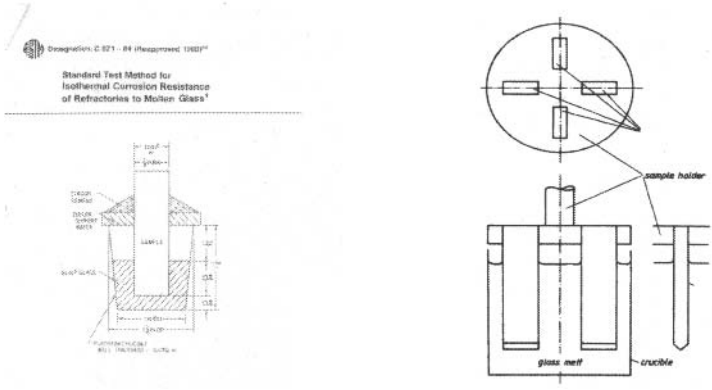

Figure 3: ASTM C-621 Method (left) and ICG TC-11 Method (right)

Since the main area of interest in a static finger corrosion test is corrosion at the metal line (or the interface between the refractory and the glass melt surface), it is important to note here that under the ASTM method, this interface is approximately 33mm up from the bottom of the sample, whereas under the TC-11 method the same interface is at approximately 60mm from the bottom. As Figure 2 shows, there can be significant differences in the ZrO_2 content in a block even when samples are taken one inch apart. Furthermore, the ASTM test calls for one round or square cross section sample per crucible, whereas the TC-11 method allows 4 bar shaped samples per crucible. These methods do not specify a common casting technique for AZS blocks, sampling location or sample placement in the test crucible. Therefore, when comparing the corrosion results from ASTM and TC-11 methods, it is important to keep in mind the differences in sample origin, size and shape.

4) COMPARISON OF AZS MADE WITH DIFFERENT MANUFACTURING PROCESSES

AZS refractories made by RHI Monofrax (in Falconer, USA) and RHI Refel (in San Vito, Italy) were compared in this study. The manufacturing processes in these plants differ mainly in terms of mold preparation and annealing. In one case, AZS blocks are left inside the molds during annealing, whereas the other process requires the blocks to be removed from the mold, while still hot.

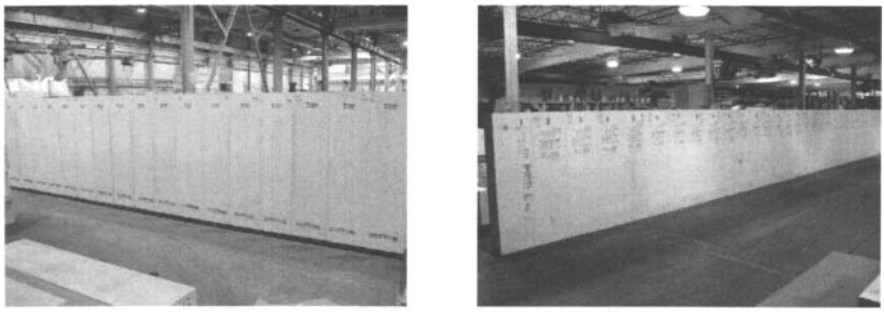

Figure 4: AZS sidewalls made at the Refel (left) and Monofrax plants (right)

In order to compare the performance of AZS made under these two different manufacturing processes, common size and shape blocks were poured. Core samples were drilled from identical locations. Core samples were first tested for chemistry and physical properties. Figures 5 and 6 show the results.

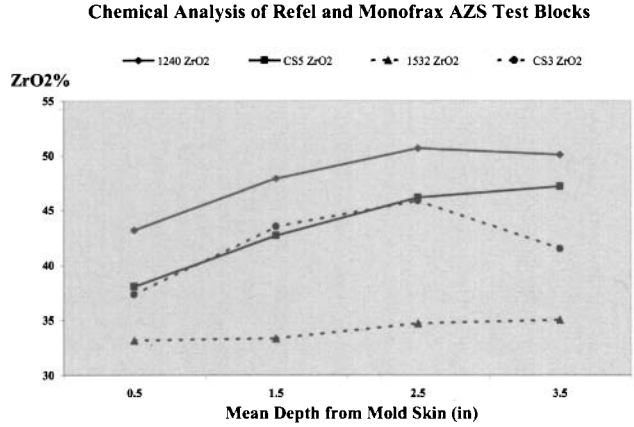

Figure 5: Chemistry variation in a 4" long finger sample. 40% ZrO_2 AZS products are CS5 and 1240 (Refel), whereas 34% AZS products are CS3 and 1532 (Refel).

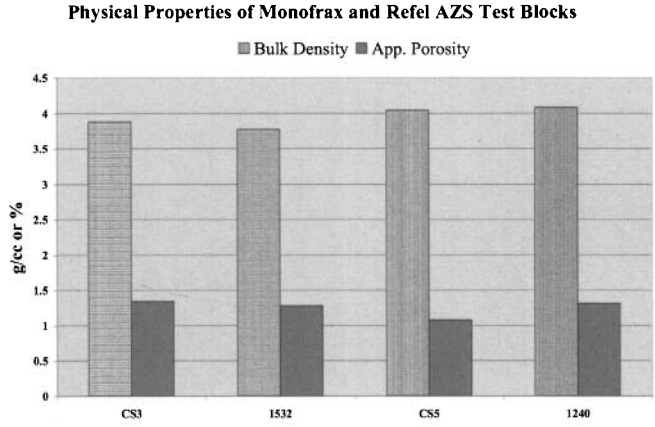

Figure 6: Physical properties measured on a 4" long finger sample

Modified ASTM C-621 static finger corrosion test method was used. Corrosion tests were performed at 1490°C and 1540°C using Soda-lime container glass. Test durations were in the range of 16h to 72h. Corrosion at the metal line was measured in terms of refractory area lost, using image analysis. Results are shown below.

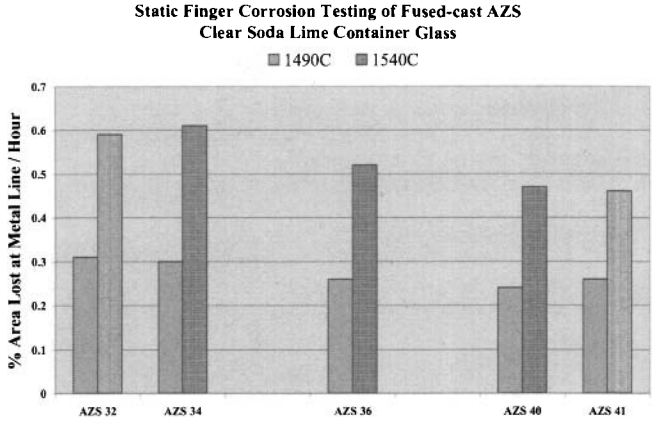

Figure 7: Corrosion resistance of Monofrax and Refel AZS. AZS 32 is Refel 1532, AZS 41 is Refel 1240; AZS 34 is CS3 and AZS 40 is CS5 from Monofrax

Following conclusions can be made from the data in figure 7:

1) The corrosion resistance of AZS 32 (Refel plant) and AZS 34 (Monofrax plant) is similar at both test temperatures.
2) The corrosion resistance of AZS 40 (Monofrax plant) and AZS 41 (Refel plant) is similar at both test temperatures.
3) The corrosion resistance of 40-41% ZrO_2 AZS is approximately 25% better than that of 32 – 34% ZrO_2 AZS.
4) The corrosion rate at 1540 °C is nearly twice as high as measured at 1490 °C, for both 32-34% and 40-41% AZS.

5) SUMMARY OF COMPARATIVE TESTING OF FUSION-CAST AZS MADE WITH DIFFERENT MANUFACTURING PROCESSES

Different manufacturing processes can indeed have an effect on the following:

- Appearance (color, surface quality etc.)
- Chemistry segregation within a block
- Microstructure evolution

Short-term laboratory testing, performed on like size blocks, under controlled conditions did not show a significant difference in the corrosion resistance of the AZS products, made at Monofrax and Refel.

6) EMERGING TRENDS IN AZS REFRACTORY APPLICATION

In the last few years, many glass companies in the NAFTA region and Europehave tested ad used lower cost AZS products in glass contact and superstructure applications. Specific examps include:

- Fused-cast AZS made in Asia
- Castable / pumpable AZS

This trend is not surprising, as manufacturers of various industrial and consumer goods hae taken on more risk in order to reduce their costs.

7) TESTING OF LOW-COST AZS

We have made an attempt to gain an insight into the lower cost products. Samples were tesd for chemistry, physical properties, microstructure, corrosion resistance and exudation behavior. n investigation #1 it was not possible to select samples from blocks of the same size. However,n investigation #2, identical size blocks were tested, with samples taken at identical locations.

7.1) Testing of Low-cost AZS; Investigation # 1

34% ZrO_2 AZS samples from 3 Asian suppliers were compared with Monofrax CS3. Samps were tested for chemistry, physical properties, exudation and corrosion resistance, using ASTM st methods. Results are shown below.

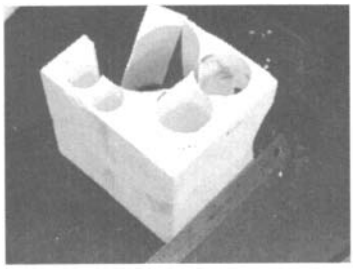

Brand A

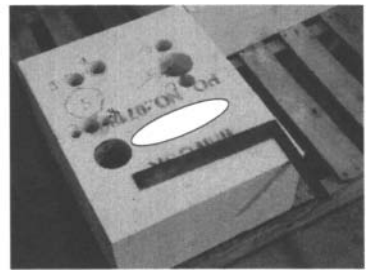

Brand B

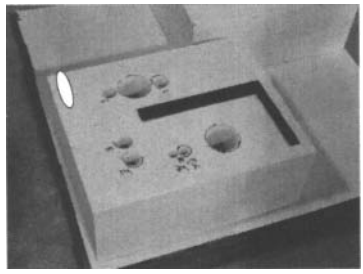

Brand C

Photos of 34% ZrO_2 AZS From Low-Cost Suppliers Tested in Investigation #1

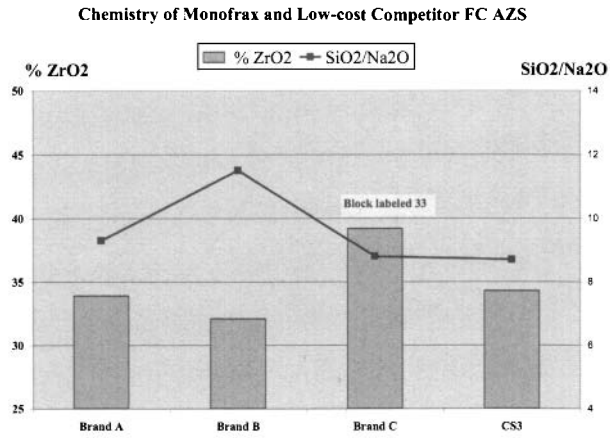

Figure 8: Chemistry of Monofrax and Low-cost 34% AZS

Brand C block was labeled 33 AZS, yet it had nearly 39% ZrO_2.

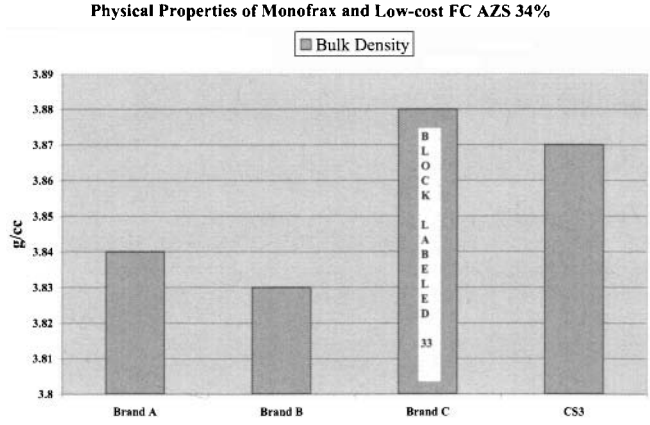

Figure 9: Physical properties of Monofrax and Low-cost 34% AZS

Brands A and B had lower bulk density than CS3. Brand C had higher density than CS3, most likely due to its higher ZrO_2 content, as shown in Fig. 8.

Investigation # 1: Exudation Test Results Following Testing at 1510 °C for 4h

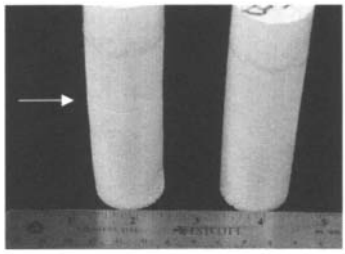

Brand A: 3.02%, 2.91 %

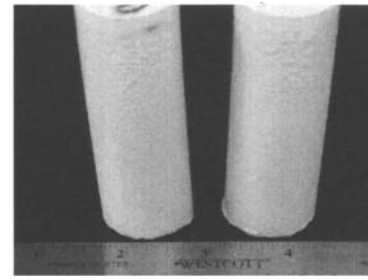

Brand B: 1.97 %, 1.66%

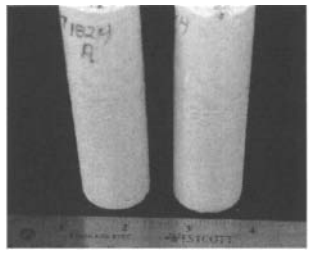

Brand C: 2.32 %, 2.20%

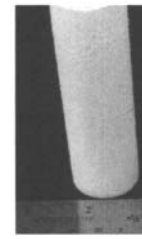

CS3: 1.54%, 1.34%

All 3 brands of low-cost AZS showed higher exudation volume than that measured for Monofrax CS3, with brands A and C showing 70% to 100% more exudation. Higher exudation is believed to be responsible for greater glass defect potential during the furnace campaign.

Investigation #1: Static Finger Corrosion Test Results

Corrosion test was performed at 1490 °C for 50 hours using a soda-lime container glass. Metal line corrosion was measured as % refractory area lost using image analysis.

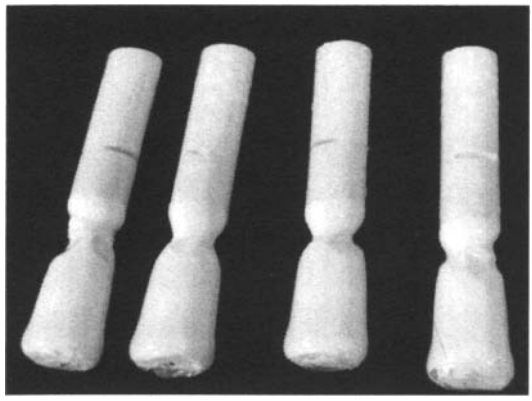

Brand C 13.1%, 12.2% Brand B 10.7%, 12.5%

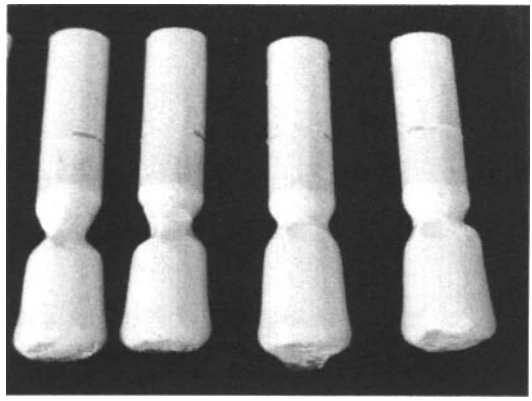

Brand A 20.1%, 20.1% CS3 11.1%, CS5 9.5%

Corrosion test data shows lower-cost brands A and C AZS performed significantly worse than CS3. Brand B had one sample with worse performance than CS3.

7.2) Testing of Low-cost AZS; Investigation # 2

In this investigation, 34% ZrO_2 AZS paving tiles were compared. The size of the tiles was 600mm x 500mm x 100mm.

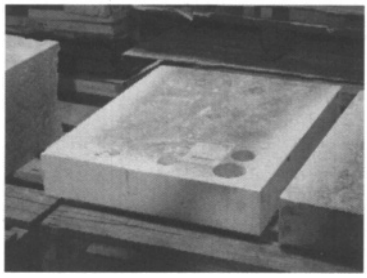

Monofrax CS3

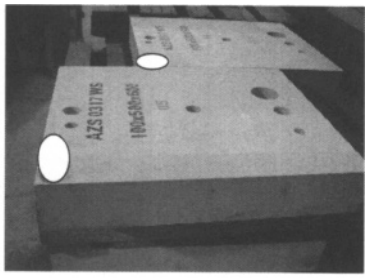

Brand XX

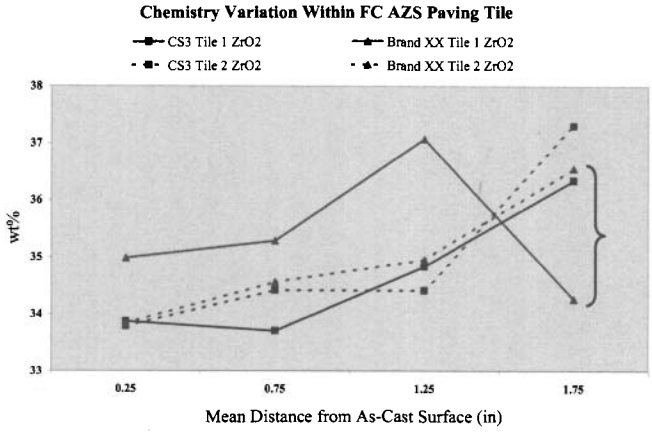

Figure 10: ZrO2 Variation Across Tile Thickness in Investigation #2

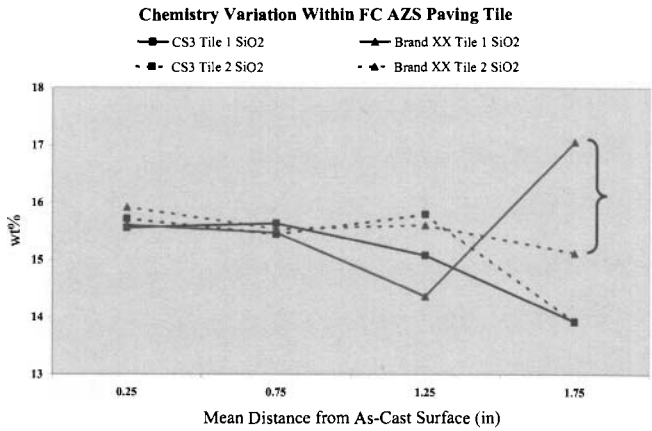

Figure 11: SiO_2 Variation Across Tile Thickness in Investigation #2

Figures 10 and 11 show greater chemistry variability in the center of the brand XX AZS tiles than seen in Monofrax CS3 tiles.

Investigation #2: Exudation test results

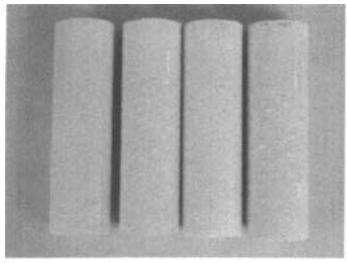

Monofrax CS3
Avg. Exudation Vol% = 1.88

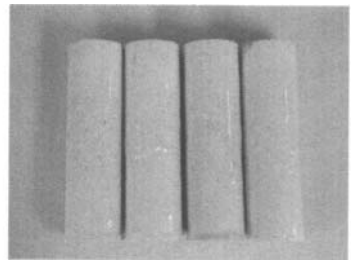

Brand XX
Avg. Exudation Vol% = 3.23

Lower-cost brand XX AZS showed 72% higher exudation volume than CS3.

Investigation # 2: Corrosion Testing of FC AZS 34% ZrO_2 Refractories, Modified ASTM C621, 1400°C, 180h, Soda Lime Container Glass

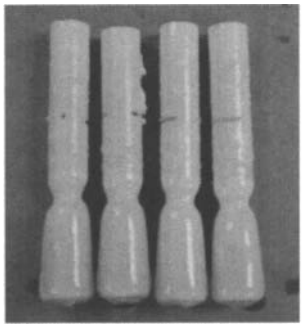

Monofrax CS3
Avg. Metal Line Corrosion = 12.2%

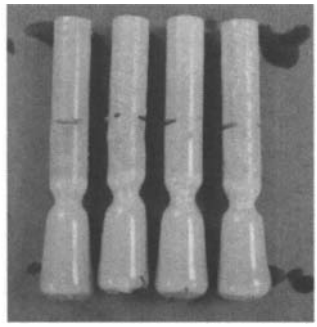

Brand XX
Avg. Metal Line Corrosion = 13.1%

Lower-cost Brand XX AZS paving tile samples showed higher rate of corrosion than Monofrax CS3 AZS

7.3) Testing of Low-cost AZS; Investigation # 3

In recent years, some glass container manufacturers have used a Castable AZS lining in place of fusion-cast AZS sidewall blocks in a glass contact application. Apparently, this decision has been partly based on the lower cost of castable AZS. In investigation # 3, we have compared samples of two different castable AZS refractories with Monofrax CS3 fusion-cast AZS.

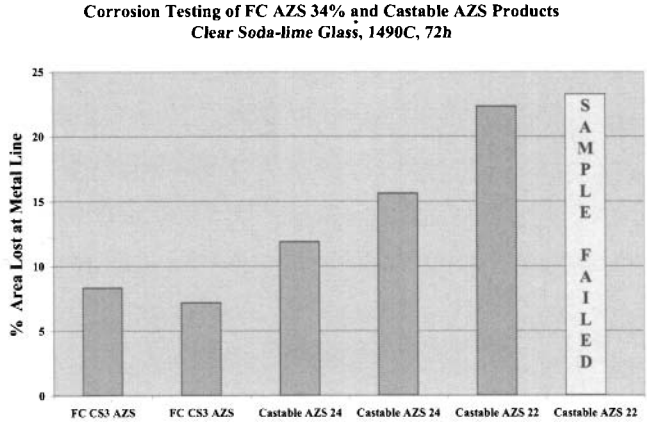

Figure 12: Results from static corrosion testing of Fusion-cast and castable AZS

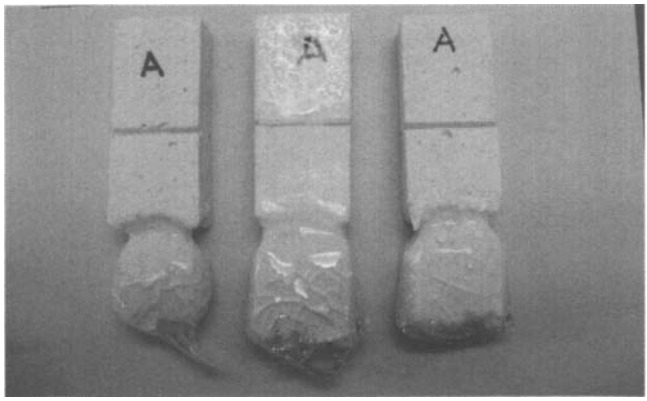

Samples on left and right are castable AZS containing 22% and 24% ZrO_2 respectively. The sample in the middle is Monofrax CS3 with 34% ZrO_2.

Though the castable AZS products contain about 33% less ZrO_2 than the fusion-cast AZS samples (22% or 24% vs. 34%), the castable AZS 24% samples corroded nearly 100% more, whereas castable AZS 22% samples corroded nearly 200% more than CS3 samples. Furthermore, the castable AZS refractory offers much greater potential for stone defects, as shown in the close-up photo of the corroded samples.

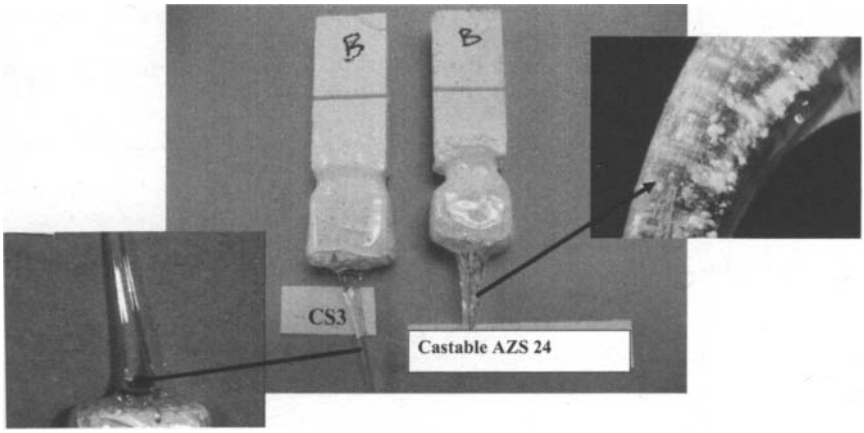

Glass adhering to the bottom of the castable sample contains numerous large refractory grains, whereas none were observed in the CS3 sample. These grains could lead to stones in the glass.

8) SUMMARY OF LOW-COST AZS EVALUATION

Three separate investigations were made to evaluate lower cost AZS. Investigations # 1 and #2 focused on lower-cost fusion-cast AZS samples from 4 manufacturers. Investigation #3 focused on lower-cost castable AZS samples. All samples were compared with Monofrax CS3 and CS5 AZS refractories, using soda lime container glass. Following conclusions can be made from the results shown above.

1) Some of the lower-cost fusion-cast AZS samples had similar overall chemistry and density as Monofrax samples. However, one sample labeled 33 AZS had the chemistry and density of 40% ZrO_2 AZS. This raises a concern regarding consistency with respect to specifications.
2) In a controlled investigation (#2), lower cost AZS showed greater variability in the chemistry of the tiles tested.
3) Most of the lower-cost fusion-cast AZS samples had higher exudation volume and higher rate of corrosion than Monofrax CS3 AZS.
4) The castable / pumpable AZS products displayed 2 to 3 times higher rate of corrosion, and a greater potential for glass defects.

9) CONCLUDING REMARKS

- More companies are producing fusion-cast AZS refractories today than ever before.
- Manufacturing processes, raw materials and overall quality control vary among the fusion-cast AZS suppliers.
- Short-term testing in laboratory conditions continues to be utilized by glass industry and refractory suppliers in selecting and promoting AZS materials.
- Test procedures vary from one continent to another, despite general recognition of the inhomogeneous structure of AZS. These procedures do not specify a standard size or casting technique for the AZS block to be tested, a common sampling location, or sample population.
- It is imperative that test samples are selected from like size blocks and identical locations, when comparing AZS made by different suppliers.
- Testing of AZS earmarked for superstructure application should be based on Regular Cast (containing shrinkage voids) blocks, whereas Void Free blocks should be used for testing for glass contact application.
- Short-term refractory test data must be correlated with long-term glass furnace campaign data (glass quality, unplanned maintenance issues, refractory wear).
- Lower-cost AZS alternatives need to be evaluated correctly and thoroughly.
- Given inferior performance of lower-cost AZS in this study, the glass industry should determine if short-term cost savings in AZS refractory procurement have truly allowed long term reduction in the cost of glass.

REFERENCES

[1] Bardhan and Mcnally, "Fusion-casting and crystallization of high temperature materials", Journal of Materials Science 15 (1980), 2409-2427

MULLITE REGENERATORS—AN OPTIMUM SOLUTION

Chris Windle and Trevor Wilson
DSF Refractories and Minerals Limited
Friden, Buxton, United Kingdom

ABSTRACT

The new generation of mullite refractories are proving to be a major success in glass furnace regenerator superstuctures, sweeping away the previously dominent position of basic refractories in these applications.

The regenerator principle for heat recovery pioneered by the Siemens brothers is now nearly 150 years old, however increased demands placed on the regenerative system have been met by improved and innovative refractories which make this system as relevant today as when first conceived.

Attributes of low thermal conductivity, low thermal expansion in conjunction with chemical stability and thermal shock resistance place mullite in the premier rank when deliberating regenerator construction.

Mullite regenerator superstructures have been widely utilised in the glass container industry with campaigns now reaching 16+ years.

The opportunities created by mullite superstructure are highlighted; specifically why mullite zoning is key to the superstructure campaign; their ability to withstand alkali in thermo-mechanical situations and finally the potential heat saving and efficiencies that can be obtained compared with basic superstructure.

In addition, the adoption of mullite regenerators for the float glass industry is discussed. Case studies are described showing mullite regenerators at campaign completion.

1. INTRODUCTION

Regenerative glass melting furnaces have undergone innovation since 1867 when Frederich Siemens introduced the concept and built the first tank at Dresden. Whilst other firing technologies have been introduced; the regenerative furnace and indeed the regenerators remain the optimum production method for many glass types.

Low NOx; long campaigns and thermal efficiency gains have placed increased demands on the regenerative system which have been met by improved and innovative refractories.

Whilst refractories in the generic "basic" family exhibit characteristics suitable to heat transfer (i.e high thermal conductivity;specific heat) and are therefore employed as the main checker heat exchange items; they are also utilised for the regenerator superstructure where attributes of relatively high thermal conductivity, expansion and creep are contrary to the objective of a highly insulated; "air tight" stable construction.

Mullite regenerator superstructures have been widely utilised in the glass container industry for many years with campaigns now reaching 16+ years.

In float glass, although mullite and associated compositions have played key roles in the lower superstructure (rider arches, rider/spanner tiles, adaptor course and mid/lower sidewalls); recent designs are incorporating these materials in the upper superstructure where traditionally basic materials have dominated.

This step change is due to mullite inherent properties of low thermal conductivity, expansion and creep, in conjunction with an ability to form "protective" layers in reaction with waste gas stream alkali.

These layers are in mutual equilibrium both thermally and chemically and their phase composition relates directly to the isothermal section of the Na_2O-Al_2O_3-SiO_2 phase diagram and follows the Na_2O concentration gradient from the hot face to the refractory interior.

The formation of these layers are crucial to mullite operation and longevity; in addition the regenerator structure is split into zones based on operating temperature; as temperature reduces the refractory mullite content should also be reduced and amorphous phase increased to combat expansile alkali reactions.

Mullite refractories derived from andalusite have structures that are particularly suited to regenerator construction; "mullite" covers a wide range of products not all of which will provide "safe" operation.

2. GENERIC REFRACTORY TYPES FOR REGENERATOR SUPERSTRUCTURE

For efficient thermal energy recovery from the waste gas stream the regenerator refractories perform two functions:-

i) heat transfer from the waste gas to combustion air stream
ii) thermal insulation of the heat transfer system; that is preventing heat flux to the surrounding environment and ensuring that extraneous air doesn't enter the system

Refractories suited to the heat transfer function should have both high heat capacity and thermal conductivity; basic and fused cast materials fit these criteria and are consequently used extensively for regenerator packing; the heat exchange surface.

Conversely the regenerator superstructure should be constructed from materials with relatively low thermal conductivity; mullite, silica and fireclay generic refractory types are appropriate, however other criteria such as thermo-mechanical and chemical stability should also be considered.

Table 1 below summarizes the desired characteristics for regenerator superstructure construction and related material properties

Table.1

Comparative Properties	Basic	Fused Cast AZS	Mullite	Silica	Fireclay
Low thermal conductivity	no	no	yes	yes	yes
Reaction with batch & alkali	resistant to alkali; fosterite formation with batch silica	Resistant to batch and alkalis (glass phase penetration)	forms stable reaction layers	corroded by batch carry-over; extensive reaction with alkali at low temperatures	alkali reaction yields glass which limits use to lower regenerator regions
Low thermal expansion	no	yes; not linear but understood	yes	yes, not linear but understood	yes
Creep resistance	dependent on grade	yes	yes	yes	no; only suited to low temperature use
Redox resistant	variable	yes	yes	yes	dependent on Fe content
Cost/unit volume	high	very high	medium	low	very low

From the analysis above, mullite based refractories would appear to be in the premier rank for regenerator superstructure utilisation, indeed for decades these materials have been used widely in the container industry.

Hindered by the perception that mullites cannot withstand the increased thermo-mechanical or thermo-chemical conditions posed by float regenerators (a legacy of traditional low mullitic compositions); these materials are now finding a foothold not only in the lower superstructure but now upper and division walls.

In addition to the properties summarised below:-

i) low thermal conductivity (fig.1)
ii) low thermal expansion (fig.2)
iii) resistant to batch carry-over (section 4)
iv) good creep resistance (fig.3)
v) protective layer formation (resists alkali;section 4)
vi) redox safe (section 4)

mullite based materials can be re-heated after tank repairs and interwoven in the construction to create an air tight installation.

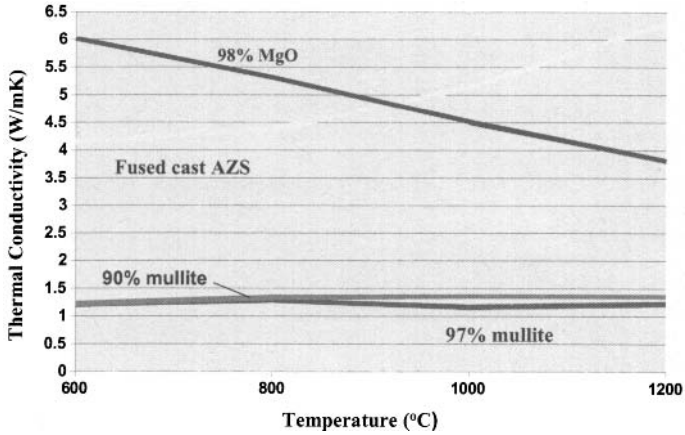

Figure 1

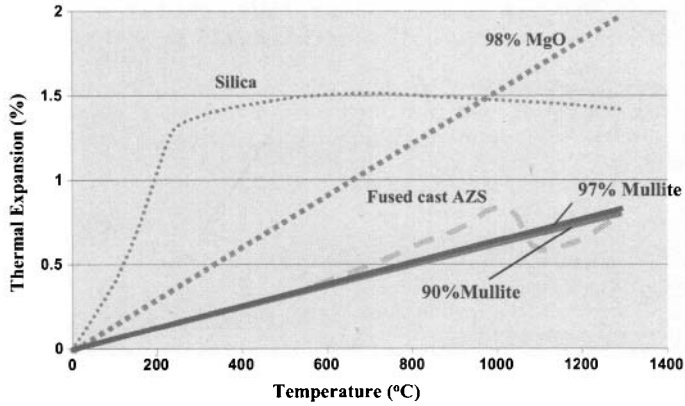

Figure 2

Table 2 overpage shows a summary of the mullites that are generally used in regenerator construction and compares them with typical data for a 98% magnesite (basic) grade. Specifically the 90, 97% and Fused Mullite compositions substitute the basic material in the upper regenerator structure; thermal conductivity, expansion and weight advantages are clear.

In regard to creep resistance both mullite and basic compositions provide stable construction, however basic refractory creep characteristics are heavily dependent on $CaO:SiO_2$ ratio and the base raw material aggregate. Compositions based on large crystal (sintered or fused) magnesia and fired to +1700°C show virtually no deformation at 1550°C, however products with similar chemistries can show major subsidence at this temperature.

Mullite materials do not have the same dependence on minor phases although naturally the maximum mullite content is desired; significantly however the creation of sealing layers on the refractory surface ensures that alkali and other batch compounds cannot penetrate the refractory interior and thermo-mechanical properties are preserved.

Table 2

% Mullite	79	81	90	97	Fused Mullite	Direct Bonded Magnesite
Bulk Density (g/cc)	2.48	2.50	2.55	2.52	2.56	2.98-3.02
Apparent Porosity (%)	13.5	13.4	14.1	18.5	17.0	15-16
CCS (MPa)	86	80	75	90	60	50-60
TSR (950°C to water)	4	8	30	16	8	2
Creep, % @ 1550°C (25th to 50th hour)	N/A	N/A	0.3	0.07	0.022	0-0.85
Thermal Expansion (% 20-1500°C)	0.72	0.54	0.91	0.72	0.80	1.5 – 2.0
Thermal Conductivity (coefficient,W/mk 800, 1000, 1200°C)	1.56 1.55 1.68	1.73 1.82 1.93	1.33 1.35 1.35	1.27 1.10 1.22	2.34 2.33 2.25	5.9 4.6 3.5

3. MULLITE REFRACTORIES DERIVED FROM ANDALUSITE

Andalusite is part of the sillimanite group of minerals which the same composition $Al_2O_3.SiO_2$, but exhibit different mineralogical properties.Formed by metamorphic processes, temperature and pressure dictate the final mineral formed; Andalusite is formed at low to moderate temperatures in conjunction with low stress (pressure), whereas Sillimanite requires much higher temperatures and pressures. Kyanite requires pressure to form but does so over a wide temperature range (figure 3)

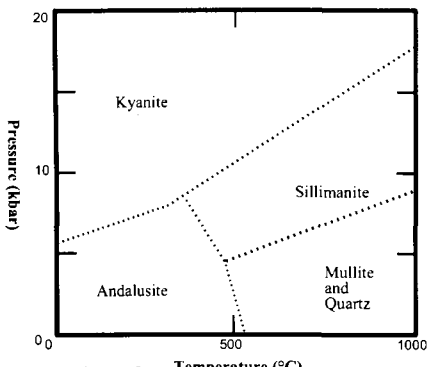

Figure 3

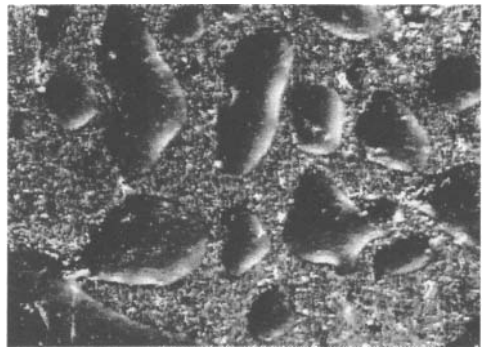

Figure 4: Secondary Electron S.E.M Micrograph. Expelled glass droplets, from a completely mullitised andalusite monocrystal

During the firing process, the sillimanite minerals dissociate to form mullite with excess silica as shown in the equation below:-

$$3(Al_2O_3.SiO_2) = 3Al_2O_3.2SiO_2 + SiO_2$$

at high temperatures (1600°C), the glass exudation from the mullitisation process is clearly visible, Fig.4 above.

4. ANDALUSITE (DUAL NATURE)

The expellation of glass from the andalusite structure begins at 1250-1300°C, and is completed by soaking at temperatures in excess of 1450°C. As mullitisation continues, the entirity of the glass formed cannot be accommodated by the structure, and 10~15% of the glass created is expelled from the grain, this equates to approximately 3.5% of the total composition.

The structure created is highly orientated mullite with a capillary network filled with a silica rich glass (~80% SiO_2). It is this composite structure that provides the unique dual nature afforded to andalusite based products, that is; the mullite jacket provides excellent resistance to deformation under load, whilst the glass trapped within the mullite when liberated from the structure by alkali interaction forms a protective glassy layer.

4.PROTECTIVE SEALING LAYERS

In operation mullite materials develop a series of boundary layers according to the isothermal section at the relevant temperature (figure 5 below):-

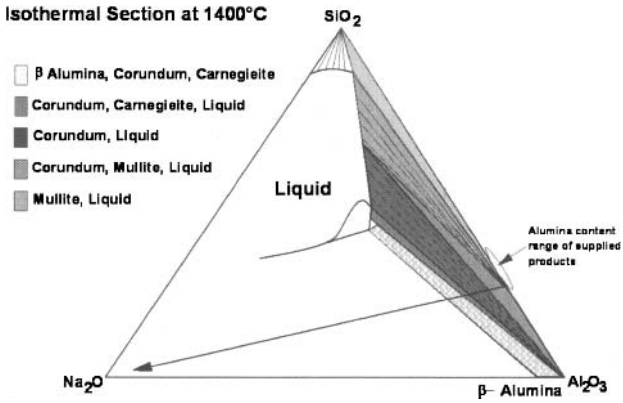

These layers are in mutual chemical equilibrium and ensure that thermal properties such as thermal expansion show gradual change from the base mullite structure to the dense corundum + glass; this prevents spalling behaviour.

Fundamentally however, the boundary layer is thermodynamically stable in the regenerator alkali laden environment and therefore wear proceeds at a minimal rate whilst the majority of the refractory is unaffected and thermo-mechanical properties are protected.

Typical microstructures developed are shown in figures 6,7 & 8:

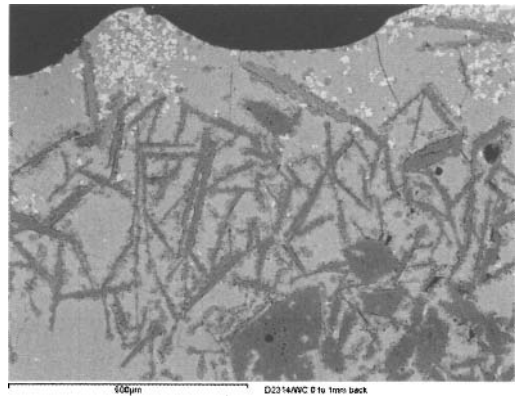

Figure 6 Dark grey corundum needles in a light grey sodium alumino-silicate glass. Note the toughening/crack stopping behaviour of the corundum needles.

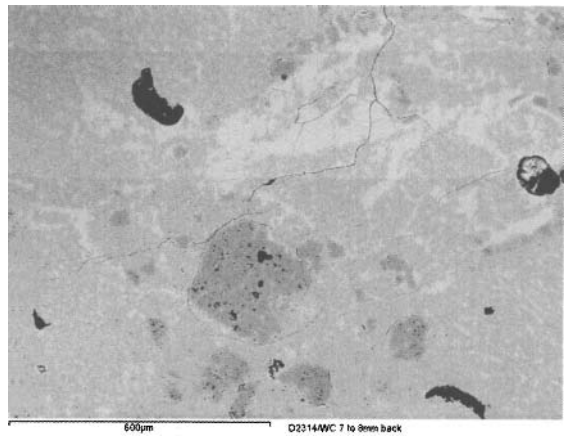

Figure 7: Mullite + glass

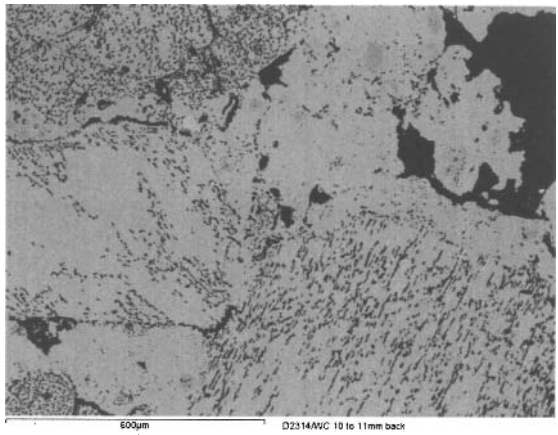

Figure 8: Mullite; unaltered structure

From figures 7 to 9 the change from dense reaction layers to unaltered composition can be observed; the Na_2O content reduces from 10-15% to <0.8% in approximately 11 mm.

5. MULLITE ZONING

Whilst mullite compositions readily form protective boundary layers at high temperatures a process which is assisted by the "dual" nature of mullites derived from andalusites; below 1270°C nepheline and β-alumina are the equilibrium phases. These sodium alumino-silicate phases are expansile and therefore will create spalling in the refractory lining. To combat this the balance of mullite crystalline phase and glass phase is altered; glass phase inherent in the brick is increased to absorb alkali without expansion.

The basic principle is shown in figure 9 below; as temperature decreases down the regenerator superstructure; refractory glass phase is increased. This means that the most crystalline high mullite refractories are utilised in the zones subject to high load and temperature.

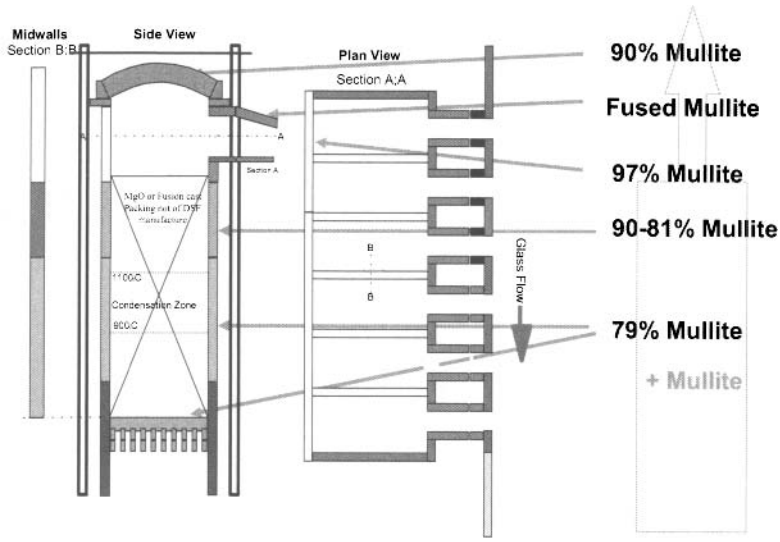

Figure 9

6. THERMAL PROFILES, HEAT FLOW & HEAT ENERGY BALANCE

Figures 10,11 & 12 show the theoretical thermal efficiencies that can be attained by switching from basic to mullite products. The beneficial heat flow (W/m2) reduction ranges from 7% on product change alone to 24% achieved by thinning the mullite layer and increasing the insulation (Figure.11). With spray insulation applied the theoretical heat flow saving is still substantial at 22% (Figure.12)

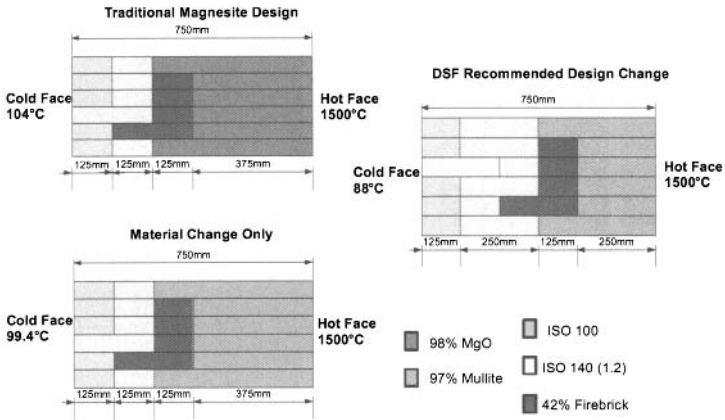

Fig.10 Temperature profile (steady state condition);upper regenerator sidewall

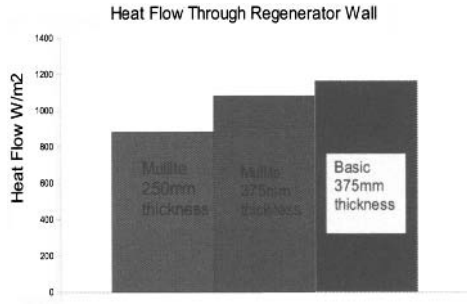

Fig.11 Heat flow through upper regenerator structure at 1500°C

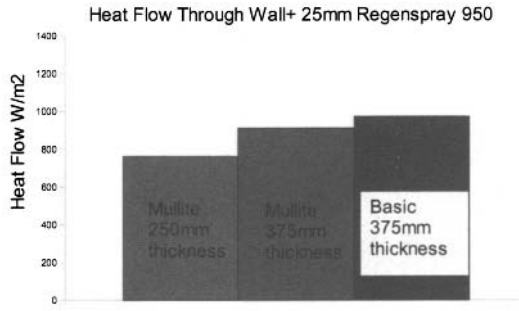

Fig.12

Heat flow; upper regenerator structure after application of insulating spray

In regard to the heat energy balance for the system; taking a typical float furnace as an example:- 1800 therms per hour are input via the burners; 800 therms per hour input via pre-heated combustion air and 1500 therms per hour lost in the waste gas stream, leaving a net input of 1100 therms per hour. The heat availability factor (HAF) is therefore 1800/1100 (1.64); therefore 1 therm/hr of increased energy requires an input of 1.64 therms/hr.

For every therm/hr saved in the regenerator structure;0.7 therms/hr are not required from the burners; that is 70% is recovered and 30% lost to the waste gas stream.

An approximate is that 35 therms/hr will be kept in the system due to the use of mullite materials in the upper regenerator structure; equating to savings into the region of several million dollars over a 16 year campaign.

7. CASE STUDIES

Figures 13 and 14 below amply illustrate the capability of mullite materials in container furnaces; more recently (last few years) mullite materials are being used in float regenerator construction.

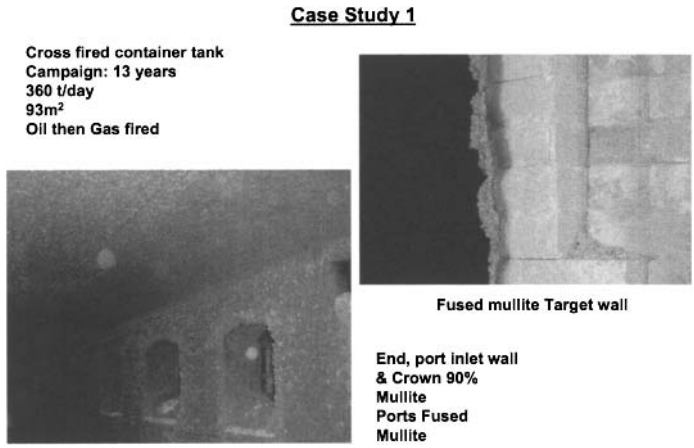

Figure 13

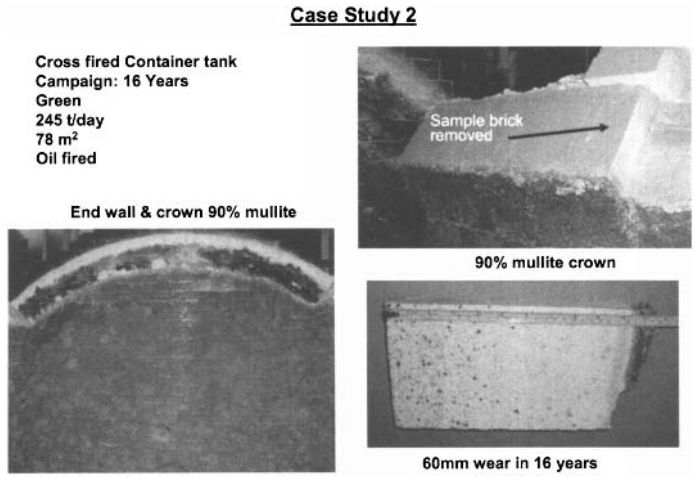

Figure 14

8. CONCLUSIONS

Mullite based materials offer significant advantages over other generic refractory types for regenerator superstructure construction namely these are:-

i) low thermal conductivity (thermally efficient)
ii) low thermal expansion
iii) resistant to batch and alkalis (through the formation of protective layers)
iv) creep resistant
v) redox resistant

Widely utilised in the container industry; these products are now finding application in the upper structures of float regenerators.

Not all mullites are the same however, in particular mullites derived from the andalusite mineral exhibit a composite structure of a mullite jacket surrounding "tubes" of glass phase. This ensures that the mullite governs thermo-mechanical behaviour whilst the glass phase is available to form a coherent protective layer, the pre-requisite for alkali resistance. These materials can be viewed as active toward their environment.

It is possible to create a 97% mullite refractory from the andalusite structure; this material has out performed traditional Fused Mullite compositions in some applications a corollary of reaction time required to form protective layers.

ACKNOWLEDGEMENTS

Figure 4	Pierre Dubreuil (1997) Andalusite:A Living Reactive Mullite, Damrec (Imerys)
Figure 6,7,8	Ceram Research, UK
Figure 10,11	Mr Trevor Wilson, Sales Manager, DSF Refractories&Minerals Ltd
Heat Energy Balance	Mr Geoff Evans GlasRef Consulting

This Page Intentionally Left Blank

Author Index

This Page Intentionally Left Blank